Bijay Kumar Sahu, 2000

AEROMAGNETICS OF SELECTED CONTINENTAL AREAS FLANKING THE INDIAN OCEAN; *WITH IMPLICATIONS FOR GEOLOGICAL CORRELATION AND REASSEMBLY OF CENTRAL GONDWANA*

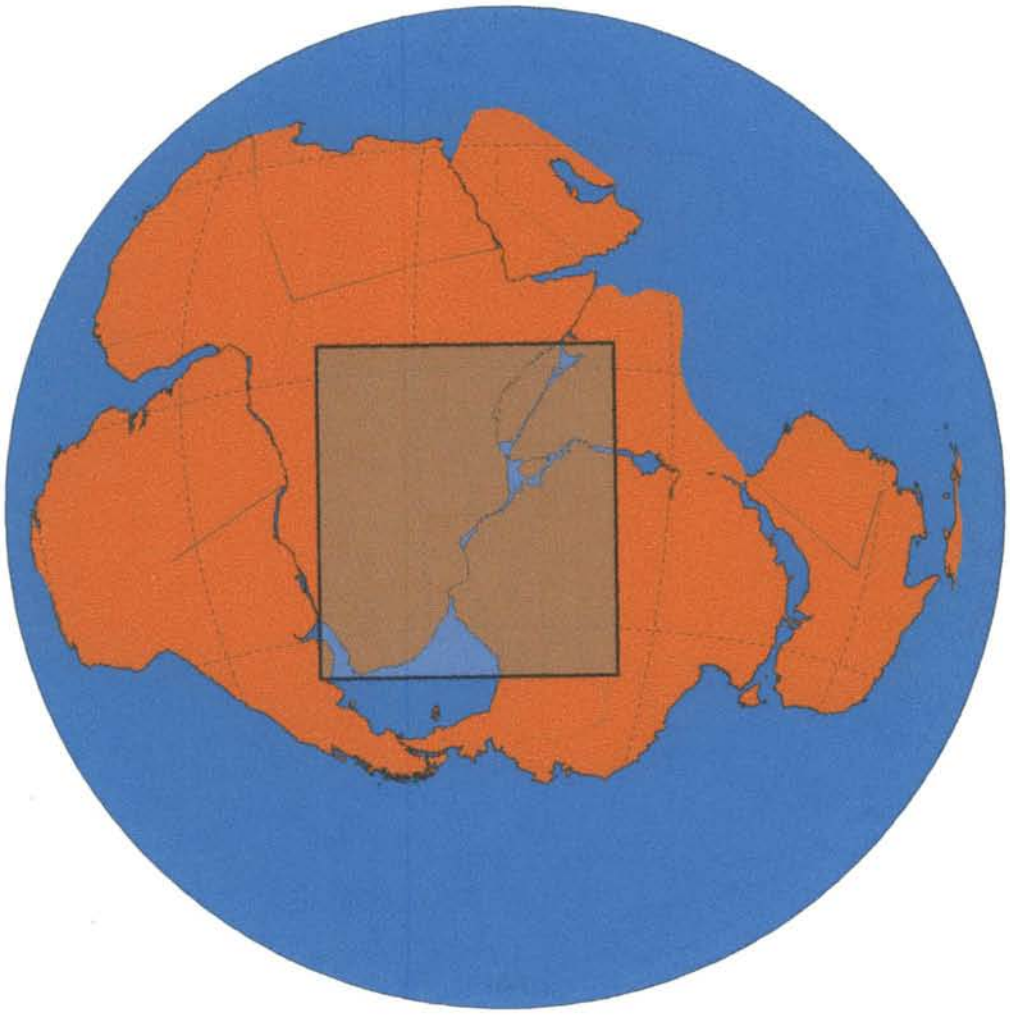

Thesis presented for the degree of Doctor of Philosophy
in the Department of Geological Sciences
University of Cape Town

September 2000

ITC

ABSTRACT

Reassembling continental fragments of Gondwana has been a subject of interest to many since almost the beginning of the last century. As a result, the broad relative position of the major continental fragments and their dispersal history is well understood using marine magnetic anomalies, coastline geometry, surface geology and limited geophysics. Uncertainty still prevails in reassembly of central Gondwana fragments flanking the Indian Ocean. This thesis aims at utilising geophysical constraints to corroborate and fine-tune the reconstruction of these fragments supported by geological evidence.

The recent geological and geochronological data of each of the fragments are reviewed. A fragment-to-fragment correlation of these data is done to find evidence for a relatively tight fit of the continents. The geology of each of the fragments is subdivided into five tectonic units for comparison.

Geophysical studies, especially aeromagnetic, are carried out in two lines — (i) comparison of aeromagnetic anomaly patterns across rifted margins and (ii) correlation of major geological features interpreted from the aeromagnetic images. A number of aeromagnetic maps are produced for correlation of anomalies and interpretation of major geological structures.

Aeromagnetic images of southern India are produced for the first time. These images reveal four distinct magnetic relief zones broadly corresponding to the litho-tectonic subdivisions. The predominantly charnockite terrain (Madurai Granulite Terrain) has higher magnetic relief than the Dharwar granite-greenstone belt to the north and the predominantly khondalite terrain to the south. Positions of most of the predefined shear zones are redefined using derivative maps and 3-D Euler deconvolution. A new trans-subcontinental shear zone named the Cannanore-Thanzavur Lineament is interpreted. A linear and high-amplitude aeromagnetic anomaly parallel to the west coast is interpreted as the eastern shoulder of the rift between India and Madagascar. Comparison of aeromagnetic anomaly patterns in southern India and south-central Madagascar strongly supports substantial dextral strike slip along West Coast Fault prior to separation between the two.

New aeromagnetic images of southern and eastern Africa clearly show many new features. Interpretation of these maps has led to the production of a tectonic map of sub-Saharan Africa. Quantitative estimation of the depth of crystalline basement below Phanerozoic sediments suggests extended crust in southern Mozambique.

Aeromagnetic maps of central Gondwana show good correlation of total field anomalies and their analytic signals between juxtaposed fragments. The long strike-length anomalies in southern Africa have counterparts in the Maudheim Province of Dronning Maud land in East Antarctica. Similarly, close juxtapositioning of Sri Lanka against southern India is argued based on similarity in magnetic trends and analytic signals.

The existing and the new aeromagnetic interpretations of various regions of central Gondwana have been digitally compiled and stored in a database, which can readily be used for preparing paleomaps of any geological age. A tectonic map of central Gondwana at 200 Ma is produced.

Integration of different layers of geoscience data (aeromagnetic and lithology) of sub-Saharan Africa, southern India and Southwest Sri Lanka reveals many new features, many of which are not clear in any one of them. A direct correlation of lithology with the corresponding aeromagnetic anomaly patterns has also been possible through the integrated images.

Review of few recent models of central Gondwana in the light of the new data suggests that the fragments can be reassembled more closely for a better correlation of geological and geophysical features.

PREFACE AND ACKNOWLEDGEMENTS

The concept of compiling, interpreting and databasing of the huge quantity of geophysical data for central Gondwana was conceived by Prof Colin Reeves in 1995. This concept led to my selection as a PhD candidate in the International Institute for Aerospace Survey and Earth Sciences (ITC) to work in the research project from October 1996. The financial and logistic support by ITC for this research is gratefully acknowledged.

I worked in the Geological Survey of India as a geologist before coming to the Netherlands. I wish to thank the Geological Survey of India for nominating me to pursue this research.

This study required both geological and geophysical knowledge. My geology background was a bonus for me in this regard. Limited training in geophysics at the Indian School of Mines, Dhanbad during M Sc and at the Geological Survey of India Training Institute was of immense help to initiate geophysical data processing. Continued discussion with Prof Colin Reeves, my supervisor in ITC, and Dr Sally Barritt further strengthened my capability in handling geophysical data. I wish to sincerely thank to both of them.

The on-going scientific co-operation between ITC and the Centre for Interactive Graphical Computing of Earth Systems (CIGCES), University of Cape Town in Gondwana research has been a major factor in successful completion of this thesis. I thank Prof Maarten de Wit for agreeing to be my University promoter. His guidance and suggestions has greatly improved my understanding of the geology of Gondwana fragments. The laboratory support of CIGCES is duly acknowledged. I am thankful to Dr Moctar Doucouré of CIGCES for his valuable discussions on various aspects of geophysics and help in comfortable stay at Cape Town during my two visits. I am thankful to Daud Jamal (Mozambique) for his fruitful discussions on the recent geochronological studies in East Africa.

I thank Saman Perera and Deepani Weerakoon (Sri Lanka), Cenk Yardimcilar (Turkey), Julius Nyakaana (Uganda), Sergio Chavez-Gomez (Cuba) and many other former students of ITC for their input in this research. Thanks are also due to the fellow PhD colleagues - Asadi Harouni (Iran), John Caranza (Philippines), Senol Özmutlu (Turkey) and Alok Porwal (India) for their valuable suggestions in many occasions. Technical support by Hans Erren and Ton Brower (ex-ITC staff) in initial stage of this research is thankfully acknowledged.

I wish to extend my sincere thanks and appreciation to Bish Kewaldar (ITC) for all his support in ITC and outside ITC. Our stay in the Netherlands would not have been so memorable but for his presence. I wish to thank Ineke Theussing, Wim Zuiderwijk and Henk Wilbrink (ITC, Delft) for their support during the research period.

I am indebted to my wife Susmita for her patience, support and understanding during all these years of my study. She has taken great pains in managing the household and taking care of our daughters Meghna and Manisha alone during my frequent absence from Delft. I greatly acknowledge the moral support of my parents, in-laws and other family members during my long absence from India.

CONTENTS

Chapter 4: GEOLOGICAL CORRELATION

Chapter 5: COMPILATION AND INTERPRETATION OF AEROMAGNETIC DATA, SOUTHERN INDIA

A. Aeromagnetic Data Compilation

B. Interpretation of Aeromagnetic Images

Chapter 6: Aeromagnetics of Southern and Eastern Africa

1. INTRODUCTION

1.1. Problem Definition

1.1.1. Gondwana Supercontinent

The concept of a single supercontinent, Gondwana (Figure 1.1) in the Southern Hemisphere was first suggested by Suess (1904) and championed by Du Toit in 1937. The scientific community has been trying to unravel the process of formation and disintegration of this supercontinent since then. This has gained momentum as the theory of plate tectonics (sea-floor spreading and continental drifting) has become formalised and accepted as one of the fundamental processes of the dynamics of the earth. Many problems pertaining to the paleopositions of the now widely-separated continents, their relation to each other in a supercontinental framework and the dynamics of their separation from the erstwhile Gondwana have still remained unsolved to the satisfaction of many.

a. Hypotheses and Uncertainties: Formation and disruption of supercontinents throughout geological history of the earth is a well-established fact now. It is also certain that a southern supercontinent called Gondwana (Figure 1.1), consisting largely of the present continents of South America, Africa, Antarctica, India, Australia and islands such as Madagascar and Sri Lanka as well as various small crustal fragments now attached to Europe and Asia, existed at the end of Paleozoic. Gondwana started disintegrating at ~200 Ma. A number of workers have attempted reconstruction of Gondwana based on coastline geometry, bathymetric contours, surface geology etc (see Smith, 1999 for review). But still uncertainty prevails about which geological features should be matched to best constrain a tight (50 to 100 km) fit of the continents – should all the geological features prior to break-up be used or only those that developed/ reactivated during the existence of Gondwana (~600 –200 Ma). It is most logical to match the later features, such as Neoproterozoic orogenic belts (*e.g.*. Pan-African, Kibaran, Braziliano), Neoproterozoic shear zones/ metamorphic belts, Permo-Triassic rift basins (*e.g.* Karoo basins of Africa, Gondwana

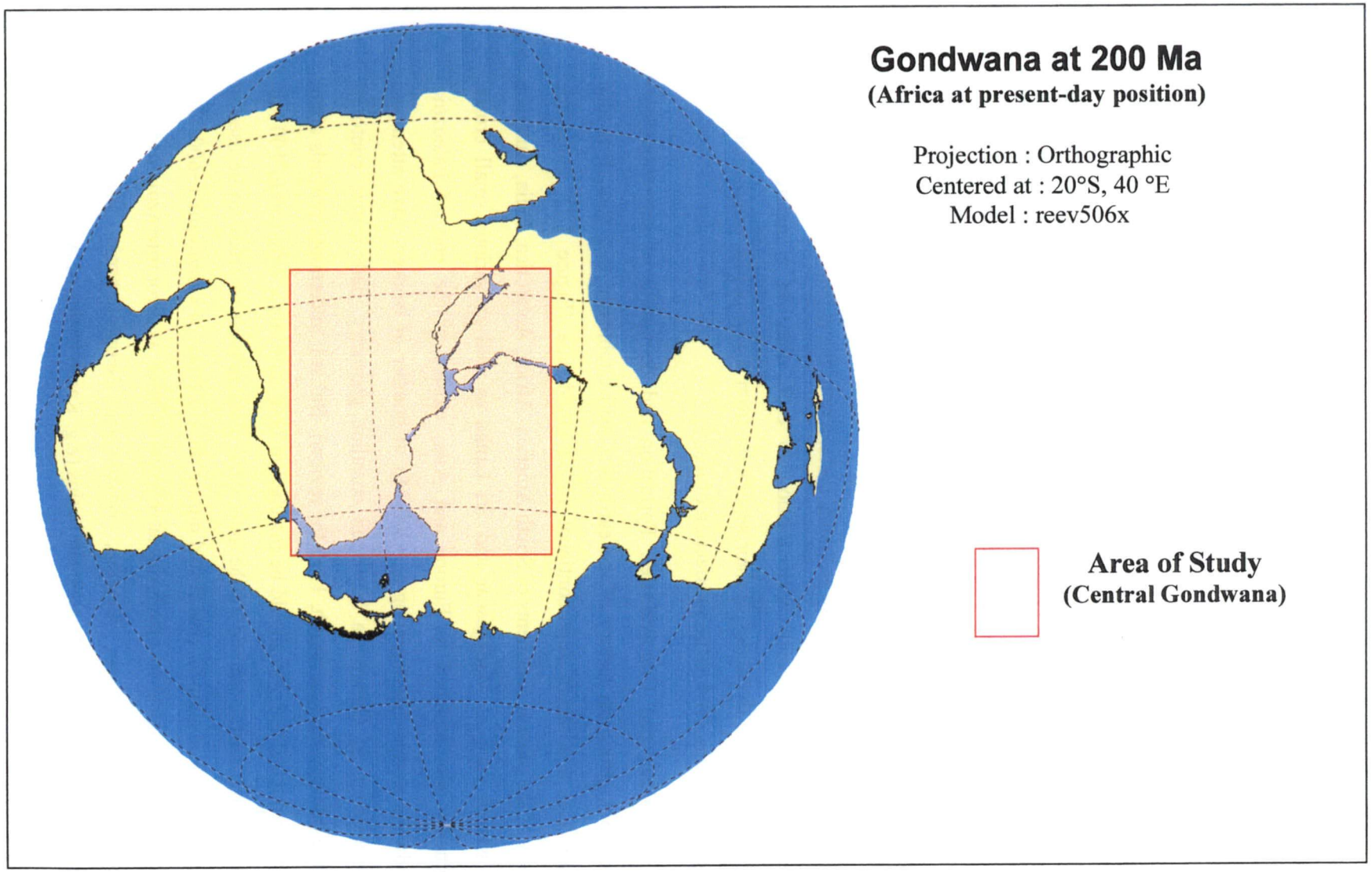

***Figure 1.1**: Gondwana model at 200 Ma (Reeves, pers. comm.) showing the study area. The model is constrained by retracing of ocean floor transforms interpreted from the satellite altimetry gravity (Smith and Sandwell, 1997).*

block of continental crust that has retained its geometrical and geological stability since a certain date, despite remaining mobile as a part of a single or more tectonic plate(s)". These blocks survive later deformation and other tectonic events that largely modify the nature of the crust surrounding them. The best examples of this are evident in southeastern Africa, where Archean cratons (Kaapvaal, Zimbabwe and Tanzania) have remained relatively unaffected by the later events like the Kibaran (~1000 Ma), the Pan-African (~500 Ma), the Karoo rifting and the latest East African rifting. It raises an important questions: do cratons survive later tectonic events because of some inherent physical properties that are distinctly different from the other crustal elements surrounding them or is their survival just a matter of chance? These questions are addressed in later chapters of this thesis.

Archean to Paleoproterozoic (pre 2000 Ma) cratons that suffered no deformation during Mesoproterozoic to Paleozoic times, constitute the fundamental nucleii in the Gondwana supercontinent and were sutured along Neoproterozoic mobile belts (Unrug, 1997). A number of relatively recent reconstructions (see Fuller 1999 for overview) have been attempted using surface/near surface geological information and coastline geometry and marine magnetic anomalies (*e.g.* Bullard *et al.*, 1965; Lawver and Scotese, 1987; de Wit *et al.*, 1988; Windly *et al.*, 1994). Little has so far been done (*e.g.* Agrawal *et al.*, 1992; Corner *et al.*, 1993; Corner, 1994; Reeves, 1999) to incorporate continental geophysical anomaly patterns. With the availability of a huge amount of geophysical data (especially aeromagnetic coverage for the continents, Figure 1.2 and satellite altimetry gravity for the oceans, Smith and Sandwell, 1997), an attempt is made here to re-assess the reconstruction models using these datasets integrated with recent geological and geochronological data.

1.1.3. Study Area

The kinematics of the breakup of Africa – South America to form the South Atlantic Ocean is rather straightforward. The evolution of the Indian Ocean, by contrast, is complex due to involvement of larger number of fragments surrounding it. Re-assembly of central Gondwana, comprising southern and eastern Africa, Madagascar, India and Sri Lanka and parts of Antarctica (Figure 1.1) across the Indian Ocean is still controversial due to the complex movement of these fragments during dispersal (*e.g.* McKenzie and Sclator, 1971; Norton and Sclator, 1979; Reeves and de Wit,

2000). The presently available evidence from surface geology, paleontology and paleomagnetism is not sufficient to constrain backtracking of continental fragments through geological times unequivocally to their predrift positions. This is largely due to inadequacy of exposed Precambrian crust and reliable geochronological and paleomagnetic data of most of the continents involved. Thus, the regional geophysical anomaly patterns of the continental fragments are used to evaluate the nature of Precambrian crust buried under thick supracrustal cover rocks and used to achieve a tight reassembly of central Gondwana. Though large parts of the study area are covered by aeromagnetic survey (Figure 1.2), interpretation of these data has been attempted mostly at local scales. In this research, digital aeromagnetic datasets are compiled, integrated and interpreted.

1.2. Aim of Research

- Compilation and Interpretation of Aeromagnetic data from South India
- Interpretation of Aeromagnetic data from southern and eastern Africa
- Compilation of aeromagnetic interpretations (published and this work) of major central Gondwana fragments
- Integration of geological and geophysical information for precise delineation of the regional geological features and tracing them across now-dispersed Gondwana fragments.
- Producing aeromagnetic maps – 1. Total field, 2. Analytic signal and 3. Interpretation - of re-assembled central Gondwana
- Producing a tectonic database and map for reassembled central Gondwana
- Reassessing the recent published models of central Gondwana reassembly using the redefined tectonic elements

1.3. Data Sources

1.3.1. Aeromagnetic Data

The aeromagnetic data used for this research fall in two categories - 1. Published interpretation maps, and 2. Existing and new digital data. A detailed account of these

basins of India). Any feature prior to the formation of Gondwana might have developed in an entirely different geological set-up on different continental fragments.

The other question is how close the Precambrian continental crusts should lie in a re-assembly with respect to each other? Both 'tight' (*e.g.* Lawver and Scotese, 1987) and 'loose' (*e.g.* Windley *et al.*, 1994; Shackleton, 1996) reconstructions have been advocated in recent years. If we accept the relatively 'loose' reconstructions like that of Windley's (*e.g.* see Figure 2.13), we must account for the nature of the crust in the wide gaps between continental fragments. In such reconstructions, it is assumed that the gaps represent areas with little or no knowledge on the nature of crust. For example, the 'loose' fit of de Wit *et al.* (1988) is based on tracing back the existing marine magnetic anomalies; the gaps between the continents, they said, would have to rely on new continental-based knowledge. Therefore, finding evidence for a close fit of continents with gaps not more than 50-100 km (similar to the width of present day rift valleys) is attempted in this study.

b. Present Work: This thesis attempts to bring two new elements to bear on the search for devising a tight re-assembly (with 50 to 100 km gaps between Precambrian rocks of conjugate fragments) of the fragments of central Gondwana as it might have appeared at the end of the Paleozoic era:

(1). The use of geophysical mapping across the marginal zones of Gondwana's central fragments – particularly aeromagnetic anomaly mapping – to enhance the structure of Precambrian crust over large areas where much of the Precambrian geology is obscured by younger cover.

(2). The use of GIS, combined with plate rotation software, to compare re-assembled digital geological and geophysical interpretation maps of the continental fragments of Central Gondwana – and redefining these reassemblies in the light of the new constraints derived from the geophysical interpretation.

1.1.2. Reconstruction

A 'craton' has traditionally been defined as a major structural unit of earth's crust, consisting of a large stable mass of Precambrian rocks, both metamorphic and igneous, which have remained unaffected by later orogenies (Whitten & Brooks, 1982). In the light of plate tectonic concepts, a craton can be redefined as "*a [large]*

block of continental crust that has retained its geometrical and geological stability since a certain date, despite remaining mobile as a part of a single or more tectonic plate(s)". These blocks survive later deformation and other tectonic events that largely modify the nature of the crust surrounding them. The best examples of this are evident in southeastern Africa, where Archean cratons (Kaapvaal, Zimbabwe and Tanzania) have remained relatively unaffected by the later events like the Kibaran (~1000 Ma), the Pan-African (~500 Ma), the Karoo rifting and the latest East African rifting. It raises an important questions: do cratons survive later tectonic events because of some inherent physical properties that are distinctly different from the other crustal elements surrounding them or is their survival just a matter of chance? These questions are addressed in later chapters of this thesis.

Archean to Paleoproterozoic (pre 2000 Ma) cratons that suffered no deformation during Mesoproterozoic to Paleozoic times, constitute the fundamental nucleii in the Gondwana supercontinent and were sutured along Neoproterozoic mobile belts (Unrug, 1997). A number of relatively recent reconstructions (see Fuller 1999 for overview) have been attempted using surface/near surface geological information and coastline geometry and marine magnetic anomalies (*e.g.* Bullard *et al.*, 1965; Lawver and Scotese, 1987; de Wit *et al.*, 1988; Windly *et al.*, 1994). Little has so far been done (*e.g.* Agrawal *et al.*, 1992; Corner *et al.*, 1993; Corner, 1994; Reeves, 1999) to incorporate continental geophysical anomaly patterns. With the availability of a huge amount of geophysical data (especially aeromagnetic coverage for the continents, Figure 1.2 and satellite altimetry gravity for the oceans, Smith and Sandwell, 1997), an attempt is made here to re-assess the reconstruction models using these datasets integrated with recent geological and geochronological data.

1.1.3. Study Area

The kinematics of the breakup of Africa – South America to form the South Atlantic Ocean is rather straightforward. The evolution of the Indian Ocean, by contrast, is complex due to involvement of larger number of fragments surrounding it. Re-assembly of central Gondwana, comprising southern and eastern Africa, Madagascar, India and Sri Lanka and parts of Antarctica (Figure 1.1) across the Indian Ocean is still controversial due to the complex movement of these fragments during dispersal (*e.g.* McKenzie and Sclator, 1971; Norton and Sclator, 1979; Reeves and de Wit,

2000). The presently available evidence from surface geology, paleontology and paleomagnetism is not sufficient to constrain backtracking of continental fragments through geological times unequivocally to their predrift positions. This is largely due to inadequacy of exposed Precambrian crust and reliable geochronological and paleomagnetic data of most of the continents involved. Thus, the regional geophysical anomaly patterns of the continental fragments are used to evaluate the nature of Precambrian crust buried under thick supracrustal cover rocks and used to achieve a tight reassembly of central Gondwana. Though large parts of the study area are covered by aeromagnetic survey (Figure 1.2), interpretation of these data has been attempted mostly at local scales. In this research, digital aeromagnetic datasets are compiled, integrated and interpreted.

1.2. Aim of Research

- Compilation and Interpretation of Aeromagnetic data from South India
- Interpretation of Aeromagnetic data from southern and eastern Africa
- Compilation of aeromagnetic interpretations (published and this work) of major central Gondwana fragments
- Integration of geological and geophysical information for precise delineation of the regional geological features and tracing them across now-dispersed Gondwana fragments.
- Producing aeromagnetic maps – 1. Total field, 2. Analytic signal and 3. Interpretation - of re-assembled central Gondwana
- Producing a tectonic database and map for reassembled central Gondwana
- Reassessing the recent published models of central Gondwana reassembly using the redefined tectonic elements

1.3. Data Sources

1.3.1. Aeromagnetic Data

The aeromagnetic data used for this research fall in two categories - 1. Published interpretation maps, and 2. Existing and new digital data. A detailed account of these

two categories in terms of their availability, reliability, advantages of using one category over the other etc. is given in Chapter 3. Details of the digital aeromagnetic datasets for each of the fragments of central Gondwana are briefly described below and the coverage is shown in Figure 1.3.

(a) Africa and Madagascar: The AMMP (African Magnetic Mapping Project) compiled data set offers a comprehensive aeromagnetic coverage of most parts of mainland Africa and parts of Madagascar in digital format (Barritt, 1993). Almost complete aeromagnetic coverage for eastern and southern Africa, the largest continuous block of Precambrian shield, is available. Interpretations of the AMMP data for certain areas have been attempted and are available in the form of recent MSc. theses (*e.g.* Nyakaana, 1994, Mubu, 1995; Abdelaziz, 1996; and Perera, 1997; Yardimcilar, 1998). Aeromagnetic coverage for Madagascar is poor outside the sedimentary basins of its western coastal regions. However, part of the Ranotsara Shear zone, an important geotectonic feature in southern Madagascar is covered.

(b) India: No original aeromagnetic data is available in the public domain. Therefore, a digital aeromagnetic dataset of southern part of India (8°N to 14°N) was generated by compilation of data digitised in this study, Sreedhar Murthy (*pers. Comm.,* 1999) and Chandrasekhar (1997).

(c) Sri Lanka: The digital dataset for the southwestern part of Sri Lanka forms a part of the AAIME Project (Erren, 1997) which was aimed at compiling aeromagnetic data for Arabia, India and Middle East. The dataset was generated by digitising of 90 contour maps at 1:31 680 scale with 10 nT contour interval (Perera, 1997). It covers ~25% of the whole country and is the only coverage undertaken of that country to date.

(d) East Antarctica: The Russian aeromagnetic data for the western Dronning Maud Land (71°S-76°S; 30°W-2°E) was compiled under the project – Geological Evolution of western Dronning Maud Land within a Gondwana framework: Geophysics subprogram by South African Committee for Antarctic Research (SACAR) between 1990 and 1994. This data was made available in digital format by Branko Corner. The original data for Enderby Land and part of Dronning Maud Land (Golynsky *et al.* 1996) could not be obtained.

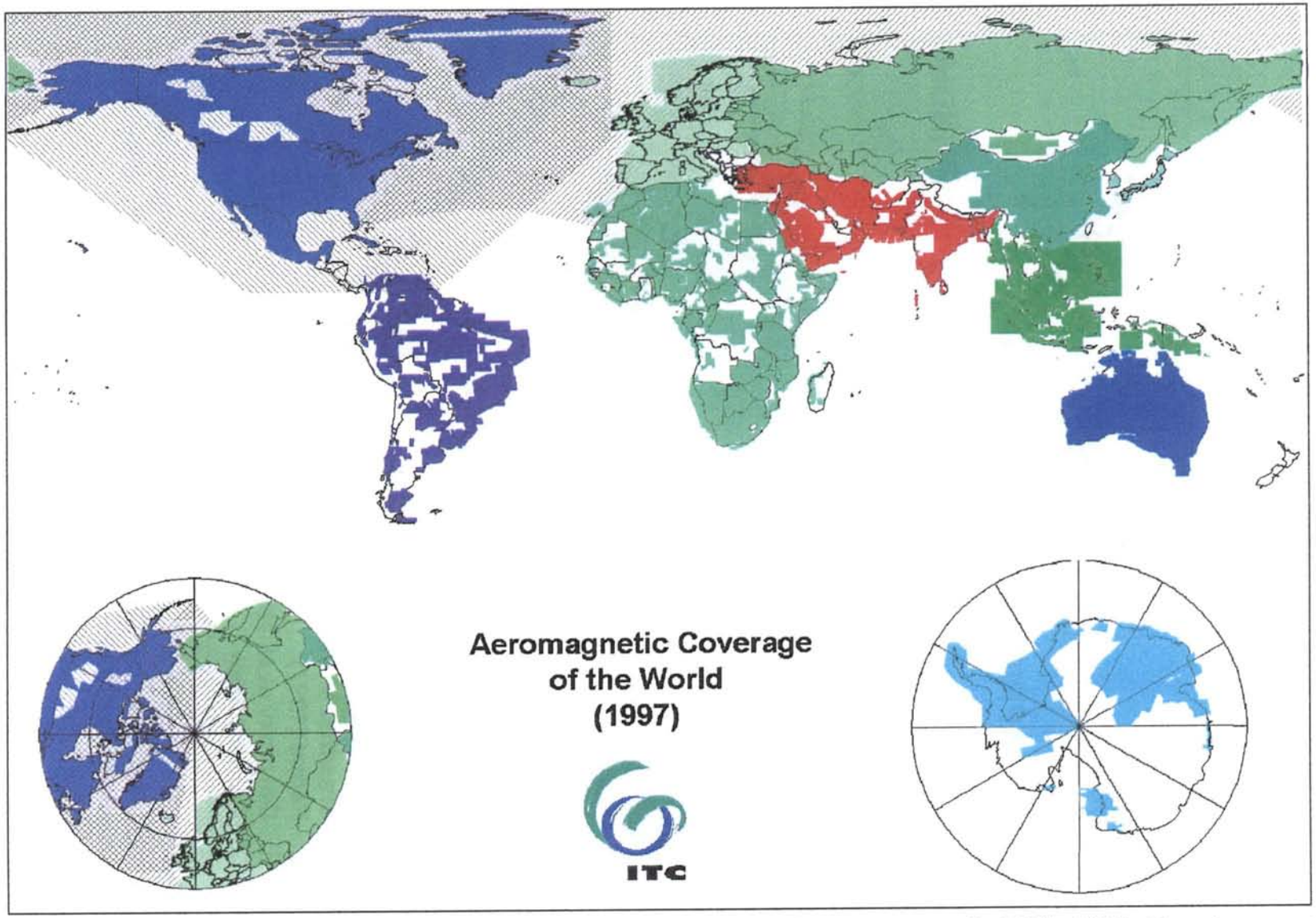

***Figure 1.2**: Map showing the aeromagnetic coverage of the world (after Reeves et al., EOS, 1998). Note the extensive coverage in India. But compilation of these datasets has so far not been done as those for Africa (African Magnetic Mapping Project), South America (South American Magnetic Mapping Project), Australia (Australian Geological Survey Organisation) etc.*

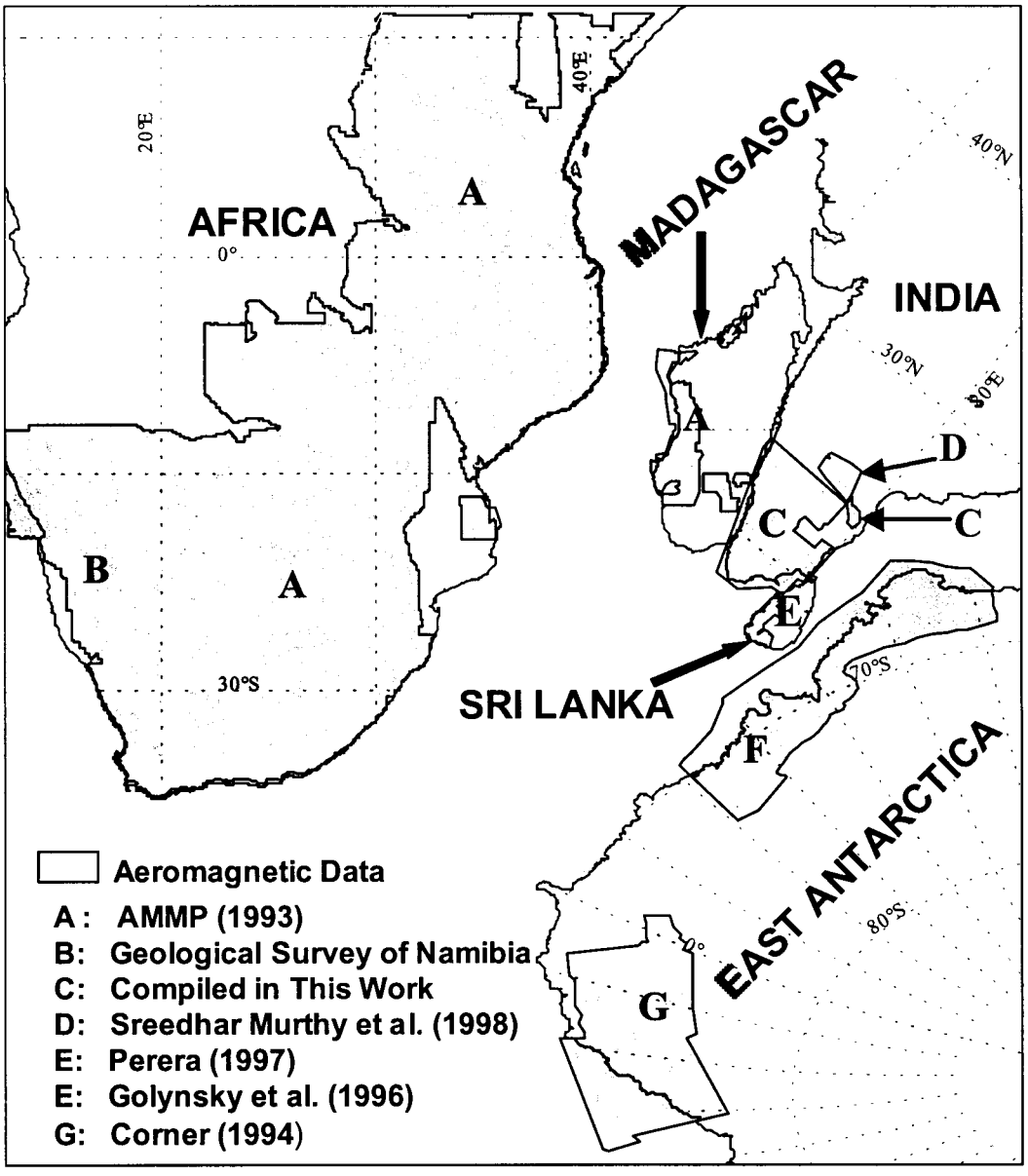

***Figure 1.3**: Aeromagnetic data coverage of the study area. The original data for Enderby Land and East Dronning Maud Land (Golynsky et al., 1996) East Antarctica could not be obtained. Reconstruction at 125 Ma, model reeve506x (Reeves, 2000, pers. com.)*

Walsh and Scotese (*http://www.scotese.com/software.htm)*; GMAP32, Torsvik and Smethurst, 1999) are available, the ATLAS software package (Atlaswin Pro, Cambridge Paleomap services Ltd., UK) was used for producing such maps. This software is capable of producing maps at any given age with a given set of rotation parameters (Euler rotation poles and angle of rotation) for the continental fragments and facilitates adding your own datasets that move along with the fragments they are attached to. The other task was to digitally compile the latest available geological and geophysical information and import them to Atlas to test the continuity of different features across the rifted continental margins at different ages. A number of geological maps and geophysical (contour and interpretation) maps have also been digitised (Table 1.1). Geophysical data for Africa (aeromagnetic), and India (aeromagnetic and gravity) and Sri Lanka (gravity) were interpreted for regional lithotectonic and structural features. Digital integration of geophysical interpretations with the geological data enabled refinement of the geological maps in many cases, especially in the areas of thick sedimentary cover (*e.g.* southern Africa). Where possible, digital datasets for other fragments have been made available for use.

Tight re-assembly of the Precambrian crustal elements has gained popularity in recent years. Thus, it is of foremost importance to precisely delineate the margins of Precambrian blocks for each of the fragments. In most of the cases the coastal tracts of continents are covered with Mesozoic and Cenozoic sedimentary rocks, obscuring the extent of Precambrian rocks. In some cases, the Precambrian continental crust might have been stretched (thinned) and therefore distorted by extension prior to Gondwana breakup. These distortions need to be restored before reassembling these fragments. Aeromagnetic surveys have proved to be useful to map Precambrian margins precisely. Digital aeromagnetic data, therefore, has been extensively used to delineate the margins of Precambrian rocks and other regional geological features like major shear zones, thrusts, faults etc.

In this research the existing geological and geophysical literature on Gondwana assembly and dispersion is reviewed and the important controversial problems are highlighted. The geology of the continents was classified into 5 broad chronostratigraphic units – 1. Archean-Mesoproterozoic (>~1400 Ma) cratons, 2. ~1000 Ma (*e.g.* Kibaran) tectonic belts, 3. Pan-African (~500 Ma) tectonic belts, 4. Karoo and Gondwana rift basins and 5. Jurassic and Cretaceous magmatism. These

units are compared between the adjacent pairs of fragments. An attempt has been made to fit closely the Precambrian fragments by establishing continuity of the later five chronosrtatigraphic units across the separated continents.

Though most parts of the study area are covered by aeromagnetic surveys, little has so far been done to interpret these data in a continental/global perspective. Identifying obscured continental scale tectonic features by interpretation of aeromagnetic data and using them for continental reconstruction should substantiate the fit achieved by geological correlation. Geophysical data for some parts of central Gondwana have been interpreted already (*e.g.* Batterham, 1983; Reeves *et al.*, 1986-87; Mubu, 1995; Perera, 1997) on local scales and are of little use in continental reconstructions unless compiled together to regional/continental scales. In this study the available geophysical interpretation (published and reliable unpublished) maps of parts of the Central Gondwana fragments have been digitally compiled. The details of the methodology are described in Chapter 3. In areas, where no credible interpretation exists, aeromagnetic data have been interpreted and incorporated into the whole compilation of aeromagnetic interpretation.

In areas where, no digital aeromagnetic data is available (*e.g.* India), hard copy contour maps were digitised to create digital data. The digital aeromagnetic datasets, thus created, were processed, imaged and interpreted. The results were appended to the already existing interpretation for the final compilation of a geophysical overlay for the whole of the study area.

The aeromagnetic images of parts of the Central Gondwana fragments are shown in a reconstructed Gondwana to visualise the continuation of major anomalies across the rifted margins. The aeromagnetic anomaly maps and the interpretation map on 1:5000 000 scale are supplied with this thesis in the back pocket as hard copies, as well as on a CD in digital format.

1.5. Software Tools

The following software packages were used for data compilation, processing, and interpretation during the research:

1.5.1. OASIS montaj

GEOSOFT (Geosoft Inc., Canada; http://www.geosoft.com) is a commercial software package available for processing and visualising geophysical data. The different programs within this package were used for processing, presentation and interpretation of geophysical data. OASIS montaj is a Windows based advanced data processing system from Geosoft Inc. designed to assist in accessing and importing data, grids, plots and images, editing, linking and visualising data, processing data and grids, analysing data, grids and maps, presenting information in maps and archiving and exporting data digitally.

1.5.2. MapInfo

MapInfo (MapInfo Professional Version 4.5, © 1985-1997 MapInfo Corporation) is a desktop mapping tool that enables the user to perform complex geographic analysis, creating thematic maps and embedding of map objects into other applications. The other important features that MapInfo offers are the importing of graphics files in a variety of formats, layout windows for preparing output, ability to change the projection of map for display and digitizing, querying capabilities, integration of different map layers and multiple views of data in three formats: Map, Browser and Graph windows.

1.5.3. Atlas

Atlas (Cambridge Paleomap Services Ltd., UK; *www://atlas.co.uk/cpsl*) is commercially available paleogeographic reconstruction tool that allows the generation of global or regional maps and reconstructions of crustal fragments at any geological time. Atlas is of special significance in the present research because of its ability to generate new models of continental reconstruction with newly generated rotation parameters for the fragments concerned. Atlas enables experimentation with various combinations of map parameters such as projection, scale, region, colour, style and grid spacing until a suitable combination is obtained.

1.5.4. TimeTrek

TimeTrek (Cambridge Paleomap Services Ltd., UK) is a supplementary system to the Atlas package and gives an animated view of the movement of continental fragments through geological time. It helps in experimenting on the position of the fragments at

different times and with different rotation parameters and enables the user to visualise the dynamic consequences of rotation parameters including cause and effect sequences of continental interactions.

1.5.5. Ilwis

The Integrated Land and Water Information System (ILWIS), a PC-based software package developed in house at ITC (www://itc.nl/ILWIS) integrates conventional GIS techniques, image processing, spatial modeling and tabular data. The availability of a wide range of facilities starting from digitizing to production of hard copy maps through data manipulation within the GIS framework makes ILWIS, when linked to Geosoft and MapInfo, a complete digital map making system. During the present research, the interpreted geological and structural maps were digitised in ILWIS to facilitate integration and comparison.

1.5.6. Reference Manager

Reference Manager (http://www.risinc.com) is a tool designed to keep track of specific references in the field of interest. It is capable of storing 30 different reference types including journals, books, conference proceedings and theses. Bibliographic retrieval is achieved by querying through one of the parameters like name of an author, keyword, periodical name, year of publication etc. It can generate bibliographies formatted in virtually any journal style appropriate for the required manuscript. This package was used for effective management of the references collected and used during the course of the research.

1.6. Thesis Layout

In Chapter 2, the existing literature and models for the assembly and breakup of Gondwana are reviewed. Gondwana reconstructions on various lines of evidence are listed and problems with such methods are highlighted.

In Chapter 3, the methodology for creation of digital geological and geophysical data databases for the study area is described in detail.

In Chapter 4, the results of the geological (lithological, structural and geochronologic) correlation between the adjacent pairs of fragments (southern Africa-Western

Dronning Maud Land, Antarctica, Enderby Land- southeastern India, India-Madagascar and Madagascar-East Africa) are evaluated.

In Chapter 5, Digital compilation of aeromagnetic data of southern India, its processing, imaging, interpretation and correlation with that of southwest Sri Lanka and Madagascar are described.

Chapter 6 deals with the methods of compilation, processing, visualisation and interpretation of aeromagnetic data for southern and eastern Africa.

In Chapter 7, the results of the geophysical correlation (geophysical anomaly patterns and interpretation) between the adjacent pairs of Gondwana fragments are discussed.

Chapter 8 describes the methods of geodata integration and a revised central Gondwana reassembly model is presented based on redefined geological and geophysical constraints. Results of comparison of this model with those published recently are discussed.

1.3.2. Gravity Data: Regional Bouguer gravity anomaly data of India digitised (Sreedhar Murthy, 1998) from the Bouguer gravity anomaly map (National Geophysical Research Institute, 1975) was used for identification of lithotectonic zones and major lineaments - in the absence of digital aeromagnetic data for the greater part of India. Bouguer gravity data for Sri Lanka was generated in this study by digitising the contour maps (1:1 000 000 scale, Hatherton *et al.* 1975).

1.3.3. Geological Data

Both hard copy maps and digital geological data were used in this study. The most recent geological maps were collected and digitised wherever necessary. The details of the data sources are given in Table 1.1.

(a) Geological Maps

- Geological map of sectors of Gondwana, de Wit *et al.* (1988)
- Geodynamic map of the Gondwana supercontinent Assembly (Unrug, 1996)
- Geological map of Antarctica, Tingey (1991), Scale 1: 10 000 000
- International Geological map of Africa (1988), CGMW/Unesco, Scale 1: 5 000 000
- Geological map of India, Geological Survey of India (1: 5 000 000, 1993 and 1:2 000 000, 1998)
- Generalised geological and Structural trend maps of southern India, Project Vasundhara, Geological Survey of India (1994), Scale 1: 2 000 000
- Geological map of Mozambique (1987), Scale 1: 1 000 000
- Geological and structural maps of Sri Lanka (1982 and 1983), Scale 1: 506 880

(b) Digital Data

- Gondwana GIS (de Wit *et al.*, 1988)
- Dyke database for southern Africa (Mubu, 1995)
- Geology of Africa, UNESCO (1985 - 1990) – Atkinson (*pers. comm.*, 1998)
- Geology of India, Geological Survey of India (1993, 1994)

- Geology of Sri Lanka, Geological Survey Department (1983)
- Geology of East Antarctica, Tingey (1991)

The sources of different data sets are summarised in Table 1.1.

***Table 1.1**: Summary of data sources*

FRAGMENTS	AEROMAGNETIC DATA SOURCE (DIGITAL)	GEOLOGICAL DATA SOURCE (DIGITAL/ANALOG)	AEROMAGNETIC INTERPRETATION
Africa	African Magnetic Mapping Project (AMMP) (Barritt, 1993)	Geological maps of Africa (CGMW/ UNESCO, 1990) – digital copy (Atkinson, 1998); Gondwana GIS (de Wit *et al.*, 1988), Van Heiningen, (1997)	This Study + Reeves (1987); Corner (1994); Mubu (1995); Yardimcilar (1998)
East Antarctica	SACAR (South African Committee for Antarctica Research) Corner, 1994	Tingey, (1991) – digitised during this study Jacobs *et al.* (1998)	Golynsky *et al.* (1996) Jokat *et al.* (1996) Corner (1994)
India	Digitised during this Study, Sreedhar Murthy (per. Comm.) and Chandrasekhar (1997)	Geological Map of India (1993) and Project Vasundara (1994) - (both digitised during this study)	This Study and Project Vasundhara (1994) Reddi *et al.* (1988)
Sri Lanka	AAIME (Erren, 1997)	Geological and Structural Maps of Sri Lanka (1983)- Digitised during this study	Perera (1997)
Madagascar	AMMP (Barritt, 1993)	Geological Map of Madagascar (Unesco, 1988) – digital copy (Atkinson, *pers. comm.*)	Yardimcilar (1998)

1.4. Research Methods

Existing reconstructed maps of Gondwana are mostly schematic in nature and often the re-assembled fragments are not shown in a single global projection. As a result the shape and size of the fragments are not always directly comparable to each other. Thus producing paleomaps of continental fragments at different ages with enhanced cartographic precision was a necessity for this research. Though a number of commercial paleomap-making software packages (*e.g.* Plate Tracker by Eldridge,

1.3.2. Gravity Data: Regional Bouguer gravity anomaly data of India digitised (Sreedhar Murthy, 1998) from the Bouguer gravity anomaly map (National Geophysical Research Institute, 1975) was used for identification of lithotectonic zones and major lineaments - in the absence of digital aeromagnetic data for the greater part of India. Bouguer gravity data for Sri Lanka was generated in this study by digitising the contour maps (1:1 000 000 scale, Hatherton *et al.* 1975).

1.3.3. Geological Data

Both hard copy maps and digital geological data were used in this study. The most recent geological maps were collected and digitised wherever necessary. The details of the data sources are given in Table 1.1.

(a) Geological Maps

- Geological map of sectors of Gondwana, de Wit *et al.* (1988)
- Geodynamic map of the Gondwana supercontinent Assembly (Unrug, 1996)
- Geological map of Antarctica, Tingey (1991), Scale 1: 10 000 000
- International Geological map of Africa (1988), CGMW/Unesco, Scale 1: 5 000 000
- Geological map of India, Geological Survey of India (1: 5 000 000, 1993 and 1:2 000 000, 1998)
- Generalised geological and Structural trend maps of southern India, Project Vasundhara, Geological Survey of India (1994), Scale 1: 2 000 000
- Geological map of Mozambique (1987), Scale 1: 1 000 000
- Geological and structural maps of Sri Lanka (1982 and 1983), Scale 1: 506 880

(b) Digital Data

- Gondwana GIS (de Wit *et al.*, 1988)
- Dyke database for southern Africa (Mubu, 1995)
- Geology of Africa, UNESCO (1985 - 1990) – Atkinson (*pers. comm.*, 1998)
- Geology of India, Geological Survey of India (1993, 1994)

- Geology of Sri Lanka, Geological Survey Department (1983)
- Geology of East Antarctica, Tingey (1991)

The sources of different data sets are summarised in Table 1.1.

***Table 1.1**: Summary of data sources*

FRAGMENTS	AEROMAGNETIC DATA SOURCE (DIGITAL)	GEOLOGICAL DATA SOURCE (DIGITAL/ANALOG)	AEROMAGNETIC INTERPRETATION
Africa	African Magnetic Mapping Project (AMMP) (Barritt, 1993)	Geological maps of Africa (CGMW/ UNESCO, 1990) – digital copy (Atkinson, 1998); Gondwana GIS (de Wit *et al.*, 1988), Van Heiningen, (1997)	This Study + Reeves (1987); Corner (1994); Mubu (1995); Yardimcilar (1998)
East Antarctica	SACAR (South African Committee for Antarctica Research) Corner, 1994	Tingey, (1991) – digitised during this study Jacobs *et al.* (1998)	Golynsky *et al.* (1996) Jokat *et al.* (1996) Corner (1994)
India	Digitised during this Study, Sreedhar Murthy (per. Comm.) and Chandrasekhar (1997)	Geological Map of India (1993) and Project Vasundara (1994) - (both digitised during this study)	This Study and Project Vasundhara (1994) Reddi *et al.* (1988)
Sri Lanka	AAIME (Erren, 1997)	Geological and Structural Maps of Sri Lanka (1983)- Digitised during this study	Perera (1997)
Madagascar	AMMP (Barritt, 1993)	Geological Map of Madagascar (Unesco, 1988) – digital copy (Atkinson, *pers. comm.*)	Yardimcilar (1998)

1.4. Research Methods

Existing reconstructed maps of Gondwana are mostly schematic in nature and often the re-assembled fragments are not shown in a single global projection. As a result the shape and size of the fragments are not always directly comparable to each other. Thus producing paleomaps of continental fragments at different ages with enhanced cartographic precision was a necessity for this research. Though a number of commercial paleomap-making software packages (*e.g.* Plate Tracker by Eldridge,

2. BACKGROUND

2.1. The Supercontinent Cycle

The concept of a cyclic order of formation of supercontinents and their breakup at least since Late Archean has been evidenced by the identification of collisional orogens and intense mountain building, episodes of glaciation and changes in the nature of life on the earth (Wilson, 1963; Bond *et al.*, 1984; Nance *et al.*, 1988; Moores, 1991; Dalziel, 1991; Unrug, 1997; Hoffman, 1999). The Wilson Cycle is the process of opening and closing of ocean basins in a cyclic order. A number of paleo-supercontinents have been described; but only the latest two or three supercontinental cycles in the last 1000 Ma are of interest in understanding the birth of Gondwana and its breakup that lead to the present day configuration of continents.

2.2. The Rodinia Concept

Piper (1975, 1982 and 1987) suggested a long-lived Rodinia (2500 –500 Ma) on the basis of paleomagnetic data. But geological evidence linking truncated Mesoproterozoic mobile belts (Bond *et al.*, 1984; Moores, 1991; Hoffman, 1991 & 1999; Dalziel, 1991; Unrug, 1996) suggests a much shorter-lived Rodinia (~1100 – 725 Ma). In these later models, the timing of formation of Rodinia is constrained by Grenville\Kibaran-aged deformation (~1100 Ma) now exposed along the margins of Laurentia, East Gondwana, Amazonia and Baltica (Dalziel, 1991). The recent reconstruction of Rodinia based on paleomagnetic studies for 1100 to 800 Ma (Weil *et al.*, 1998) resembles those proposed on geological grounds for Laurentia, East Gondwana, Baltica, São Fransisco-Congo and the Kalahari cratons. The geodynamic map of Gondwana supercontinent assembly (Unrug, 1997) provides an insight into the Neoproterozoic breakup of the Rodinia supercontinent (Figure 2.1). Breakup and reorganisation of continents initiated at ~ 725 Ma with the separation of tectonic elements later forming East Gondwana from the Pacific margin of Laurentia (Borg

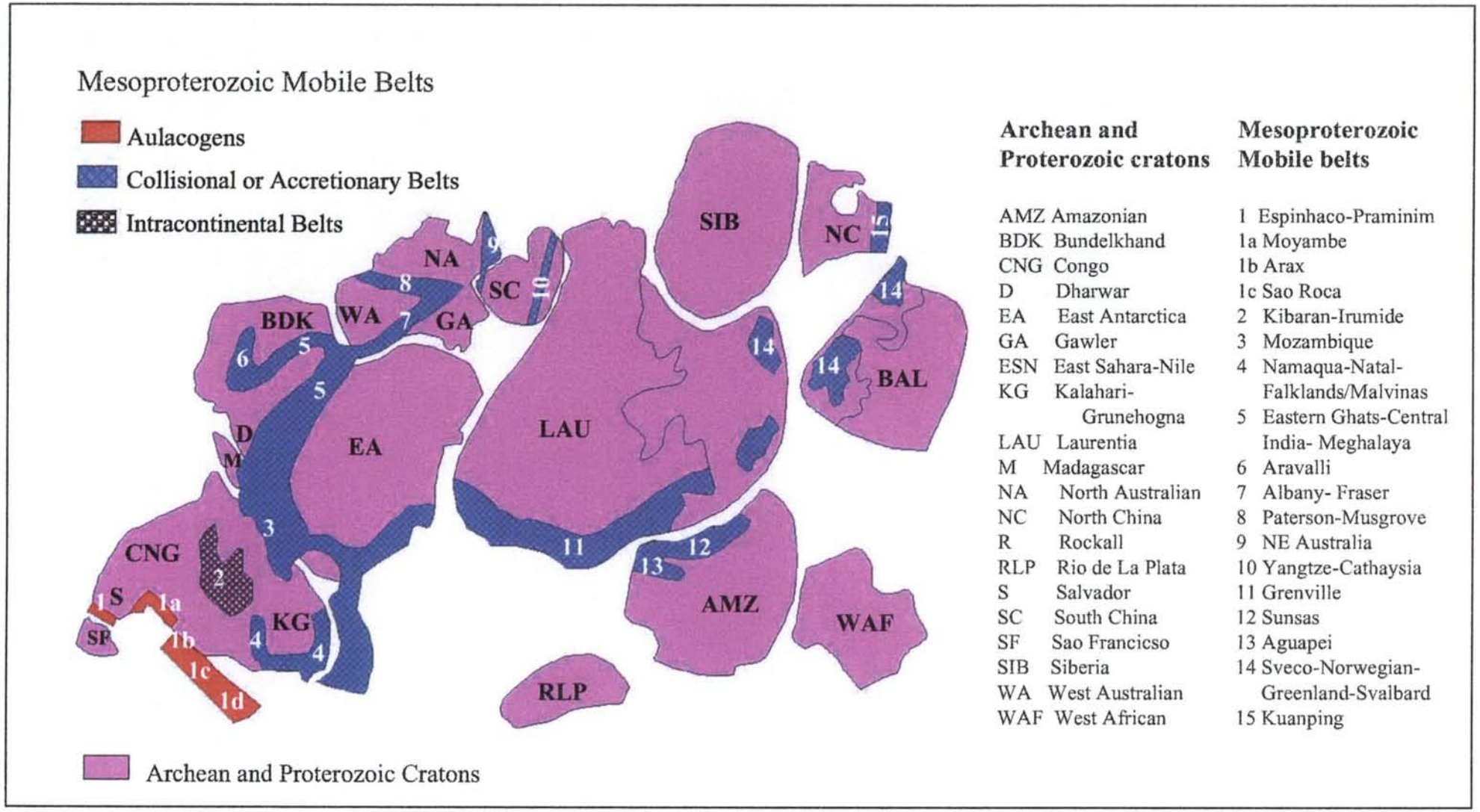

***Figure 2.1**: Possible Assembly of Rodinia Supercontinent at ~1000 Ma (after Unrug, 1996). Archean-Mesoproterozoic cratons are welded together along Mesoproterozoic (~1100 - 1000 Ma) collisional belts.*

and dePaolo, 1994; Park, 1994; Hoffman, 1999). Powell *et al.* (1993) argue that the disintegration of Rodinia started at 725 Ma with the breaking away of Laurentia from East Antarctica and Australia. However, others have suggested different modes and ages of breakup. For example, Bond *et al.* (1984) suggested a time range of 625 to 555 Ma for rifting of Laurentia from a Late Proterozoic supercontinent based on tectonic subsidence analysis.

2.3. Chronology of Gondwana Assembly and Breakup

Reorganisation of cratonic blocks following the Neoproterozoic breakup of Rodinia gave birth to Gondwana – a megacontinent consisting of five major Archean-Proterozoic cratons, welded together by Pan-African and other contemporaneous orogenic belts (*e.g.* de Wit *et al.*, 1988; Hoffman, 1998). However, the precise chronology of the formation and disruption of the Gondwana supercontinent has long been a matter of debate. Li and Powell (1993) suggest that Gondwana did not exist until the end of the Cambrian or Early Ordovician (~ 510 Ma), as the paleopoles from east and west Gondwana show significant divergence before this time. On the other hand, Radhakrishna and Mathew (1996) suggest juxtaposition and collision between the African and Indian continental nuclei along the Mozambique Belt that marked the amalgamation of East and West Gondwana in the Late Precambrian (~ 800-750 Ma) on the basis of paleomagnetic studies. Recent compilation of lithological and chronological data (Unrug, 1996) suggests that disintegration of Rodinia started at about 725 Ma. But this date is debated and still remains inconclusive.

Re-assembly of different continental fragments into a new supercontinent (Gondwana) started at ~725 and continued up to ~500 Ma (Unrug, 1997). Thus, the breakup of Rodinia and assembly of Gondwana were partly contemporaneous. Central parts of Gondwana remained united until about 200 Ma, when rifting started to turn to drifting of cratonic fragments away from each other. Central Gondwana suffered relatively less tectonic disturbance, except the development of a number of intracontinental rift basins during the period Permo- Carboniferous to Early Jurassic (Karoo basins of southern and eastern Africa, Gondwana basins of India etc.). The history of the formation of the Phanerozoic supercontinent Pangea (Bullard *et al.*, 1965) consisting of Laurentia and Gondwana is still less understood. Though the

Early Jurassic paleomagnetic poles from Gondwana and Laurentia coincide broadly, Triassic and Permian mean poles for Gondwana differ significantly from those of Laurentia (Smith and Livermore, 1991). Based on this difference in the APWPs, Smith and Livermore (1991) postulated the existence of a transform zone (translational plate boundary) between Laurussia (Laurentia + Baltica) and Gondwana prior to their amalgamation in Early Jurassic to form Pangea. Besse and Ricou (1998) suggested an alternative model for formation of Pangea based on new paleomagnetic data from Gondwana and Laurussia. A broad summary of the assembly and disruption history of Gondwana and other supercontinents is given in Figure 2.2.

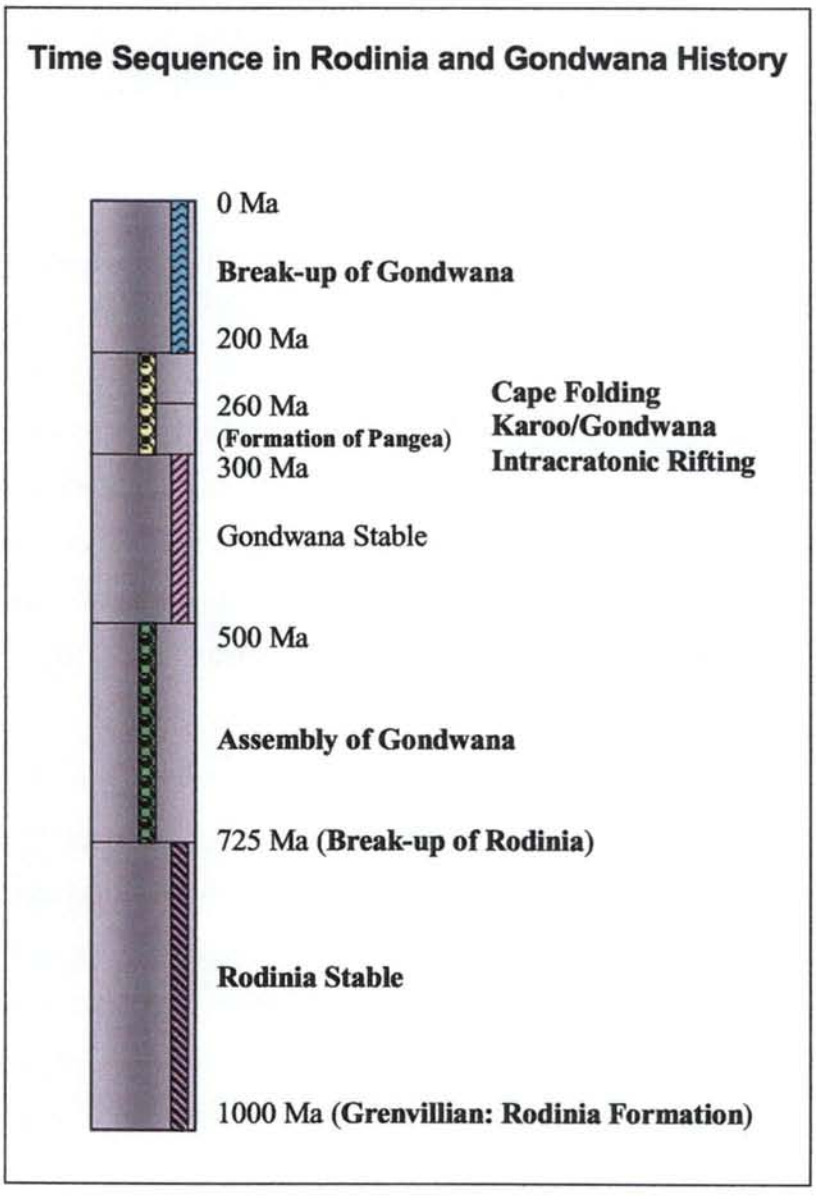

***Figure 2.2**: Summary of major events in assembly and break-up of Rodinia and Gondwana*

Breakup of the Gondwana supercontinent is recognised as a major geodynamic event in the history of the earth and has been attributed to a number of tectonic processes caused by membrane stresses, trench suction, slab pull and hot spots (Smith, 1999 and references therein). By the Early Permian, earth forces had begun to strain the continental crust and rifts developed at already existing planes of weakness, represented by deep and subvertical faults and shear zones, paleosuture zones, margins of Archean cratons etc., in response to regional extension. The Gondwana continents broke apart during a geologically short period (Triassic to Jurassic times), coinciding with intrusion of major dyke swarms and eruption of huge volumes of flood basalts. The initial separation started about 180 Ma ago (Late Jurassic) essentially as a two plate system, with spreading between West Gondwana (Africa-South America) and East Gondwana (Antarctica-India-Madagascar-Australia-New Zealand) (de Wit *et al.*, 1988; Reeves and de Wit, 2000). From the geological and palaeomagnetic evidence it is known that Central Gondwana drifted from the southern polar region to the subequatorial latitudes between mid Paleozoic and early Mesozoic time (Powel and Li, 1994, Grunow, 1999; Smith, 1999).

2.4. Collisional Tectonics and Formation of Gondwana

It is now well established that the Gondwana supercontinent was formed by collisional tectonics along Pan-African/Brassiliano (1.0 –0.5 Ga) orogenic belts (*e.g.* Hoffman, 1999). Though, traditionally, a two Gondwana – West and East – collision has been advocated by many (*e.g.* Stern, 1994; Shackleton, 1996), Gondwana can be divided into 3 separate blocks (Figure 2.3) - West Gondwana (comprising the Amazonia craton of South America and the West African craton), Central Gondwana (Congo and Kalahari cratons of Africa and Grunehogna Province of East Antarctica) and East Gondwana (Eastern Madagascar, Indian peninsula, Sri Lanka and East Antarctica Shield, Australia). The collision between West Gondwana and Central Gondwana took place along the north-south Brasilliano Mobile Belt and its northward continuation to western Africa, where it is referred to as the Trans-Saharan Mobile Belt (Figure 2.4). Similarly, paleomagnetic evidence suggests that Central and East Gondwana (India, Australia, East Antarctica with Madagascar and Sri Lanka) were

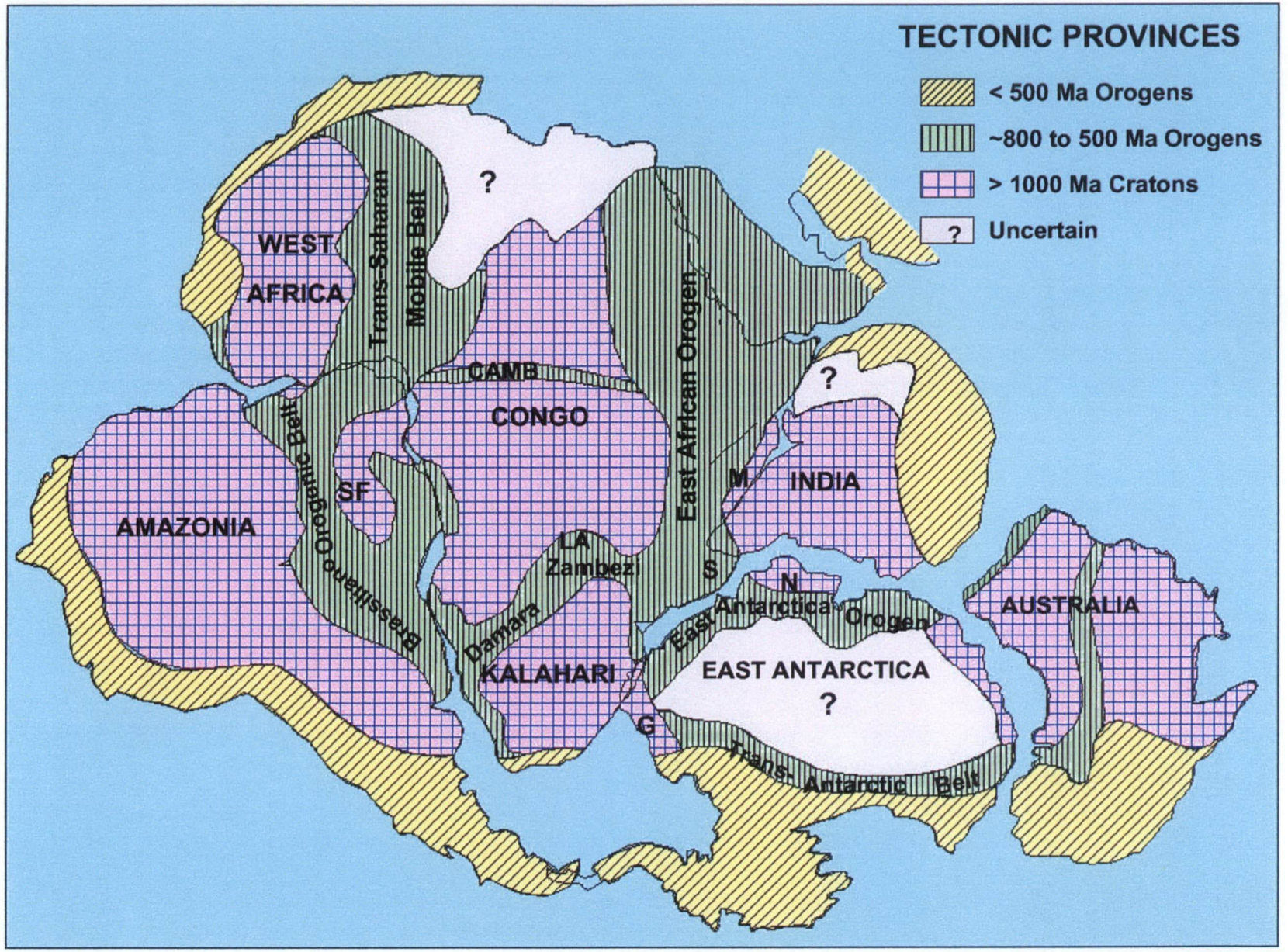

***Figure 2.3**: Gondwana supercontinent comprising at least ten pre-1000 Ma cratons welded together by Pan-African/ Brasilliano orogenic belts (modified from Hoffman, 1999). SF:Sao Francisco, G: Grunnehogna, N: Napier Complex, S: Sri Lanka, M: Madagascar, CAMB: Central African Mobile Belt, LA: Lufilian Arc. West Gondwana: Amazonia and West Africa; Central Gondwana: Kalahari, Kango and Sao Francisco; East Gondwana: East Antarctica, India, Sri Lanka, western Madagscar and Australia.*

separated by the Mozambique Ocean (Li and Powell, 1993), the closure of which led to their collision in the Late Neoproterozoic along East African Orogenic Belt (Stern, 1993 & 1994). Though the timing of these collisional episodes has been resolved reasonably well, the position and extent of the suture(s) within these broad collision belts are still uncertain. Figure 2.4 shows the locii of two possible north-south suture

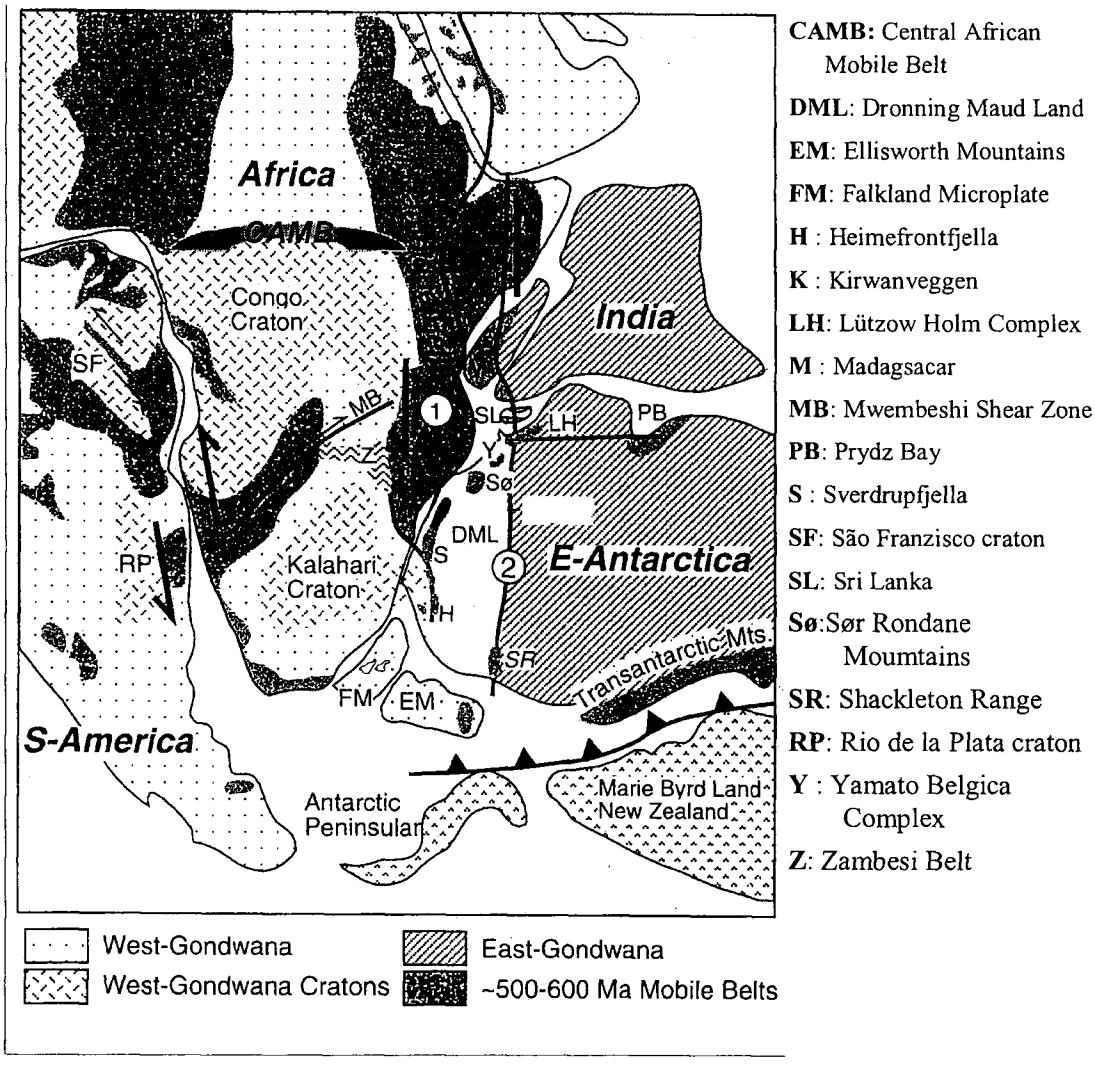

***Figure 2.4**: Positions of two possible suture zones between East and West Gondwana: 1. Shackleton, 1996, 2. Grunow et al., 1996 and Wilson, et al., 1997 (from Jacobs et al., 1998)*

zones between Central and East Antarctica: (1) based on geological and paleomagnetic evidence, Shackleton (1996) suggested a suture that extends from the ophiolite sequences in the Arabian-Nubian Orogenic Belt in Arabia (Behre, 1990

&1997) through north-central Kenya, the eastern end of the Zambezi Belt and finally to western Dronning Maud Land, and (2) based on paleomagnetic and geochronological evidence Grunow *et al.* (1996) and Wilson *et al.* (1997) argued in favour of a suture zone farther east extending northward from the Shackleton Range in East Antarctica through the Lützow Holm Complex, East Antarctica, Sri Lanka, southern India, central Madagascar up to Somalia in the Nubian Shield.

2.5. Reassembling Gondwana

Reassembling Gondwana fragments to their predrift configuration has been attempted by various workers since almost the beginning of the last century. The methods applied for such continental reconstruction are briefly reviewed in the following subsections.

2.5.1. Coastline Geometry and Continental Margins

Pioneers (Wegener, 1915 and du Toit, 1937) of the 'continental drift' theory suggested continental reconstruction models primarily based on matching of present day coastlines and lithofacies of the 'Gondwana' sequences of adjacent continents (*e.g.* Dwyka glacial deposits in Africa and South America). Though later workers have tried reconstructions based on geological and geophysical evidence (*e.g.* marine magnetic anomalies), matching of coastline geometry still remains a key aspect. But as the coastlines in most cases do not represent the true boundary between the continental and oceanic crusts, the continental margins – which might in some cases, extend well beyond the coastline - should be preferred to the coastlines in any continental reassembly. Bullard *et al.* (1965) first suggested a computer-aided tight reassembly of the continents around the Atlantic Ocean (Figure 2.5). Their fit was not made at the present coastlines, but at the line where continental shelf slopes down steeply down the sea floor (~1000m) – what they considered as the true boundary between continents and oceans. Smith and Hallam (1970) also considered 500 fathoms (~1000m) bathymetric contour as the true continent-ocean boundary and suggested a tighter fit for the Du Toit's original Gondwana. The continent-ocean boundary problem has been summarised by Smith (1999). Though the nature of ocean –continent transition is now better understood, the position of the present ocean-continent boundary is still not well known.

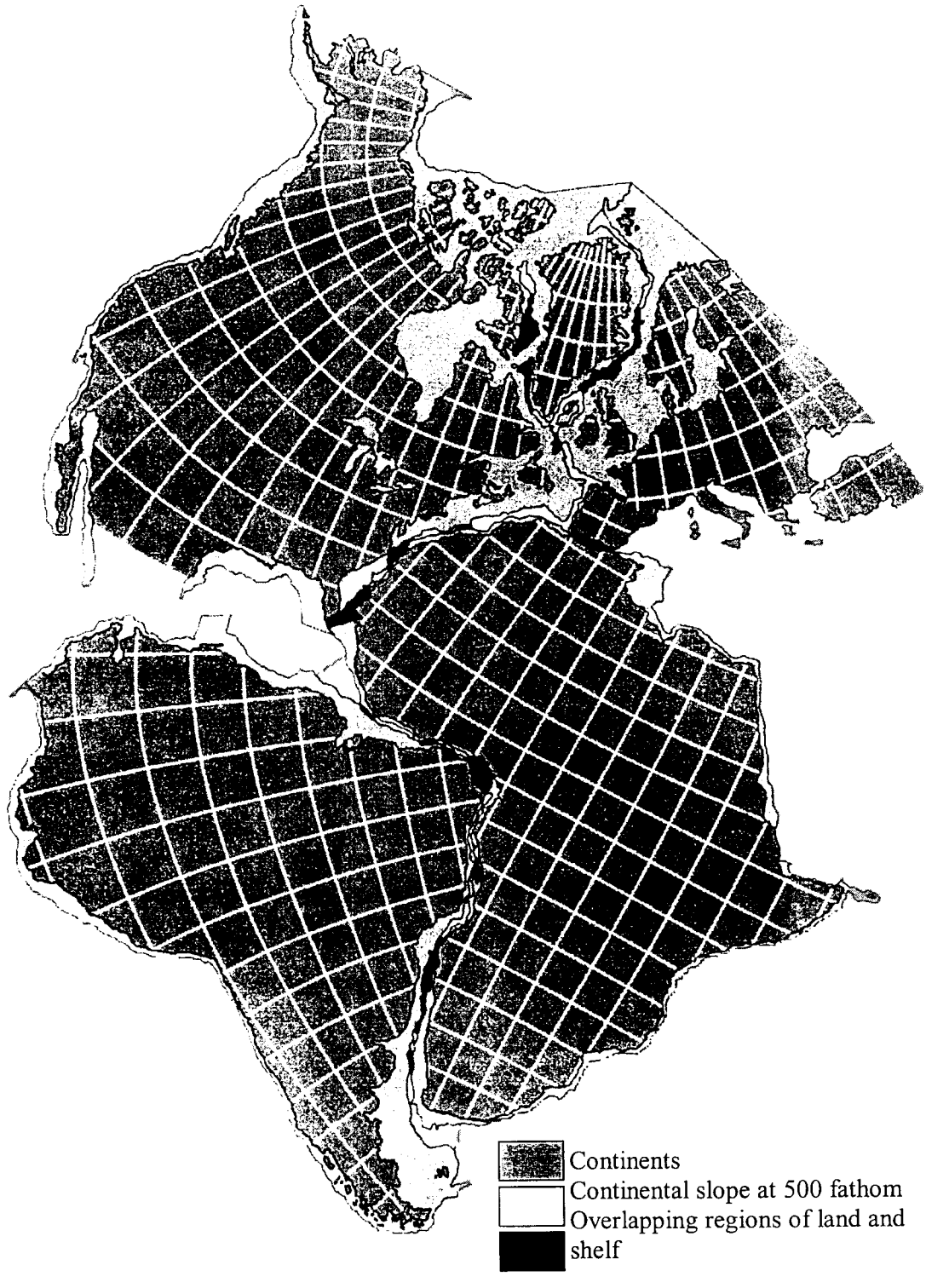

***Figure 2.5**: The first computer generated geometric fit of continents at 500 fathom (1000m) contour line by Bullard, Everett and Smith (1965).*

Reeves (1999) has addressed some problems of delineating and matching continental margins. Gravity measurements, being the direct function of lithospheric density variation, often depict a clear picture of the continental margins, which may be used for geometrical fit of continents. An example of such a fit between Antarctica and Australia is shown in Figure 2.6. Now that the high- resolution satellite altimetry derived gravity data for whole of the world's oceans (Smith and Sandwell, 1997) is available; the boundaries between continental crust and oceanic crust can be mapped rapidly with relative ease. These margins, in turn, can be used to achieve precise geometric fit of continents. However, these margins might still have been distorted (extended) during breakup and thus need to be restored to their pre-rift configuration before a final tight fit can be considered. Matching pre-rift geological features can be used to achieve this.

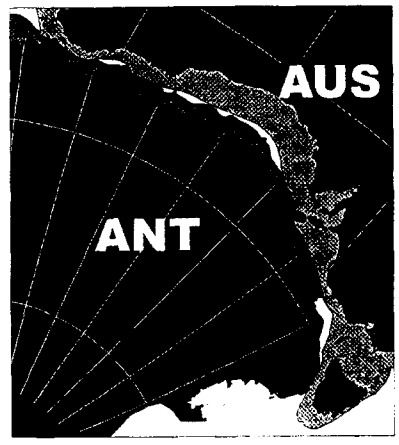

***Figure 2.6**: Antarctica-Australia fit based on gravity interpretation of continental margins (Reeves, 1999): light and dark grey shades represent extended continental crust.*

2.5.2. Matching Geological Features

Comparison of geological characteristics (*e.g.* lithology, structure, metamorphism and geochronology) between adjacent pairs of continental fragments is of prime importance in their reassembly to the predrift configuration within limits of 50 to 100 km between conjugate margins.

(a) Lithology

Correlation of the rock types of adjacent continental fragments plays an important role in continental re-assembly. The lithologies, in principle, should show a high degree of similarity across the rifted margins of the continents that were once together. For example, the granulite belts of southern India have a remarkable similarity with those in Sri Lanka (Yoshida *et al.*, 1996) and in Madagascar (Ghosh, 1999). Similarly, correlation between the Early Phanerozoic sedimentary basins - the Urfjella Group of western Dronning Maud Land, East Antarctica and parts of the Natal Group of southern Africa has been established based on their litho-assembages- quartz-arenites,

arkoses, conglomerates and siltstones (Groenewald, 1993). Unrug (1997) has compiled the geological correlation for the Gondwana fragments and has shown the continuity of different Neoproterozoic (1000 – 500 Ma) lithotectonic belts in the supercontinent Rodinia (Figure 2.1). However, geology (especially Precambrian geology) can change across the rifted margins, which often show a preference for pre-existing suture zones and/or mobile belts - *e.g.* Karoo rifts around the edge of the Zimbabwe craton. Thus, matching geology for continental reassembly should not form the sole criteria.

(b) Structure

Matching of deep-seated crustal structures (faults, rift valleys, alignment of dyke swarms and plutons) is significant in continental reconstructions. Based on matching of major vertical-dipping shear zones in the central Gondwana fragments, a number of models (*e.g.* Windley *et al.*, 1994; de Wit *et al.*, 1995 and de Wit *et al.*, 1998) have been proposed. More recently Reeves *et al.* (1999) and Sahu and Reeves (1998) have correlated the geophysically interpreted boundary between the Rayner Complex and the Napier Complex in Antarctica, the Palghat-Cauvery Shear Zone in southern India and the Ranotsara Shear Zone in Madagascar in a tight reassembly of central Gondwana. However, correlation of such crustal structures should be done with caution, particularly where the geological history of the structures is not well understood. Systematic study of each of such structures in terms of their age of development, litho-assemblages, metamorphic history, reactivation phases and kinematics of movement should be a pre-requisite before matching them with each other.

De Wit *et al.* (1998) suggested a number of pairs of 'piercing points' (Table 2.1) – defined as points where vertical/subvertical and linear geological features (*e.g.* boundary between lithotectonic units, tectonic lineaments like faults, shear zones having similar geological history) transect the continent-ocean boundary. These pairs of points on the margins of the drifted continents can be used as reference points for continental reconstruction.

***Table 2.1**: Description and Location of pairs of piercing points referred in Figure 2.15*

Points	Description	Location of Piercing Points (Lat; Long)
A	Eastern Margin of Karoo Rift in southern Madagascar	13.600; 39.480
A1	Karoo rift fault in Tanzania	-8.625; 39.334
B	Ampahiny Shear Zone in southern Madagascar	-24.869; 44.777
B1	Xixano-Chivaro Shear Zone in northern Mozambique	-8.979; 39.489
C	Vorokofortra Shear Zone in southern Madagascar	-25.237; 46.222
C1	Achankovil Shear Zone in southern India	9.454; 76.314
D	Ranotsara Shear Zone in Madagascar	-24.220; 47.372
D1	Either of the shear zones in southern India	
	i. Palghat-Cauvery	10.830; 75.907
	ii. Karur-Kambam-Painavu-Trichur	10.830; 76.150
	iii. Bhavani	11.962; 75.297
E	Lurio Thrust Front in northern Mozambique	13.344; 40.521
E1	Thrust boundary between Highland and Vijayan Complexes, Sri Lanka	6.096; 80.967

(c) Geochronology

The earliest and break-through work to test continental drift based on comparison of radiometric ages by Hurley *et al.* (1967) demonstrated the usefulness of radiometric ages in understanding the time of assembly and breakup of continents. Since then, geochronology has been used as one of the most favoured tools in continental reconstruction. Advanced techniques of isotopic age determination of rocks and minerals have enabled to provide precise ages for their crystallisation, metamorphism and deformation, which form the key to correlation of contemporaneous geological events. Unfortunately, the geochronological data for most parts of the continental fragments are inadequate and in many cases, the reliability of the existing data is questioned (*e.g.* Ghosh, 1999). A few recent models of Gondwana reconstruction constrained mainly by precise isotopic data have been proposed by de Wit *et al.*, 1998 (Figure 2.15), Ghosh, 1998 and Mezger and Cosca., 1999 (Figure 2.16) and Kröner *et al.* (2000).

2.5.3 Matching Geophysical Features

Symmetric magnetic anomaly patterns on either side of mid-oceanic ridges (magnetic isochrons) and paleomagnetism have extensively been used to understand the history of ocean development and paleopositions of continents (*e.g.* McElhinny, 1970; McKenzie and Sclator, 1971, Norton and Sclator, 1979; Besse and Courtillot, 1988, van der Voo and Meert, 1991, Grunow, 1999). But continental reassembly based on comparison of geophysical anomaly patterns over the continents and/or the features interpreted from these anomalies has rarely been attempted. Mapping crustal structures at depth or in areas of little or no outcrop (*e.g.* most parts of Australia, Botswana) has successfully been achieved with geophysical surveys (especially airborne geophysical methods – aeromagnetic and radiometric). Delineation and comparison of crustal structures derived from geophysical anomalies and comparison of anomaly patterns between adjacent continental fragments should provide additional constraints for their re-assembly.

(a) Reconstruction based on MAGSAT data

Von Frese *et al.* (1987) attempted the first ever-continental reconstruction (Figure 2.7) on the basis of satellite magnetic anomaly patterns (MAGSAT) on a global scale. Striking correlation of satellite magnetic anomalies has been observed along the rifted margins between South America and Africa and Australia and Antarctica. On the other hand, the correlation is very poor for the Africa-Madagascar-India-Antarctica fit (Figure 2.7) in a Late Neoproterozoic (560 Ma) reconstruction model (Smith *et al.*, 1981). This mismatch of anomalies across rifted margins may be attributed either to the post-rift modification of the magnetic characteristics of the crust or problems in the continental reassembly itself. For example, the strong negative anomaly in Cameroon, West Africa might be due to post-breakup sources. Therefore, any such mismatch should be analysed critically with respect to the geological characteristics, especially age, of the causative sources of these anomalies. In a India-Madagascar-East Africa reassembly (Agrawal *et al.*, 1992), MAGSAT anomalies show one to one correlation between India and Madagascar, whereas a prominent mismatch in anomaly pattern is evident from a large magnetic positive in Madagascar (1 in Figure 2.8) which does not match to a well-defined negative anomaly along East African margin (2 in Figure 2.8). A similar fit between the east coast of India and Enderby

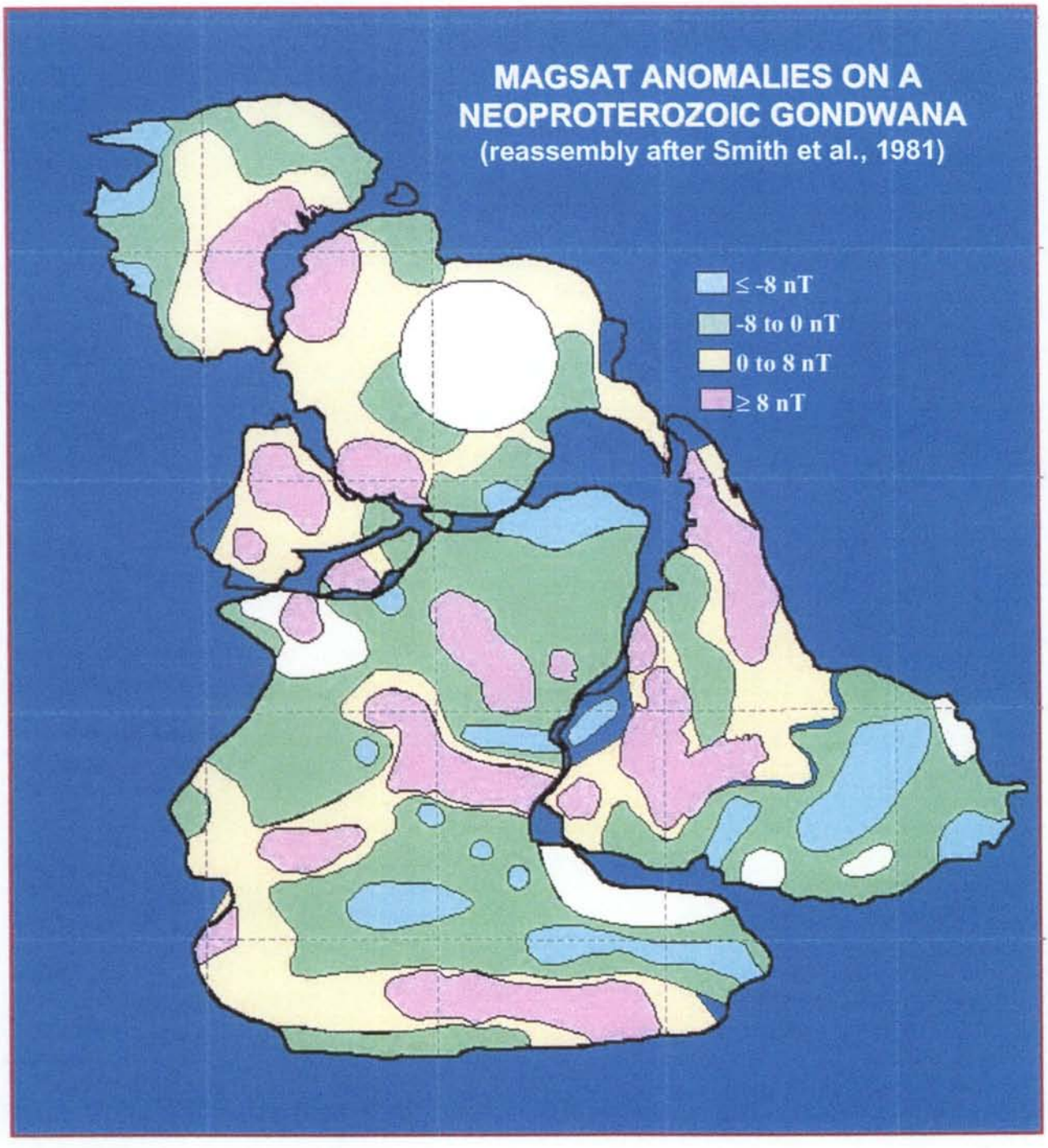

***Figure 2.7**: Schematic presentation of MAGSAT anomaly patterns in a reassembled Gondwanaland (modified from von Frese et al., 1987) - Note strong correlation of anomalies between central Africa and South America and Antarctica and Australia*

Land, East Antarctica has also been suggested by Mishra (1984) based on comparison of MAGSAT anomaly patterns However, the resolution of MAGSAT data is far from satisfactory for a tight fit of continents (50 to 100 km) for comparison of anomaly patterns across the rifted margins.

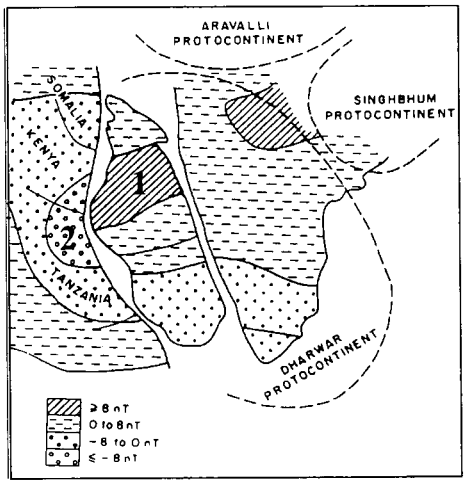

***Figure 2.8**: MAGSAT anomalies across South India, Madagascar and East Africa (after Agrwal et al., 1992)*

(b) Aeromagnetics and Continental Reconstruction

Reconstruction of conjugate continental fragments based on aeromagnetic anomaly patterns also has been attempted by a number of workers. Strangway and Vogt (1970) have shown similarity in the nature of banded magnetic features across the rifted margins of parts of West Africa and northeastern South America. Correlation of long strike-length magnetic anomalies of southern Africa, the Falkland plateau and Dronning Maud Land (East Antarctica) suggests that the Beattie anomaly of southern South Africa continues eastward to Dronning Maud Land in East Antarctica through the Falkland plateau (Corner *et al.*, 1991 & 1994). Aeromagnetic comparison between southwestern Sri Lanka and northern Mozambique (Perera, 1997) casts doubt on the idea of the Highland Complex of Sri Lanka being the eastern counterpart of the Lurio Shear Belt of Mozambique. Reeves *et al.* (1986/87) suggested a closer proximity of Madagascar to the East African coast than indicated in many reconstructions constrained by mostly geological evidence. A similar close-fit between Madagascar and East Africa has been suggested based on the correlation of geological features like major lineaments and plutons interpreted from aeromagnetic data (Yardimcilar, 1998).

(c) Reconstruction based on satellite altimetry-derived gravity data

A dynamic model for reconstruction of the continental fragments across the Indian Ocean based on retracing the ocean floor features (active and fossil transforms) interpreted from the satellite altimetry-derived gravity data (Smith and Sandwell, 1997) has been suggested by Reeves and de Wit (2000, 2000). Creation of the whole Indian Ocean has been described in four distinct phases or regimes between the period

168 and 0 Ma (Figure 2.9). This model seems to satisfy the continental plate movements in reverse time by keeping the transform termini coincident and colinear.

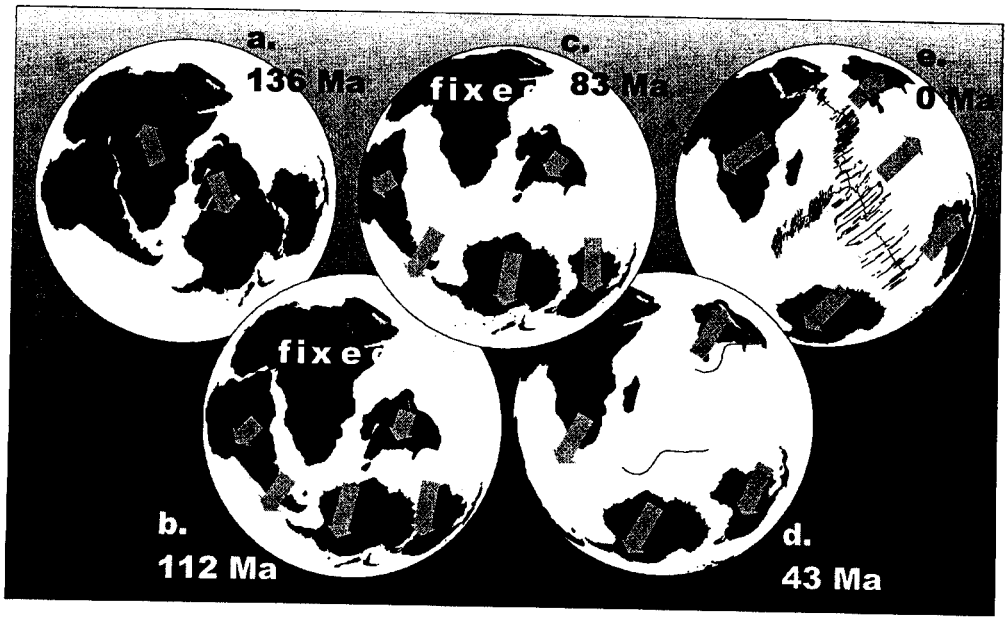

***Figure 2.9**: Four regimes of Gondwana disruption based on retracing the transforms of the Indian Ocean (from Reeves and de Wit, 1998)*

(d) Gravity Anomalies and Continental Reconstruction

Though gravity anomalies are suitable for identification of deep crustal structures that could be used as markers for continental reassembly, comparison of gravity anomaly patterns across the rifted margins is not much of use as it is difficult to separate the gravity effects of the tilted margins from those attributable to the crustal geology. The first step towards a gravity map of Gondwana has been taken by Doucouré *et al.* (1998 & 2000). However, earlier workers have attempted continental reconstruction based on gravity in parts of Gondwana. For example, Agrawal *et al.* (1992) correlated Bouguer gravity anomaly

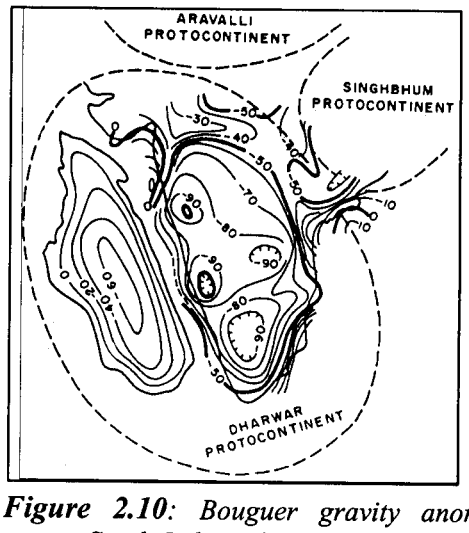

***Figure 2.10**: Bouguer gravity anomaly across South Indian shield and Madagascar (from Agrawal et al., 1992)*

patterns between South Indian Shield and Madagascar (Figure 2.10). They have shown that steep gravity gradients exist across rifted margins- west coast of India and east coast of Madagascar. Similarly, Corner *et al.* also used gravity data in support of the extension of the Kaapvaal craton into Dronning Maud Land.

2.6. Important models of Gondwana reconstruction: a review

Geoscientists from various disciplines have suggested a number of reconstruction models for central Gondwana.

2.6.1. Lawver and Scotese (1987)

A tight reconstruction of central Gondwana (Figure 2.11) was suggested by Lawver and Scotese (1987) using – (1) marine magnetic anomalies in the Somali basin, in the Mozambique basin and off the coast of East Antarctica, (2) lineaments in Madagascar and India and (3) juxtaposition of charnockite localities in southern India and Enderby Land, East Antarctica. The fit between Madagascar and East Africa was achieved by

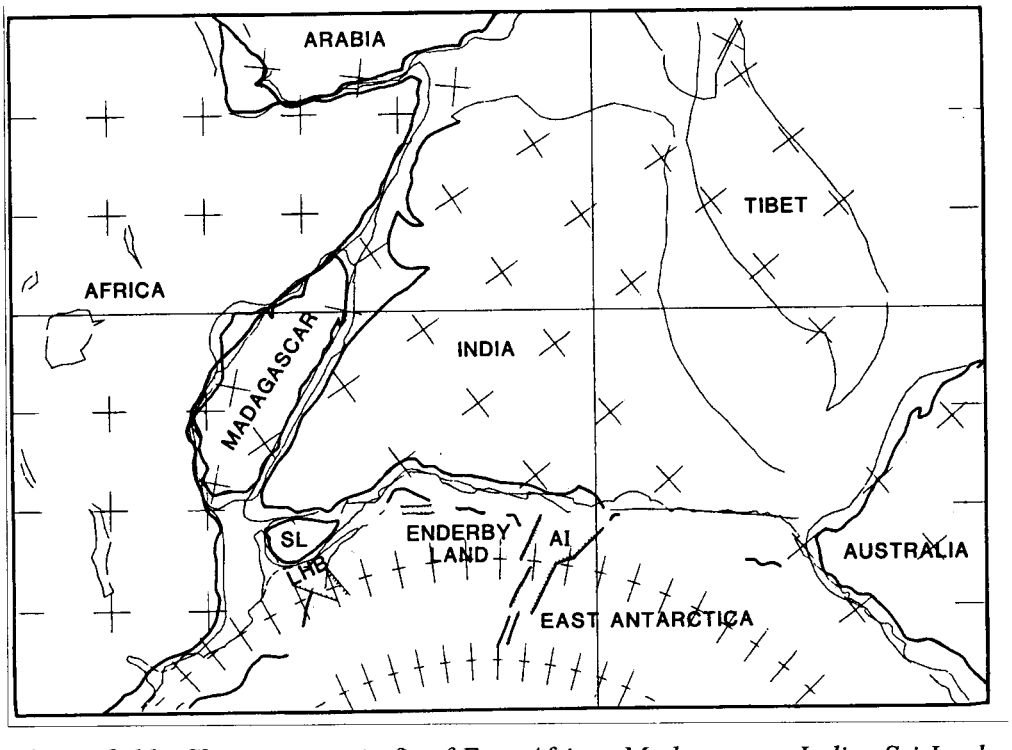

***Figure 2.11**: Close geometric fit of East Africa- Madagascar- India- Sri Lanka- East Antarctica (after Lawver and Scotese, 1987). Africa is held fixed in its present-day position. SL: Sri Lanka, LHB: Lützow-Holm Bay, AI: Amery Ice Shelf.*

the constraints from magnetic anomalies in the Somali basin, whereas India-Sri Lanka- East Antarctica fit is constrained by the matching occurrences of charnockites. Though this model provides a close geometric fit of these fragments, the question remains whether simple occurrence of charnockites in India, Sri Lanka and Enderby Land should constrain their fit without reliable age data from these charnockites. Since then, a large number of isotopic data from these terrains have been obtained and used in later reconstructions. Matching of marine magnetic anomalies certainly does not constrain such tight fit, as the oldest anomalies are located far off the present coastlines. Thus it seems that the fit has been achieved by matching the 500-fathom bathymetric contour.

2.6.2. Pinna *et al.* (1995)

The proposed model for central Gondwana reconstruction (Figure 2.12) by Pinna *et al.* (1995) is primarily based on their exhaustive study of the geology of the Mozambique Belt in northern Mozambique and its correlation with similar geological settings in the adjacent fragments. In this model, the Mozambique Belt is considered as the collision zone between two major continental areas: the Archean Indo-Antarctic block including eastern Somalia and Madagascar, and the central African block. Sri Lanka is juxtaposed to northern Mozambique based on the similarity in litho-assemblages and tectonothermal history, consistent with the models proposed by de Wit *et al.* (1988) and Kröner *et al.* (1991). The Highland Complex of Sri Lanka (Figure 2.12) is correlated to the Lurio Supergroup of northern Mozambique, whereas the Wanni and Vijayan Complexes (Figure 2.12) are considered as the equivalents of the Chiure Supergroup (Figure 2.12). However, comparison of aeromagnetic interpretation in both the areas (Perera, 1997) reveals the absence of any counterpart of the Lurio Shear Zone in Sri Lanka, which leads to the conclusion that the Lurio tectonic belt might pass either north or south of Sri Lanka or else the eastward extension of it is terminated against some pre-existing structure between northern Mozambique and Sri Lanka. Pinna *et al.* (1993) correlate the boundary between the East Antarctic craton and the remobilised Archean-Proterozoic rocks of the Sør Rondane Mountains with the Achankovil Shear Zone of southern India. However, later models (*e.g.* Sahu and Reeves, 1998) using aeromagnetic interpretations suggest a correlation between the Palghat-Cauvery Shear zone in southern India (Geological

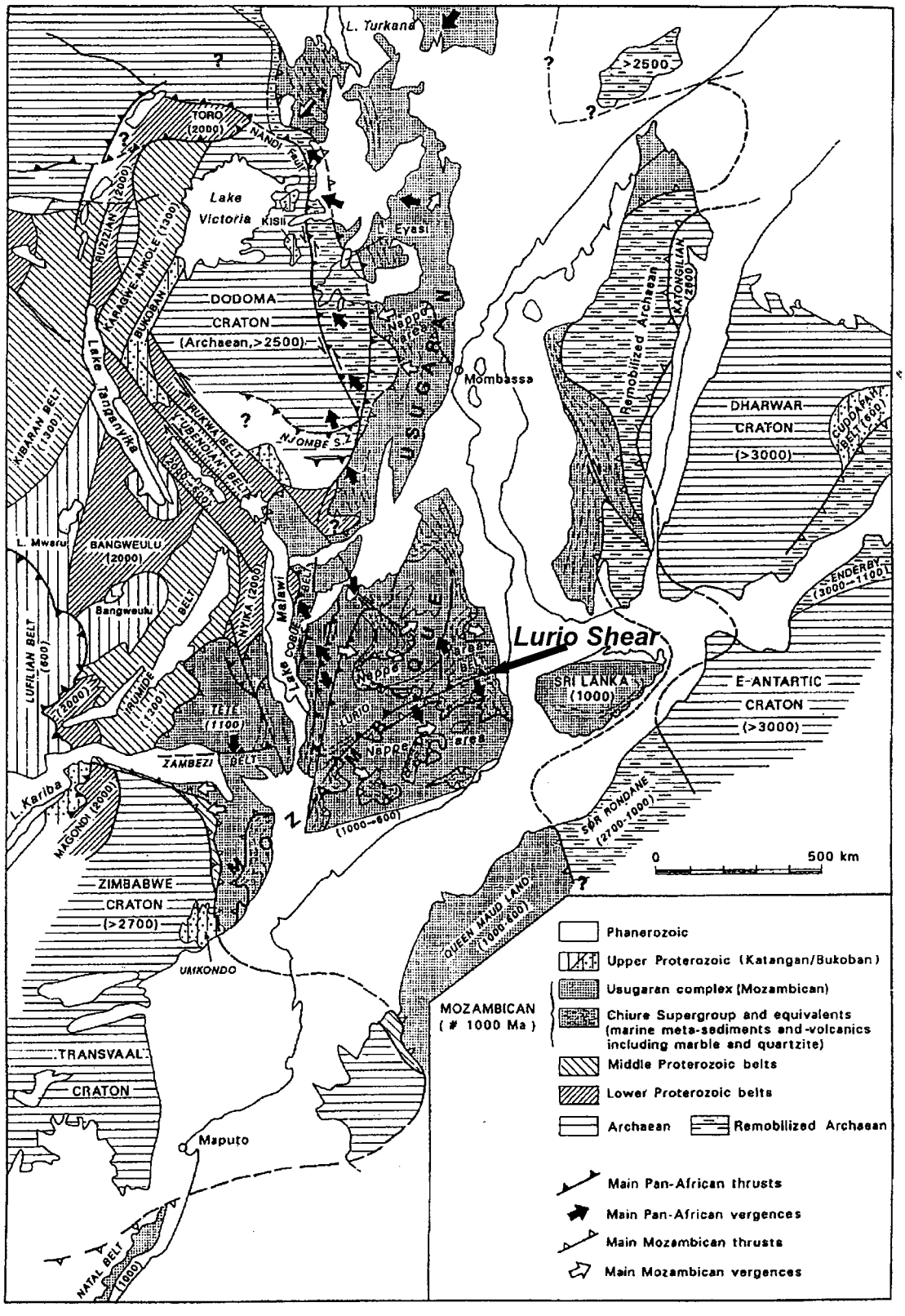

***Figure 2.12**: Central Gondwana reconstruction on the basis of geological similarities (from Pinna et al., 1995). Note the Lurio Shear Zone does not show continuity in Sri Lanka; in stead, the linear eastward extrapolation of this shear passes through the gap between India and Sri Lanka in this reassembly.*

Survey of India, 1994) and that of the boundary between the Rayner Complex and the Napier Complex, East Antarctica (Golynsky *et al.*, 1996).

2.6.3 Windley *et al.* (1994)

A model for central Gondwana reconstruction (Figure 2.13) has been presented by Windley *et al.* (1994) summarising the correlation of Precambrian structural elements and metamorphism of eastern Africa, Madagascar, southern India and Sri Lanka suggested by earlier workers. In their model the Ranotsara Shear Zone of south-

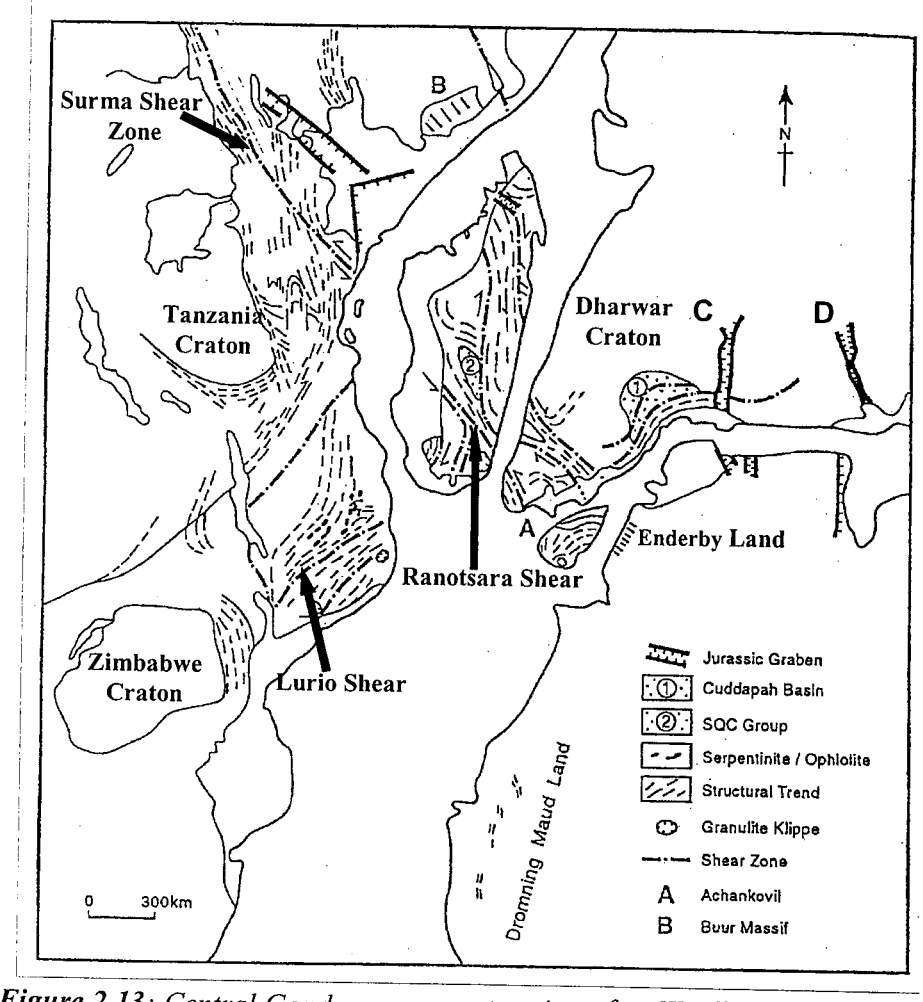

***Figure 2.13**: Central Gondwana reconstruction after Windley et al. 1993): **A**: Achankovil Shear, **B**: Buur Massif, **C**: Godavari graben, **D**: Mahanadi graben. The position of Madagascar is shown well south of most other models (e.g. Reeves, 1986/87; Yardimcilar and Reeves, 1998)*

central Madagascar is correlated with the Achankovil Shear Zone of South India in the east and either the Surma Shear Zone (Bonavia *et al.*, 1992) or the parallel Ashwa

Shear zone (Chorowicz *et al.*, 1987) of East Africa in the west due to their common characteristics of sinistral movement and orientation. Their other argument for the correlation of the Achankovil Shear Zone (ASZ) with the Ranotsara Shear Zone (RSZ) is the presence of granulite facies metamorphism of Pan-African age (Choudhary *et al.*, 1992; Paquette *et al.*, 1994) in the regions immediately south of both the shear zones. But this has been contested by Ghosh (1999), who reported occurrences of Pan-African granulites from both north and south of the ASZ. Ghosh prefers the Karur-Kambam-Painvu-Trichur (KKPT) shear zone, a newly derived shear zone, as counterpart of the RSZ in India (Figure 2.14). In the India-Sri Lanka fit (Kriegsman, 1993), the Achankovil Shear Zone passes just south of Sri Lanka. Similarly a hypothetical 100-150 km wide right-lateral axial high grade shear zone of Madagascar is correlated with the Burr massif of southern Somalia in the west and with the right-lateral high-grade Palghat-Cauvery Shear Zone across southern India (Drury *et al.*, 1984) based on geological similarities- (1) enclaves of granulite facies belts of Archean age, (2) presence of folded stratiform ultrabasic-basic complexes in the Palghat-Cauvery Shear zone and the Archean craton to the north in India (Weaver, 1990) and the Androna–Beforona belt in Madagascar.

2.6.4. De Wit *et al.* (2000)

The recent model of central Gondwana reconstruction (Figure 2.15) by de Wit *et al.* (1998; 2000) is based on matching of Neoproterozoic shear zones that are well-constrained by geochronological data. The Neoproterozoic shear zones in the southern parts of Madagascar and India cut host rocks with ages between 800 and 2600 Ma, formed under similar high-grade metamorphic conditions and which have a similar polyphase metamorphic history. The age of early shear deformations of the host rocks in Madagascar occurred between 650 to 627 Ma. Latter episodes occurred around 600-610 Ma and continued up to 500 Ma. The north-south shear zones (Vorokafortra Shear Zone) formed between 610-608 Ma have a similar thermal history to the Achankovil Shear Zone of southern India that dates between 610-570 Ma. The left-lateral Ranotsara Shear Zone developed between 520-550 Ma is correlated with any of the three major shears zones (KKPT, Bhavani, PCSZ; Figure 2.15).

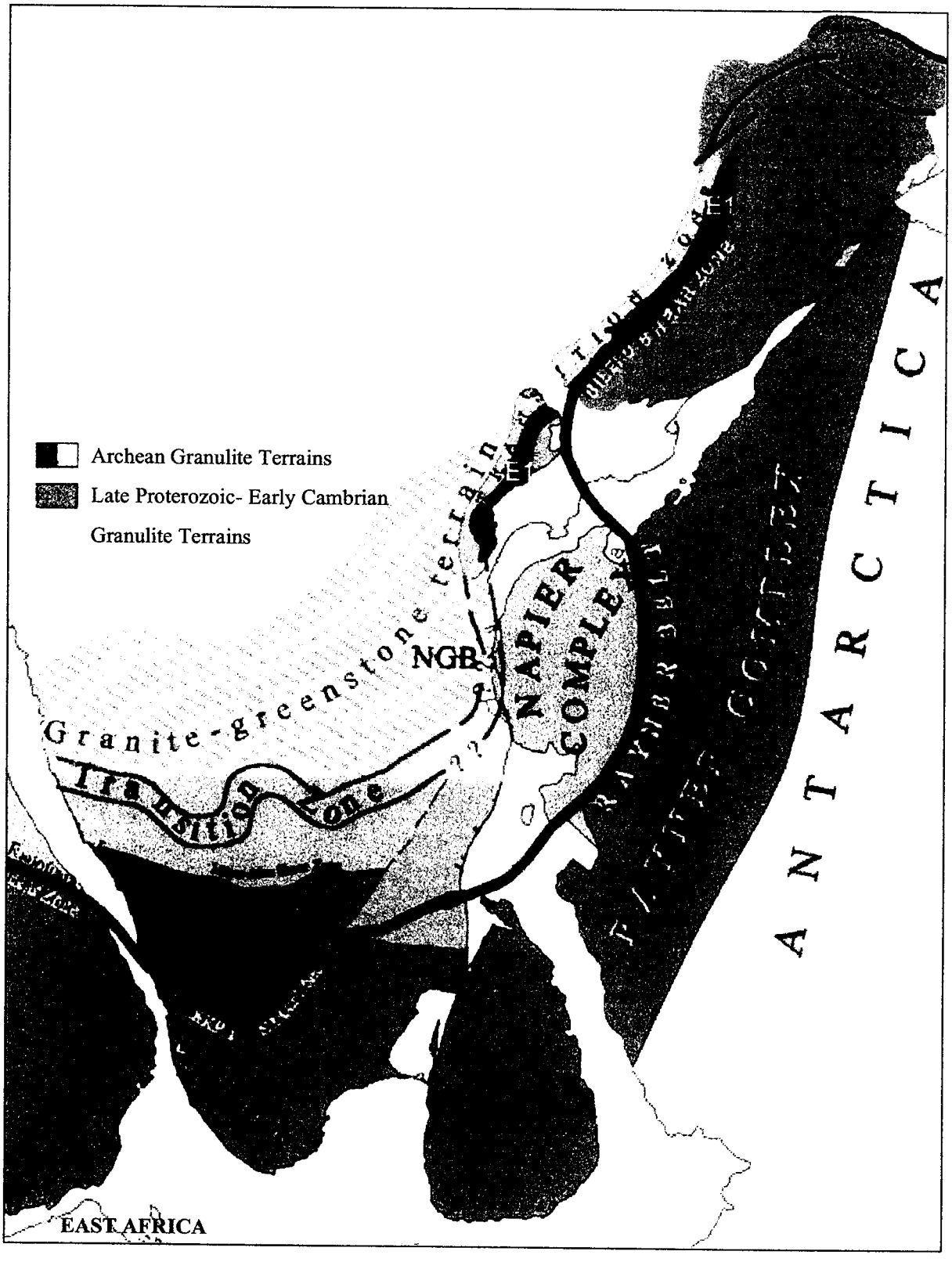

***Figure 2.14**: Relative positions of Madagascar, East Antarctica and Sri Lanka with respect to India in Gondwana (from Ghosh, 1999).The newly defined KKPT Shear Zone in southern India is correlated with the boundary between Napier and Rayner Complexes in the east and with the Ranotsara shear zone in Madagascar.*

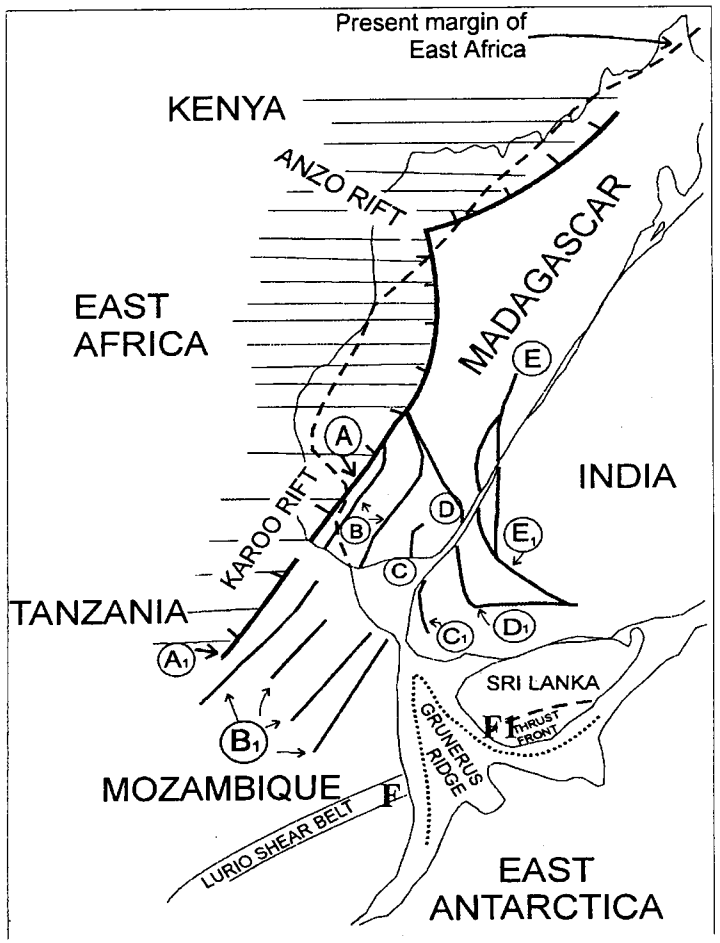

Location	Geological Features	Description	AGE (Ma)
A Madagascar	Eastern margins of	subvertical normal	350-250
A1 Tanzania	Karoo Rift	faults	350-250
B Madagascar	Ampahiny/Vorokafortra	subvertical ductile shear	630-605
B1 Mozambique	Xixano-Chivaro	Ductile Lineaments	~600
C Madagascar	Tranomaro	subvertical ductile	>560
C1 India	Achankovil	shear zones	610-570
D Madagascar	Ranotsara	subvertical ductile-	550-530
D1 India	KKPT	brittle shear zones	570-560
E Madagascar	Ifondiana	subvertical ductile-	>550
E1 India	PCSZ/Moyar	brittle shear zones	722 - 600

KKPT : Karur-Kambam-Painavu-Trichur Shear Zone (Ghosh et al.,1999)

PCSZ : Palghat-Cauvery Shear Zone

Figure 2.15 :Reconstructed central Gondwana based on the position of geochronologically constrained shear zones (after de Wit et al., 2000). For details of the dating in individual shear zones/lineaments, see references in de Wit et al. (2000).

2.6.5. Mezger and Cosca (1999)

The recent reconstruction of India-Sri Lanka-Antarctica (Mezger and Cosca, 1999) is primarily based on the new mineral ages of the Eastern Ghats Belt of eastern India and its correlation with the adjacent fragments (Figure 2.16). From the geochronological data it is evident that the central and eastern parts of the Eastern Ghats Belt have a thermal history similar to that of the Rayner Complex, East Antarctica with a major granulite facies metamorphism at ~1000 Ma and a later overprint during Pan-African times. This Pan-African orogenic activity is the major tectonothermal event in Sri Lanka (Hölzl *et al.*, 1994) and the Lützow-Holm complex of Antarctica (Shirashi *et al.*, 1994). In another recent reconstruction (*e.g.* Unrug, 1996), the high-grade terrains of Sri Lanka and southern India are correlated with the Lützow-Holm and the Rayner Complexes of East Antarctica. In this reconstruction the Napier Complex and the Rayner Complex are juxtaposed with the southern and northern parts of the Eastern Ghats Belt respectively. The Napier Complex is considered as an exotic terrane without any correlative segment in the Eastern Ghats belt of India. This analysis is based on - (1) absence of high-grade and ultra high temperature metamorphism, (2) lack of discernible Pan-African overprint and (3) presence of exclusively Archean material as indicated by Nd-model ages (Black and McCulloch, 1987) – in the Napier Complex. Ghosh (1999) correlates his KKPT (Figure 2.14) with the boundary between the Rayner and Napier Complex in the east and with the RSZ in the west (Figure 2.14)

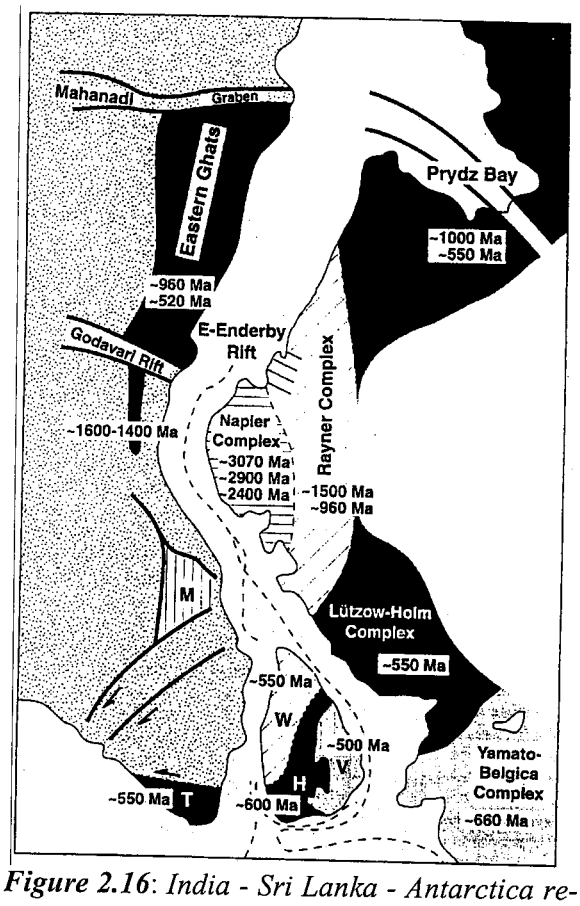

***Figure 2.16**: India - Sri Lanka - Antarctica re-assembly with ages of major Metamorphic episodes (from Mezger & Cosca, 1999); T: Trivandram Complex, M: Madras Granulite V: Vijayan Complex, H: Highland Complex, W: Wanni Complex.*

based on geochronological evidence separating Archean granulites from those of Neoproterozoic-Early Cambrian age.

2.7. Discussion

Most of the above-described models of Gondwana reassembly are non-unique and often based on correlation of Precambrian geology with uncertain or imprecise dating. In order to test the geometric fit of continents, paleomaps with high cartographic precision (50-100 km) with a global projection must be a pre-requisite. Once equipped with the capability of high precision paleomap-making, the question arises what – coast line, 200m bathymetric contour, 1000m bathymetric contour, margins of Precambrian continental crust - should we match? Matching the Precambrian continental crust probably answers the above ambiguity, as they represent the true continental nuclei, which moved as the whole or parts of tectonic plates prior to the formation of Gondwana. The other question is how close should the conjugate margins lie in a prebreak-up configuration. This requires attention to the pre-drift rifting history of an unknown width of crust/lithosphere that is now present only in an extended or attenuated form. This problem is addressed in Chapter 8. It is only through correlation of geological features ranging in age from ~700 Ma to ~ 200 Ma – the period during which Gondwana was in existence – rather than comparing the whole Precambrian geological history of the continents - that reliable fits may be achieved. Mismatch of Precambrian geology across rifted continents, however, may mean little if the continents were rifted apart along a pre-existing suture.

3. CONTINENTAL SCALE GEOPHYSICAL AND GEOLOGICAL DATA COMPILATION

3.1. Introduction

Vast quantities of geophysical and geological data are underutilised for correlation among continental fragments of erstwhile Gondwana primarily due to incompatibility and inaccessibility of various datasets. The datasets are often presented as hard copy paper maps at different scales and projections. Thus, it is hard to directly correlate this information from one fragment to another in continental reassembly. It is, therefore, necessary to convert these datasets into digital format for effective manipulation – e g. changing of projections and scales, adding new data, revising/editing the existing information. Geophysical interpretations, especially aeromagnetic and gravity, for several areas exist only at local scales and in isolation. These datasets need to be digitally compiled on regional/continental scales for effective use in correlation among continents in reassembly. In this study, several geological (Table 3.1) and geophysical (Table 3.2) maps were digitised, suitably modified and interpreted, where necessary. The digital databases were then stored in *ATLAS* format (refer to Appendix V for an example of the file type), which could readily be used for preparing maps for any geological age, testing different reconstruction models and developing a working model for Gondwana. This database could be modified in future with new data input. The database is supplied on a CD-ROM in the back pocket of this thesis.

This chapter deals with the collection of different datasets and methods of digital compilation. Interpretation results are described in following chapters.

3.2. Geophysical Data

Geophysical data (aeromagnetic and gravity) used for this research falls in two broad categories – (1) Hard copy maps: Interpretation maps and Contour maps, and (2) Digital data.

3.2.1. Hard-copy Maps

Hard copy paper maps were used to create digital geophysical datasets for the areas, where no original data was available.

a. Interpretation Maps

A number of published and unpublished aeromagnetic and gravity interpretation maps (Table 3.1) were used for creating a digital database and continental-scale compilation. Aeromagnetic interpretation maps for East Antarctica were obtained from Corner, 1994 (Western Dronning Maud Land), Jokat *et al.*, 1996 and Golynsky *et al.*, 1996 (Eastern Dronning Maud Land and Enderby Land). Aeromagnetic interpretation maps for parts of Africa were obtained from MSc theses (Mubu, 1995 for southern Africa; Abdelaziz, 1996 for parts of southern and eastern Africa; Nyakkana, 1994 for parts of Tanzania and Uganda). Aeromagnetic interpretations by Batterham *et al.*, (1983) for Tanzania and Reeves *et al.* (1986/87) for Kenya were also used for compilation. Regional aeromagnetic data for southern and eastern Africa and southern India were interpreted in the present study. Interpretation map for Southwest Sri Lanka was taken from Perera (1997).

b. Contour Maps

Published aeromagnetic contour maps of southern India (Reddi *et al.*, 1988) and NGRI[1] (1975-1978) were used for creating digital database. The Bouguer gravity contour map of Sri Lanka (Hatherton *et al.*, 1975) was also used to create new digital dataset.

3.2.2. Digital Data

a. Aeromagnetic Data

Aeromagnetic data for most parts of southern and eastern Africa and parts of Madagascar were available in digital format from the African Magnetic Mapping Project (AMMP, Barritt, 1993). This data was available in gridded format with 1 km grid cell size reduced to 1 km terrain clearance. Gridded total field aeromagnetic data for Namibia was obtained from the Geological Survey of Namibia. This data was

[1] *National Geophysical Research Institute, Hyderabad, India*

Table 3.1: Summary of geophysical data used for this research

Fragment	Area	Data Type	Source	Remarks
East Antarctica	Eastern Dronning Maud Land and Enderby Land	Aeromagnetic	Golynsky *et al.* (1996)	Published interpretation
	Western Dronning Maud Land	Aeromagnetic	Corner (1994)	Gridded data at 2000 m cell size; Interpretation by Corner (1994)
Africa	Southern Africa	Aeromagnetic	AMMP (1993)	Digital gridded data (1000m grid size); interpreted in this study
			Geological Survey of Namibia	Gridded data at 2000m grid size; compiled with AMMP data of southern Africa and interpreted in this study
	East Africa	Aeromagnetic	AMMP	Digital gridded data (1000m grid size)
			Batterham *et al.* (1983)	Interpretation map of Tanzania
Madagascar	South central and Western Madagascar	Aeromagnetic	AMMP, Barritt (1993)	Digital gridded data (1000 m grid cell size)
			Yardimcilar (1998)	Interpretation by Yardimcilar during his MSc in ITC
India	Southern India	Aeromagnetic	NRSA of India (1981-'94) and NGRI (1981-1984)*	Digital data from Sreedhar Murthy (1999) and Chandrasekhar (1997) and this study. compiled and interpreted in this study
	Whole India	Bouguer Gravity	NGRI of India (1975)	Digitised from contour map by Sreedhar Murthy (1998)
Sri Lanka	SW Sri Lanka	Aeromagnetic	Perera (1997)	Digital compilation and interpretation by Perera during his MSc in ITC
	Whole Sri Lanka	Bouguer Gravity	Hatherton *et al.*, Sri Lanka (1975)	Digitised from the Bouguer gravity contour map in this study

AMMP: African Magnetic Mapping Project, GSD: Geological Survey Department, NRSA: National Remote Sensing Agency, NGRI: National Geophysical Research Institute. See Figure 1.3 for various data sources.
*refer to Table 5.1 (Chapter 5) for survey specifications

processed and merged (refer to Chapter 6 for details) with the AMMP data of southern Africa in this study. The data for Western Dronning Maud Land was obtained from Corner. This dataset is of very low-resolution, mostly flown at a coarse line spacing of 20 km except for the southeastern part over the HU Sverdrupfjella, Ahlmannryggen and Kirwanveggen where the data was acquired at a relatively close line-spacing of 5 km. Higher resolution, but old aeromagnetic contour maps of southwestern Sri Lanka ware digitised by Perera (MSc, 1997) and under the AAIME Aeromagnetics of Arabia, India and Middle East) project. The survey was conducted in 1956-57 with 150 m constant terrain clearance and 400 to 800 m line spacing. Data for southern India was partly created during the present study by digitising the published contour maps (Reddi *et al.*, 1988) and NGRI (1978-1981) contour maps. Parts of the digital data were also obtained from Sreedhar Murthy (1999, pers. comm.) and Chandrasekhar (1997). Most of the southern Indian data used here were acquired at 4 km line spacing and 1500 to 2850 m flying height with an objective of studying the regional tectonic setting.

b. Gravity Data

Bouguer gravity data generated from widely spaced gravity stations from India, Sri Lanka and parts of Africa were used as supporting evidence to the aeromagnetic and geological interpretation for regional structures. The interpretation of these datasets is described in Chapter 7.

(i) India

Bouguer gravity data was available from Sreedhar Murthy (1999, pers. Comm.). The digital data (*Figure* 3.1) was created from the published contour maps on 1:5 000 000 scale (National Geophysical Research Institute, 1977) by onscreen digitising using the Auto Trace and Digitise (ATD) tool (Sreedhar Murthy *et al.*, 1998). The contour interval of these maps was 10 mgal.

(ii) Sri Lanka

Bouguer gravity contour map of Sri Lanka (Hatherton *et al.*, 1975) was digitised (Figure 3.2) in the present project to create a digital database, produce enhanced images and interpret the deep crustal features. The contours were digitised on-screen

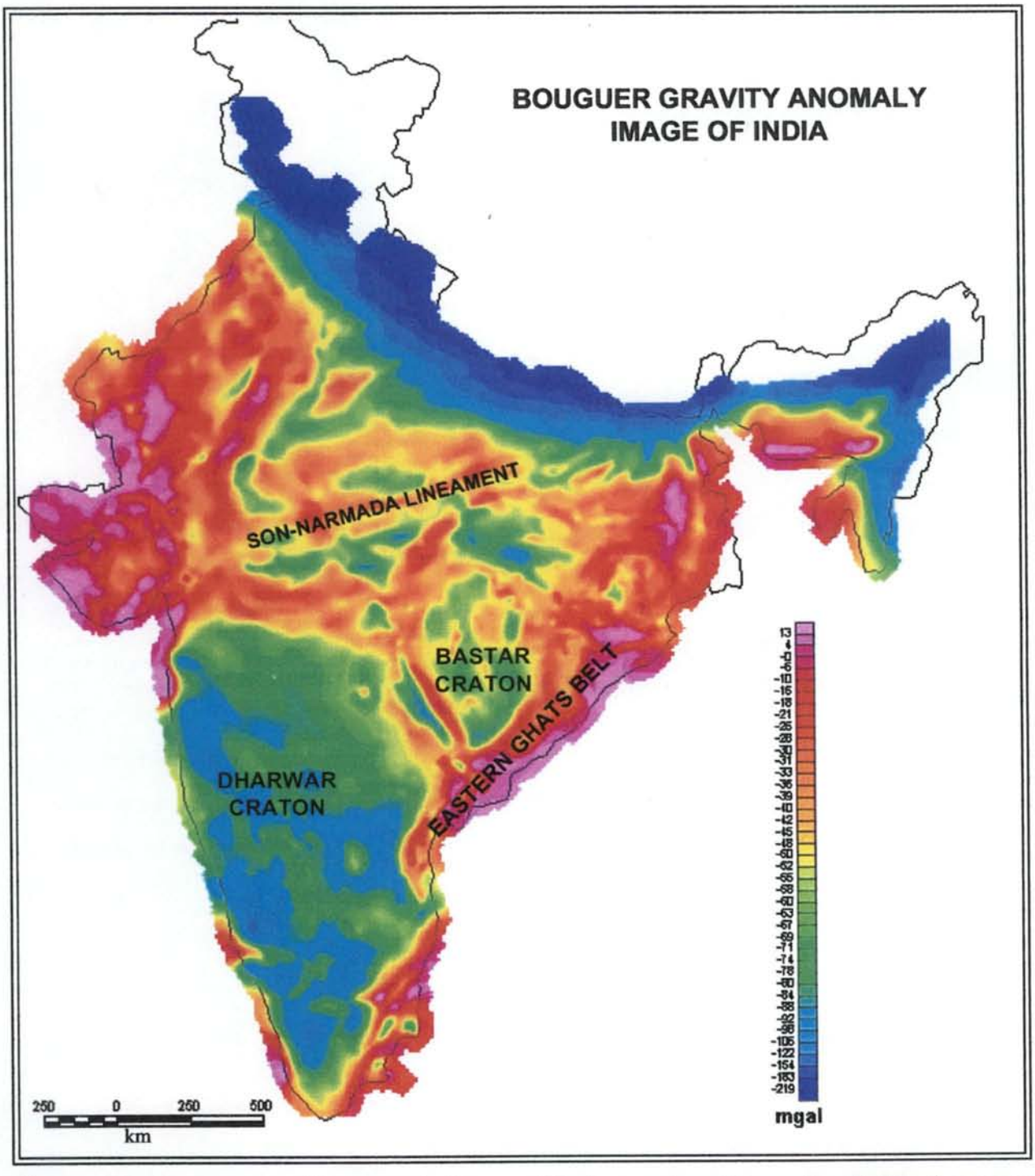

***Figure 3.1**: Bouguer gravity anomaly image of India produced from the digitised contour map (I: 5 000 000, NGGRI, 1977). Note the high gravity values in the Eastern Ghats Belt and low gravity values over Archaean cratonic areas. See Chapter 7 for interpretation of this gravity data.*

using the *Digitise* tool in *OASIS montaj* (*Geosoft*®) from 1: 1 000 000 scale map with contour interval of 5 mgal.

(iii) Southern Africa

Digital format Bouguer gravity data for southern Africa (Figure 3.3) was obtained from the Geological Survey of Namibia (1998, Rainer Wackerle - Senior Geophysicist). The data was available as Geosoft grid (4 km x 4 km). This data was mainly used to delineate the deep crustal structures and to substantiate the features interpreted from aeromagnetic data (see chapters 6 and 7 for details).

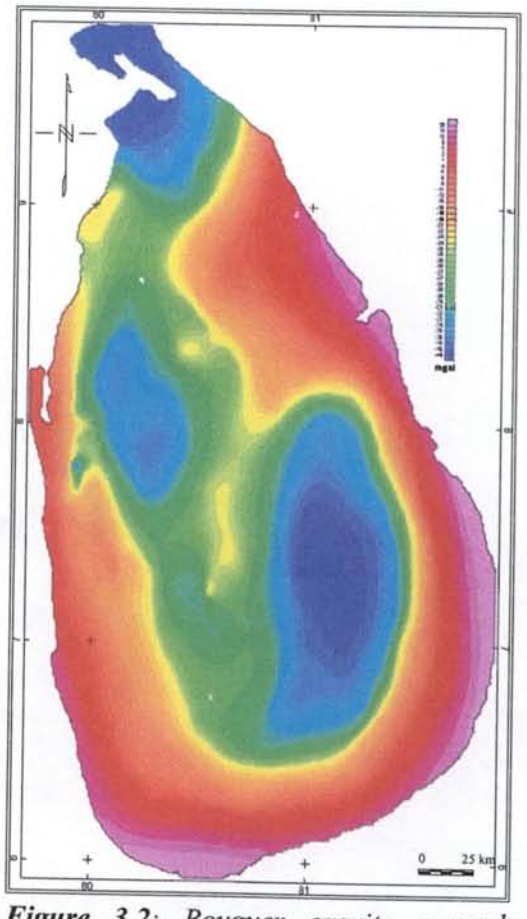

***Figure 3.2**: Bouguer gravity anomaly image of Sri Lanka (digitised from 1: 1000 000 contour map, Hatherton et al., 1975)*

3.3. Continental Scale Aeromagnetic Data Compilation

The published and unpublished aeromagnetic interpretations and the interpretations carried out in this study were compiled together in continental scales for the central Gondwana fragments in order to produce an aeromagnetic interpretation map. The methodology followed for compilation is summarised in Figure 3.4.

3.4. Geological Data

Geological data were mostly available as published geological maps and literature. Recent geological maps of India (Figure 3.5), Sri Lanka and Antarctica were digitised in the present research. The details of the digital data used are summarised in Table 3.2.

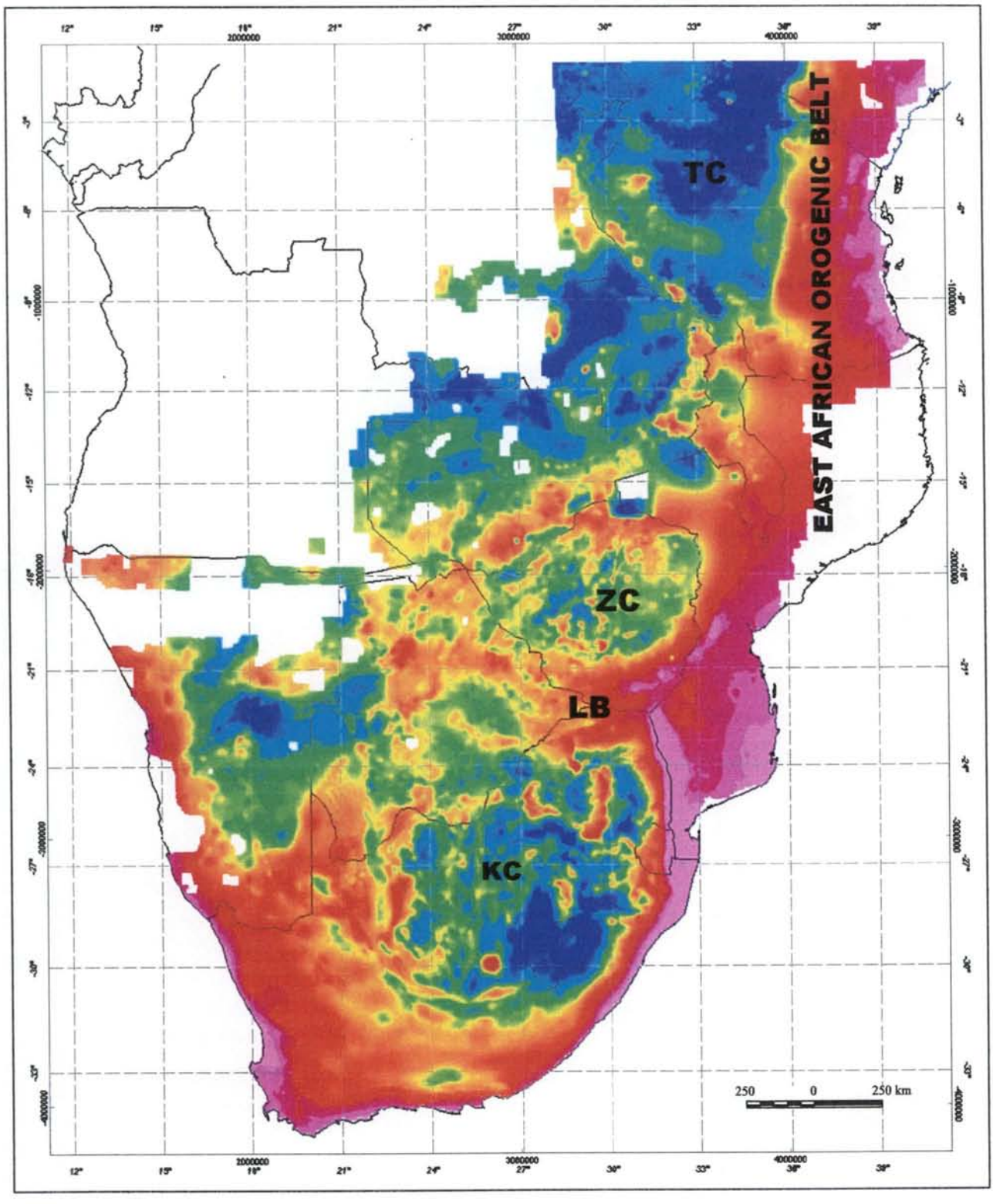

***Figure 3.3**: Bouguer gravity anomaly image of parts of southern Africa (Data source: Namibian Geological Survey). Image produced from 4 km x 4 km grid on Mercator projection. KC: Kaapvaal craton, LB: Limpopo Belt, ZC: Zimbabwe Craton, TC: Tanzania Craton. See Chapters 6 and 7 for interpretation of this data.*

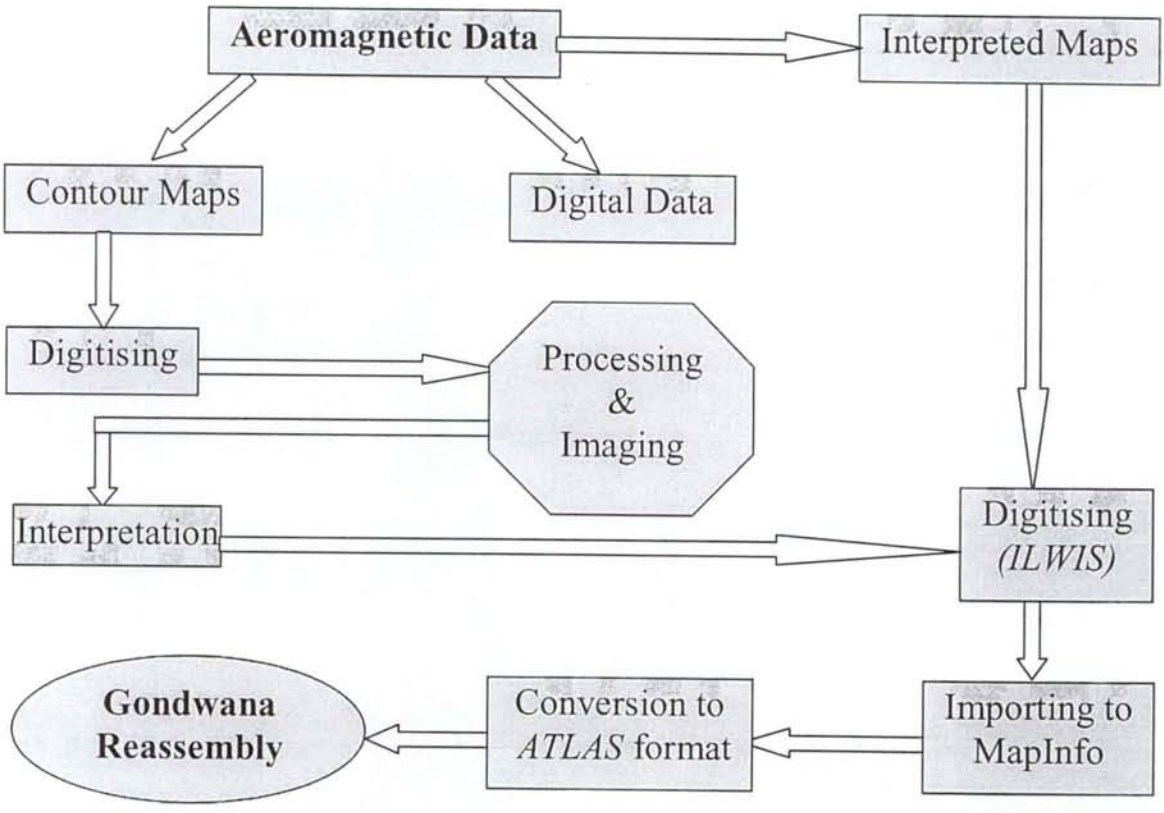

***Figure 3.4**: Flow chart of aeromagnetic data compilation for paleomap preparation*

***Table 3.2:** Details of digital geological data used in the research*

Continent	Geological Maps	Scale	Remarks
India	GSI[2], 1993	1:5 000 000	Digitised in this study
	GSI, 1994	1:2 000 000	Digitised in this study
Sri Lanka	GSD[3], Sri Lanka, 1983	1: 506 880	Digitised in this study
Madagascar	ASGA/UNESCO, 1990	1: 5 000 000	Digital data obtained from Atkinson (pers. comm.)
Africa	ASGA/UNESCO, 1990	1: 5 000 000	Digital data obtained from Atkinson (pers. comm.)
Antarctica	Tingey, 1991	1:10 000 000	Digitised in this study

[2] *Geological Survey of India, Calcutta.*
[3] *Geological Survey Department of Sri Lanka (now known as Geological Survey and Mines Bureau)*

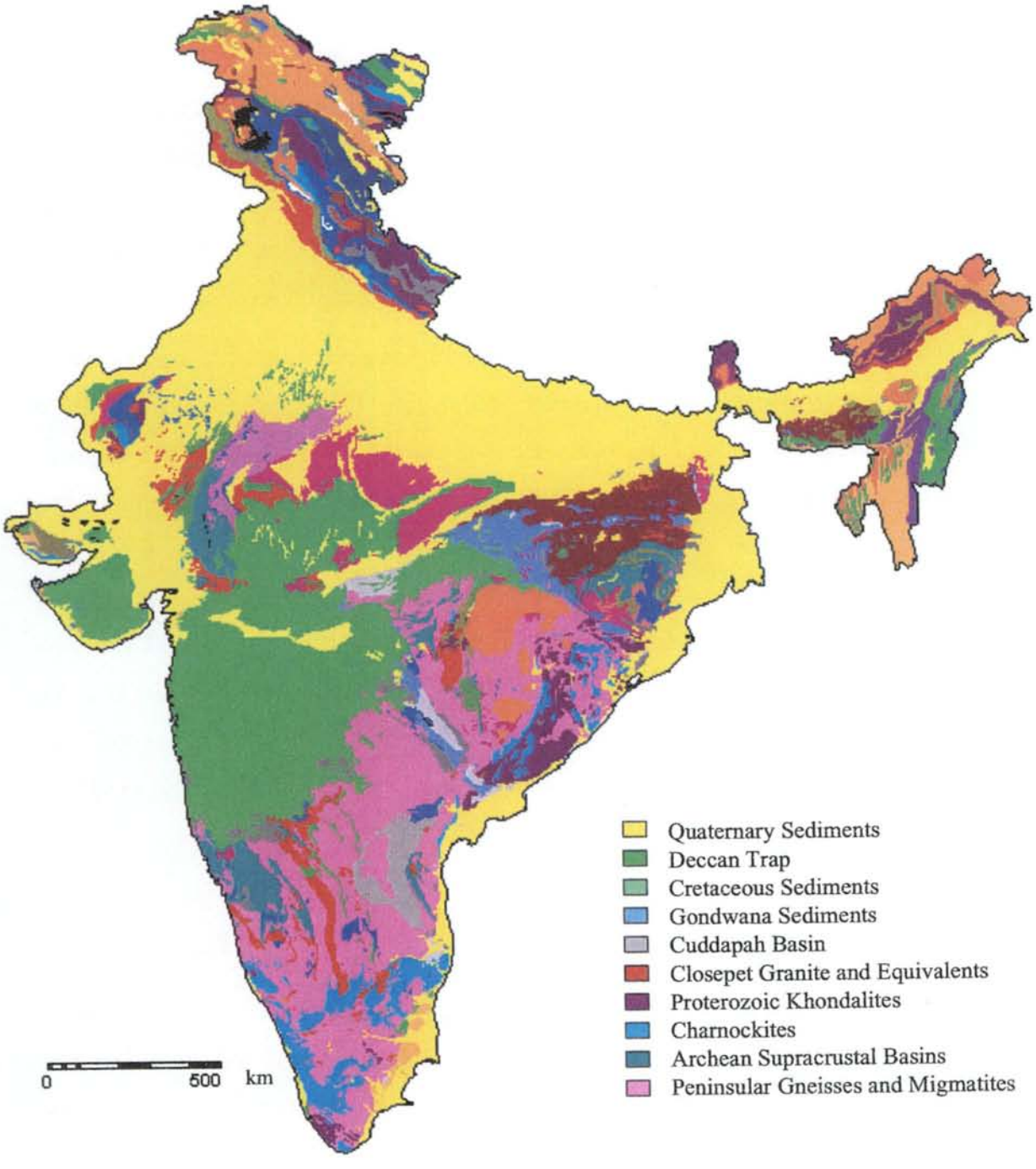

Figure 3.5: *Geological map of India produced from the digital geological database created in this study. The digital geology was created from Geological map of India (1: 5 000 000), Geological Survey of India, 1993. Only the major litho-units of southern India are shown in the legend.*

3.5. Digital Data Capture

The hard copy interpretation maps were digitised using *ILWIS®*® and *MapInfo*® software tools. The quality of digital data depends, to a great extent, on the scale and accuracy of the source maps from which these are digitised. As most of these hardcopy maps do not contain detailed projection information, it was often time-consuming to determine the projection parameters as accurately as possible.

The aeromagnetic contour maps for parts of South India were digitised using a simple program written in *GWBASIC* (Asfaha and Erren, 1990) and a Calcomp 9100 digitising table. The digitising operation was carried out by moving the digitizer cursor along the flight lines and capturing the x, y and z (easting, northing and magnetic field) values at the points of intersections between flight path and contour lines. The captured data were stored as *. xyz files in ASCII format. The Bouguer gravity contour map of Sri Lanka was digitised using the *Digitise* tool in *ILWIS®*. As most of the contour maps were hand-drawn in the pre-computer era, accuracy of these maps depends, in parts, on the personal expertise of the person drawing the contours. All the geological and geophysical interpretation maps were digitised using the *Digitise* tool in *ILWIS®* and CALCOMP digitising table.

3.6. Aeromagnetic Data Interpretation

Huge aeromagnetic data sets of different parts of the world (*Figure* 1.2 in Chapter 1) have been acquired since about 1950 with widely varied specifications and techniques. Most of these data sets are available only as contour/profile maps and are under-utilised. The importance of compilation of these data sets on continental and even global scales has been realised now by the geoscientific community for a better understanding of subsurface geology and global tectonics. Continental scale compiled aeromagnetic data for South America (SAAMP), Australia (Tarloski *et al.*, 1996) and Africa (AMMP – Barritt, 1993) are now available for interpretation. Data sets for parts of Arabia, India and Middle East compiled at ITC (International Institute for Aerospace Survey and Earth Sciences, the Netherlands) under AAIME (Erren, 1997) fill a major gap in global aeromagnetic coverage. Aeromagnetic datasets for southern

and eastern Africa and southern India were processed and analysed for continental scale aeromagnetic features. These interpretations along with the existing interpretations were compiled together in this study. These interpretations, in combination with limited gravity interpretation and geological data, were used to find geophysical constraints for a tight reassembly of the central Gondwana fragments flanking the Indian Ocean. The following steps were involved in achieving the aeromagnetic interpretation.

3.6.1. Processing

The AMMP data was used for aeromagnetic interpretation of most parts of southern and eastern Africa and parts of Madagascar. The AMMP data was made available in gridded format (1000 m grid cell size). The gridded data of Namibia (Geological survey of Namibia) was merged with the AMMP data to obtain a near complete aeromagnetic coverage of southern and eastern Africa. The details of further processing are described in Chapters 6 and 7. The south Indian aeromagnetic data was compiled and processed in this study (refer to Chapter 5 for details of processing). The 250 m gridded data of Sri Lankan (Perera, 1997) was resampled to 1000 m cell size and upward continued to 2000 m for comparison with the low-resolution data of southern India. The Antarctica data (Western Dronning Maud Land, Corner, 1994) was also regridded to 1000 m cell size for comparison with that of southern Africa. The Russian data covering Eastern Dronning Maud Land and Enderby Land could not be obtained despite our best efforts.

3.6.2. Data Presentation

The gridded aeromagnetic data were used to produce a number of images and interpretation maps at suitable scales for each of the fragments (*e.g.* on 1: 5 000 000 for Africa - Maps 6.1 - 6.7; and on 1: 2 500 000 for southern India – Maps 5.2 - 5.4 enclosed in back pocket) using Mercator projection, same as that of the AMMP data. The various maps produced are – 1. Total field shaded relief map, 2. Vertical derivative map, 3. Analytic Signal map, 4. Vertical Derivative of Analytic Signals and 5. 3D Euler depth map. The utility of these maps in data presentation and interpretation is described in Chapters 5 and 6.

3.6.3. Interpretation

(a) Qualitative Interpretation

Aeromagnetic maps were interpreted for regional features like tectonic boundaries between cratons and surrounding mobile belts, major faults and shear zones, dyke swarms, subsurface volcanic rocks etc. Qualitative interpretation involved zoning of a magnetic map by outlining the zones each of which has a characteristic anomaly pattern or "thumbprint" that is distinctly different from the patterns surrounding it and correlating these zones with the corresponding lithologies. Thus, zoning of magnetic anomalies helps in mapping subsurface extensions of geological units, which have limited exposure. Grey scale total field magnetic maps were used for zoning. Vertical derivative maps and shaded relief maps were used for delineating linear features. 3D analytic signal[4] maps were used as an alternative to the 'reduced-to-pole' for simplification of complex magnetic anomalies at low magnetic latitudes like southern India and eastern Africa.

(b) Quantitative Interpretation:

Rough estimates of depth and positions of the magnetic sources were carried out for all the aeromagnetic data using 3D Euler deconvolution technique (Reid *et al.*, 1990). Magnetic edges could be mapped precisely from the linear alignment of depth solutions. An example of effective use of Euler solutions for mapping magnetic contacts is shown in Figure 3.6, where clustering of depth solutions is prominent along the Lurio Shear Zone in northern Mozambique. Similarly, deeper solutions are clustered in the northeastern part defining the boundary between the Precambrian rocks of the Mozambique Belt and younger sediments. Quantitative interpretation for depth of burial and dimensions of the magnetic sources of selected anomalies was carried out using the *Geosoft® Magmod* software tool. Spectral analysis of total field

[4] *Analytic signal is defined as the square root of the sum of the squares of the vertical and two horizontal derivatives of the total magnetic field T (Qin, 1994). The peaks of the analytic signals correlate directly with their causative bodies and are positioned symmetrically over them, as they are independent of the inclination of the magnetic field. This avoids the difficulties often faced in the conventional process of reduction-to-pole for non-vertical T. Preliminary interpretation also has been possible by processing the derivatives of the analytic signal amplitude, instead of the original analytic signal amplitude, which gives a more efficient separation of anomalies caused by close sources (Debeglia and Corpel, 1997).*

and eastern Africa and southern India were processed and analysed for continental scale aeromagnetic features. These interpretations along with the existing interpretations were compiled together in this study. These interpretations, in combination with limited gravity interpretation and geological data, were used to find geophysical constraints for a tight reassembly of the central Gondwana fragments flanking the Indian Ocean. The following steps were involved in achieving the aeromagnetic interpretation.

3.6.1. Processing

The AMMP data was used for aeromagnetic interpretation of most parts of southern and eastern Africa and parts of Madagascar. The AMMP data was made available in gridded format (1000 m grid cell size). The gridded data of Namibia (Geological survey of Namibia) was merged with the AMMP data to obtain a near complete aeromagnetic coverage of southern and eastern Africa. The details of further processing are described in Chapters 6 and 7. The south Indian aeromagnetic data was compiled and processed in this study (refer to Chapter 5 for details of processing). The 250 m gridded data of Sri Lankan (Perera, 1997) was resampled to 1000 m cell size and upward continued to 2000 m for comparison with the low-resolution data of southern India. The Antarctica data (Western Dronning Maud Land, Corner, 1994) was also regridded to 1000 m cell size for comparison with that of southern Africa. The Russian data covering Eastern Dronning Maud Land and Enderby Land could not be obtained despite our best efforts.

3.6.2. Data Presentation

The gridded aeromagnetic data were used to produce a number of images and interpretation maps at suitable scales for each of the fragments (*e.g.* on 1: 5 000 000 for Africa - Maps 6.1 - 6.7; and on 1: 2 500 000 for southern India – Maps 5.2 - 5.4 enclosed in back pocket) using Mercator projection, same as that of the AMMP data. The various maps produced are – 1. Total field shaded relief map, 2. Vertical derivative map, 3. Analytic Signal map, 4. Vertical Derivative of Analytic Signals and 5. 3D Euler depth map. The utility of these maps in data presentation and interpretation is described in Chapters 5 and 6.

3.6.3. Interpretation

(a) Qualitative Interpretation

Aeromagnetic maps were interpreted for regional features like tectonic boundaries between cratons and surrounding mobile belts, major faults and shear zones, dyke swarms, subsurface volcanic rocks etc. Qualitative interpretation involved zoning of a magnetic map by outlining the zones each of which has a characteristic anomaly pattern or "thumbprint" that is distinctly different from the patterns surrounding it and correlating these zones with the corresponding lithologies. Thus, zoning of magnetic anomalies helps in mapping subsurface extensions of geological units, which have limited exposure. Grey scale total field magnetic maps were used for zoning. Vertical derivative maps and shaded relief maps were used for delineating linear features. 3D analytic signal[4] maps were used as an alternative to the 'reduced-to-pole' for simplification of complex magnetic anomalies at low magnetic latitudes like southern India and eastern Africa.

(b) Quantitative Interpretation:

Rough estimates of depth and positions of the magnetic sources were carried out for all the aeromagnetic data using 3D Euler deconvolution technique (Reid *et al.*, 1990). Magnetic edges could be mapped precisely from the linear alignment of depth solutions. An example of effective use of Euler solutions for mapping magnetic contacts is shown in Figure 3.6, where clustering of depth solutions is prominent along the Lurio Shear Zone in northern Mozambique. Similarly, deeper solutions are clustered in the northeastern part defining the boundary between the Precambrian rocks of the Mozambique Belt and younger sediments. Quantitative interpretation for depth of burial and dimensions of the magnetic sources of selected anomalies was carried out using the *Geosoft® Magmod* software tool. Spectral analysis of total field

[4] *Analytic signal is defined as the square root of the sum of the squares of the vertical and two horizontal derivatives of the total magnetic field T (Qin, 1994). The peaks of the analytic signals correlate directly with their causative bodies and are positioned symmetrically over them, as they are independent of the inclination of the magnetic field. This avoids the difficulties often faced in the conventional process of reduction-to-pole for non-vertical T. Preliminary interpretation also has been possible by processing the derivatives of the analytic signal amplitude, instead of the original analytic signal amplitude, which gives a more efficient separation of anomalies caused by close sources (Debeglia and Corpel, 1997).*

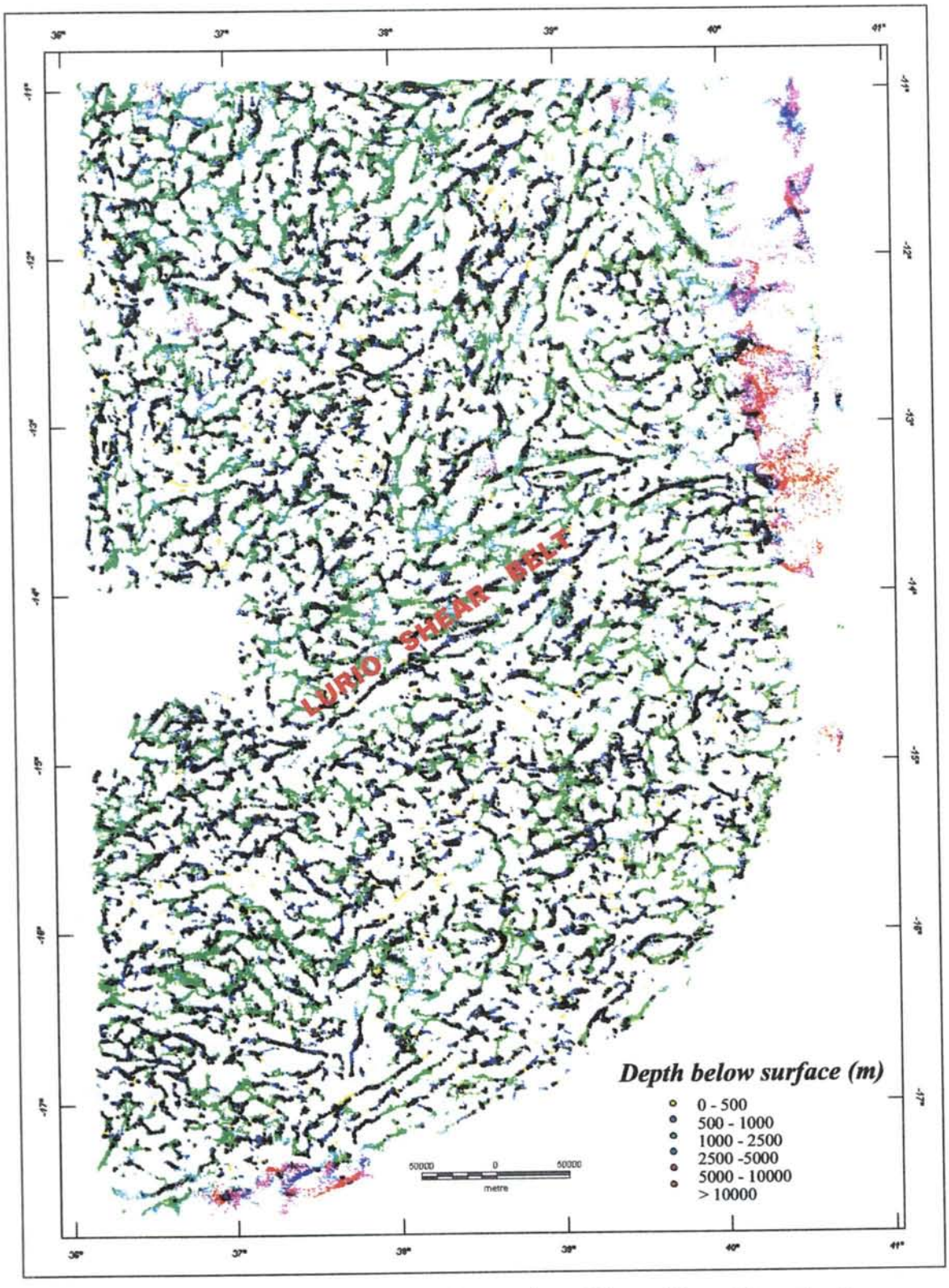

***Figure 3.6**: Euler 3D depth solutions for northern Mozambique. Note the linear alignment of depth solutions along the Lurio Shear Zone and the clustering of deeper solutions in the northeastern part defining the faulted boundary between the Mozambique Belt and younger sediments*

magnetic data for some areas was carried out to estimate the approximate depth range of magnetic populations.

3.7. Generalisation of Geology

Fine details of each geological unit of local importance are not of much use in geological correlation at continental scales. So it was necessary to generalise the geology of each fragment into broad lithotectonic units prior to their correlation. The generalisation was based on lithological assemblages, magmatic and tectonothermal (metamorphism and deformation) ages and break in regional structural trends. Geology of each fragment was classified into 4 tectonic domains.

1. Pre-Kibaran (>~1000 Ma) Shields: it is now well accepted that the Neoproterozoic supercontinent Rodinia (Figure 2.1 in Chapter 2), the precursor to Gondwana, was formed at ~1000 Ma by collision tectonics among continental masses (*e.g.* Unrug, 1997; Hoffman, 1999). It is, therefore, important to group together all the crustal elements that were cratonised (*i.e.* tectonically stabilised) prior to this collision and which have not been affected by the later tectonothermal/orogenic events. Examples of such shield areas are the Kalahari craton of southern Africa and the Rayner Complex of East Antarctica.

2. Terrains affected by 1000 to 500 Ma tectonothermal events: A number of tectonothermal events took place between ~1000 Ma and ~500 Ma - formation of Rodinia, its breakup and formation of Gondwana (*e.g.* de Wit *et al.*, 1988; Unrug, 1997; Kröner *et al.*, 1999). Identification and correlation of such terrains (*e.g.* East African Orogenic Belt, Madagascar, Southern Granulite Terrain of India) are important for understanding of geological events that led to the breakup of Rodinia and formation of Gondwana.

3. Upper Paleozoic-Mesozoic Intercontinental Sedimentary basins: These are Upper Carboniferous to Lower Jurassic intracratonic rift basins (*e.g.* Karoo basins of Africa, Gondwana basins of India) developed in wide areas of almost all the Gondwana fragments. As these basins developed during the existence of Gondwana (post-assembly and pre-breakup), correlation of these basins across rifted margins provides useful constraints for Gondwana reassembly.

4. Syn-breakup magmatism: Wide-spread magmatic activities in the form of eruption of voluminous mafic lava (*e.g.* Karoo volcanics in southern Africa, Cox, 1992, Duncan *et al.*, 1997; Deccan Traps in western India, Watts and Cox, 1989; Elliot and Fleming, 2000; Ferrar volcanics of East Antarctica) and intrusion of huge dyke swarms (*e.g.* North Botswana dyke swarm, Reeves 1978 and 2000) took place during Jurassic and Cretaceous periods – synchronous with Gondwana breakup. Classification of these magmatic episodes based on geological characteristics and their age of emplacement provides valuable constraints on the time and location of breakup between hitherto conjugate fragments.

The classified geological terrains were digitised as polygons using *ILWIS*® and *MapInfo* . The digitised geology was rasterised for integration with geophysical datasets

3.8 Creation of Database in Atlas[5] Format

The digitised geological and geophysical data were imported to MapInfo as **.mif* files (see Appendix IV for an example). The *mif* files, in turn, were converted to **.atl* (*ATLAS* format files) for direct use in the paleomap-making programs (*ATLAS* and *TimeTrek)* using a basic program *MiftoAtl* (Reeves, 1997, pers. comm.; see Appendix VI for the program). Each geophysical/geological unit was time-windowed and attached to the respective continental fragment for display in paleomaps only in the period during which it was in existence. For example, all the Pre-Kibaran geological terrains were assigned a time-window of 4000 to 0 Ma, whereas the Karoo and Gondwana basins were assigned a time-window of 300 to 0 Ma. This helps in selective viewing of the geological terrains at different ages as they evolved. An example of such a time-windowed data for Peninsular India is shown in Figure 3.7. Similar databases were created for all the fragments.

---

[5] *Atlas (*.atl) files are simple READ format ASCII files (see Appendix V for an example). The first two lines (optional) describe the Title of the data. The third line READ fragment code (e.g. READ 400) indicates that the following lines contain data for the respective fragment (e.g. 400 for Africa). The fourth line states the total number of coordinate pairs including Dummy Coordinate pairs for time-window, if any, and mode of display of the data (line, points etc). The fourth line is followed by co-ordinate pairs. The coordinate pairs are followed by 0 in the last line that indicates the end of that particular data.*

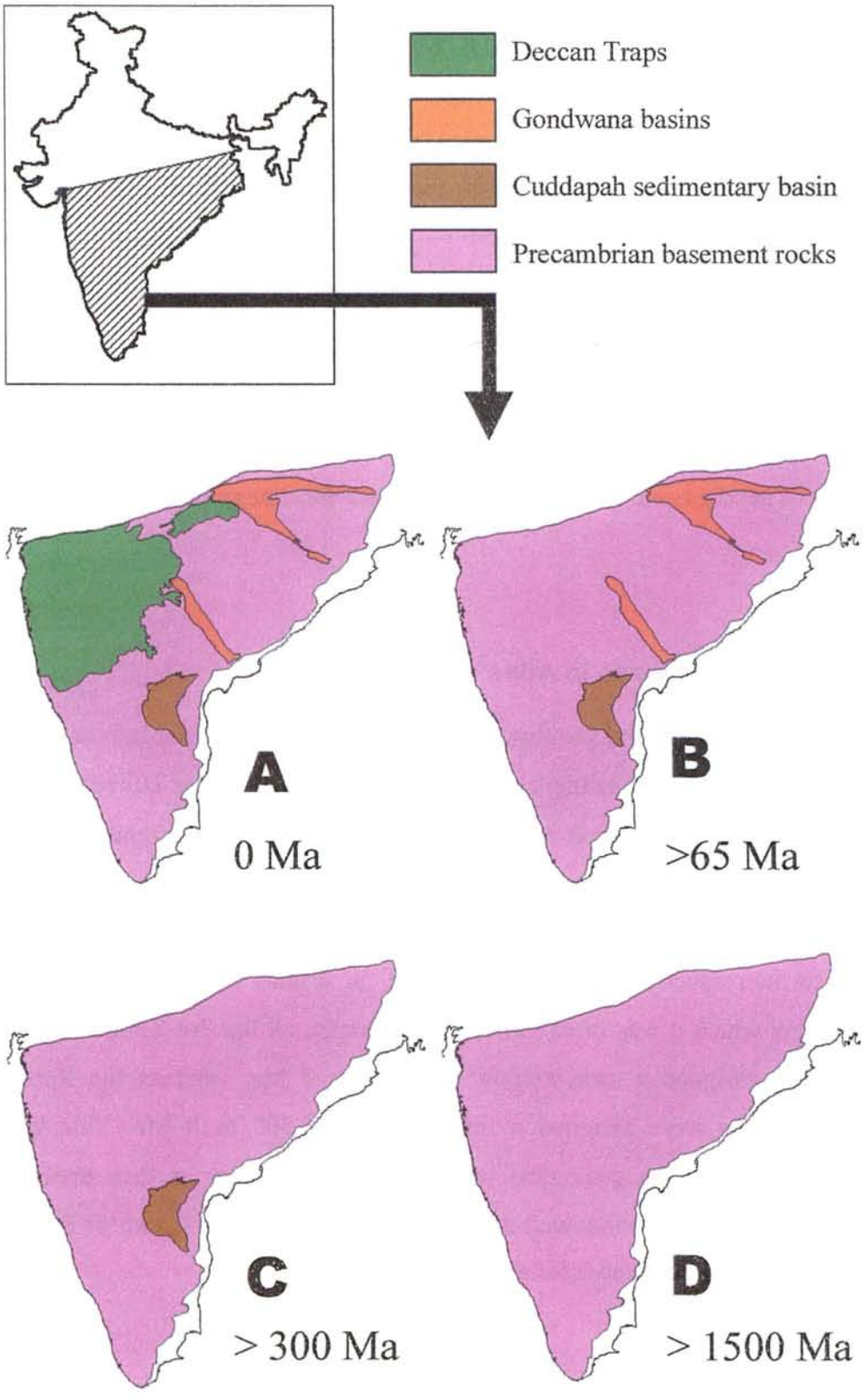

***Figure 3.7**: Peninsular India at different geological ages. A: Present day, B: before 65 Ma, C: before 300 Ma, D: before 1500 Ma*

3.9. Gondwana Reassembly

Once all the data are in Atlas format, the geological and geophysical features move with the fragments to which they are attached. Thus, paleomaps at different ages could be produced with relative ease to test the continuity of these features across the drifted margins in a reassembled Gondwana. It was also possible to test the validity of different models of Gondwana reconstruction and fine-tune some of the reconstructions with the help of these datasets. Reassembly of central Gondwana based on the geological and geophysical evidence is discussed in detail in Chapter 8. This database could further be modified in future as and when new data is available for central Gondwana fragments.

4. GEOLOGICAL CORRELATION

4.1. Introduction

The timing and nature of amalgamation of continental fragments into large supercontinents during the Neoproterozoic period and their subsequent breakup into present day continents have been a subject of ongoing debate. Though a number of models have evolved to explain the mode and timing of their amalgamation and separation, the precise paleopositions of the continental fragments (southern and eastern Africa, East Antarctica, India, Sri Lanka and Madagascar) and their changes with time during the formation of the Indian Ocean have not been satisfactorily resolved. Here we take a closer look at the lithotectonic and geochronological correlation between adjacent pairs of continental fragments, as it is of prime importance for finding the predisruption configuration of Gondwana. An attempt is made here to compile and review the existing data and suggest a reliable fit for central Gondwana.

Assembly and break-up of Gondwana is one of a number of cycles (Wilson, 1963; Bond *et al.*, 1984; Dalziel, 1991) of formation of super-continents followed by disruption throughout Earth's geological past. If we presume that Gondwana was a mosaic of older continental blocks welded together along sutures formed in response to collisional tectonics, then in many places, the fragments might be expected to have split along these pre-existing zones of weakness. If so, the resulting fragments need not have matching geology on either side of the latest rift. Such evidence (geological difference) does not, then, necessarily argue against a reassembly based on other constraints like paleomagnetism, paleontology etc. On the other hand, it has been observed that ~50% of the total rifted Gondwana margins are oblique to the previous structures (Krabbendam and Barr, 2000). Many rifts cut across rigid continental blocks and the geology on either side should match to a great degree when reassembled (Figure 4.1). Thus, similarity of geology across a pair of reassembled margins is an argument in favour of former juxtaposition; difference in geology, however, should not form the sole criteria against such juxtaposition.

The time span between Archean to Early Jurassic has been divided into 4 chrono-tectonic sub-divisions. The rock types, geochronology, deformation history etc. of each of these tectonic subdivisions in adjacent pairs of fragments are compared in this chapter.

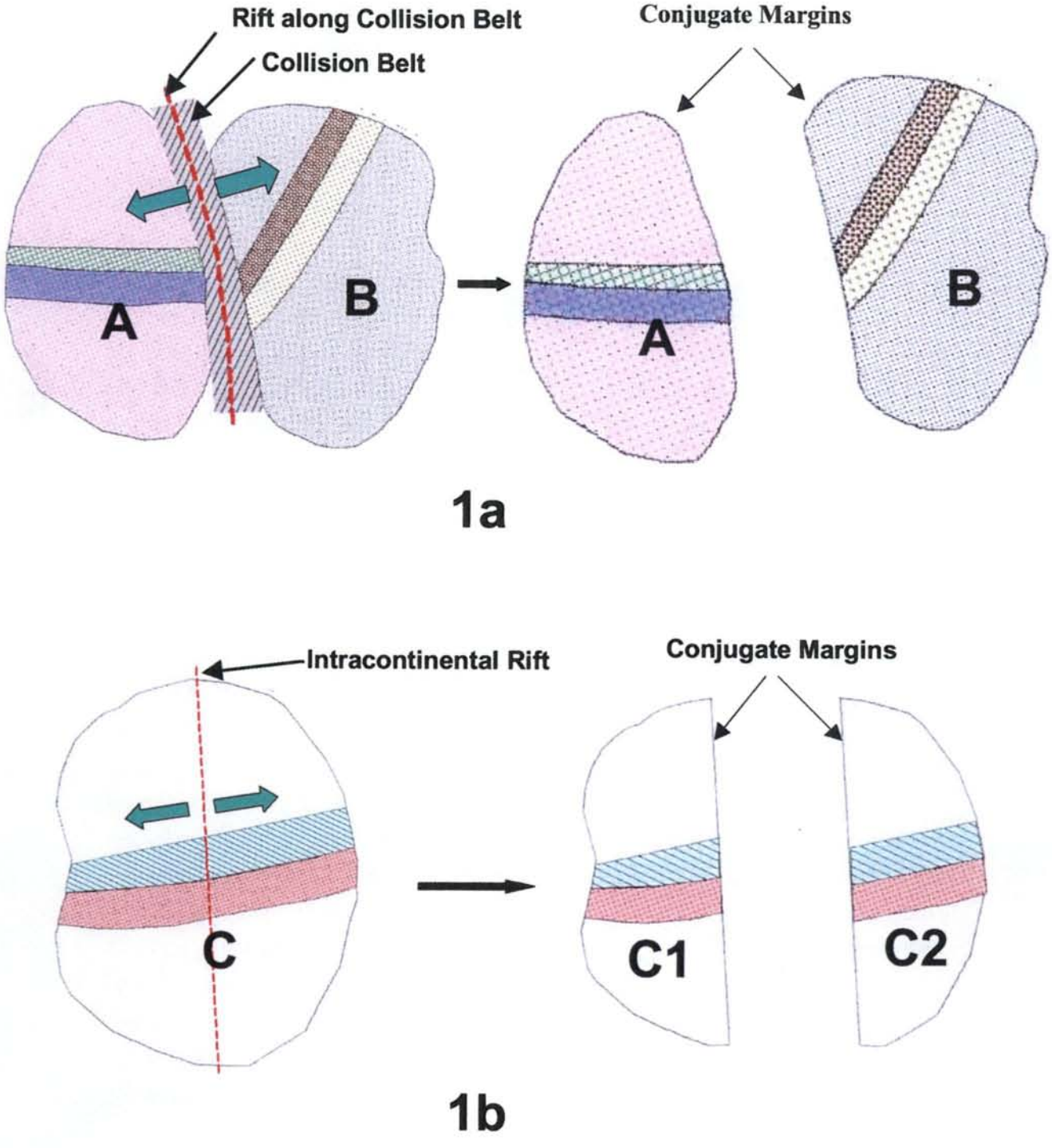

Figure 4.1: *Cartoon figures demonstrating the principle of geological correlation across rifted margins in two different cases. 1a - a supercontinent formed by collision of two terrenes (A & B) of completely different geology splits into two continents along the collision zone. The geology of these continents do not match when reassembled. 1b - A single continent (C) splits into two (C1 and C2) by intracontinental rifting. The geology of these two rifted continents should match when reassembled.*

1. **Archean Cratons and Pre-Kibaran Supracratonic Sequences:** This includes the Archean cratons and Pre-Kibaran supracrustal sequences which have attained cratonisation before ~1000 Ma.
2. **Kibaran-age Orogeny:** This is a ~1100 - 1000 Ma orogeny identified across all the Gondwana fragments and thought to have been developed in response to collisional tectonics between continental blocks during the formation of Rodinia supercontinent. This is equivalent to the Grenvillian orogeny of North America.
3. **Pan-African Tectonothermal Event:** The original idea of the ±500 Ma thermal event in East Africa (Pan-African) of Kennedy (1964) has subsequently been modified to include magmatic and metamorphic ages between 900 and 500 (Shackleton, 1996). But in this thesis, the term Pan-African has been used to define thermo-tectonic events of 550±50 Ma.
4. **Late Paleozoic-Jurassic Karoo/Gondwana Sedimentation and Volcanism:** A series of extensional intracratonic volcano-sedimentary basins developed in Sub-Saharan Africa, western Madagascar, central and eastern India, South America and Australia during Late Carboniferous to Early Jurassic.

4.2. Southeastern Africa and Dronning Maud Land, East Antarctica

Geological correlation between western Dronning Maud Land and southeastern Africa suggests essentially similar crustal evolution from Archean until Mesozoic. Assembly of this part of Gondwana took place before ~1000 Ma as both the terrains are transected by ~1000 Ma orogenic belts. The Late Archean to Meso-Proterozoic granite-greenstone rocks and the volcano-sedimentary sequences of the Kaapvaal and the Zimbabwe cratonic provinces of southern Africa are comparable with the Grunehogna Province of western Dronning Maud Land with respect to their lithostratigraphy, metamorphism and deformation, geochronology and tectonic evolution.

4.2.1. Archean Cratons and Supracratonic Sequences

The Precambrian rocks of southern Africa include two major Archean cratonic fragments- the Kaapvaal craton in the south and the Zimbabwe craton in the north, separated by the Limpopo belt, which has been intensely deformed and metamorphosed at ~2700 Ma and ~2000 Ma (Barton and van Reenen *et al.*, 1992; Kröner *et al.*, 1999) granulite terrain (Figure 4.2). Western Dronning Maud Land

comprises the Archean Grunehogna Province fringed by discontinuous blocks of ~1000 Ma granulite and gneisses of the Maudheim Province (Figure 4.3)

a. Southern Africa

(i) The Kaapvaal Craton:

The Kaapvaal Craton of southern Africa (Figure 4.2) represents one of the oldest known cratonic fragments, where a large portion of relatively pristine Mid-Late Archean rocks has been preserved. The craton covers an area of ~ 1.2×10^6 km^2 and comprises predominantly Archean basement rocks - massive and foliated granitoids, gneisses and relicts of volcano-sedimentary greenstone belts, which are overlain by Archean to Mesoproterozoic supracrustal cover rocks (*e.g.* (Brandl and de Wit 1997);

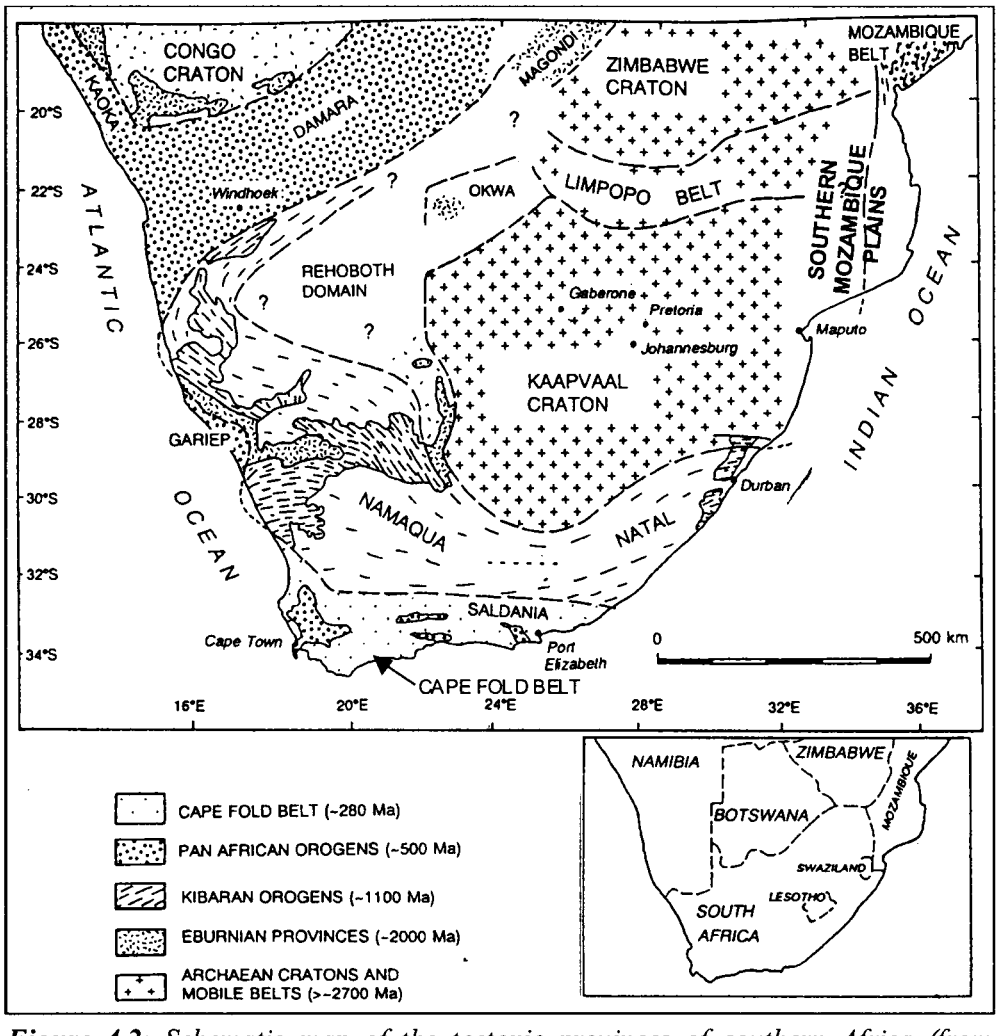

***Figure 4.2**: Schematic map of the tectonic provinces of southern Africa (from Thomas et al., 1993). Note isolated outcrops of Pan-African rocks in Cape Fold Belt (Saldanian Province)*

Carlson, *et al.*, 2000). The craton has been intruded by the Bushveld Complex, the world's largest mafic layered intrusion, at ~2.0 Ga (Brandl and de Wit, 1997 and references therein). The boundaries have been reasonably well defined by geochronological, structural and aeromagnetic data. The craton is bounded: to the east by the Lebombo monocline formed during the break-up of Gondwana; to south and southwest, by the Proterozoic Namaqua-Natal Belt. The northern margin is less well defined and has been interpreted to lie beneath the central zone of the Limpopo Belt (de Wit *et al.*, 1993; Roering *et al.*, 1992). However, aeromagnetic data suggests the boundary to lie approximately along a 10 km wide vertical shear zone (Corner *et al.*, 1991 and Corner, 1998). De Wit *et al.* (1992) have subdivided the craton into a number of discrete Archean tectonic sub-domains with thrust and faulted boundaries.

The Archean history of the craton spans over 1.2 x 10^9 years from 3.60 to 2.50 Ga (*e.g.* Tankard *et al.*, 1982; Compston and Kröner, 1988; Hunter, 1991). The ancient core, which forms the eastern and southeastern part of the craton, comprises the ancient Gneiss Complex (3.64 Ga, Compston and Kröner, 1988) and the Barberton greenstone terrains. The granitoid basement in the central and western parts of the craton is poorly exposed and dated at ~3.12 Ga (Armstrong *et al.*, 1990). The northern Kaapvaal craton contains a number of greenstone belts (Murchinson, Pietersberg etc.), associated tonalitic gneisses (3.01 – 2.87 Ga, Barton, 1990) and a series of younger post-tectonic granites. U-Pb zircon ages (2.88 – 2.78 Ga, Grobler and Walraven, 1992) from the granitoid rocks of western Kaapvaal Craton suggest a Late Archean crustal evolution. The Archean basement rocks of the craton, at places, are overlain by Late Archean supracratonic sequences (Dominion, Witwatersrand, Pongala Transvaal basins).

(ii) The Zimbabwe Craton

The Zimbabwe craton (Figure 4.2), lying north of the high-grade Limpopo Belt, is an Archean granite-greenstone province and covers an inferred area of ~268,000 km^2 (Blenkinsop *et al.*, 1997). The craton is surrounded by three orogenic belts: to the northwest, the Magondi Mobile Belt (2.0 – 1.8 Ga); to the north and east, the Zambezi Mobile Belt (1.0 – 0.5 Ga) and to the south, the Limpopo Belt (2.6- 2.0 Ga). It is covered by Tertiary Kalahari sands to the west. The craton consists of older granitoids, greenstone belts, intrusive complexes, younger granites and the ~2.5 Ga Great Dyke. These rocks range in age from ~3.6 to 2.6 Ga (Petters, 1991 referred in Blenkinsop *et al.*, 1997). The basement complex of the Zimbabwe craton is nonconformably overlain by relatively unmetamorphosed volcano-sedimentary sequences of predominantly clastic sediments in the northeast. The Zimbabwe Craton

is notable for its large number of greenstone belts and the high proportion of greenstone to granitoids (~20%).

(iii)The Limpopo Mobile Belt

The Kaapvaal and Zimbabwe cratons are separated by the ENE-trending Limpopo Province, an intensely deformed granulite belt (Figure 4.2). It comprises three crustal domains, the northern, central and southern zones (Watkeys, 1983) and has been modelled as a collisional orogen that developed in response to collision between the Kaapvaal and the Zimbabwe cratons (Roering *et al.*, 1992). Two episodes of high-grade metamorphism at ~2.7 Ga and ~2.0 Ga (Kröner *et al.*, 1999) have been recognised in the Limpopo Belt.

(iv) Late Archean to Mesoproterozoic Supracratonic Sequences

A number of Late Archean to Mesoproterozoic supracrustal sequences of southern Africa developed on the Archean basement rocks of the Kaapvaal, Limpopo and Zimbabwe provinces. The cratonic cover includes the Pongola, Witwatersrand, Transvaal, Waterberg, Soutspanberg, Ntingwe and Umkondo Groups. The Umkondo, Waterberg, Soutspanberg and Ntingwe successions, preserved near the margins of the Kaapvaal and Zimbabwe cratons, contain immature fluvial to shallow marine sediments. These successions are characterised by the ubiquitous presence of the earliest known red beds (sediments with ferric pigmentation) indicating the prevalence of oxidising conditions during their deposition. The sedimentary/volcanic rocks ratio varies depending upon the tectonic setting of basins in which these rocks were deposited. Tholeiitic volcanic rocks overlying the sedimentary sequences are reported from the Soutspanberg and the Umkondo Groups. Predominant south to southeast paleocurrent directions have been reported from the Soutspanberg and Waterberg groups indicating a north/northwesterly provenance.

Geochronological data suggest Late Archean ages (3.10 – 2.5 Ga, Armstrong *et al.*, 1990; Robb *et al.*, 1991; Roering *et al.*, 1990) for the Dominion, Witwatersrand, Pongola and Transvaal Groups, and ~2.0 – 1.1 Ga (Allsopp *et al.*, 1989) for the later supracratonic sequences.

b. Western Dronning Maud Land, East Antarctica

(i) The Grunehogna Province - cratonic basement and the supracrustal rocks

The Grunehogna Province of western Dronning Maud Land (Figure 4.3) comprises relatively undeformed and unmetamorphosed Archean and Proterozoic rocks. The Archean basement rocks are exposed in patches only in the western part of the Grunehogna province and are represented by ~3000 Ma granites (Barton et al, 1987).

The Proterozoic Ritscherflya Supergroup, making up the rest of the Grunehogna province, comprises fluvio-marine sedimentary rocks overlain by a sequence of continental tholeiitic basalts and basaltic andesites (Watters *et al.*, 1991) ranging in age from 800 to 1000 Ma (Moyes and Harris, 1996). The sedimentary rocks include greywackes, arenites, siltstones, mudstones and intraformational conglomerates suggesting, from the base upwards, shallow marine, tidal flat, braided stream and alluvial fan deposits (Ferreira, 1986). Paleocurrent directions suggest a southwestern provenance for these sediments.

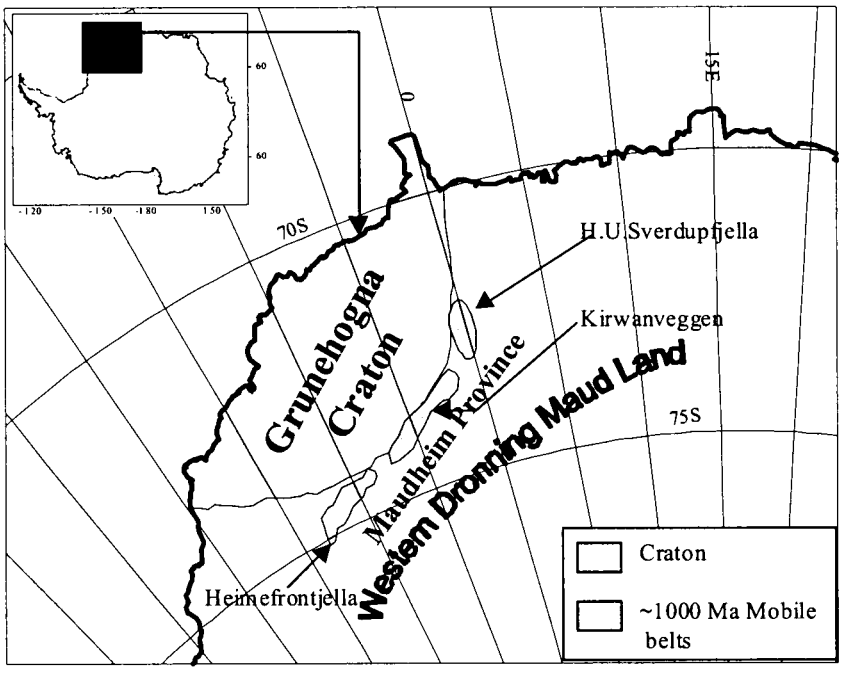

***Figure 4.3**: Schematic representation of Precambrian rocks of Western Dronning Maud Land, East Antarctica*

The rocks of the Ritscherflya Supergroup are weakly deformed with the strata generally dipping between 2° to 10° NE or SE (Groenewald *et al.*, 1995). Wide-ranging isotopic ages (800 to 1800 Ma) for the sediments and volcanic rocks have been suggested (Wolmarans and Kent, 1982; Moyes and Barton, 1990). However, recent studies using Sm-Nd and Rb-Sr systematics have lead to provisional conclusions that the sedimentation took place around 1080 Ma followed by the period of magmatism between 800 and 1000 Ma (≅Kibaran).

c. Discussion:

The southern African cratons comprise granite-greenstone basement rocks ranging in age from 3.65 Ga to 2.6 Ga. Though no greenstone belts have been reported from the Grunehogna Province, the granite occurring to the western extremity is of similar age (~3000 Ma) as those of the eastern and southeastern parts of the Kaapvaal craton. Granites from the two terrains have marked differences in their geochemical characters (Barton *et al.*, 1987) suggesting separate magmatic sources. However, the geochemical differences derived on the basis of 10 whole rock analyses from a rather limited outcrop should not be considered as representative of the entire granitic mass of the Grunehogna Province.

The supracratonic sequences - the Umkondo, Soutspanberg and Ntingwe Groups of southern Africa are broadly similar in lithostratigraphic character to the Ritscherflya Supergroup. Ferreira (1986) has correlated the Ritscherflya Group with the Umkondo Group, situated on the eastern flank of the Zimbabwe Province, based on sedimentary characteristics. But the ultramafic intrusions and volcanic rocks of the Umkondo Group, though similar in character, differ from those of Ritscherflya Supergroup in geochronology (1080±140 Ma age for the Umkondo volcanics by Allsopp *et al.*, 1989).

***Table 4.1**: Summary of comparison between Mesoproterozoic supracrustal groups of Kaapvaal and Grunehogna cratons (modified from Groenewald, 1993 and Groenewald et al., 1995)*

	Kaapvaal Craton	***Grunehogna Craton***
Groups/ Supergroups	Waterberg, Soutpansberg, Umkondo Groups	Ritscherflya Supergroup
Lithology	conglomerates, sandstones, arkoses, siltstones, mudstones, tholeiitic basalts and andesite	greywackes, arenites, siltstones, mudstones, intraformational conglomerates, tholeiitic basalts and basaltic andesites
Depositional Envrionment	shallow marine, tidal-flat, lacustrine, braided alluvial	shallow marine, tidal flat, braided streams, alluvial fan
Paleocurrent	south, southeast and east	northeast
Geochrono-logy	~1800 Ma : sedimentation ~1100 Ma: volcanism	~1080 Ma: sedimentation 800-1000 Ma: magmatism

4.2.2. The Kibaran-age (~1400 - 1000 Ma) Mobile Belts

The ~1000 Ma orogenic cycle, conceived to be a major tectonothermal event, has been widely recognised across almost all the fragments of Gondwana. It is postulated that these orogenic belts have been formed in response to the collision of cratonic fragments during their accretion to form the Rodinia Supercontinent. The cratonic provinces of southern Africa and East Antarctica are surrounded by a number of such orogenic belts as described below.

a. Southern Africa

The ~1400 -1000 Ma orogeny in Africa is widely known as the Kibaran tectonothermal event (see Cahen *et al.* 1984 for review) and is represented by the Namaqua-Natal and the Mozambique belts in southern Africa.

(i) The Namaqua-Natal belt

The Namaqua-Natal Belt is a low-pressure/high-temperature polymetamorphic terrain along the southern margin of the Kaapvaal at ~1200 Ma during a major period of continental growth (Joubert, 1986). The belt extends eastward from Namaqualand in the west, under the Karoo sediments, to Natal in the east coast of southern Africa. The western part of the belt, the Namaqua Province, is a complexly deformed poly-orogenic low to *high-grade* gneissic terrain last affected by the Kibaran Orogeny at ~1000 Ma (Tankard *et al.*, 1982). The eastern part of the Namaqua Province contains arc-related volcano-sedimentary sequences (~1.3 Ga, Cornell *et al.*, 1990) which are intruded by calc-alkaline granitoids. The proportion of granitic rocks increases westwards and southwards. The metamorphic grade increases southwards from amphibolite facies to granulite facies (Moore, 1989).

The Natal Province consists of three tectonostratigraphic domains bounded by southward dipping thrusts (Thomas, 1989). The oldest rocks (~1.3 to 1.0 Ga, Thomas and Eglington, 1990) in the southern Margate and Mzumbe terrains comprise arc-related felsic to mafic metavolcanics with subordinate metasediments. The Tugela terrain in the north consists of layered mafic volcanics (~1.2 Ga, Barton, 1983) intruded by mafic ultramafic complexes and serpentinites and alkaline granitoids. The accretion of these three terrains onto the craton took place by northeast directed thrusting. As in the Namaqua Province, the grade of metamorphism increases southwards, away from the Kaapvaal craton.

Thomas (1989) and Thomas *et al.* (1993) identified a number of discrete east-west elongated terrains which were accreted by a series of thrusts. This process resulted in a series of NE-SW and NW-SE trending terrains in the Natal and Namaqua provinces during the Kibaran Orogenies. In a Gondwana context, similar lithotectonic terrains

have been reported from the Falkland Islands and western Dronning Maud Land in East Antarctica (*e.g.* Groenewald *et al.*, 1995; Jacobs *et al.*, 1998).

(ii) The Mozambique Belt

The Mozambique Belt (Figure 4.2) is a north south Proterozoic mobile belt along much of the east coast of Africa comprising gneisses-migmatite basement and metamorphosed volcano-sedimentary cover sequences. The basement is predominantly composed of high-grade ortho- and para-gneisses, migmatites. Protoliths of orthogneisses were emplaced and deformed at two distinct phases at 1100 to 850 Ma and ~500 –600 Ma (Pinna *et al.*, 1993; Kröner *et al.*, 1997; Jamal *et al.*, 1999). But still there is argument as to whether or not ~1000 Ma event is a tectonic (deformation) event or just a magmatic event and the major thrusting event might be of only 500-600 Ma (Jamal, 2000, *pers. comm.*).The supracrustal units comprise marine sedimentary rocks and calc-alkaline and tholeiitic rocks associated with ultramafic-mafic sequences. Synmetamorphic shearing, blastomylonitisation and regional thrusting to the east and southeast are the major tectonic products of the ~1000 Ma event (Mozambican orogeny of Pinna *et al.*, 1993). Low-grade metasedimentary rocks (phyllite, sandstone, conglomerate and marble) unconformably overlie the basement rocks. The metamorphic grade ranges from mid-amphibolite facies in the south and widespread granulite facies in the north. The belt is dominated by thrust-nappe tectonics. **b. Dronning Maud Land**

(i) The Maudheim Province

The ~1000 Ma orogeny in Dronning Maud Land, East Antarctica is exposed as three discrete blocks in the Maudheim Province - the H.U.Sverdrupfjella in the east, the Kirwanveggen in the south and the Heimefrontfjella in the southwest (Figure 4.3) – in the Maudheim Province (Groenewald *et al.*, 1995; Board and Frimmel, 2000). All the three blocks consist of intensely deformed granulite and amhibolite facies gneisses of ages ranging from 1200 to 900 Ma. The H.U.Sverdrupfjella block consists of an amphibolite facies rock assemblage in the west and partially retrogressed granulites in the east (Grantham *et al.*, 1995). These rocks include calc-alkaline orthogneisses, paragneissic metacarbonates and pelites, quartzo-feldspathic paragneisses and metapelites. The Kirwanveggen area of the central Maudheim Province comprises predominantly quartzo-feldspathic gneisses of volcanic origin (Wolmarans & Kent, 1982) with minor amounts of calc-silicates and other metasedimentary rocks. The Heimefrontfjella forms the western block of the Maudheim mobile belt consisting of metamorphosed relics of a magmatic arc in the north, a back-arc basin the central part filled with sedimentary and bimodal volcanic rocks (Bauer *et al.*, 1998). These rocks

were metamorphosed under amphibolite to granulite facies conditions and intruded by a number of post-Kibaran mafic dykes.

The rocks of the Maudheim Province have suffered polyphase deformation and metamorphism involving thrusting and recumbent folding with predominantly northwestward transport directions (Grantham *et al.*, 1995). The early folding and thrusting with NW vergence signifies a collisional orogeny in the earliest part of the terrain evolution. The rocks have been subjected to medium to high pressure (8-12 kbar) and temperature (ranging from 750 to 850°C) metamorphic conditions. Decompressive retrograde metamorphism of the high-grade rocks has been reported from the eastern H.U.Sverdrupfjella and has been attributed to the Pan-African imprints.

Attempts have been made (Grantham *et al.*, 1988; Groenewald *et al.*, 1991, Pinna *et al.*, 1993) to correlate these orogenic belts and establish their continuity from southern Africa to East Antarctica. The ~1000 Ma orogenic belts of southern and eastern Africa (Mozambique, Natal and Namaqua Provinces) have been correlated with the Maudheim Province of East Antarctica by Grantham *et al.* (1988) and Groenewald *et al.* (1991). The ~600 - 450 Ma tectonothermal activity (Pan-African event) overprinted on the ~1000 Ma event identified in the Mozambique orogenic province (Sacchi *et al.*, 1984 and Pinna *et al.*, 1993) is found in the Maudheim Province. Syntectonic granite intrusions in the Maudheim province have yielded a well-constrained whole-rock Rb-Sr date of 519±17 Ma (Moyes & Barton, 1990). No evidence of any Pan-African tectonothermal activity has been found in the Natal Province as no isotopic data reveal ages younger than 850 Ma.

New U-Pb SHRIMP zircon and Sm-Nd data (Jacobs *et al.*, 1998) of rocks from the coastal stretch of central Dronning Maud Land indicate that the oldest rocks in this area are Mesoproterozoic in age (1080 – 1130 Ma). 570-515 Ma metamorphism of the intrusive granites in the region suggests Pan-African activity in the area. ENE-WSW trend of Pan-African syn-tectonic granitoids and a number of ductile sinistral shear zones occur in the area, which suggests that central DML may represent the southern continuation of the Mozambique Belt in East Antarctica.

4.2.3. Pan-African Event in southern Africa and western Dronning Maud Land

A widespread Late Neoproterozoic-Early Paleozoic tectonothermal event ranging in age from ~550 to ~450 Ma has been identified in most Gondwana fragments (*e.g.* Pinna *et al.*, 1993; Unrug *et al.*, 1997). This orogeny has mostly affected the earlier mobile belts resulting in intense folding and thrusting and retrograde metamorphism and magmatism. At times the intense deformation of this orogeny has obscured all the

earlier deformational and metamorphic history. The Gariep, Damara and Saldanian orogenic provinces of southern Africa are examples of Pan-African belts. In the present context, the effects of the Pan-African deformation on the Mozambique and Natal belts is discussed and correlated with that of the Maudheim province of western Dronning Maud Land. In southeastern Africa, direct evidence of tectonothermal overprinting is restricted to the Mozambique belt. Sacchi *et al.* (1984) recognised gentle folding related to the emplacement of 500 Ma old granites in the Lurio belt. Widespread resetting of isotopic systems, particularly Rb-Sr and K-Ar, has misled many earlier workers to consider the entire Mozambique Belt of Pan-African age. But Pinna *et al.*, (1993) suggested that major crustal growth took place during 1100-950 Ma, the Pan-African event being an intracontinental tectonic event with extensive deformation of the Mozambican continental crust and very little crustal addition. Metamorphism during the Pan-African period was mainly retrogressive. The basement and the supracrustal rocks were subjected to Pan-African thrusts, transcurrent shear zones and folds. Recent geochronological work by Kröner *et al.*, 1997 and Jamal (*pers. comm.,* 2000) reveals extensive Pan-African events in the Neoproterozoic East African Orogen to the north.

Imprints of the Pan-African orogeny have been reported from all the three exposed segments of the Maudheim Province (Figure 4.3). In H.U.Sverdrupfjella (Figure 4.3), this event is marked by alkaline granite intrusion at ~520 Ma, and subsequent thrusting and folding with NW vergence and intense refoliation accompanied by whole-rock Rb-Sr isotope resetting at ~500 Ma (Groenewald *et al.*, 1993). Similarly, biotite blocking-temperature-ages of 475 Ma have been reported from Kirwanveggen (Elworthy, in Wolmarans and Kent, 1982). In Heimefrontfjella, the rocks were tectonothermally overprinted by ~500 Ma events, resulting in northwest directed thrusts and retrograde metamorphism under greenschist facies conditions (Bauer, *et al.*, 1998).

The well-documented Pan-African overprint of the Mozambique and the Maudheim belts suggests that they were in lateral continuity during the period. The northwesterly vergence of the Pan-African thrusts in both the Mozambique and the Maudheim Provinces suggests a northwesterly tectonic transport of these belts over the cratonic blocks. The decompressive retrogression in metamorphism during this period has been attributed to tectonic exhumation through thrusting and emplacement of these blocks above low-grade tectonostratigraphic units (Groenewald *et al.*, 1995). Pan-African deformation has been reported from the sediments of the Natal Group. However, absence of any evidence of Pan-African deformation or retrogression in the Kibaran-age Natal Metamorphic rocks and presence of the Saldanian Belt of Pan-

African age with thrust faulting, intense folding and extensive granitoid magmatism suggest that the Mozambique-Maudheim Pan-African orogeny probably changed its trend to southwest into the Saldanian Belt instead of extending westwards into the Natal Belt.

4.2.4. Phanerozoic Correlation

Several intracratonic depositional basins, preserving evidence of the syndepositional

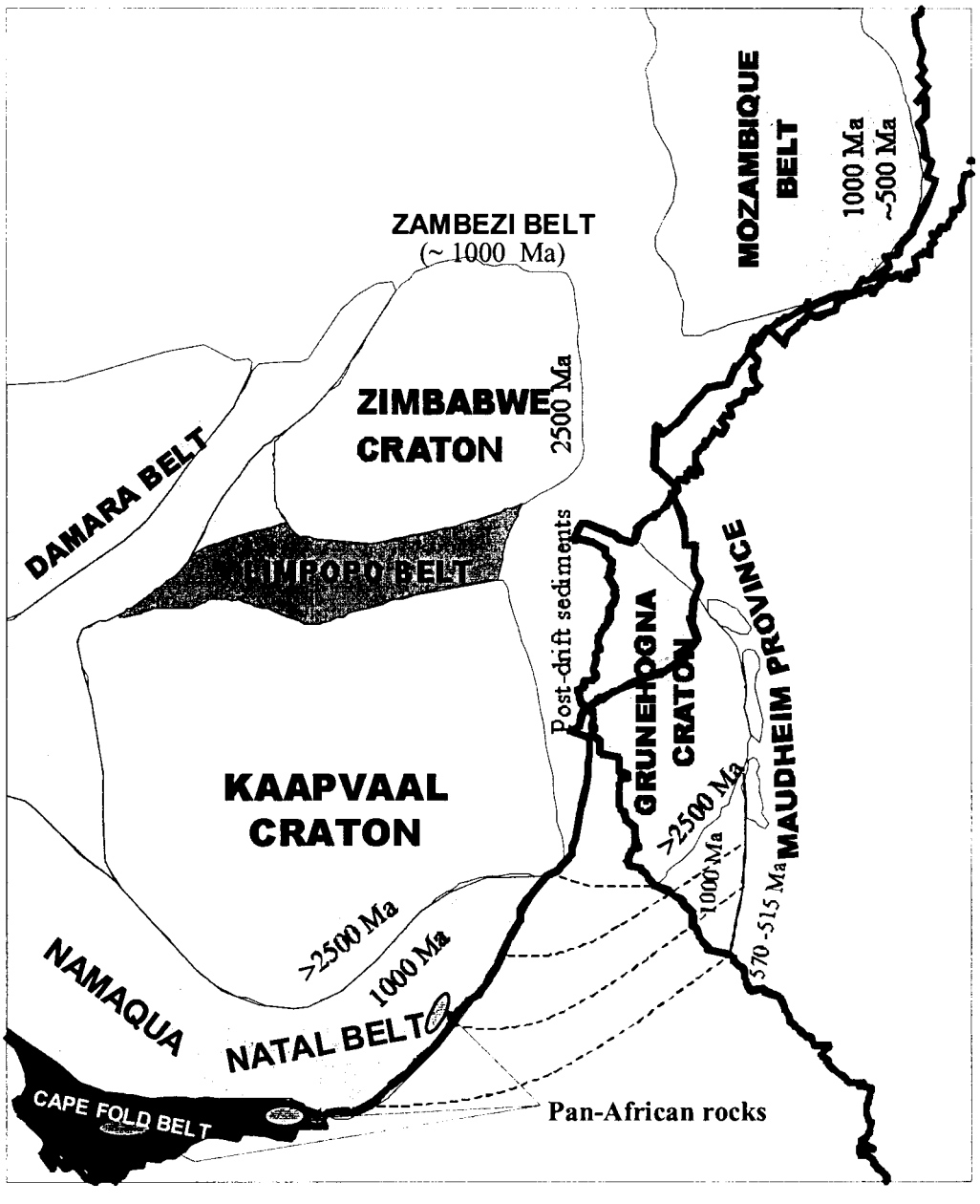

Figure 4.4: Correlation of Precambrian geology between southern Africa and Western Dronning Maud Land, East Antarctica in a Gondwana configuration. Note few isolated patches of Pan-African rocks in the Cape Fold Belt.

tectonic elements, like the development of a large number of growth faults and plutonic and volcanic activity, have developed in both regions after the Pan-African Orogeny. Post-Pan-African tectonic-sedimentary provinces of southern Africa include Cape and Karoo basins. However, lesser sequences like the Klipheuwel Formation (now regarded by many as the lowermost part of the Cape Supergroup) of SW Cape and the Natal Group of Natal are of specific significance due to their geological similarities with the Urfjell Group of Kirwanveggen of Dronning Maud Land. The Early Phanerozoic sedimentary rocks of the Klipheuwel Formation and the Natal Group comprise conglomerates, arkoses and siltstone suggesting an alluvial fan depositional environment. The Early Phanerozoic sedimentary basin, the Urfjella Group in the Kirwanveggen area of western Dronning Maud Land is lithostratigraphically similar to the parts of the Natal group as both the groups consist predominantly of quartz arenites, arkoses, conglomerates and siltstone (Groenewald, 1993). Consistent southwest to south-southwest paleocurrent directions and the poorly sorted nature of the conglomerates suggest a similar paleogeographic environment for both the groups. Relicts of undeformed and unmetamorphosed Permo-Carboniferous cover sediments have been reported from Heimefrontfjella (Bauer *et al.*, 1998 and references therein) and Kirwanveggen (Tingey, 1991). These sediments show evidence of glacio-fluvial depositional environment, similar to the famous Dwyka Formation of the Karoo basin.

a. Synbreak-up Magmatism

A large volume of continental flood basalts (Karoo volcanics) has errupted at ~183±1 Ma (Duncan *et al.*, 1997) in southern and eastern Africa. These basalts are well preserved along the Lebombo monocline (Figure 4.5a and 5b). A north-south trending MORB-like dolerite dyke swarm (Rooi Rand Dolerites), distinctly different in composition from the rest of the Karoo basalts, has intruded the Karoo sedimentary sequence and the overlying volcanic rocks (Duncan *et al.*, 1990), and is thus younger than the Karoo flood basalts. These dykes are clear on aeromagnetic images. It is suggested that a direct temporal relation exists between the intrusion of these dykes and initiation of rifting along the Lebombo monocline, which ultimately resulted in the opening of the Indian Ocean and breakup between southern Africa and East Antarctica. Early Jurassic tholeiitic volcanic rocks and a number of Jurassic mafic intrusive rocks in western Dronning Maud Land (Figure 4.5a) have also been described by Tingey (1991). A number of Jurassic dolerite dykes and basalt flows reported from the northeastern part of Heimefrontfjella have been considered

M: Madagascar, S: Sri Lanka, NA: New Amalfi Sheet, DI: Dufek Intrusion

***Figure 4.5a**: A tight-fit configuration of southeast Africa and Western Dronning Maud Land showing the Lebombo Monocline and the Explora Escarpment (from Cox, 1992). The index map shown in the left is a fit of central Gondwana at 200 Ma by Reeves and de Wit (2000).*

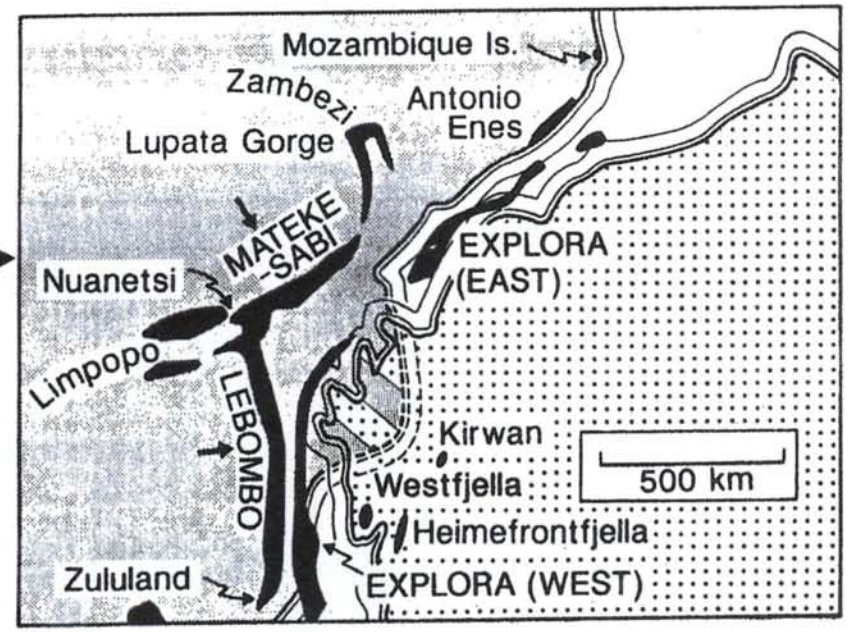

syntectonic with Gondwana break-up (Speath and Schüll, 1987). Similarly ~180 Ma old dolerite dykes and basalts have been reported from Kirwanveggen by Harris *et al.* (1991). Encarnación *et al.* (1996) have reported ages between 180 and 183 Ma for Ferrar dolerites and basalts.

Neethling (1972) correlated these intrusions with the Karoo dolerites of southern Africa (Figure 4.5b) based on geochemical similarities. Recent U/Pb dates of 183-184

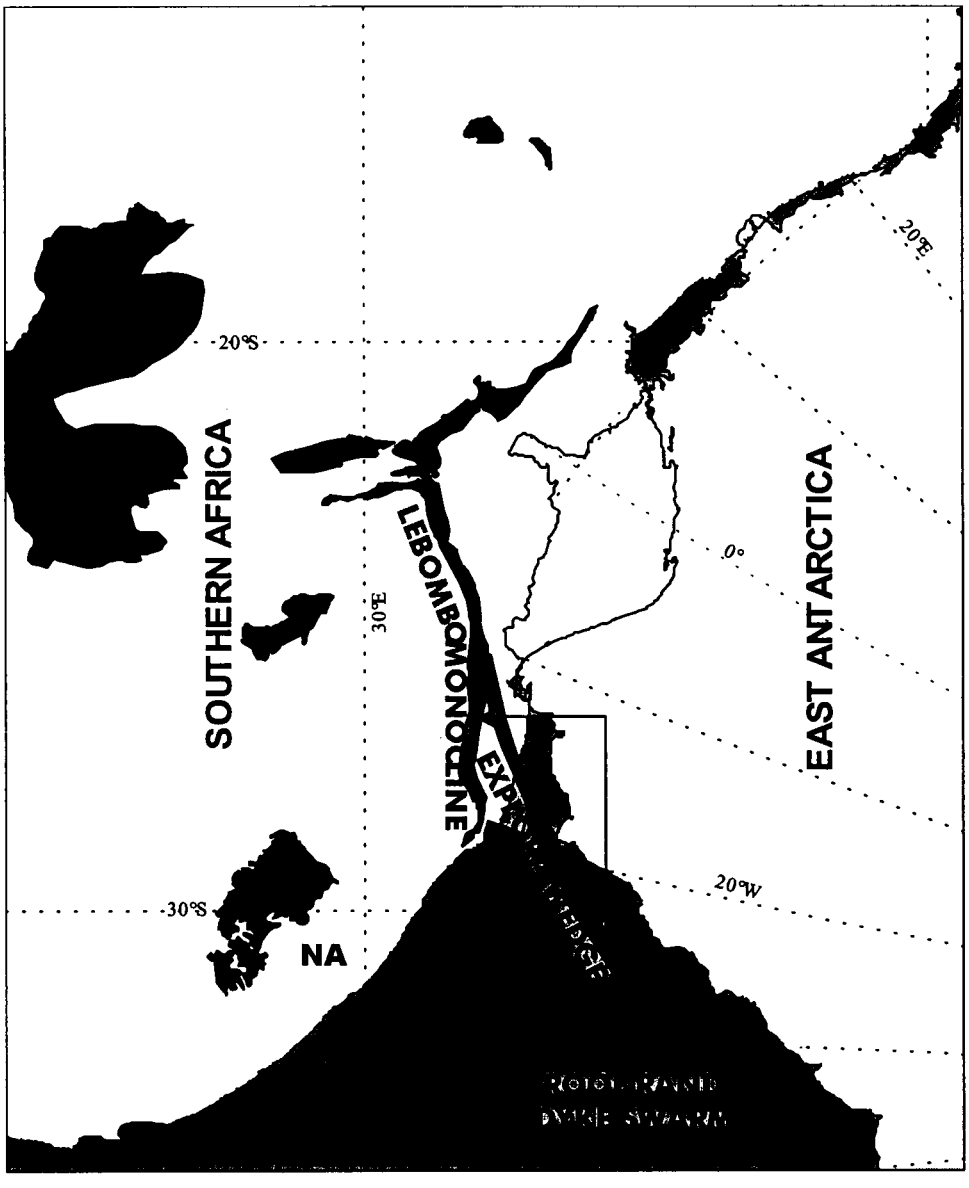

***Figure 4.5b**: Matching of the Lebombo Monocline, southern Africa and the Explora Escarpment in a pre-drift configuration (Reeves 506 model). The off-shore Explora Escarpment is from the geophysical interpretation by Jokat et al., 1996; and the Karoo volcanics (green) are from the geological maps, UNISCO, 1990. NA: New Amalfi Sheet*

Ma for Ferrar and New Amalfi sheet in South Africa (Figure 4.5b) (Encarnación *et al.*, 1996) and for the Dufek intrusion (Minor and Mukasa, 1997) clearly demonstrate contemporaneiety of Ferrar and at least a part of the Karoo magmatism at a resolution of ~1 Ma. Elliot and Flemming (2000) suggested a single source for the Karoo and Ferrar magmas associated with a tripple junction in the proto-Weddell Sea region based on tectonic and geochemical relationship between the two. Storey (1995) also suggested a single synbreak-up magmatic province for the Karoo and Dronning Maud Land and Ferrar basalts and has related these to the Bouvet plume. Cox (1992) has shown a remarkable correlation between the Karoo volcanism along the Lebombo and Mateke-Sabi lineaments in southeastern Africa and the Explora Wedge off the coast of western Dronning Maud Land (Figure 4.5a).

Both the western and eastern part of the Explora Wedge show a high degree of parallelism with the Lebombo and Mateke-Sabi volcanics that suggests the contemporaneity of their eruption. In the recent model based on retracing the active and paleo-transforms of the southern Atlantic ocean (Reeves and de Wit, 2000), however, the Lebombo monocline (digitised from the geological map of Africa, CGMW\UNESCO, 1990) lies north of the Explora wedge interpreted from the geophysical data (Jokat *et al.*, 1996) at ~183 Ma (Figure 4.5b). Thus both the linear volcanic belts together represent an elongated axis of east-west crustal extension followed by fissure type of eruption.

4.3. Enderby Land (East Antarctica) and Southeastern India

Enderby Land of East Antarctica is juxtaposed to southeastern India in most of the recent Gondwana reconstructions (Windley *et al.*, 1994; Mezger and Cosca, 1999, Reeves and de Wit, 2000) based on geological and geophysical constraints. A brief summary of the geology of both the terrains is described below to evaluate these fits.

4.3.1. Peninsular India (South of Son-Narmada Lineament)

The Precambrian basement of peninsular India comprises an assemblage of Archean cratons and Proterozoic mobile belts transected by a network of Neoproterozoic-Early Paleozoic shear zones (Naqvi and Rogers, 1987; GSI, 1994 & 1998, Ghosh, 1999). There are three major Archean cratons – the Dharwar craton in the south, the Bastar craton in the centre and the Singhbhum craton in the north (Figure 4.6) - separated by Gondwana rift valleys (≅ to the Karoo rifts in Africa). The Archean cratons are bounded by Late Archean to Neoproterozoic high-grade granulite terrains in the south – the Southern Granulite Terrain and in the east -Eastern Ghats Belt (Geological Survey of India, 1998).

(a) The Dharwar Craton

The Dharwar craton, largest among the three cratons, is a classic Archean granite-greenstone province that exposes large sections of continental crust through a continuous transition from upper to lower crust. It grades into the granulite terrains in the south, is bounded by a thrust front along the western margin of the Eastern Ghats mobile belt in the east and the Godavari rift in the north. The craton extends right up to the west-coast (Figure 4.6). It is divided into Western Dharwar (WD) and Eastern

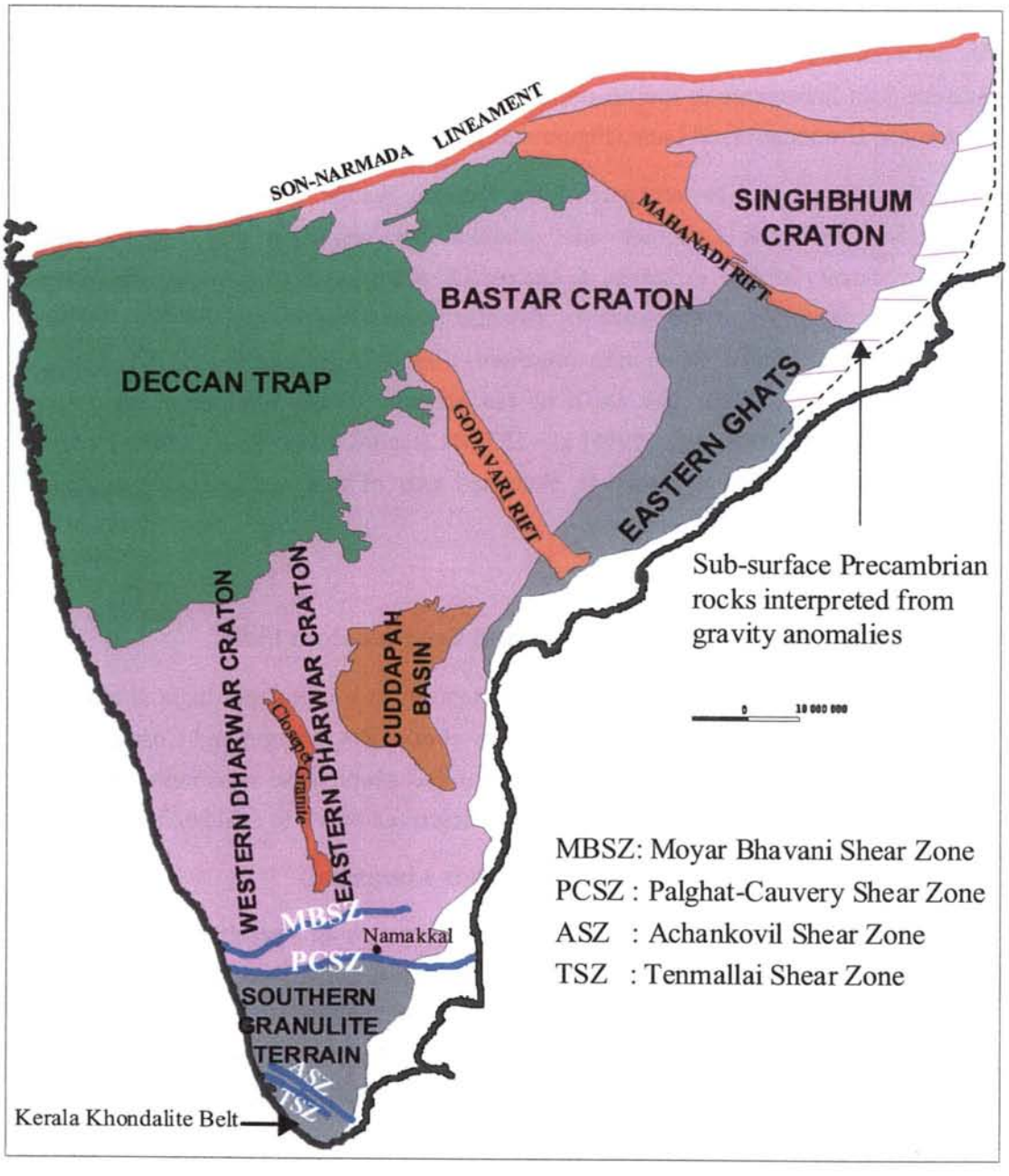

***Figure 4.6**: Simplified geological map of peninsular India (modified from geological maps of Geological survey of India (1993, 1994 & 1998), Ghosh (1999) and geophysical interpretation (this thesis).*

Dharwar (ED) cratons separated by the north-south trending Closepet Granite (summary by Divakar Rao *et al.*, 1990). The sialic basement represented by tonalite/trondhjemite gneisses forms the principal rock type throughout the craton. These basement gneisses are partly covered by relicts of Late Archean volcano-sedimentary sequences- referred to as greenstone belts and are intruded by Late Archean granitoids (Closepet granite and equivalents).

The major differences between the eastern and western parts of Dharwar Craton (Rogers and Giral, 1997) are – (1) earlier evolution of the basement rocks in the Western Dharwar craton (3.4 to 3.0 Ga, Meen *et al.*, 1992) than that of the Eastern Dharwar craton (3.0 ~2.5 Ga, Krogstad *et al.*, 1989); (2) extensive emplacement of the ~2.5 Ga granitoids (Closepet granite and equivalents) in the EDC but sparse in the WDC; (3) The WDC contains extensive Late Archean greenstone belts, whereas in the EDC greenstone belts are comparatively rare.

The principal structural trends in the western Dharwar craton are approximately north-south as evident from the orientation of the major schist belts and the Closepet Granite (Figure 4.6), major shear zones and small-scale structures like regional gneissic foliation and schistosity (Mukhopadhyay, 1986; GSI, 1994; Ghosh, 1999). The greenstone belts in the southern part of the craton are relatively small and metamorphosed to amphibolite facies, whereas, those in the north are larger and only at greenschist facies metamorphism. The general structural trend in ED changes from N-S in the southern part to NW-SE in the north. Metamorphic conditions in the gneiss-granulite transition zone are in the range of 6 to 8 kbar and 700° to 800°C (Naqvi and Rogers, 1987 and the references therein). The schist belts are mostly at greenschist facies metamorphism with amphibolite facies near the margins

Geochronological data from the Dharwar craton is sparse. Isotopic ages from different parts of the Peninsular Gneiss range from 2.9 to 3.4 (Meen *et al.*, 1992; Peucat *et al.*, 1993). Jayanand and Peucat (1995) suggested three periods of accretion (3.4 Ga, 3.3 to 3.2 Ga and 3.0 to 2.9 Ga) for the Peninsular Gneiss on the basis of clustering of isotopic data. U-Pb SHRIMP dating of detrital zircons from metapelite from the Sargur Schist belt indicates 3580-3130 Ma age for their provenance (Nutman *et al.*, 1992). Mafic and felsic volcanic rocks of the schist belts range in age from 2.4 to 2.5 Ga (Taylor *et al.*, 1984, Bhaskar Rao *et al.*, 1992).

(i) The Cuddapah Basin

The crescent-shaped Cuddapah basin (Figure 4.6) in the eastern extremity of the Dharwar craton is a Meso-Neoproterozoic platformal cover sequence laid unconformably across the Peninsular gneisses. It extends over a length of 400 km in

north-south direction with a maximum width of 145 km (Nagaraja Rao *et al.*, 1987). The basin is characterised by over 6000m of red-coloured, arenaceous-pelitic succession with local carbonates and volcanic rocks. Sediments in the western part are essentially undeformed with gentle eastward dips to the centre of the basin. On the contrary, the sediments in the eastern part are isoclinally folded with steeply dipping inverted strata. The basin is tectonically overlain to the east by an Archean thrust mass, which includes the Dharwar-type Nellore schist belt (Kalia and Tewari, 1985). Deep seismic soundings (Kalia *et al.*, 1979) suggest that this thrust and several other sympathetic imbrications within the basin are steeply inclined and penetrate down to the base of the crust.

Isotopic age data from the Cuddapah basin is scarce. Basalt units from lower Cuddapah sequence gives Rb-Sr dates of 1583±147 Ma (Crawford and Compston, 1969). The upper sequences of the basin are of Late Neoproterozoic age.

b. The Bastar and Singhbhum Cratons

The Bastar cratonic block sandwiched between the Dharwar and Singhbhum cratons in the south and north respectively, is less well understood. It is bounded by the eastern Ghats front in the east, the Son-Narmada Lineament in the northwest, the Godavari rift in the south and the Mahanadi rift in the north (papers in the volume edited by Dutta *et al.*, 1990). The western extension of the craton is however not clear due to thick cover of the Deccan basaltic province. Sparse isotopic data for the basement gneisses suggest a Middle Archean age (Sarkar *et al.*, 1990). The basement gneisses are covered by greenschist facies volcano-sedimentary supracrustal sequences. Though Archean to Mesoproterozoic metamorphic ages have been suggested based on stratigraphic constraints, no isotopic data is available to substantiate it. It is recommended to refer to the volume edited by Dutta *et al.* (1990) for a comprehensive review of this craton.

The Singhbhum craton in eastern India is a 250 km long (east-west) by up to 170 km wide Archean block. It is bounded – (1) on the north by the 200 km long Singhbhum Thrust that separates the low-grade metamorphic rocks to the south from the overthrust higher grade (amphibolite facies metamorphic rocks of the Singhbhum-Dalbhum mobile Belt on the north and (2) on the south by the Sukinda Thrust against granulite facies rocks of the Eastern Ghats Belt (Naqvi and Rogers, 1987). The Singhbhum cratonic block consists of granite/gneiss basement complex and associated supracrustal sequences. The basement gneisses and granites are generally middle Archean, stabilised at ~3.0 Ga or older (Saha *et al.*, 1986, Moorbath and Taylor, 1988). The gneisses are complexly intermingled with supracrustals of the Older Metamorphic Group and overlain by numerous other suites, the oldest of which is the

Iron Ore Group (Rogers and Giral, 1997 and references therein). The Older Metamorphic Group (OMG) consists of mica schists, quartzites, calc-silicates and amphibolites. These metasediments are intruded by igneous and meta-igneous rocks of >3.0 Ga age. Rogers and Giral (1997) suggested that the OMG might represent fragmented remains of a former greenstone belt. The Iron Ore Group contains ~7.5 km of folded volcanogenic and meta-sedimentary materials intruded by mafic-ultramafic rocks.

c. Proterozoic Granulite Terrains

The Dharwar granite-greenstone craton is bounded by Neoproterozoic granulite terrains - the Southern Granulite Terrain and the Eastern Ghats Mobile Belt in the south and east respectively. These blocks are composed of predominantly high-grade metasediments and charnockites.

(i) The Eastern Ghats Belt

The Dharwar craton is bordered by a prominent NE-SW trending elevated physiographic region in the east known as the Eastern Ghats Belt (EGB) stretching from Nellore in the south to the Mahanadi Rift in the north (Figure 4.6). The belt comprises essentially highly deformed high-grade metamorphic rocks- charnockite (ortho-pyroxene-bearing quartzo-feldspathic gneisses, leptynite (garnet-perthite-quartz ± plagioclase gneisses) and khondalite (quartz-garnet-sillimanite-biotite ± graphite ± cordierite gneisses) (Ramakrishnan *et al.*, 1998). The Eastern Ghat gneisses have a general NE-SW trend, parallel to the overall trend of the belt and are transected by a number of later shears (Chetty, 1996). The contact between the Eastern Ghats and the Dharwar craton has been modelled as a sutured contact primarily based on a steep gravity gradient (Subrahmanyam, 1983).

The available isotopic age data suggest an extended history of evolution from Late Archean to latest Neoproterozoic. Rb-Sr and Sm-Nd model ages have yielded ages of ~3.0 to 2.9 Ga for the oldest khondalites and charnockites (Perraju *et al.*, 1979 and Paul et al, 1990). A ~2.6 Ga metamorphic event has been suggested by Perraju, *et al.* (1979). Rb-Sr whole rock ages (1200 –1400 Ma) obtained from one of the unreformed massive anorthosite bodies (alkaline plutons) by Sarkar *et al.* (1981) suggest the presence of a pre-1400 Ma granulite facies regional metamorphic episode. Recent isotopic data depicts metamorphic episodes at ~1000, 800 and 550-500 Ma (Shaw *et al.*, 1997; Mezger and Cosca, 1999) suggesting the EGB was intensely affected by Neoproterozoic tectonothermal activities (≅ Kibaran and Pan-African episodes of Africa).

(ii) The Southern Granulite Terrain

The *low-grade* granite-greenstone rocks of the Dharwar craton grade into the high-grade gneissic and charnockitic terrain to the south known as the Southern Granulite Terrain (SGT). The SGT is subdivided into two prominent blocks- (1) the Madurai Granulite Block (MGB) occupying the area between the southern transition zone of the Dharwar craton and the Achankovil Shear Zone (ASZ), and the Southern Khondalite Block (SKB) to the of ASZ. The MGB consists predominantly of charnockite massifs. These massifs comprise massive charnockite and enderbite with mafic granulite and high-grade metasedimentary enclaves and are surrounded by both ortho- and para-granitoid gneisses and amphibolite to granulite facies supracrustal rocks. The SKB comprises predominantly khondalites, calc-silicates, quartzites and amphibolites.

Geochronological data from south of the Palghat-Cauvery Shear zone is sparse. Single crystal zircon dates (zircon evaporation) suggest protolith ages of 2.4 Ga and ~2.1 Ga for meta-granites and charnockites respectively (Bartlett *et al.*, 1995 and Jayanand *et al.*, 1995). Neoproterozoic thermal events have been recorded from both the blocks of the SGT - ~1.65 Ga from Palghat area (Ghosh, 1999 – using conventional single zircon dating) and ~1.8 Ga from Southern Khondalite Block (Kelly *et al.*, 1997). Zircon evaporation ages of ~560 Ma have been reported from charnockites of Kodaikanal area (Barlett *et al.*, 1995; Jayanand *et al.*, 1995). Santosh *et al.* (1989) obtained ages between ~760 to ~550 Ma (Rb-Sr mineral isochrons) for a number of granitic bodies in the SGT. A granulite facies metamorphic event at ~550 to 520 Ma has also been reported from charnockites, khondalites and cordierite gneisses (Unnikrishanan-Warrior *et al.*, 1995; Jayanand *et al.*, 1995).

Until recently, no Archean age was reported from the SGT. However, Ghosh (1999) has obtained single crystal zircon dates of ~2.9 Ga from mafic granulites of the Namakkal area (Figure 4.6) and biotite gniesses from the Palghat area. Ghosh also reported ~2.5 Ga granites and tonalites from large areas of the SGT north of the Palghat-Cauvery Shear Zone (PCSZ). These dates suggest that the Dharwar craton may be extended farther south, at least up to the PCSZ.

d. Major Shear Zones of Peninsular India

A number of subvertical trans-continental shear zones with dominant strike-slip movement have been recognised (Drury and Holt, 1980, Drury *et al.*, 1994, GSI, 1994) based on Landsat imagery, structural trends and geophysical data. The three most important shear zones from north to south are- 1. The Moyar-Bhavani shear zone, 2. The Palghat-Cauvery Shear Zone and 3. The Achankovil Shear Zone (Figure

4.6). These shear zones have tectonic significance in a Gondwana sense due to their potential for correlation with similar zones in other Gondwana continents.

(i) The Moyar-Bhavani Shear Zone

The Moyar–Bhavani Shear Zone (MBSZ) is a part of a complex anastomising shear system of southern India. The east-west trending MBSZ splits into the WNW-ESE trending Moyar Shear Zone (MSZ) in the north and the arcuate NE-SW trending Bhavani shear zone (BSZ) in the south. Based on the swing in the regional strike from N-S through NE-SW to roughly E-W and finally to NE-SW from north to south, Drury and Holt (1980) interpreted the MSZ as a 20 km wide dextral shear zone. They also noted the presence of new planar and linear fabrics, extensive augen gneiss and retrogression in the high-grade metamorphic rocks along MSZ. The BSZ marks the southern limit of the Nilgir Hill Massif. The MBSZ bends to the NE in the eastern part and finally merges with the shears along the eastern boundary of the Cuddapah Basin that have affected the Neoproterozoic rocks. This observation lead Drury *et al.* (1984) to suggest a Neoproterozoic age for the MBSZ.

(ii) The Palghat-Cauvery Shear Zone (PCSZ)

The southern boundary of the intricate shear system of southern India is defined by the E-W trending Palghat-Cauvery Shear Zone (PCSZ). Though the PCSZ has not been well defined by the satellite imagery due to alluvial cover in most parts, later workers (GSI, 1994; Chetty, 1996) have documented the presence of the shear zone based on geological and geophysical evidence. Ramakrishnan (1993) considered the PCSZ as the southern boundary of the Dharwar craton. However, recent field observations, structural analysis and geochronological evidence (Ghosh, 1999) do not support this view.

(iii) The Achankovil Shear Zone (ASZ)

The Achankovil Shear zone (ASZ), south of the PCSZ, is a NW-SE trending shear zone that was first recognised by Drury *et al.* (1984) based on abrupt change in structural trends across it. The NNE-SSW strike of the lithological units in the north abuts against the lineament and changes to NW-SE in the south. Drury *et al.* (1984) have interpreted sinistral strike-slip movement along the ASZ. However, limited structural analysis shows the contrasting nature of the shear zone - dextral (Sacks *et al.*, 1997) and sinistral (Rajesh *et al.*, 1998). Geological mapping across the shear zone (GSI, 1995a & b) depicts a gradual change in the litho-tectonic strike across the lineament suggesting no significant strike-slip movement along this shear zone. Ghosh (1999) argued that the ASZ represents a flattened fold limb rather than a simple shear based on structural trend analysis.

(iv) The Karur-Kambam-Painavu-Trichur (KKPT) Shear Zone

Ghosh (1999) recognised this new shear zone (Figure 5.16) south of PCSZ based on striking contrasts in structural style and lithological assemblages across it. He related the arcuate nature of KKPT to a late regional fold axis. To the south of KKPT, the terrain is dominated by khondalite, paragneisses and abundant calc-silicates and quartzites. To the north, the area is predominantly underlain by granitic and tonalitic gneisses with mafic granulites, BIF and associated metasediments. Ghosh (1999) further reported ~2.5 Ga and 2.0 Ga old detrital zircons from khondalite and associated metasediments south of KKPT and dates older than ~2.9 Ga from the BIF and associated rocks north of KKPT.

Though it is likely that all these shear zones have suffered multiple phases of shearing and reactivation, recent structural and isotopic studies (Deters-Umalauf *et al.*, 1997; Ghosh, 1999) suggest that the MSZ, the BSZ, the PCSZ have evidence of a thermal peak between ~600 and 610 Ma and show an overall dextral sense of movement. However, there is no record of considerable strike-slip movement along any of these shear zones.

4.3.2. Enderby Land, East Antarctica

The coastal and near-coastal areas of East Antarctica between Enderby Land and Dronning Maud Land are composed of Precambrian metamorphic and plutonic rocks. The Napier Complex (Figure 4.7) is composed of high pressure-high temperature metamorphic rocks (granulite facies), whereas the Rayner Complex to the south (Figure 4.7) comprises both reworked rocks of the Napier Complex and Late Proterozoic igneous and metamorphic rocks formed by magmatic and sedimentary processes (Black *et al.*, 1987)

a. The Napier Complex

The Napier Complex, occupying the coastal areas of Enderby Land between 50°E and 58°E, is an Archean high-grade block surrounded by Proterozoic belts in the east, south and west (Tingey, 1991). The complex consists predominantly of gneissic enderbites, charnockites and granite gneisses with minor lenses and xenoliths of volcano-sedimentary supracrustal rocks (Kamenev, 1993). The supracrustal rocks include quartzite, meta-ultrabasites, meta-anorthosites and BIF schists. These rocks have suffered greenschist facies to ultra high-grade granulite facies metamorphism and polyphase deformation evident from the refolded recumbent folds, nappes and

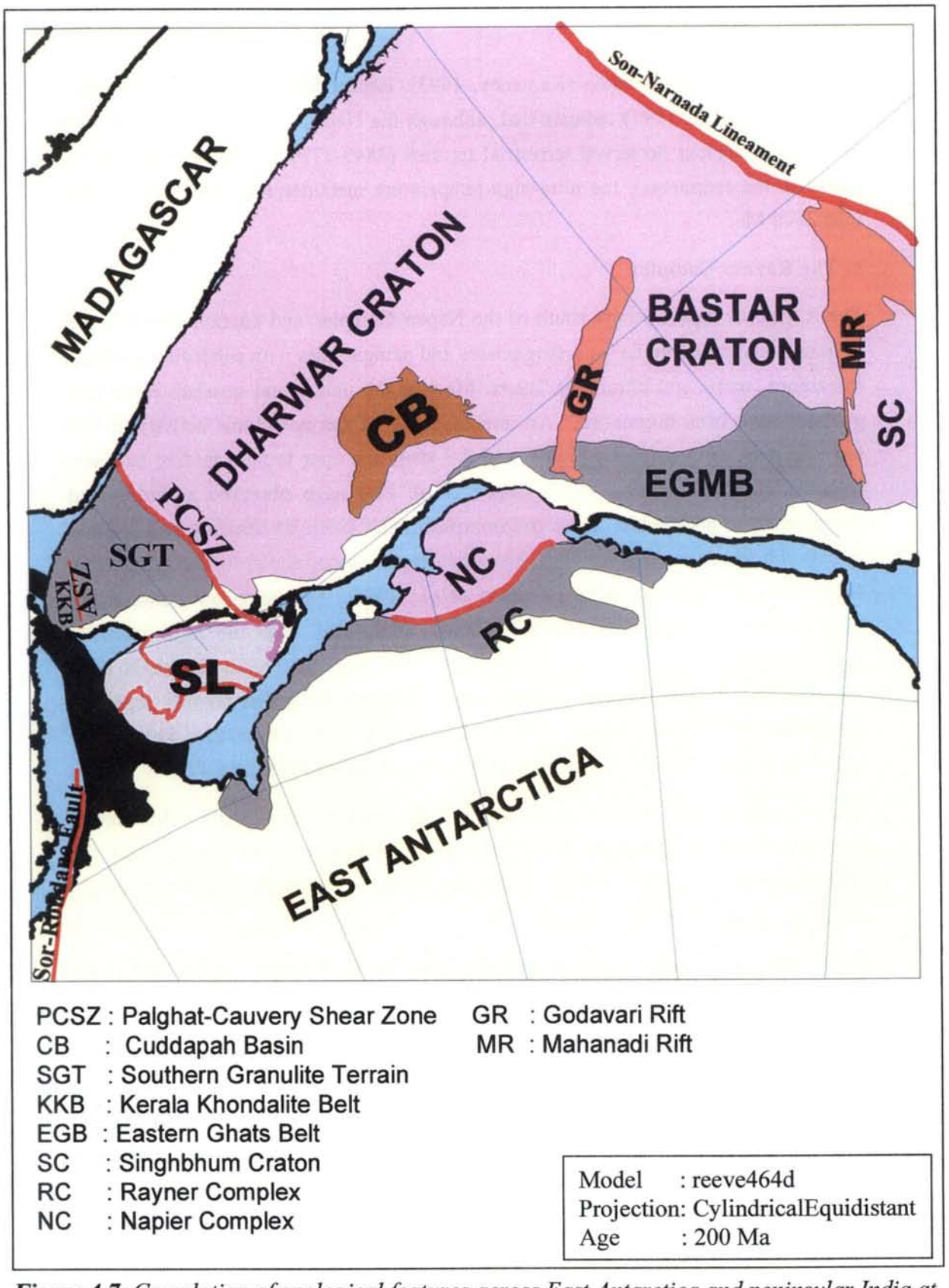

***Figure 4.7**: Correlation of geological features across East Antarctica and peninsular India at 200 Ma.*

tectonic layering by thrusting (Kamenev, 1993). Recent SHRIMP U-Pb zircon data (Harley and Black, 1997) indicate that, although the Napier Complex represents one of the most ancient preserved terrestrial terrains (3840-3770 Ma dates from detrital grains in the sediments), the ultra-high-temperature metamorphic event is not older than 2840 Ma.

b. The Rayner Complex

The Rayner Complex occurs south of the Napier Complex and contains amphibolite to transitional granulite facies orthogneisses and paragneisses with subordinate pelitic, calcareous, mafic and ultramafic layers. Most of the pelitic and quartzo-feldspathic gneisses have been migmatised. An intense phase of thermotectonic activity at 960 Ma with peak metamorphism (750°C and 7-8 kbar) and open to tight folding has been reported by Black *et al.*, (1987). Black *et al.* also have observed a widespread overprinting of greenschist facies metamorphism and localised shearing and faulting at 550-500 Ma (Pan-African). The Rayner Complex is correlated to the Proterozoic Granulite belts in South India (Yoshida *et al.*, 1996). The boundary between the Rayner and the Napier complexes, recently interpreted from the high intensity magnetic anomaly patterns by Golynsky *et al.* (1996), may be correlated with the east-west trending Palghat-Cauvery Shear Zone of southern India that broadly separates the Archean Peninsular gneisses in the north from Proterozoic migmatites, khondalites and charnockites (Project Vasundhara, GSI, 1994) in the south (Figure 4.6).

The two parallel NW trending shear zones in the southern tip of India - Achankovil Shear Zone and the Tenmallai Shear Zone (Figure 4.6) seem to be lined up with the western boundary faulted margin of the Sør Rondane mountains (Golynsky *et al.*, 1996) in a reassembled Gondwana.

4.3.3. Neoproterozoic Tectonothermal event in Peninsular India and East Antarctica

The area south of the PCSZ contains abundant evidence of Neoproterozoic activity (≡Pan-African), including amphibolite facies gneiss with a Rb-Sr whole rock date of 550 Ma (Hansen *et al.*, 1985). Garnet whole rock Sm-Nd dates of ~550 Ma and 450-350 Ma from the Kodaikkanal granulites south of the PCSZ have been interpreted as ages of peak metamorphism and cooling respectively by Jayananda *et al.*, 1995. Similar isotopic dates have been obtained from the Nagercoil charnockite massif in the southernmost tip of India with Sm-Nd mineral ages of 558-517 Ma and Rb-Sr (cooling) ages of 484-440 Ma (Choudhary *et al.*, 1992; Unnikrishnan-Warrier *et al.*, 1995). The ~500 Ma (Sm-Nd garnet whole rock ages) event has also been reported from the rocks of the Eastern Ghats Mobile Belt (Paul *et al.*, 1990,Yoshida *et al.*,

1995, Shaw *et al.*, 1996). Granitic intrusion at ~700 Ma and greenschist facies metamorphism at ~500 Ma have been identified in the Rayner Complex by Black *et al.* (1987). So both the Rayner Complex and the granulite terrains south of the PCSZ in southern India have similar overprint ages, equivalent to that of the Pan-African terrains of Africa.

4.3.4. Summary of Geological Correlation between southern India and Enderby Land, East Antarctica

The oldest ages reported from the rocks of the Archean craton north of the PCSZ range from 3.6 Ga to 2.6 Ga (Nutman *et al.*, 1992; Peucat *et al.*, 1995). The terrain south of the PCSZ has mostly 2.4-2.2 Ga Rb-Sr biotite ages (Peucat *et al.*, 1995). Recent isotopic study (Ghosh, 1999) suggests sporadic occurrence of Archean rocks south of PCSZ up to KKPT (Figure 2.14). A narrow belt of Mg-rich metapelites exposed as cordierite gneisses and charnockites (Achankovil metasediments), along the southern margin of the ASZ (Figure 4.6) is characterised by relatively younger Nd model-ages in the range of 1.5-1.2 Ga sharply contrasting with the Paleoproterozoic ages from the Kerala Khondalite Belt (Bartlett *et al.*, 1995; Brandon and Meen, 1995).

The Napier Complex forms the oldest known terrain in East Antarctica with model Nd ages ranging from 4.0 to 3.1 Ga (Harris *et al.*, 1996). Recent ion-microprobe studies in the Napier Complex have yielded dates of 2980±9 for emplacement of charnockite, a very high-grade tectonothermal event at 2837±15 Ma and a high-grade tectonothermal event ranging from 2456+8/-5 to 2481±4 Ma (Harley & Black, 1997).

Though, geochronologically, the Dharwar craton and the Napier Complex show similar evolutionary history, lithologically they are distinctly different. The Dharwar craton predominantly comprises a low-grade granite-greenstone assemblage, whereas the Napier Complex represents an Archean high-grade granulite terrain. The Dharwar craton grades into the Southern Granulite Terrain (SGT). Archean ages (~2.9 to 2.5) have been recorded from the transition zone between the low-grade Dharwar craton and the high-grade SGT (Ghosh *et al.*, 2000). This transition zone might represent the uplifted block of the extended Dharwar craton and is possibly the counterpart of the Napier Complex in Enderby Land, as both the terrains show evidence of granulite facies metamorphism at ~2.5 Ga and are virtually unaffected by the Pan-African tectonothermal activities.

The rocks of the Rayner Complex have been dated in the range of 2.3 to 1.3 Ga (model ages, Black *et al.*, 1987). These granulites have suffered charnockitisation and granitic magmatism between 550-525 Ma (Shirashi *et al.*, 1994). Thus, the boundary between the two contrasting terrains – the Napier and the Rayner complexes - might

represent a terrane boundary and can be a key to correlation with similar boundaries in India in a Gondwana reassembly. Several prospective shear zones, described as terrane boundaries in southern and eastern India, qualify for consideration as the Indian counterpart of the Napier-Rayner Boundary (NRB). Though kinematics of the Indian shear zones show Neoproterozoic activity, absence of such a record from the RNB makes it difficult for correlation. Ghosh, (1999) suggested a possible correlation between his KKPT and the RNB based on ages of granulites across these shear zones. This problem will be discussed in Chapters 5 and 6 with additional geophysical constraints.

4.4. East Antarctica – Sri Lanka

4.4.1 Sri Lanka

Sri Lanka, as a small Gondwana fragment, has attracted relatively little attention in most of the previous reconstructions. With a broad agreement on the paleopositions of major fragments – Africa, South America, Antarctica, India, and Australia – the focus now has turned to the smaller fragments – Madagascar, Sri Lanka and Seychelles - to fill the remaining gaps in Gondwana. Unlike Madagascar and Seychelles, Sri Lanka is located in a triangular gap surround by India, East Antarctica and East Africa. Thus Sri Lanka has the possibility of being a constituent part of any one or all of these three fragments.

Cooray (1994) has classified the widely distributed Precambrian rocks of Sri Lanka into three major lithotectonic units (Figure 4.8, Table 4.2) - a northwestern amphibolite to granulite facies terrain (Wanni complex: WC), a central granulite facies terrain (Highland complex: HC) and a southeastern amphibolite facies terrain (Vijayan Complex: VC). HC and VC have been separated by a thrust and the former is superposed over the later (Büchel, 1994). Structural and kinematic analysis suggests that the WC is thrust over the HC (Tani, 1997). Aeromagnetic studies in SW Sri Lanka have also substantiated the presence of three distinct lithotectonic units (Perera, 1997). The geology of the three lithotectonic units of Sri Lanka is summarised in Table 4.2.

4.4.2. Geochronology of Sri Lanka

Nd model ages from the Precambrian rocks of Sri Lanka (Milsenda *et al.*, 1988 & 1994) depict three distinct age provinces broadly corresponding to the three lithotectonic units (Figure 4.8). These data show that the initial crustal growth of the Highland Complex took place between 3.4 to 2.0 Ga, whereas that of the Wanni and the Vijayan Complexes occurred between 2.0 and 1.0 Ga. Kröner *et al.* (1991) have

shown that the regional high-grade metamorphism in the HC and WC occurred between 665 and 550 Ma, whereas earlier studies depicted peak metamorphism at ~1000 Ma (Burton and O'Nions, 1990 a&b). Intrusion of granitoids occurred between

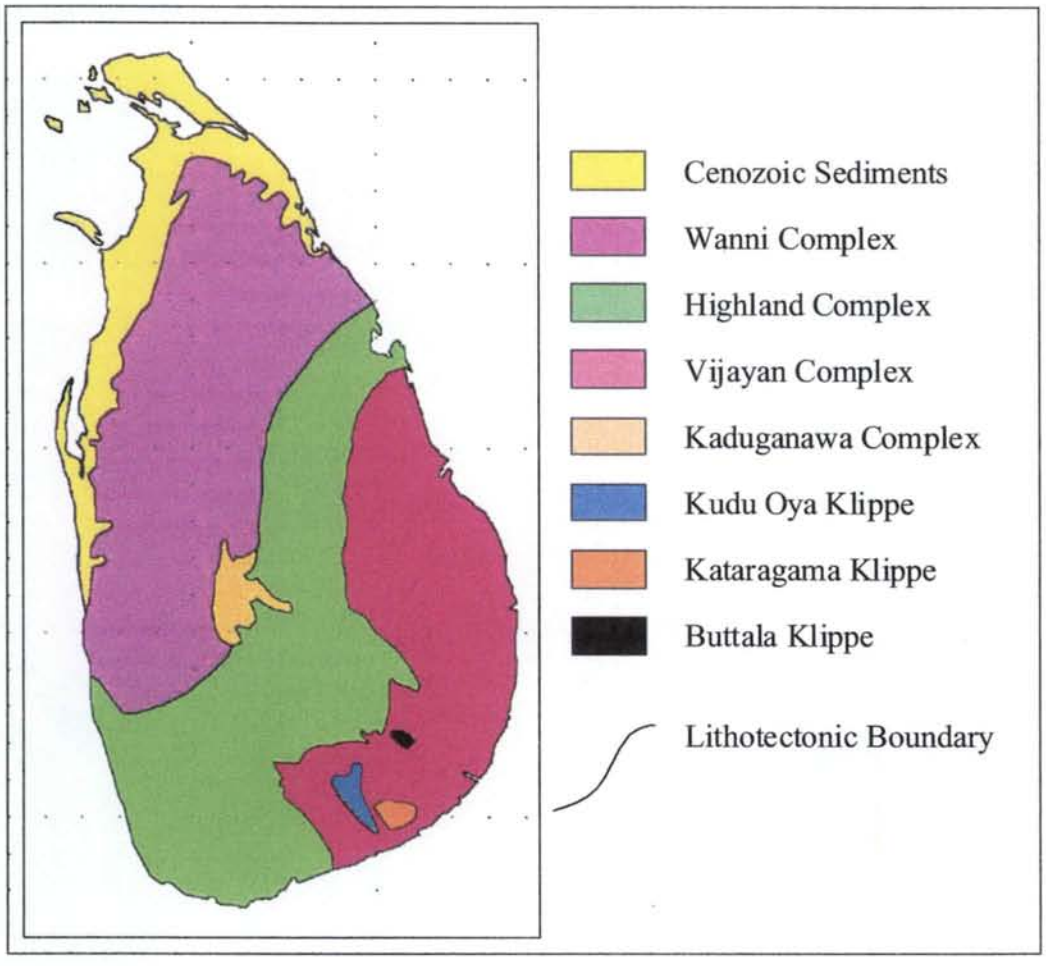

***Figure 4.8**: Generalised geological map of Sri Lanka showing major lithotectonic subdivisions (modified from Cooray, 1994)*

~1900 and 670 Ma in HC, ~1025 Ma in VC and ~ 1100 – 800 in WC (Hölzl *et al.*, 1994; Kröner *et al.*, 1994). Compilation U-Pb zircon ages by Shiraishi *et al.* (1994) with reference to the terrain boundaries (Milsenda *et al.*, 1994) suggest peak metamorphic ages of ~610-550 Ma in the HC, 550-500 Ma in the VC and ~1100 Ma in the WC. But Hölzl *et al.*, (1994) maintain that regional high-grade metamorphism in all the complexes occurred less than 670 Ma ago. Post tectonic granitoids and pegmatites have intruded throughout all the three complexes at ~550 Ma (Hölzl *et al.*, 1994).

4.4.3. Lützow-Holm Bay area, East Antarctica

The Lützow-Holm Complex (LHC in Figure 4.9) comprises calcareous, pelitic and quartzo-feldspathic metasediments intruded by basic and ultrabasic rocks (Shiraishi *et*

***Table 4.2**: Lithological and Geochronological correlation among three lithotectonic units of Sri Lanka*

	Vijayan Complex	Highland Complex	Wanni Complex
Lithology	Granitoid gneisses, migmatites, discrete metasedimentary xenoliths	Pelitic, intermediate and mafic gneisses and granulites, Quartzite and dolomitic marble, Charnockites, minor ultrabasic rocks	Granitoid intrusives (charnockite and migmatite gneisses, Pelitic gneisses, Quartzite and dolomitic marble
Geochronology	Initial Crust formation: 1000 – 1800 Ma Plutonism : ~1000 Ma Peak Metamorphism : 500 – 550 Ma	Initial Crust formation: 2000 - 3000 Ma Granulite facies Metamorphism, Folding and Charnockitisation: 550 – 610 Ma	Initial crust formation: 1000 – 1200 Ma Amphibolite to granulite facies metamorphism : ~1100 Ma Charnockitisation : 530 – 590 Ma

al., 1994). Ubiquitous occurrence of isolated blocks of ultramafic rocks within the metasediments is significant due to the fact that these rocks represent derivatives of various parts of layered mafic complexes (Hiroi *et al.*, 1991). The LHC is bounded by the Late Proterozoic Rayner Complex in the east and the Yamato-Belgica Complex (YBC) in the southwest. The metamorphic grade of the LHC increases from upper amphibolite facies in the east to granulite facies in the SW and decreases again to amphibolite facies in the Yamato- Belgica area further southward (Hiroi *et al.*, 1991).

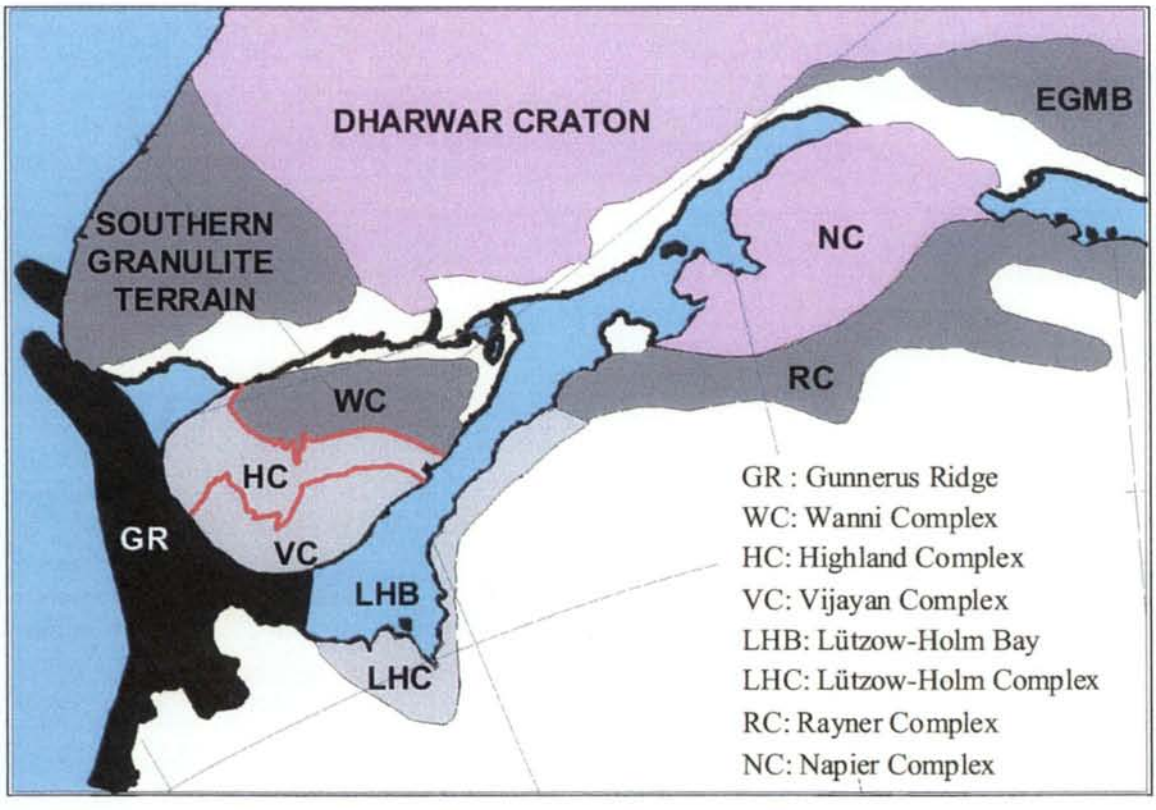

***Figure 4.9**: Geological correlation between the Lützow-Holm Complex, Enderby Land, Antarctica and Sri Lanka (modified from Shirashi et al., 1994). Reconstruction model reeve464d at 200 Ma by Reeves (pers. comm.2000).*

A transitional zone of amphibolite facies – granulite facies occurs in the Prince Olav Coast. High-grade granulite facies rocks predominantly occur in the Lützow-Holm Bay area. The rocks have been subjected to at least two phases of deformation- early isoclinal to tight folds with axial planes trending NW-SE to N-S and later open to tight cross folds with axial planes E-W to NE-SW (Shiraishi *et al.*, 1985 referred in Shiraishi *et al.*, 1994). The D1 folds are contemporaneous with the regional metamorphism. Two phases of discordant mafic dyke intrusion have been reported from the LHC (Shiraishi *et al.*, 1988). The older dykes are deformed and

metamorphosed to the same grade as of the host rocks and the later ones are undeformed and only slightly metamorphosed.

Rb-Sr whole-rock isochron dates ranging between ~680 and ~1200 Ma (Shibata *et al.*, 1986 referred in Shiraishi *et al.*, 1994) suggest a Neoproterozoic metamorphic event. However, ion microprobe U-Pb (SHRIMP) data (Shiraishi *et al.*, 1994) show the presence of ubiquitous ~500-550 Ma dates over the entire area except three locations with ~1000 Ma dates indicating high-grade regional metamorphism and intense folding during Early Cambrian rather than Neoproterozoic. This observation suggests that the ~1000 Ma (Kibaran/Grenvillan) deformation is highly obscured by the intense Pan-African deformation. Thus, it casts doubt on the very existence of a ~1000 Ma orogeny in these areas. The ~1000 Ma ages obtained from 3 locations may represent protolith ages rather than being a wide-spread orogenic episode, as reported from northern Mozambique recently (Jamal, *pers. comm.*, 2000)

4.4.4. Discussion

Recognition of ~500 Ma tectonothermal events in the East Antarctica Shield provides significant evidence for an improved fit to the relative locations of the once contiguous fragments of Gondwana. Shirashi *et al.* (1994) have shown a ubiquitous presence of ~500-550 Ma dates from different parts of the LHC that signifies a widespread regional metamorphism during Neoproterozoic (≅Pan-African) period. This result also shows that the regional granulite metamorphism in the LHC coeval to that of ~500 Ma in the adjacent Rayner Complex. Study of geochronological data from Sri Lanka clearly exhibits 550-610 Ma metamorphic ages for the high-grade granulite rocks of the Highland Complex.

Moreover, other geological attributes - lithology, tectonic deformation and metamorphic history - of the Highland Complex of Sri Lanka and the Lützow-Holm Complex of East Antarctica show marked similarities between them. Presence of lithological assemblage of dolomitic marbles, quartzites and pelitic gneisses in both the terrains suggest a shallow-water continental margin or intracontinental basin depositional environment. Both the terrains comprise upper amphibolite to granulite facies metasediments, gneisses and granulites of Paleoproterozoic to Neoproterozoic-Early Paleozoic ages and intruded by granitoids at ~500 Ma. The high-grade granulite facies rocks of the Lützow–Holm Bay area, in particular, are similar to those of the Highland Complex. Both the terrains suffered intense deformation accompanied by granulite facies metamorphism during Pan-African times (~550 Ma). Thus it is evident from the above geological considerations that both the terrains formed parts of a continuous Proterozoic Province that suffered peak metamorphism during Pan-African time. However, the Wanni Complex also suffered a peak metamorphism at

~1100 Ma (Burton and O'Nion, 1990), much earlier than that of the Highland Complex. This metamorphic event might be correlated with the ~1000 Ma metamorphic event of the Rayner Complex. The geological correlation between these two terrains is summarised in Table 4.3.

***Table 4.3**: Geological correlation between the Lützow-Holm Complex, East Antarctica and the Highland Complex, Sri Lanka*

	Lützow-Holm Complex (East Antarctica)	**Highland Complex (Sri Lanka)**
Lithology	Pelitic, intermediate and mafic gneisses and granulites; Quartzites and dolomitic marble; Migmatites in the east, Granites and pegmatites	Pelitic, intermediate and mafic gneisses and granulites; Quartzites and dolomitic marble; Charnockites; minor ultrabasic rocks
Deformation	NW-SE to N-S trending early isoclinal to tight folds; E-W to NE-SW trending later tight to open folds	Early recumbent, isoclinal folds; Later upright open folds superimposed on earlier folds
Metamorphism	Upper amhibolite facies in the east; Granulite facies in SW; Peak meta-morphism at 800-850°C and 7-8 kbar	Upper amhibolite to granulite facies Peak metamorphism at 700-900°C and 5-9 kbar
Geochronology	~2900-1500 Ma : Upper Intercept of in metasediments ~520-550 Ma : Upper amphibolite to granulite facies metamorphism; Folding ~500 Ma: Granite and pegmatite intrusion	3000-2000 Ma : Initial crust formation 550-610 Ma : Granulite facies metamor-phism; Folding; Charnockitisation ~550 Ma: Granite and pegmatite intrusion

4.5. India - Sri Lanka

The geological details of southern India and Sri Lanka are described in sections 4.3.1 and 4.4.1 respectively. A detailed account of the geochronological correlation between theses two terrains is discussed in this section.

4.5.1. Geochronologic Correlation

Systematic isotopic studies (model Nd-ages) of the Precambrian rocks of Sri Lanka have revealed three distinct age provinces (Milisenda *et al.* 1988,1994), broadly corresponding to the three lithotectonic units. The model ages of the rocks of the Highland Complex, the oldest of the three provinces, ranges from 2.9 to 1.9 Ga, that can be compared with the spread in model Nd ages from the KKB of south India (Figure 4.6). The rocks of the Wanni Complex range in ages from 1.9 to 1.2 Ga and can be correlated with the rocks of the Achankovil metasediments (1.4-1.2 Ga) from southern India. The Vijayan Complex forms the youngest age province in Sri Lanka

with model Nd ages ranging from 1.5 to 0.8 Ga, that finds no correlatable rocks in southern India.

4.5.2. Neoproterozoic (≅Pan-African) Event

Pan African tectonothermal events have been identified in all the three lithotectonic units of Sri Lanka. The latest tectonothermal activity in the Highland Complex, represented by ductile faults, gentle folds, granite-pegmatite intrusion and incipient charnockite formation under low pressure amphibolite facies conditions, has been dated in the range of 450 to 570 Ma (Kröner *et al.*, 1987; Kagami *et al.*, 1990; Hölzl, 1991). The Wanni Complex has suffered the latest phase of metamorphism at ~500 Ma (Rb-Sr and Sm-Nd mineral isochron ages by Hölzl *et al.*, 1991). U-Pb zircon studies of the rocks of the Vijayan Complex by Kröner *et al.* (1987) have revealed that a metamorphic event occurred at ~550 Ma. Incipient charnockite formation has been recorded from both the granulite terrains in South India and NW Sri Lanka. The youngest of these charnockites from both the terrains has been dated at ~500 Ma (Yoshida & Santosh, 1994) suggesting a simultaneous deformation and metamorphic phase during Pan-African time.

4.6. India - Madagascar

4.6.1. Madagascar

The Precambrian geology of Madagascar has been summarised by Windley *et al.* (1994). The Precambrian rocks of Madagascar are cut across by a NW-SE trending tectonic lineament, the Ranotsara Shear Zone (RSZ in Figure 4.10) in the south-central part. Southern Madagascar south of the RSZ is predominantly occupied by paragneisses mostly deformed and metamorphosed under granulite and upper amphibolite facies conditions, whereas areas to the north of the RSZ are predominantly underlain by granitic orthogneisses, migmatites and sparse volcano-sedimentary sequences (Windley *et al.*, 1994, Kröner *et al.*, 2000). Traditionally, the RSZ is regarded as the boundary between predominantly Neoproterozoic rocks of the south and the Late Archean rocks of the north. But the extent of Archean basement in Madagascar has been questioned by recent workers (Paquette and Nédélec, 1998, Tucker *et al.*, 1999, Kröner *et al.* 2000, Collins *et al.*, 2000) based on geochronological evidence.

a. Northern Madagascar

Collins *et al.* (2000) have subdivided the Precambrian terrain to the north of RSZ into five tectonic units (Figure 4.10) separated from each other by a shear zone or a

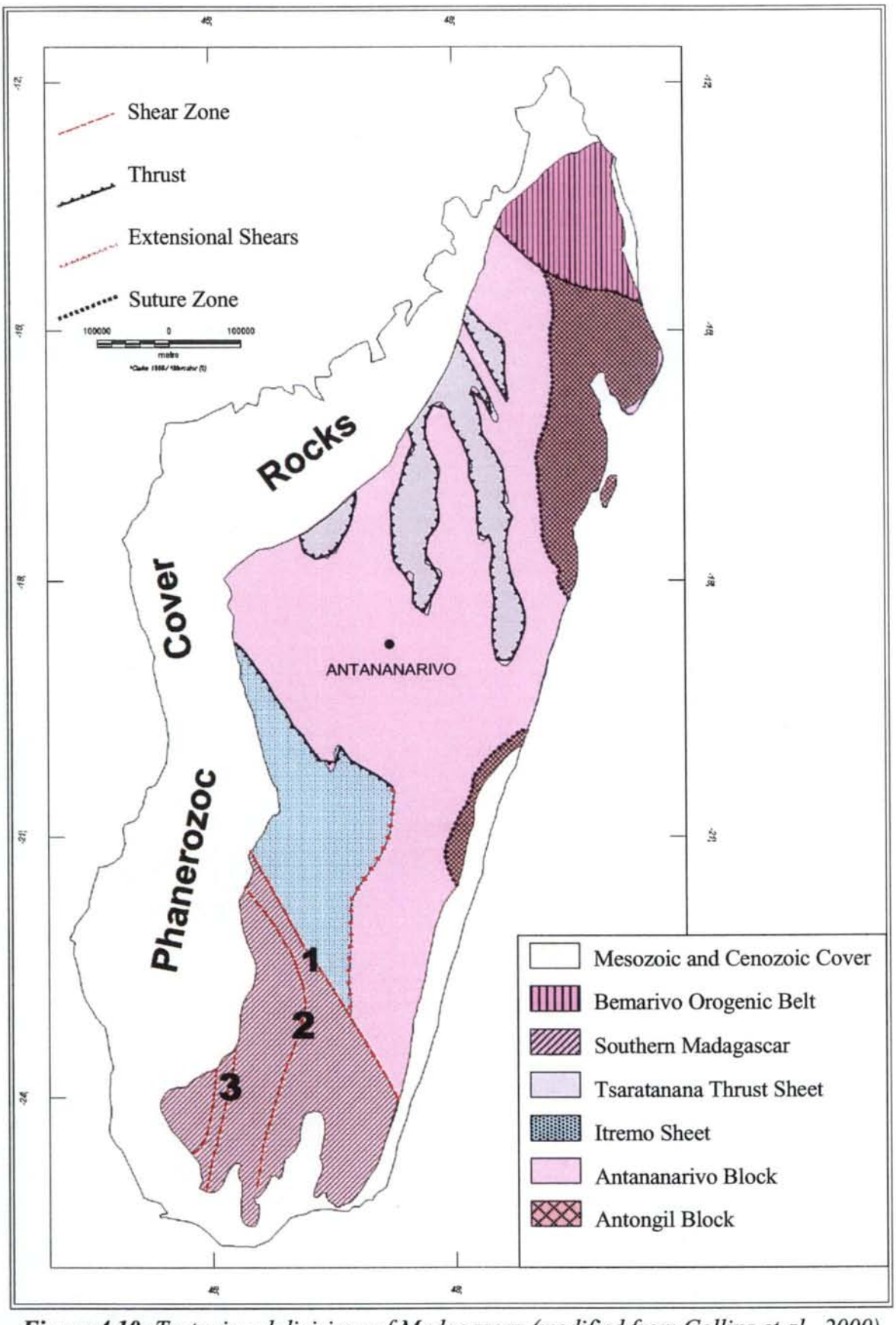

***Figure 4.10**: Tectonic subdivisions of Madagascar (modified from Collins et al., 2000) 1: Ranotsara Shear Zone(RSZ), 2. Vorokafotra Shear ,3. Ampahiny Shear.*

regionally significant unconformity. The Antonglil block comprises Archean gneisses and granite, which have escaped Proterozoic high-temperature metamorphism and deformation. The Antananarivo block consists of granulites, orthogneisses and granites and was thrust over the Antongil block from west to east in Late Proterozoic. Collins *et al.* (2000) have interpreted the boundary between these two blocks as a suture zone (Betsimisaraka suture). The Antananarivo block is structurally overlain by the Itremo sheet to the southwest and the Tsaratanna thrust sheet to the east and north. The Itremo sheet comprises Mesoproterozoic sediments thrust from west to east over the Antananarivo block between 1850 and 800 Ma. The Tsaratanana thrust sheet consists of Archean mafic and granitic gneisses that was thrust over the Antananarivo block before 890 Ma and deformed again during the closure of the Betsimisaraka suture. The Bemarivo orogenic belt in the north was thrust from northeast to southwest over the already amalgamated Antananarivo-Tsaratanana-Antogil tectonic unit during Late Cambrian.

b. Southern Madagascar

Southern Madagascar south of the Ranotsara Shear Zone comprises a complex Precambrian terrain of high-grade metamorphic rocks with a history of polyphase deformation during Neoproterozoic (de Wit *et al.*, 2000) The area has been divided into six tectonic belts (Windley *et al.*, 1994) based on variation in structural style across major shear zones described below.

(i). The Ampanihy and Vorokafotra Shear Zones:

The Ampanihy and Vorokafotra shear zones, the three major Neoproterozoic ductile shear zones, cut the terrain in a ~ north-south direction in southern Madagascar. Three phases of shear deformation between 608 and 650 Ma have been reported from the area (de Wit *et al.*, 1998 and 2000). The early phases (D_1 and D_2) of simple shear deformation during 650 – 620 Ma produced east-verging recumbent folds and ductile thrusts. The late phase (D_3) produced subvertical S-tectonites between 608 and 610 Ma.

(ii). The Ranotsara Shear Zone

The Ranotsara Shear Zone (1 in Figure 4.10) comprising NE-SW trending en echelon shears divide the Malagasy shield into a southern Proterozoic gneissic and schistose terrain and a northern Mid-Late Archean ortho- and paragneisses. De Wit *et al.* (1998 and 2000) have established a left lateral movement of these en echelon shears that have developed during the last phase of the Pan-African thermal episode between 550 and 520 Ma.

4.6.3. India – Madagascar fit

Geometrically, the west coast of India and east coast of Madagascar fit well along their straight coastlines, when juxtaposed. Recent geochronological studies (Paquette and Nédélec, 1998; Tucker *et al.*, 1999; Kröner *et al.*, 2000; Collins et al, 2000) have revealed that the extent of pristine Archean crust is limited only to the northeastern part of Madagascar (Antongil and parts of Antananarivo blocks in Figure 4.10). Though few Late Archean protolith ages (Tucker *et al.*, 1999; Kröner *et al.*, 2000) have been reported from the Antananarivo block in central Madagascar, the rocks of central Madagascar have mostly been affected by wide-spread magmatism during 800- 530 Ma. A widespread high-grade metamorphic event ~550 Ma has been recorded from most parts of central and southern Madagascar. Notable absence of Kibaran-Grenville (~1000 Ma) age magmatism and metamorphism in Madagascar suggests that it did not play a major role in the accretionary history and formation of Rodinia, as thought earlier. On the contrary, the ~550 Ma granulite facies metamorphism, similar to those in southern India and Sri Lanka, probably reflects the timing of amalgamation of East and West Gondwana.

The southern regions of both India and Madagascar comprise complex Precambrian terrains of high-grade metamorphic rocks with polyphase deformational history and late charnockite formation. These terrains also have been subjected to intense deformation and granulite facies metamorphism during Late Neoproterozoic and Early Paleozoic (Pan-African) resulting in the development of a number of ductile shear zones (Ampanihy and Vorokafortra shear zones in Madagascar and Achankovil and Palghat-Cauvery shear zones in southern India, Figure 4.11). A number of reconstructions between India and Madagascar have been attempted based on correlation of these shear zones. Similarity in metamorphic history between the rocks south of the ASZ in South India (~558 Ma by Choudhary *et al.*, 1992) and immediately south of RSZ in Madagascar (560-580 Ma by Paquette *et al.*, 1994) led Windley *et al.* (1994) to correlate the ASZ with the RSZ. Rajesh et al (1998), on the basis of kinematic analysis of the asymmetric features along the SW edge of the ASZ, have concluded that the ASZ indicated primarily dextral shear and ruled out the possibility of ASZ being the eastern counterpart of the Ranotsara Shear Zone that is sinistral in nature. But Sacks *et al.*, (1997) have recorded both sinistral and dextral sense of movement along ASZ, supporting the views of Windley *et al* (1994). De Wit *et al.*, (1995) and Harris *et al.*, (1996) have linked the Ranotsara Shear Zone with the Palghat-Cauvery Shear Zone based on lithological and geochronological similarities. But recent structural and geochronological work by Ghosh (1999) suggests a link between the RSZ and Karur-Kambam-Painvu-Trichur Shear (KKPT in Figure 2.14).

The crystalline basement rocks of Southwestern India are composed of Late Archean gneisses which were subjected to high-grade metamorphism around 2500 Ma and a high-grade metamorphic event in the far south during Late Neoproterozoic times (Jayanand and Peucat, 1995; Barlett *et al.*, 1998; Raith *et al.*, 1999). Kröner *et al.* (2000) argue that lack of ~820 to 720 Ma magmatism, a prominent event in Madagascar and Sri Lanka, in southern India does not support a direct link between Madagascar and India. But Ghosh (1999 and 2000) has recorded a number of Neoproterozoic thermotectonic events in southern India including granitic intrusions at ~800 to ~525 Ma. Thus Kröner's argument based on the non-existence of ~800 Ma magmatism in southern India does not find favour. Moreover, the Neoproterozoic (~548 Ma) charnockitisation identified in southern India (Ghosh, 1999) is also present in southern and central Madagascar (~550 Ma high-grade metamorphic event, de Wit *et al.*, 2000; Kröner *et al.*, 2000). Thus, juxtaposition of southern India and Madagascar appears to have firm footing. Synthesis of lithology and geochronology of both Madagascar and southern India leads to the following conclusions.

1. Both the western Dharwar craton and the Antongil Block of northwestern Madagascar consist of Archean (> 3.0 Ga) gneisses, granites and metasediments. The rocks have been subjected to greenschist to lower amphibolite facies metamorphism and have escaped Neoproterozoic thermotectonic events.

2. Archean protoliths in southern India extends farther south of the PCSZ at least up to KKPT (Figure 2.14) thus contradicting the concept of PCSZ being the southern boundary of the Dharwar craton. Neoproterozoic (~800 to 520 Ma) thermotectonic activities (magmatism and granulite metamorphism) have been recorded as far north as the 'Fermor line'[1] (Fermor, 1936). Similarly, recent geochronologic studies suggest sporadic Archean protolith ages (~2500 Ma, Tucker *et al.*, 1999; Kröner *et al.* 1999) for the rocks of the Antananarivo block. These rocks have suffered magmatism and high-grade metamorphism during ~800 to ~550 Ma.

3. Ortho- and paragneisses and the Neoproterozoic charnockites of southern Madagascar are similar to those in southernmost part of India. The only Paleoproterozoic (~2250 Ma) age from southern Madagascar suggests the presence of

[1] *Fermor (1936) divided Peninsular India into a charnockitic terrain in the south and east, and a non-charnockitic terrain in the north. The rocks of the charnockitic terrain retain evidence of intense ductile deformation and high-grade metamorphism. The charnockitic terrain was considered a mobile belt adjacent to the non-charnockitic terrain, the Dharwar craton. Fermor considered that the boundary between these two provinces represents a fundamental litho-tectonic boundary along which there must have been considerable vertical movement. This boundary, since then, is known as the 'Fermor line'.*

limited remobilised basement rocks, as in the case of southern India. de Wit et al (2000) have also reported ~2500 Ma basement rocks in southern Madagascar.

4. The shear zones both from southern India and southern Madagascar bear evidence of reactivation during Neoproterozoic (~550 to ~600 Ma). Present knowledge on the geochronology of southern India and Madagascar supports a probable link between the KKPT and RSZ that constrain the position of Madagascar with respect to southern India in a predisruption configuration.

4.7. Madagascar - East Africa

The paleoposition of Madagascar is crucial due to its location in the transition zone between East and West Gondwana in almost all reconstructions. Recent geochronological and structural studies both in Madagascar and in East Africa have clarified the long-standing idea of Madagascar being a remobilsed Archean fragment belonging to East Gondwana. A summary of geology of the East African terrains and its comparison with that of Madagascar is given here.

4.7.1. East Africa

a. The Tanzania Craton

The Late Archean Tanzania Craton in Tanzania, western Kenya and south-eastern Uganda comprises predominantly high-grade orthogneissic granitoids in the south and low-grade volcano-sedimentary supracrustal sequences intruded by shallow level granitoid plutons in the north (Borg and Shackleton, 1997). It is limited to the east and south-east by the Paleoproterozoic Usagaran Belt (2.0 –1.8 Ga) and the Neoproterozoic (900-500 Ma) Mozambique Belt. To the southwest, the Tanzania Craton is bounded by the Paleoproterozoic (2.0 Ga) Ubendian Belt and westward by the Neoproterozoic Karagwe-Ankolean belt and early Paleozoic Bukoban system (Borg and Shackleton, 1997). The northern limit of the craton is uncertain. The granite-greenstone association grades into the complexly deformed Ugandan Basement Gneisses of northern Uganda (Cahen *et al.*, 1984). The granitoid gneisses have yielded ages between 2.93 and 2.53 Ga (Maboko, 2000 and Pinna *et al.*, 1999).

b. East African Orogen

The East African Orogen (Figure 4.11; Stern, 1994; Meert and Van der Voo, 1997) includes the low-grade terrains of the Arabian-Nubian shield in the north and the high-grade gneissic assemblages known as the Mozambique belt (Kennedy, 1964; Pinna *et al.*, 1993; Shackleton, 1996). The belt extends over 2500 km along the

eastern part of Africa from Egypt to Mozambique making it one of the longest orogenic belts in the world.

The near-coastal belt along the east coast of Africa extending from northern Mozambique to northern Somalia through Tanzania and Kenya (Mozambique Belt) is composed mainly of high-grade gneiss, granulite, migmatite and orogenic plutonic rocks of Neoproterozoic age (Pinna *et al.* 1993). Low-grade metasedimentary rocks unconformably overlie the Mozambican basement and both the basement and cover rocks have suffered deformation and metamorphism during Pan-African time (800-550 Ma). In northern Mozambique, emplacement of granitoids between ~850 to 1100 Ma) has been reported by Pinna *et al.* (1993) and Kröner *et al.*, (1997). Both Kibaran (~1300 –1000 Ma) and Pan-African (~550 Ma) ages have been reported (Pinna *et al.*, 1993; Kröner *et al.*, 1997; Jamal *et al.*, 1999) from areas south of the Lurio Belt in central Mozambique. Recent SHRIMP dating by Jamal (*pers. comm., 2000*) does not show significant Kibaran-age crustal material in northern Mozambique. But Nd model ages from the southern Tanzania segment of the Mozambique Belt lie in the range of 1400 to 900 Ma (Möller, 1994). Thus, the northern extent of the Kibaran orogeny in the East African Orogenic Belt is still uncertain and needs further field and isotopic studies.

c. Karoo Rift Basins of Eastern Africa and Madagascar

A number of Permo-Triassic rift basins (Karoo basins) constitute the bulk of the coastal plains of both East Africa and western Madagascar (*e.g.* Henkel, 1994; van Heiningen, 1997). In Tanzania, the Karoo basins (Kreuser *et al.*, 1990; TPDC, 1995) are represented by the NE trending Selous and Ruvu basins which are separated from the north-south trending Jurassic rift basins (Ruvuma, Mandawa and basins). The Western Madagascar comprises an extensive sequence of gently westerly dipping Phanerozoic sedimentary rocks within three basins, referred to, from north to south, as the northeast Diego and Majunga basins and the ~ north- south Marondova basin (Figure 4.11).

The Selous basin of east Africa and the Mujanga basin of SW Madagascar (Figure 4.11) represent the complimentary parts of a pre-drift Karoo basin. Presence of a Mid-Jurassic break-up unconformity separating non-marine Karoo clastics and lacustrine shales from overlying marine carbonates, marls, shales (Clifford, 1986) in both the basins is a strong evidence for their spatial continuity prior to the break-up in Mid-Jurassic. The enormous amount of sediment accumulation between Upper Carboniferous and Mid-Jurassic indicates that the rift developed for more than 100 Ma before drifting started. Thus, the re-assembly of Karoo rift basins in east Africa and Madagascar is by far the strongest evidence for a predrift juxtaposition of East

Africa and Madagascar. The paleomagnetic studies (Rakotosolofo *et al.*, 1999) and aeromagnetic studies (Yardimcilar and Reeves, 1998) also strongly corroborate the fit achieved by correlating Karoo rift basins of the conjugate fragments.

4.7.2 Madagascar-East Africa link

Madagascar is placed between West and East Gondwana in most reconstructions (*e.g.* Reeves *et al.*, 1986/87; Kriegsman, 1995; Groenewald et al., 1995). Recent advances in geochronological (Paquette and Nédélec, 1998; Tucker *et al.*, 1999; Collins *et al.*, 2000; Kröner at al., 1999), paleomagnetic (Rakotosolofo *et al.*, 1999) and geophysical studies (Yardimcilar, 1998) have substantiated earlier views and helped in achieving a tighter reassembly of Madagascar with East Africa. Identification of widespread ~800 to 550 Ma magmatism and high-grade metamorphism in both the terrains suggests much of Madagascar was a part of the broader East African Orogeny which developed due to collision between East and West Gondwana during Neoproterozoic times. The Archean terrains in the northeastern part of Madagascar, probably, were the western extension of the Dharwar craton of India in East Gondwana, which collided with the Tanzania craton and adjacent Precambrian terrains.

4.8. Discussion

From the extensive literature survey it is concluded that central Gondwana, comprising eastern and southern Africa, East Antarctica, Sri Lanka, southern India and Madagascar, comprised a number of Pre-Kibaran shields (including Archean cratonic nucleii and Paleo-Mesoproterozoic mobile belts cratonised prior to Kibaran orogeny). These shields are separated by Late Mesoproterozoic (Kibaran-Granville) to latest Neoproterozoic-Early Paleozoic (Pan-African) orogenic belts. The comparable cratonic fragments include the Kalahari craton (Kaapvaal and Zimbabwe cratons) and Tanzania cratons of Africa, the Grunehogna Province of East Antarctica and the Dharwar, Bastar and Singhbhum cratons of south and central India ranging in age from 4.0 to 2.5 Ga. The Proterozoic mobile belts comprising the Natal-Namaqua belt and East African Orogenic Belt of southern Africa, the Maudheim province of East Antarctica, the Highland Complex of Sri Lanka, the Southern Granulite Terrain of India and the Neoproterozoic granulite terrains of southern and central Madagascar constitute a network of mobile belts formed by collision among Pre-Kibaran shields during formation of Rodinia and/or Gondwana. The presence of Permo-Carboniferous intracontinental sedimentary basins associated with syndepositional tectonism in Africa (Karoo sediments and volcanics), India (Gondwana basins) and similar basins in western Madagascar is indicative of similar paleoclimatic conditions during the

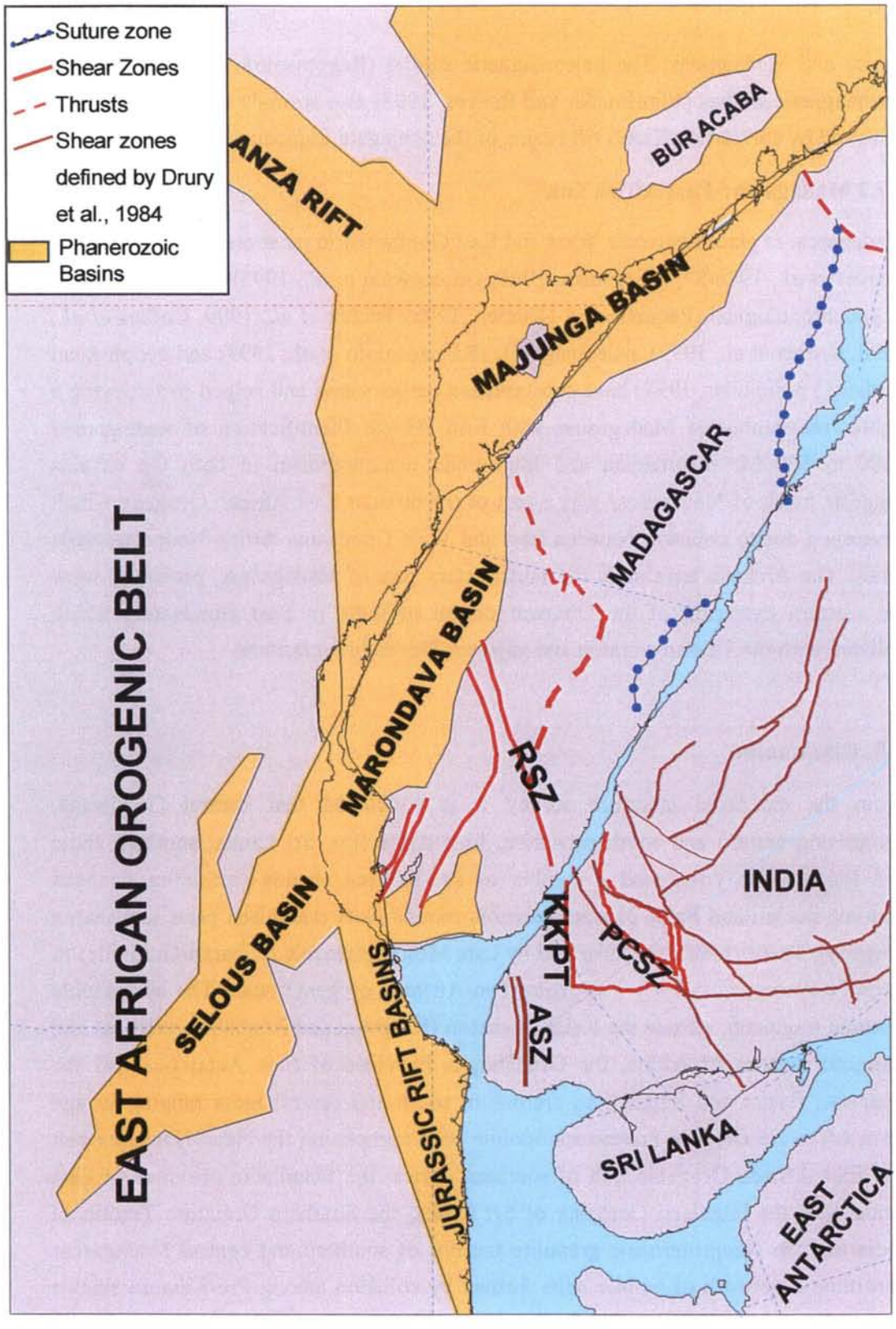

***Figure 4.11**: East Africa Madagascar fit based on correlation of Phanerozoic rift basins. Note the alignment NE-SW trending Permo- Triassic basins (the Selous basin in Tanzania and the Marondava basin in Madagascar) in the reassembly. The Selous-Marondava basin was separated by the N-S East African Jurassic rifts.Reassembly model: reeves506.*

Upper Palaeozoic period. Syndepositional magmatism in the Karoo basins is interpreted to be related to an extensional tectonothermal regime in the east coast of Africa during initial rifting between West and East Gondwana.

Though it is certain that Madagascar was a part of East Africa during Paleozoic and Upper Mesozoic period, its association prior to the close of Mozambique Ocean is still uncertain. There might be three possible cases – 1. part of India, 2. part of East Africa or 3. parts of both India and East Africa. Recent geochronological, structural and tectonic studies (*e.g.* Tucker *et al.*, 1999; Kröner *et al.*, 1999 and 2000; Collins *et al.*, 2000; de Wit *et al.*, 2000) favour the first and/or last case due to the following reasons.

1. The Archean Antongil block (Figure 4.10) was a part of the Dharwar craton. Both these terrains are comprised of gneisses and granitoids of >3.0 Ga and have escaped Proterozoic high temperature metamorphism and deformation.

2. The granitoids of Antananarivo block that have yielded both Late Archean to latest Proterozoic ages are geochronologically similar to those of the high-grade granulite terrain (refer to transition zone in Figure 2.14).

3. Southern and south-central Madagascar with a pronounced high-grade metamorphic event at ~ 550 Ma might be the western extension of the Southern Granulite Terrain of India. Identification of this high-grade metamorphic event in southern India, southern and central Madagascar and East African Orogenic Belt suggests these terrains were already in physical continuity prior to ~550 Ma. So the amalgamation of East Gondwana and West Gondwana as a result of closure of the Mozambique Ocean must have taken place before 550 Ma, producing the high-grade metamorphism common to both areas. The extensive shear zones both in southern India and Madagascar suggest significant compression in both the terrains at ~620-600 Ma. Thus, the collision process might have started as early as ~620 Ma and must have completed before the high-grade metamorphic event at ~550 Ma.

5. COMPILATION AND INTERPRETATION OF AEROMAGNETIC DATA, SOUTHERN INDIA

This chapter consists of two sections. Section 'A' deals with the methodology used for compilation, processing and visualisation of aeromagnetic data of southern India. Results of the interpretation of processed data are described in Section 'B'. The aeromagnetic and the geological maps are enclosed at the end of the Chapter.

A. Aeromagnetic Data Compilation

5.1. Status of Aeromagnetic Survey in India

Airborne geophysical survey operations in India started in 1967, and since then over 1670 000 km^2 have been covered by multisensor and aeromagnetic surveys (GSI, 1995c). Parts of western and eastern India were covered using multisensor surveys by American companies under the Operation Hard Rock Project during 1967-68. In the second phase, parts of western and central India were covered by BRGM/CGG of France during 1971-72. Large parts of the Son-Narmada Lineament and the Cuddapah basin were covered during 1978-81 for tectonic studies. Regional aeromagnetic surveys of parts of southern and eastern India were carried out by the National Remote Sensing Agency of India (NRSA) under the National Programme of Aeromagnetic Survey project. The Airborne Mineral Surveys and Exploration (AMSE) wing of the Geological Survey of India has been engaged in multisensor airborne geophysical data acquisition since 1986 with its Twin Otter aircraft. AMSE has covered over 73 000 km^2 by aeromagnetic, aeroelectromagnetic and aeroradiometric surveys over potential mineral belts of India. The status of the airborne geophysical survey in India is summarised in the table 5.1 and shown in Figure 5.1.

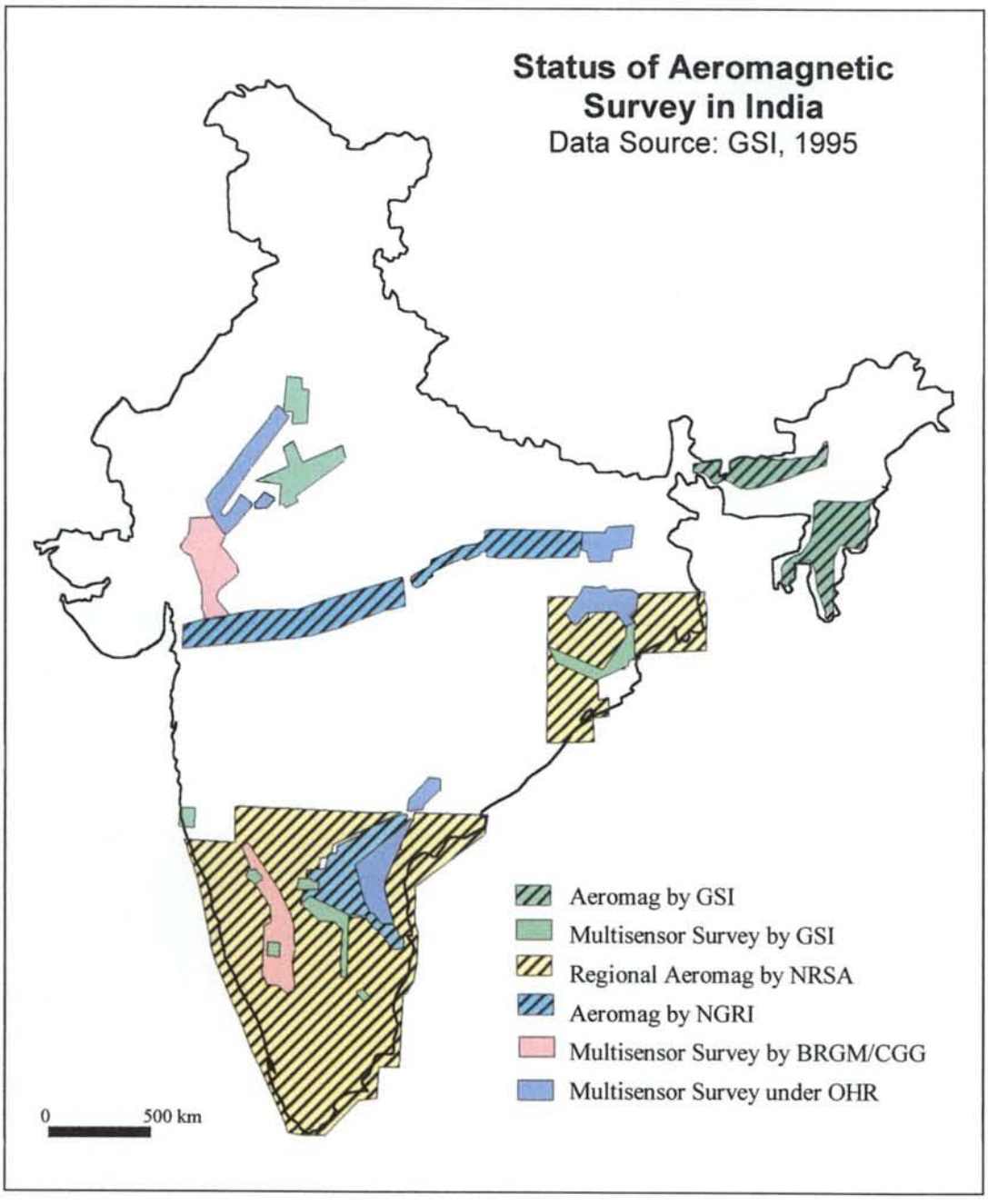

Figure 5.1: *Aeromagnetic coverage of India by different agencies up to 1995. Data compiled from Catalogue of Aero-geophysical Maps of India (Geological Survey of India, 1995)*

5.2. Digital Compilation of Aeromagnetic Data of India

Although most parts of India are covered by regional aeromagnetic surveys and low-flying high-resolution surveys in specific areas, no progress has so far been made in digital integration of these datasets on a national scale. The results of these surveys

Table 5.1: Status of Aeromagntic Coverage of India (Data compiled from the Catalogue of Aero-geophysical Survey of India, 1995)

Project	**Flying Agency**	**Year**	**Type of Survey**	**Area Covered** (sq km)	**States/Regions**	**Survey Specification**		**Purpose**
						Line Spacing (metres)	Flying Height (metres)	
OHR	Aeroservice Corp. and Parsons Corp., USA	1967 –68	Multisensor	97 395	Rajasthan, Bihar,West Bengal, Andhra Pradesh	*na*	*na*	Mineral and ground water resources
BRGM/CGG	BRGM/CGG, France	1971-72	Multisensor	76 460	Rajasthan, Gujarat, Karnataka	500	120	Mineral resources
	NGRI, India	1978-81	Aeromag	142 982	Son-Narmada Lineament and Cuddapah basin	1000	150 (500 feet)	Tectonic studies
NPSA	NRSA, India	1981-1994	Aeromag	11 96 058	Karnataka, Kerala, Tamilnadu, Andhra Pradesh, Orissa, Bihar, West Bengal, Madhya Pradesh, Maharastra, Goa	4000	1500 – 2850 (5000 – 9500 feet)	Regional aeromagnetic maps of the entire country to elucidate lithostructural and tectonic features, basement configuration etc
	AMSE, GSI	1986-1994	Multisensor	73 670	Tamilnadu, Karnataka, Orissa, Andhra Pradesh	500	50	Mineral exploration in potential mineral belts of India
Special Projects For ONGC	AMSE, GSI	*na*	Aeromag		Agartala and Silchar Block, West Bengal, Assam and Arunachal Pradesh, NE India	*na*	*na*	Oil Exploration
Special Project for NPC	AMSE. GSI		Multisensor		Rajapur and Devgarh area, Maharastra	*na*	*na*	*na*

AMSE: Airborne Mineral Surveys and Exploration, **GSI**: Geological Survey of India, **BRGM**: Bureau de Recherché Geologiques et Minieres, **CGG**: Compagnie Generale de Geophysique, **NGRI**: National Geophysical Research Institute, **NRSA**: National Remote Sensing Agency, **ONGC**: Oil and Natural Gas Commission (India), **NPSA**: National Programme of Aeromagnetic Survey, **NPC**: National Power Corporation, **OHR**: Operation Hard Rock; *na*: not available

are mostly available as hard copy contour maps which need to be digitised before compilation. Moreover, it is not possible to take advantage of the modern visualisation techniques for delineating regional features without digitally compiled datasets. Thus, India together with Antarctica represents a major gap in the aeromagnetic map of Gondwana (Figure 1.1). Digital compilation of the aeromagnetic datasets over parts of southern India (between 8°N and 14°N) has been carried out during this study. Existing hand-contoured maps have been digitised, processed, merged into a single dataset and then imaged using modern software tools like GEOSOFT. The aeromagnetic images thus produced have been interpreted for regional geological features that are often obscured by sedimentary cover and/or highly weathered rocks. The aeromagnetic anomaly patterns and the interpreted geological features are compared with those of south-west Sri Lanka and southern Madagascar for continental re-assembly.

5.3. Data Source and Quality

The data for southern India were acquired by regional aeromagnetic surveys (NRSA) flown at 4 km line spacing and 5000 to 9500 feet (1500 to 2850 m) high, apart from the Area G which forms the southern part of the Cuddapah basin coverage by NGRI with 1 km line spacing and 150m flying height. The datasets were presented as contour maps on 1:250 000 at contour interval of 20 nT. The area was flown by north-south and northeast-southwest flight lines. The specifications of different surveys are shown in Table 5.2 and Figure 5.2.

5.4. Aeromagnetic Data Processing

5.4.1. Processing Sequence Digital compilation of aeromagnetic data involves a number of steps from digitising of contour maps to producing high quality images. The processing sequence is summarised in the following flow chart.

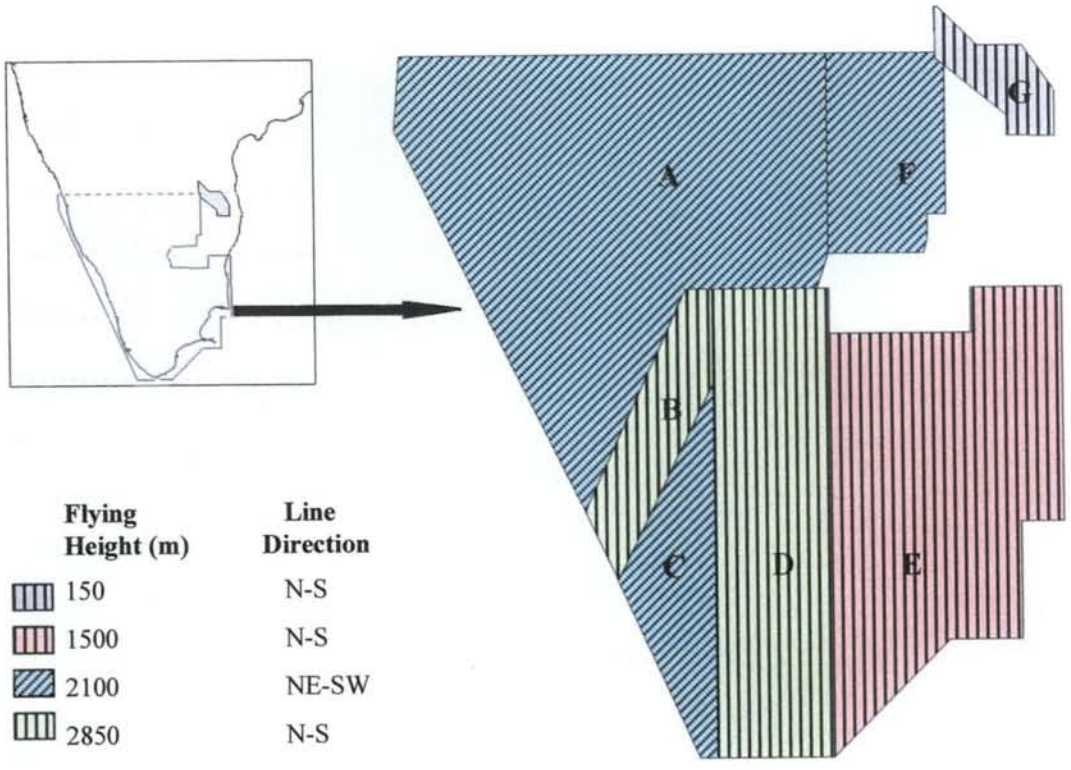

***Figure 5.2**: Map showing the aeromagnetic survey specifications of different blocks in southern India*

***Table 5.2**: Survey specification of aeromagnetic surveys in southern India*

Survey Area (refer Figure 5.2)	Year of Survey	Flying Height (m)	Line Spacing (m)	Flying Direction
A	1981-85	2850	4000	NE-SW
B	1981-85	2850	4000	NE-SW
C	1981-85	2100	4000	NE-SW
D	1981-85	2850	4000	N-S
E	1981-85	1500	4000	N-S
F	1981-85	2100	4000	NE-SW
G	1978-81	150	1000	N-S

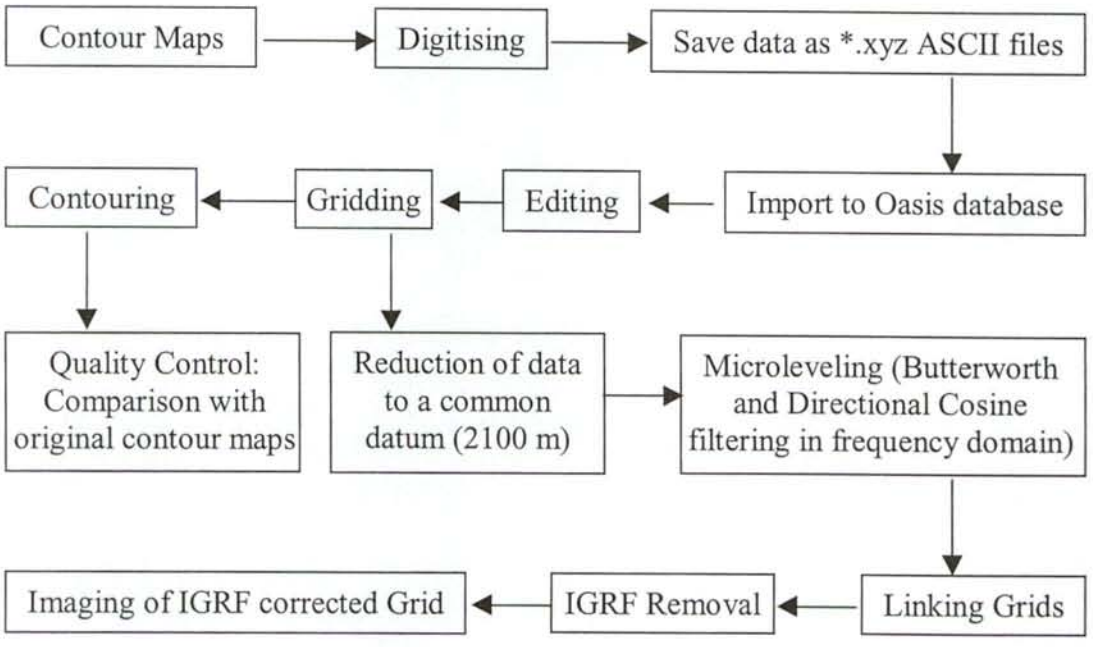

5.4.2. Digitising of Contour Maps

Processing of analogue aeromagnetic data starts with digitising contour and profile maps. The results of regional aeromagnetic survey were presented by GSI/NRSA/NGRI as contour maps on 1: 250 000 scale with 20nT (10 nT for the area G by NGRI) contour interval. The contour maps for areas A, B, C, D and E were scanned and digitised on-screen using the ATD (Auto Tracing and Digitising) method (Sreedhar Murthy *et al.*, 1998) at AEG (Association of Exploration Geophysicists), Hyderabad. The magnetic values were captured at regular intervals along the contour lines. Contour maps for the Area F in Figure 5.2 were digitised at ITC by Chandrasekhar (1997), using a CALCOMP® digitising table and a DOS based basic program developed in-house (Asfaha and Erren, 1990). Contour maps on 1:250 000 scale for the southern part of the Cuddapah basin (Area G in Figure 5.2) were digitised on-screen by the author using a MapBasic program (*Digga* in *MapInfo*). In the last two cases, the magnetic values were captured at the intersection points between the contour and flight lines. The data, in both the cases, were stored as ASCII files in *.xyz format defining the total field magnetic values (z) at each x, y co-ordinate points. The main limitation of any method of data capture that uses contour lines is that the dynamic range of the digitised data is governed by the contour interval

rather than the sensitivity of the magnetometer. Picking intersections of contours with flight lines has some advantages over other approaches, however.

5.4.3. Gridding and Contouring

The *.xyz data files generated by digitising the contour maps were imported to OASIS databases for editing digitising errors and further processing. Gridding was done separately for each of the datasets using the minimum curvature interpolation method, adequate to preserve the information content of the input data, with the help of the Rangrid program in Oasis montaj™ (Geosoft Inc.). As the spacing between flight lines is approximately 4 km, a grid cell size of 1000m (one fourth of the average line spacing) was selected which is adequate to reconstruct the anomalies caused by surface sources and also comparable with that of the AMMP (African Magnetic Mapping Project) data. The gridded data were contoured and compared with the original contour maps to assess the quality of digitising. The computer contoured maps showed close similarity with the original maps signifying the degree of accuracy achieved.

5.4.4. Linking Survey Grids

Viewing the results of separate surveys in a regional sense necessitates simultaneous display of data from all the surveys of that region. But simply viewing assembled surveys simultaneously is not of much use if there is a marked difference (step) in the background level of the results from one survey to another. This often leads to the generation of dominant artifacts along the survey boundaries (Figure 5.3) that have no geological significance. This difference, in most cases, may be attributed to poor leveling of data. In the present case, the area was covered by six surveys with varying survey parameters like flying height, flying direction etc. Therefore, it was necessary to follow a number of steps in processing individual grids before linking them together for a regional compilation.

a. Reduction of Grids to a Common Datum

Because the surveys were carried out at different flying heights ranging from 1500 to 2850 m (Table 5.1 and Figure 5.1), all the grids needed to be reduced to a common datum before further processing and merging. A datum of 2100m was chosen because the majority of the area under consideration was flown at that height. Thus, the

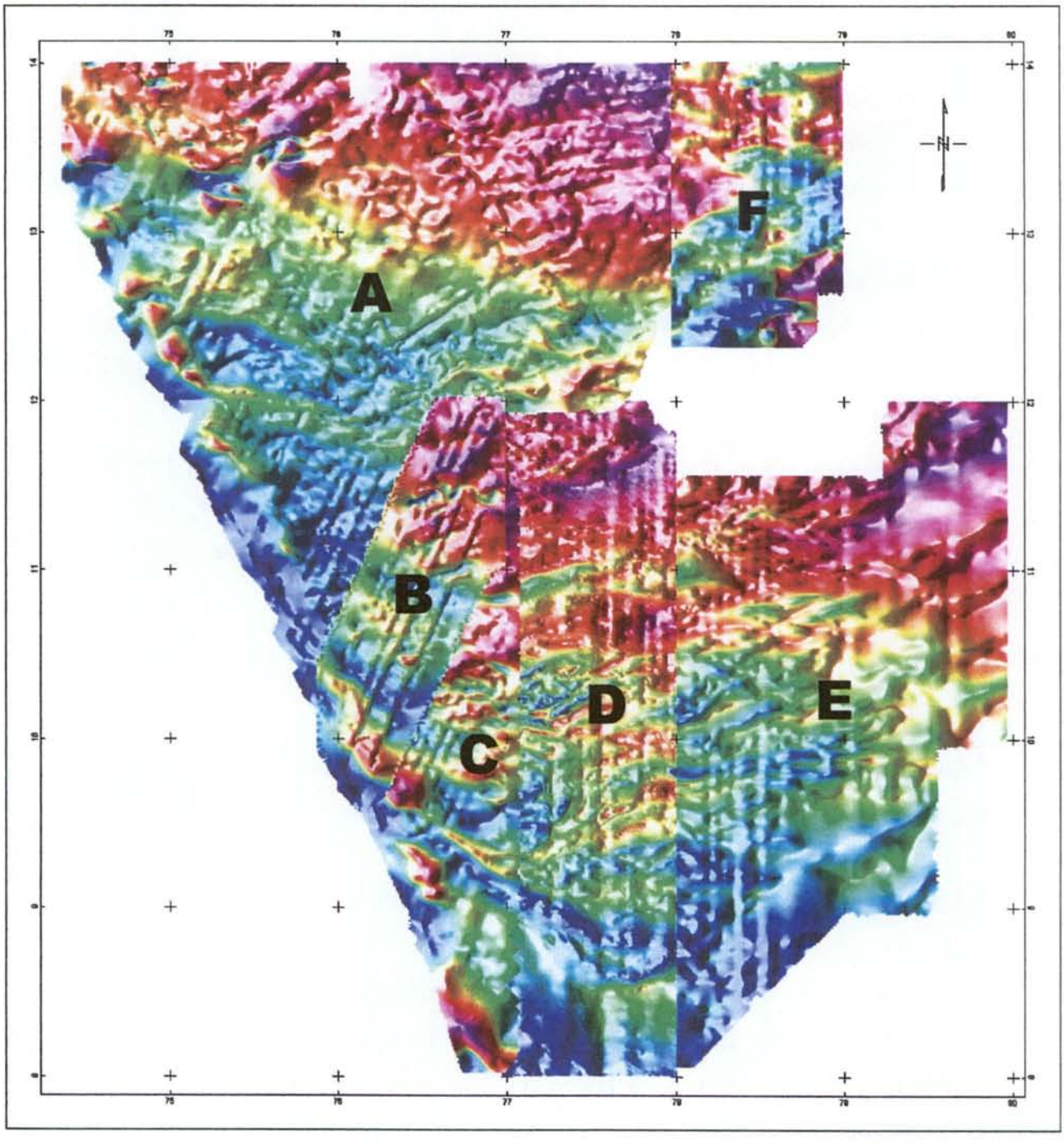

***Figure 5.3**: Mosaic of preprocessed grids - note the strong strip-related noise in all the grids and also mismatches along the survey boundaries.It is difficult to interpret the data without filtering out this noise*

easternmost survey grid (E in Figure 5.1) was upward continued by 600 m, whereas the central grids (B & D in Figure 5.1) were downward continued by 750 m using the 2D FFT processing techniques in the MAGMAP tool of GEOSOFT® to reduce all the grids to the 2100 m level as that of the grids A, C and F. Care must be taken for downward continuation of magnetic data as there is often a risk of introducing noise to the original data. However, in the present case no significant noise was observed in the downward continued grid. There will be considerable difference in the observed magnetic values at different levels of survey due to decrease in magnetic intensity with increasing separation between the source and the survey datum. This will lead to mismatch between surveys when compiled.

b. Microlevelling

Some flight path levelling errors were evident in the initial grids as narrow elongate anomalies along the flight lines (Figure 5.3). Some of these artifacts are also clearly depicted in the original contour maps. This noise is often so prominent that it suppresses the real anomaly pattern of the images, making it difficult to interpret real anomalies. Moreover, the very aesthetic appearance of the images is much diminished due to the emergence of such noise. Thus it was necessary to minimise this effect, a process often referred as decorrugation, and was achieved by applying decorrugation filters (Minty, 1991). Filtering was done using the 2-D FFT Processing System in Geosoft (MAGMAP). The grids were transformed into spatial frequency (wave number) domain and the following steps were carried out for each grid for microlevelling.

1. A high-pass Butterworth filter set to 4 times the average line spacing (=16 km) was applied to the original grid (D, Figure 5.4) in order to pass frequencies of the order of the line separation and the filtered grid was saved as D_1.

2. A directional cosine filter (90°- perpendicular to the survey direction) was applied to grid D_1, in order to pass the wavelengths only in the direction of flight lines producing a filtered grid D_2. Suitable directional filters (90° for grids D and E and 300° for grids A, B, C and F in Figure 5.2) were applied to respective grids. A mild degree of cosine function of 0.25 was used to remove a minimum required amount of line-related anomalous values without much affecting the real

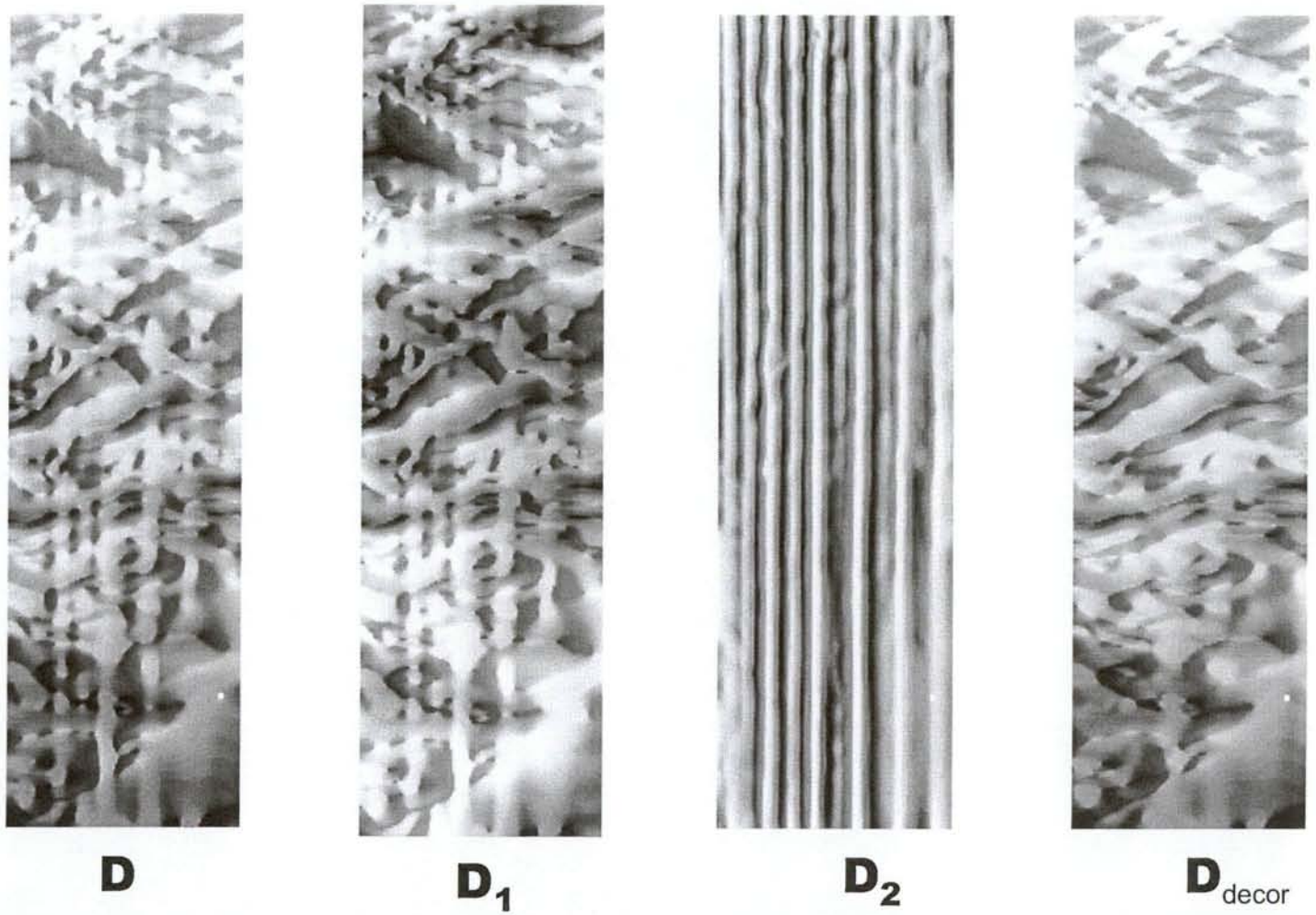

***Figure 5.4**: Figure showing the original (D), the filtered grids (D_1 & D_2) and the decorrugated grid (D_{decor}). Note the north-south line-related noise in grid D, the strong north-south noise components in grid D_2 after applying the decorrugation filters and the final decorrugated grid (D_{decor}) with much reduced level of line-related noise*

3. Anomalies due to geological sources. No microleveling was done for Area G (Figure 5.2), as no significant line related noise was noticed in the initial grid.

4. The resultant grid D_2 (Figure 5.4) was subtracted from the original grid (D) to get the corrected grid D_{decor}.

$$\text{Grid D} \xrightarrow{\text{decorrugation filters}} \text{Grid } D_2$$

$$\text{So, Grid } D_{decor} = \text{Grid D} - \text{Grid } D_2$$

c. Merging of Grids

Computer contouring was done for each of the decorrugated grids to compare magnetic values and patterns at the edges of the adjacent grids. Minor adjustments were carried out balance any mismatches (steps) in magnetic values at the edges of adjacent grids. Merging of grids was done systematically from west to east using the suture method of the GridKnit tool in OASIS. The suture method defines a suture line inside the overlap area between the two grids, along which the grids will be joined (Geosoft GridKnit™, Tutorial and User Guide). A mismatch in the grid values is corrected by adjusting the grids on either side of the suture path by averaging the values of both the grids along the suture line and then adjusting the values adjacent to the suture path for a smooth transition between the two grids. A user-defined suture path (red line in Figure 5.5) can also be applied in cases of irregular survey boundaries. Figure 5.5 illustrates the method of linking grids by suture method.

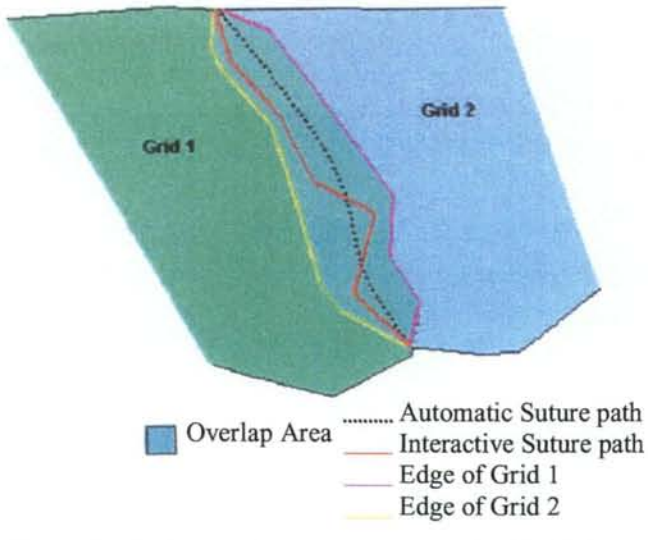

***Figure 5.5**: Figure showing suture paths for linking grids in the GridKnit tool (modified from Tutorial and User's Manual, Geosoft GridKnit™)*

5.4.5. IGRF Correction

The contour values around 40 000 nT (comparable to IGRF 1980 in this area) in the original contour maps suggest that no constant value or trend had been subtracted from the original data during early processing prior to contouring. This implies that the regional (non-geologic) field component still persists in the magnetic data. So it was necessary to remove the regional field represented by the International Geomagnetic Reference Field (IGRF) for the corresponding epoch of survey from the total magnetic field (observed value) to obtain the anomalous field due to the crustal sources according to normal convention. As most of the surveys were carried out in the early eighties, a regional IGRF grid (Figure 5.6b) for 1980 was removed from the merged grid (Figure 5.6a). The IGRF value for each of the grid nodes of the merged grid was calculated using the IGRF tool in Oasis and then subtracted from the processed merged grid to obtain the final grid (Figure 5.6c).

5.5. Map Presentation

5.5.1. Shaded Relief Image

Directional sun-shading of the total field magnetic data can be done with varying inclination (elevation) and declination (azimuth) angles of the illumination source. Shaded relief images prove to be useful in determining geological strike and delineating linear features like faults, shear zones etc. as they enhance the visibility of features in a desired direction and suppress those in other directions. In theory, a shaded relief image represents the first horizontal derivative of the total magnetic field in a given direction – thus, the near surface features that are not well resolved in a simple colour raster map tend to appear better in shaded relief maps (Milligan *et al.*, 1982). Shaded relief images of the area were visualised interactively with varying elevation and azimuth of the illumination source. It was found that shading parameters of 30° azimuth and 45° elevation gave the best results in enhancing the visibility of most of the desired features (Figure 5.7) to facilitate interpretation of major structures. In the shaded relief image, most of the magnetic anomalies strike nearly east-west or NW-SE, without any significant north-south trending anomaly. This can be attributed to the natural suppression of magnetic anomalies over north-south striking bodies at

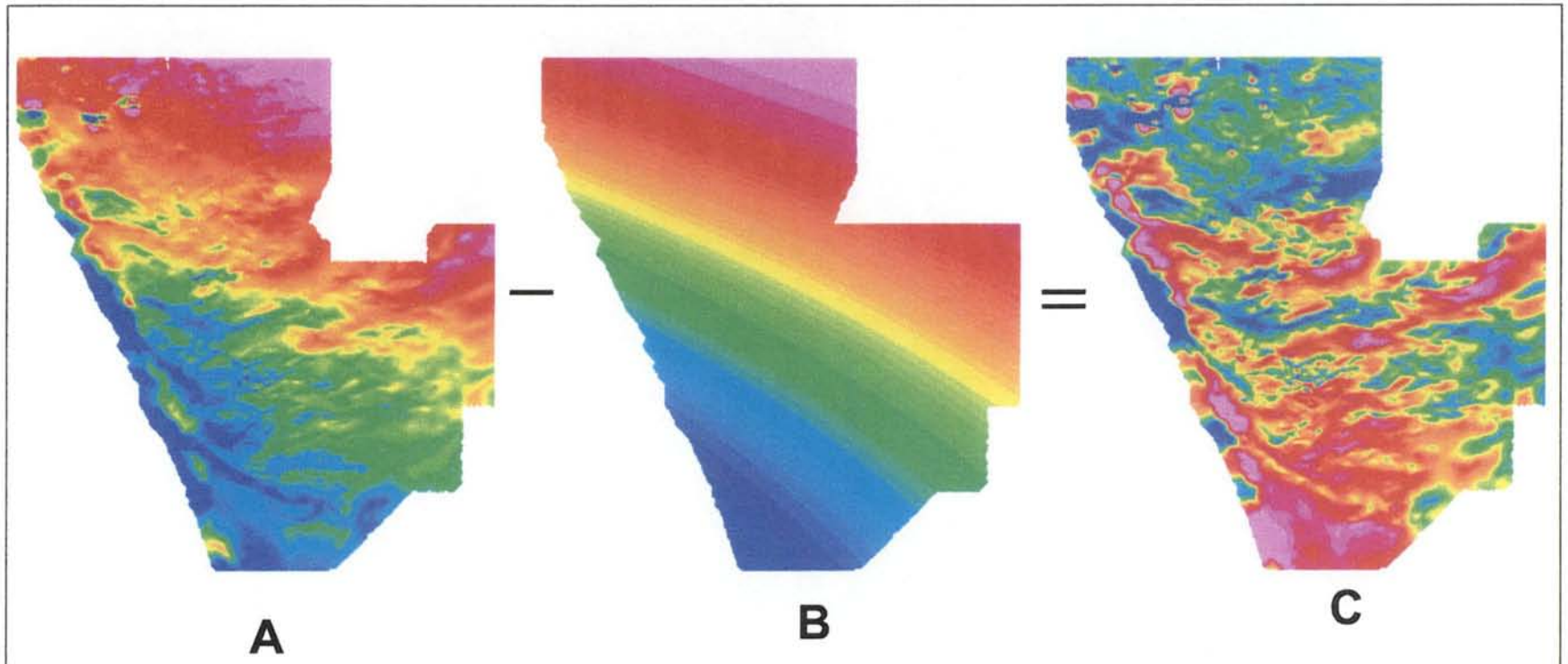

A: Processed aeromagnetic grid prior to removal of IGRF; **B**: IGRF grid for 1980 for the same area; **C**: IGRF corrected grid

A - B = C

Figure 5.6 *:Images demonstrating removal of IGRF from the observed data. Note the emergence of anomalies due to crustal sources in image C after removal of IGRF, regional field, (image B) from grid A.*

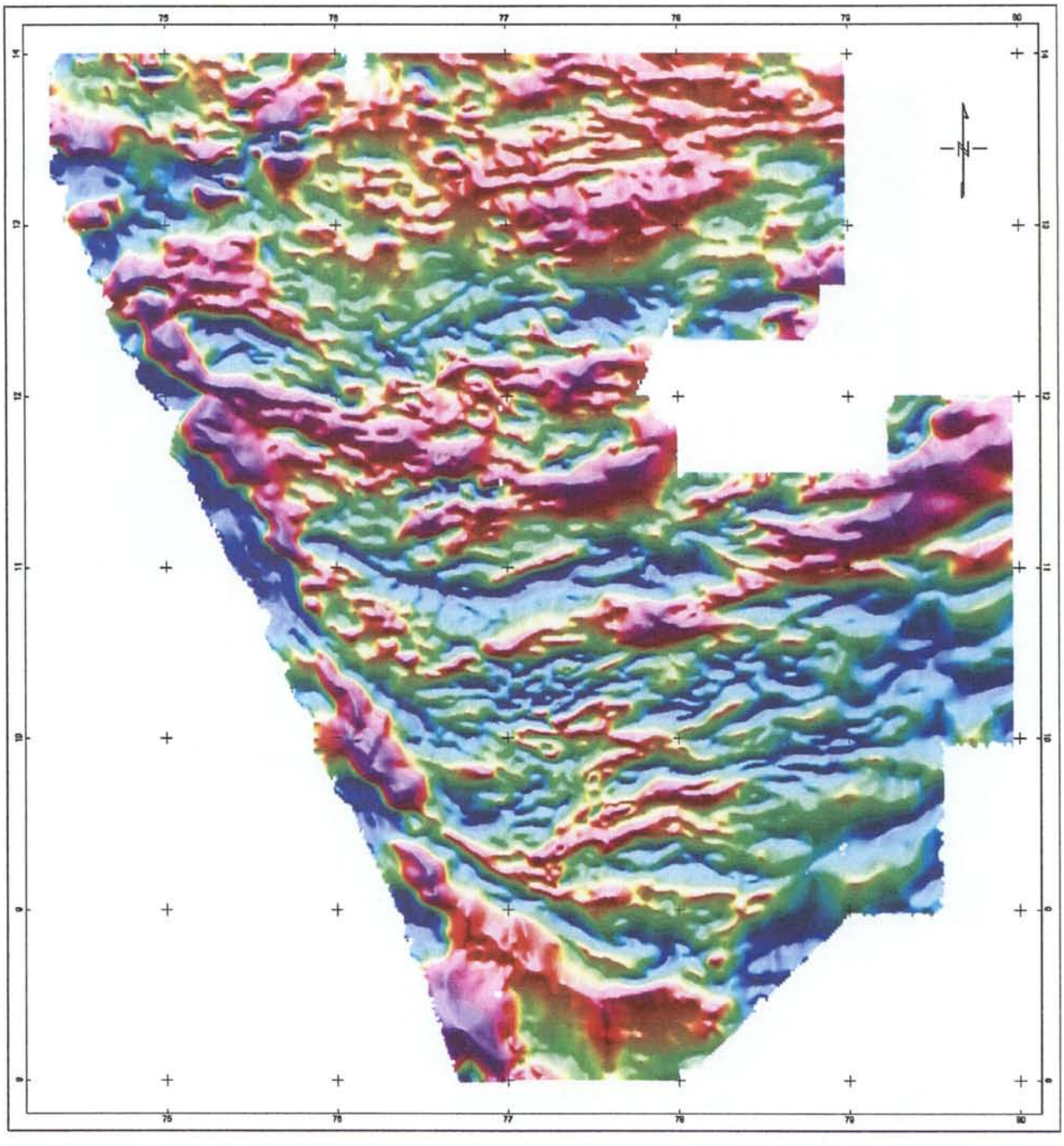

***Fig 5.7**: Shaded relief total field Aeromagnetic map of southern India. Note the virtual elimination of line related noise in the grids and mismatches along the survey boundaries after processing. Compare the preprocessed map (Figure 5.3) and processed map (this figure).*

low magnetic inclinations. A detailed explanation of the suppression of anomalies due to north-south striking sources is given in the next section.

5.5.2. Vertical Derivative Image

The first vertical derivative of the total magnetic field in an aeromagnetic survey is theoretically equivalent to observing the vertical gradient directly with magnetic gradiometers. A vertical derivative image enhances the response from the shallow sources, suppressing deeper ones (Reeves, 1998). Thus, closely-spaced sources can be better differentiated on the derivative maps than the colour raster image of the total magnetic field. Higher orders of derivative might help in resolving the closely-spaced sources better, but often the noise in the data becomes more prominent than the signal, causing ambiguity in interpretation. In the present study, as the area was flown at 1500 to 2850 m high, the colour raster image of the total field mostly represents high wavelength anomalies due to deeper sources. The first vertical derivative (Figure 5.8) sharpens the anomaly amplitudes thus helping in identification of more geological features.

5.5.3. Analytical Signal

The analytical signal is defined as the square root of the sum of the three orthogonal gradients of the total magnetic field (Roest, et al, 1992; Qin, 1994) and is expressed as

$$A(x,y) = \sqrt{(\partial T/\partial x)^2 + (\partial T/\partial y)^2 + (\partial T/\partial z)^2}$$

where, $A(x,y)$ is the amplitude of analytical signal at location x, y and T is the observed magnetic field at x, y.

Peaks of the analytical signals correlate directly with their causative bodies and are positioned symmetrically over them. Analytical signals of the total magnetic field are virtually independent of the inclination of magnetisation. Analytic signals serve as a better tool than reduction to pole for the interpretation of total field (ΔT) magnetic anomalies in low and middle magnetic latitudes, where reduction to pole often results in exaggeration of north-south trending features and/or noise. As there is a tendency for natural suppression of magnetic anomalies due to north-south trending geological

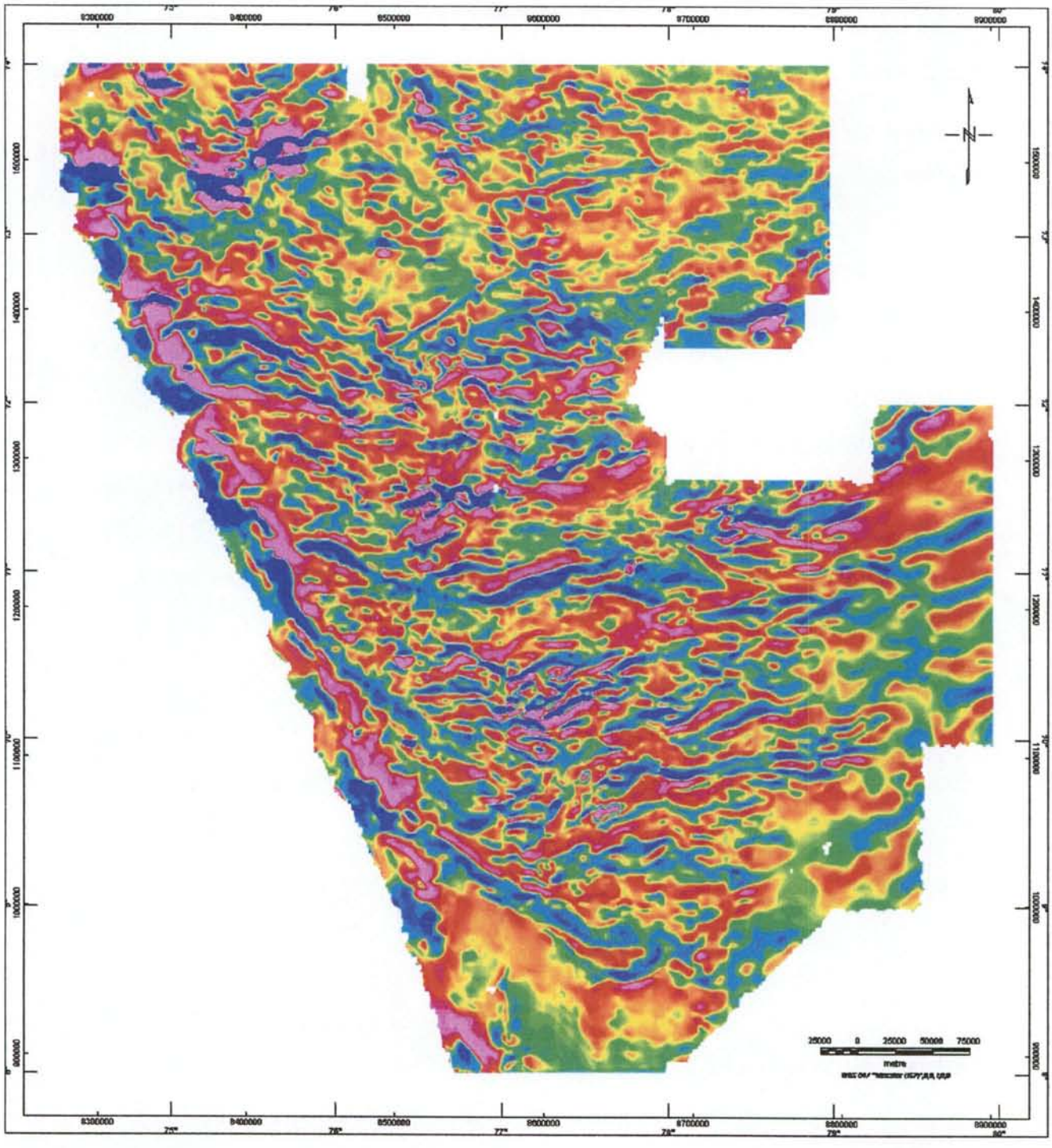

***Figure 5.8**: First Vertical Derivative image of the Total Field Aeromagnetic data. Note the enhancement in sharpness of the magnetic anomalies.*

sources at low magnetic latitudes like southern India (where, I = 2° to 9°), it is often the exaggerated noise that forms the bulk of the anomalies in a reduced to pole map (Figure 5.9). Thus, an analytic signal technique (Figure 5.10) was used as an alternative tool to the 'reduction-to-pole' method to simplify interpretation of the anomalies. The analytical signal is a function of the distance to the magnetic source and the intensity of magnetisation – the closer the source the greater the anomalous field and greater the analytical signal.

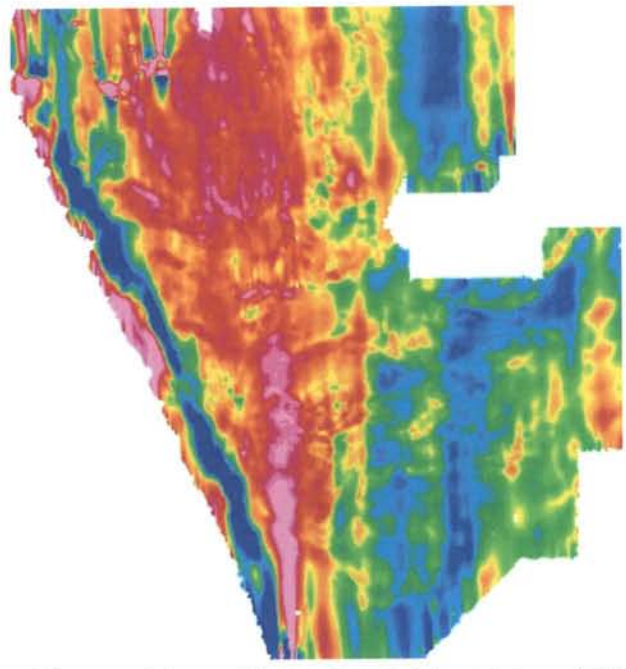

Figure 5.9: *'Reduced-to-Pole' total field aeromagnetic map of Southern India. Note the exaggerated north-south anomalies, mostly due to line related noise*

5.5.4. 3D Euler Deconvolution

3D Euler deconvolution is a boundary and depth estimation method for potential field data which requires minimum assumptions about the initial source parameters and is defined by the equation

$$(x-x_0)\partial T/\partial x + (y-y_0)\partial T/\partial y + (z-z_0)\partial T/\partial z = N(B-T)$$

where, (x_0,y_0,z_0) is the position of a magnetisation whose total field is measured at (x,y,z), B is the background level of the potential field at position (x,y,z) and N, the structural index, is the degree of homogeneity related to the rate of change of potential field with distance from the source (Thompson, 1982, Reid *et al.*, 1990). Thus the Euler deconvolution provides a useful means of gaining a broad idea on the depth and location of various magnetic sources in a given area provided the right parameters like grid cell size, window size and the structural index are selected. It is a faster method of covering the whole area for depth and boundary estimation of magnetic sources than modeling of individual anomalies for this purpose. It also helps in delineating

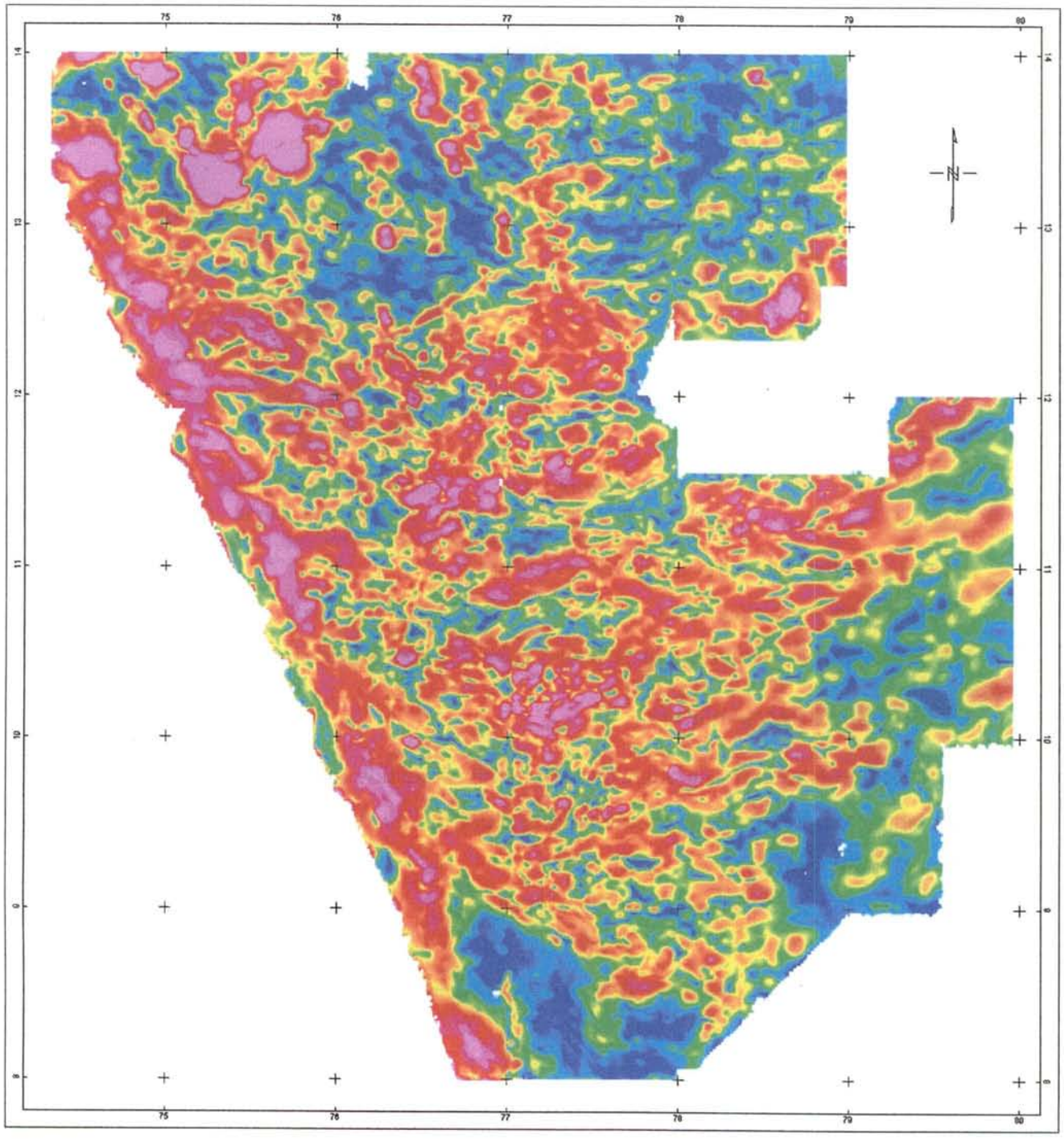

***Figure 5.10**: Analytic Signal map of the total field aeromagnetic data of Southern India.The magnetic anomalies are relatively simpler than those in the total field aeromagnetic map (Figure 5.7). Note the difference in anomaly patterns between the northern and south-central parts of the map.*

linear geological features (e.g. fractures and offsets) more precisely due to clustering of focussed solutions along these features. For magnetic data, the significant advantage of Euler deconvolution is that it is insensitive to magnetic inclination, declination and remanence. But the use of Euler depths must be done with care as depth error varies considerably depending upon the line spacing. A course line spacing will increase the depth error, whereas the location is usually more accurate within the limits of line spacing and grid cell size. Thus, the Euler solutions must be used with the full knowledge of survey and processing parameters.

As the area under discussion was flown at heights ranging from 1500 to 2850m with 4 km line spacing, a grid cell size of 1000m serves to map all the anomalies due to surface sources and hence can be considered suitable for use in Euler deconvolution. Though Fairhead *et al.* (1994) have argued that a 4x4 window size (*i.e.* 4 km x 4 km window for 1 km grid cell size) is adequate for 1 km grid, it has been observed that it is too small a window to incorporate substantial variation in the magnetic field in the present study area. On the other hand, a 10x10 window has proved to adequately represent the broad anomalies arising from deep sources as well as moderate anomalies from relatively shallow sources without significant effects from multiple sources. Structural index (N) – a measure of the rate of change of potential field with distance – is the most important attribute for obtaining sharp focussed results. A list of structural indices and the corresponding geological models is given in Table 5.3. In the present case, as it is a regional interpretation and we are interested in magnetic contacts and lineaments, Euler solutions were calculated for both indices 0 and 1. However, the results for the index 1 (Figure 11), seem to be better than those for index 0. The depth ranges have been plotted in Figure 11 after subtracting the flying height (2100m) from the calculated depth values. At any rate, all the magnetic sources lie within the upper crust.

Structural Index	Simple Source Model
0.0	Contact
0.5	thick step
1.0	Sill/Dyke
2.0	Pipe
3.0	Sphere

***Table 5.3**: Summary of structural indices for simple models in a magnetic field*

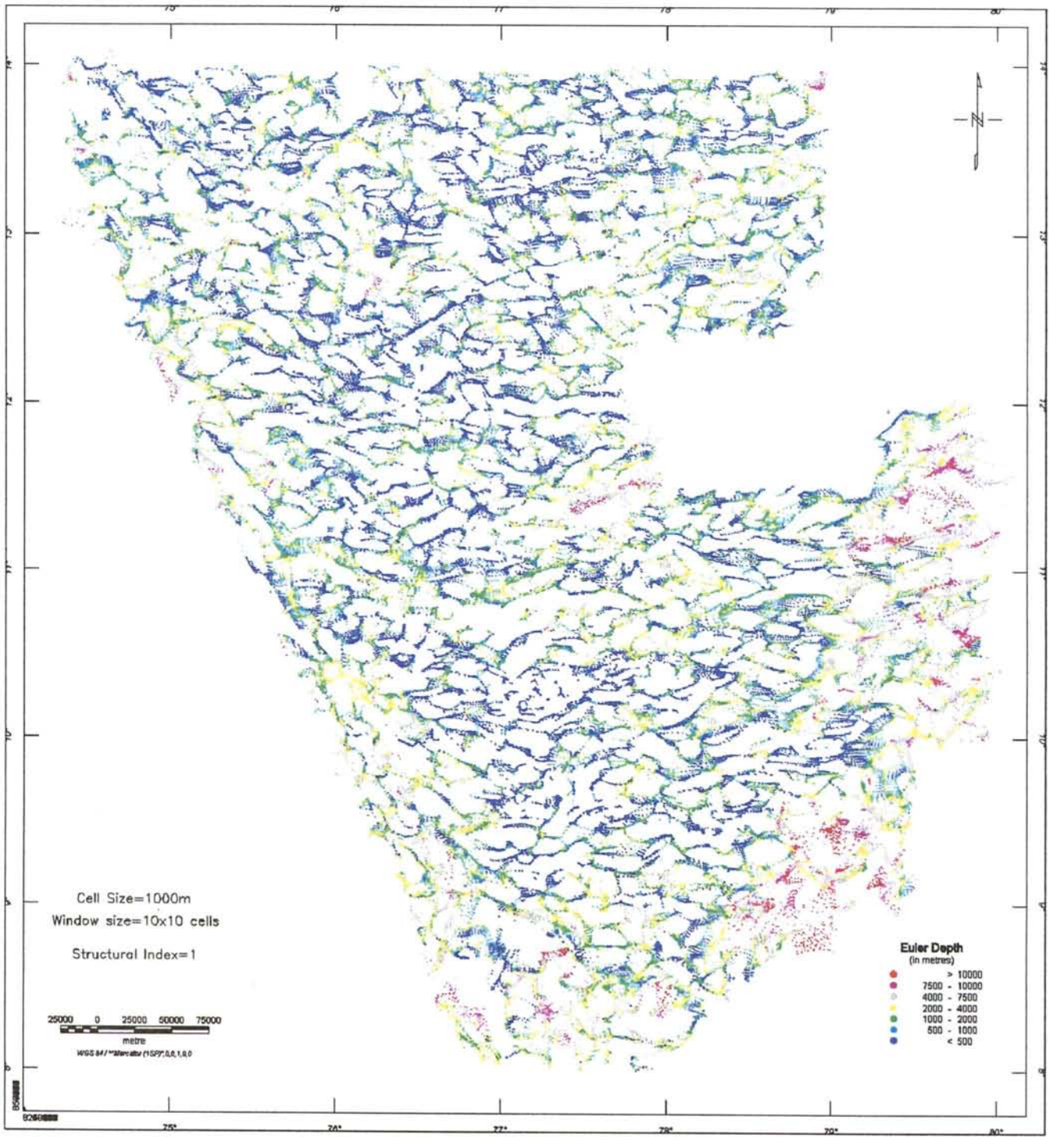

***Figure 5.11**: Euler deconvolution depth map of Southern India. The values correspond to depth below ground surface. Note the clustering of deep solutions (>7.5 km) in the southeastern part of the map, where the basement rocks are buried under thick sequences of Phanerozoic sediments.*

5.6. Spectral Analysis

In order to estimate the approximate depth range of magnetic populations and facilitate designing filter parameters for filtering in the wave-number domain, the radially-averaged power spectra for the total magnetic field grid data of the area was generated. Depths of the ensemble of causative bodies were determined by measuring the slopes of the linear branches of the spectra (Figure 5.12) and dividing these by 4π (Spector and Grant, 1970). The spectral analysis indicates that the anomalies in the area arise due to at least 4 distinct ensembles of magnetic sources at 130 m, 360 m, 7 km and 16 km depth below ground surface. Most of the magnetic populations lie in the range of 0 to 360m depth. However, these estimates can only be used as a rough guide to the depth of populations of magnetic sources.

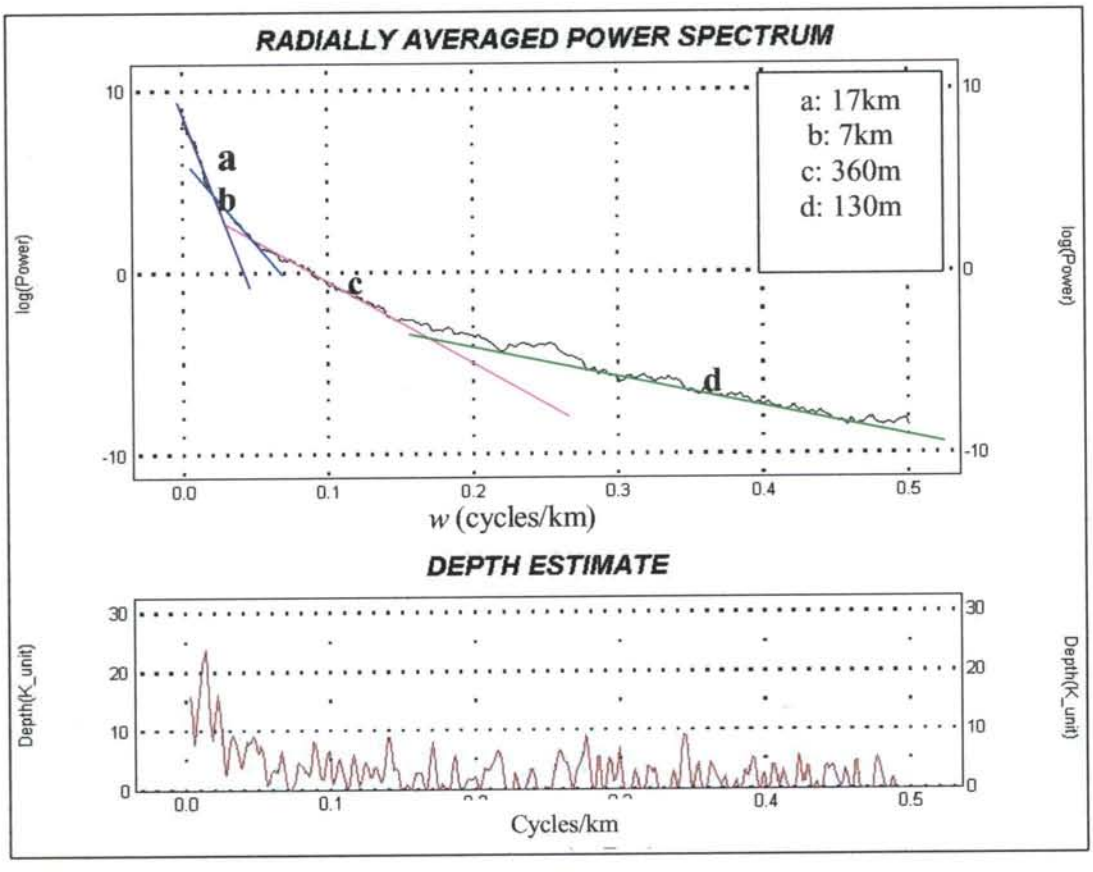

***Figure 5.12**: Radially-averaged wavenumber spectrum for the total magnetic field at 2100 m terrain clearance over Southern India. Straight-line branches indicate source ensembles at depths 17 km, 7 km, 0.36 km, and 0.13 km.*

5.7. Summary and Conclusions on Compilation and Imaging

1. Compilation and processing of aeromagnetic datasets acquired through varying survey parameters and different time span is an essential first step towards interpretation of geological sources in a regional perspective. The difference between the figures 5.3 (pre-processed mosaic of individual datasets) and 5.7 (compiled image of the same datasets) provides an insight into the value of such an exercise.

2. Advantages of images over contour maps are also evident from the above mentioned figures. Aeromagnetic images enhance the visual perception of geology-related information drastically.

3. Visualisation of linear geological features can be enhanced and artifacts suppressed selectively by changing the illumination inclination and declination.

4. Vertical derivative maps enhance shallow sources, suppress the deeper ones and provide better resolution for closely spaced sources related to near-surface geology. Figure 5.8 demonstrates the usefulness of such processing for structural interpretation.

5. Analytic signal technique provides an alternative to the reduction-to-pole for aeromagnetic data interpretation in low latitude areas like South India. Euler deconvolution technique is useful for semi-quantitative interpretation of the positions and depths of burial of causative sources

6. Digital compilation of the existing aeromagnetic data (hard copy and digital) for whole of India needs to be completed urgently so that maximum possible benefits of the modern processing, imaging and interpretation techniques can be used to aid and accelerate exploration of water, minerals and hydrocarbon resources.

7. An aeromagnetic image of image of India will be of immense help, in tectonic analysis and filling the gap in an aeromagnetic interpretation of whole of Gondwana.

B. Interpretation of Aeromagnetic Images

5.8. Problems in Interpretation of Aeromagnetic Data over Precambrian Terrains

Aeromagnetic data interpretation upgrades our knowledge on the geometry of magnetic basement through providing a unique window for comparison of lithotectonic and structural features at a regional (subcontinental) scale. Magnetic interpretation of Precambrian terrains is often difficult due to their complex geological and tectonic evolution. The main causes of this complexity are – 1. uneven distribution of magnetic minerals (magnetite) in the rocks, 2. polyphase deformation and associated metamorphism and 3. variable remanent magnetisation in some rocks. Low magnetic inclination (2° to 9°), wide line spacing (~4 km) and high survey altitudes (1500 t0 2850m) and some ~north-south striking litho units (Closepet granite etc., Figure 5.13), especially in the northern part of the study area add to the complexity of magnetic interpretation of the high-grade metamorphic terrains of southern India. However, careful data processing, imaging and modeling using modern techniques has enabled the production of a credible interpretation map of the region.

5.9. Interpretation Methodology

As the dataset is of relatively low resolution, only the magnetic anomalies of the medium and deep magnetic sources are fully represented and the near-surface geology is imperfectly recorded. The data has been primarily used to interpret of regional structure and lithotectonic units. A few selected anomalies have been modelled for quantitative estimation of source parameters like depth to the top of a unit and/or dip of the body. A modified interpretation scheme was devised primarily based on the concepts of Reeves *et al.* (1990) and Reeves (1992). The approach to interpretation follows the scheme below.

1. Study of the recent geological maps of the area to be acquainted with the rock types, their regional trends, structural style, grade of metamorphism etc. and linear structural features like faults, shear zones etc.

2. Classifying rocks based on magnetic characteristics – rock types responsible for producing magnetic anomalies and those magnetically transparent.

3. Producing aeromagnetic maps (shaded relief, vertical derivatives, 3D analytical signal and Euler deconvolution) at the same scale and projection same as that of the corresponding geological map. These maps were produced on 1: 2 500 000 scale with polyconic projection.

4. Draping of grey scale shaded relief (total field aeromagnetic) image over geology for correlation and interpretation of major tectonic features

5. Zoning of the magnetic anomaly maps based on anomaly patterns considering – frequency of magnetic axes (highs and lows) within a unit, magnetic relief patterns, shape of individual anomalies (circular, long-strike-length, convoluted etc.) and general background level within a particular zone.

6. Refining geological maps based on continuity of magnetic anomaly patterns from areas of relative abundant outcrop to the areas of low outcrop density and those devoid of any outcrop due to magnetically transparent sedimentary cover or high degree of weathering.

7. Delineation of linear/curvilinear features like faults, shear zones, dykes etc from magnetic anomaly patterns and linear clustering of Euler depth solutions and integrated image of geology and magnetics.

8. Estimation of depth to the top of the sources and their dimension by quantitative inverse modelling of selected anomalies.

5.10. Regional Geology of southern India

Southern India is predominantly underlain by Archean granite-greenstone rocks of the Dharwar craton to the north and high-grade gneissic terrain of the Southern Granulite Terrain to the south. The Dharwar craton is divided into Western and Eastern Dharwar cratons (Figure 5.13) separated by the north-south trending Closepet granite

(Naqvi and Rogers, 1987, GSI, 1998). The Western Dharwar craton is composed of Peninsular Gneisses – a suite of low-K granitoid gneisses, relicts of greenstone belts and intrusions ranging in composition from ultramafic to acidic (Jayanand and Peucat 1995; Geological Survey of India, 1994 & 1998). The principal structural trend in the Western Dharwar craton is north-south as evident from the orientation of the major greenstone schist belts and the Closepet Granite (Figure 5.13). The Eastern Dharwar Craton, east of the Closepet Granite, contains high-grade gneisses, schist belts, granites and undeformed supracrustal sedimentary basins. The general structural trend changes from north-south in the southern part to NW-SE in the north.

The low-grade schistose rocks of the Dharwar craton grade into high-grade gneissic rocks of the Southern Granulite Terrain to the south. The Southern Granulite Terrain is broadly divided into two lithotectonic units separated by the NW-SE trending Achankovil Shear Zone (ASZ in Figure 5.13). The area between this shear zone and the Dharwar craton (referred henceforth as Madurai Block) is predominantly occupied by charnockite massifs with mafic granulite and enclaves of high-grade metasedimentary rocks. The area south of ASZ consists predominantly of khondalite (referred henceforth as Southern Khondalite Block, Figure 5.13). A number of Proterozoic gabbro-anothosite-alkali complexes occur within the Southern Granulite Terrain.

A number of subvertical trans-continental shear zones cut across the Precambrian terrains of southern India (Figure 5.13, Drury and Holt, 1980; Geological Survey of India, 1994). The Moyar-Bhavani Shear System in the northern part of the study area consists of the WNW-ESE trending Moyar Shear Zone and the NE-SE trending Bhavani Shear Zone. This shear system has affected Neoproterozoic charnockites in the eastern part. This is consistent with Ghosh (1999), who dated the movements between 500 and 550 Ma along these shear zones. The east-west trending Palghat-Cauvery Shear Zone (PCSZ) is considered by many (*e.g.* Ramakrishan, 1993) as the southern boundary of the Dharwar craton. Though the presence of PCSZ was not revealed in the satellite imagery (Drury and Holt, 1980), it has been well documented in later works by the Geological Survey of India (1994) and Chetty (1996) based on geological and geophysical evidence. The NW-SE trending Achankovil Shear Zone (ASZ) occurring to south of the PCSZ was recognised from the abrupt change in

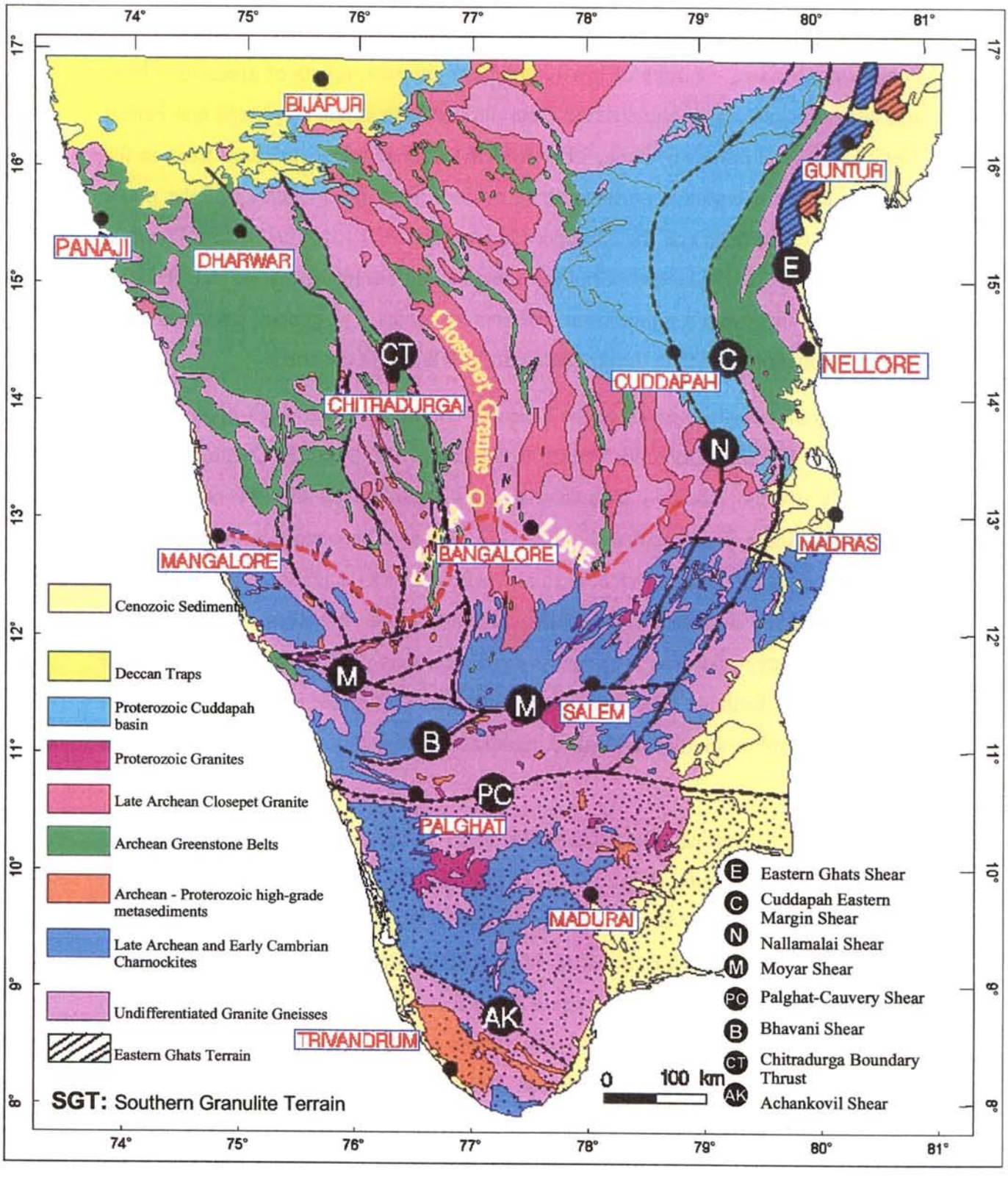

***Figure 5.13**: Geological map of southern India (after GSI, 1994 and Ghosh, 1999) with major shear zones interpreted from satellite imagery by Drury et al., (1980 &1984).*

structural trends (interpreted from satellite imageries) across it (Drury *et al.*, 1984). The NNE-SSE strike of the lithological units in the north abuts against the ASZ and changes to NW-SE in the south.

5.11. Magnetic Characteristics of Metamorphic Rocks

Magnetic anomaly patterns of an area are largely controlled by the distribution of magnetic minerals (mostly magnetite) in the rocks (Clark and Emerson, 1991). Thus irregular anomaly patterns are indicative of heterogeneous magnetite distribution in rocks. Magnetic susceptibility, the constant of proportionality between the induced magnetisation and the inducing field, is largely a function of magnetite content of rocks. Thus susceptibility contrast is not necessarily diagnostic of lithological classification, which is primarily based on silicate mineral assemblage (Clark and Emerson, 1991). Magnetite and/or hematite are common magnetic minerals in most metamorphic rocks. Generally, magnetite in metamorphic rocks is created by breakdown of ferromagnesian minerals during metamorphism. Prograde metamorphism from amphibolite to granulite facies leads to increased production of magnetite as a result of breakdown of ferro-magnesian minerals like biotite and amphibolite (Skilbrei *et al.*, 1991). Study of magnetic petrology of a transition zone between amphibolite and granulite facies in northern Norway by Olesen *et al.* (1991) has revealed that a gradual increase in magnetite content from ~0.05% in the rocks of amphibolite facies to over 1% in granulite facies rocks. Though, there is no systematic study on the distribution of magnetite in the metamorphic rocks of southern India, the expected results could presumably be similar due to the fact that the amphibolite facies rocks of the Dharwar craton grade into the high-grade gneissic rocks of the Southern Granulite Terrain. So an increase in the magnetite content from north to the south could be expected in southern India.

5.12. Qualitative Interpretation

5.12.1. Magnetic Relief Zones and Tectonic Domains

Though a detailed correlation of the lithological units with the aeromagnetic anomaly patterns has been difficult due to low resolution of the survey (high flying height and

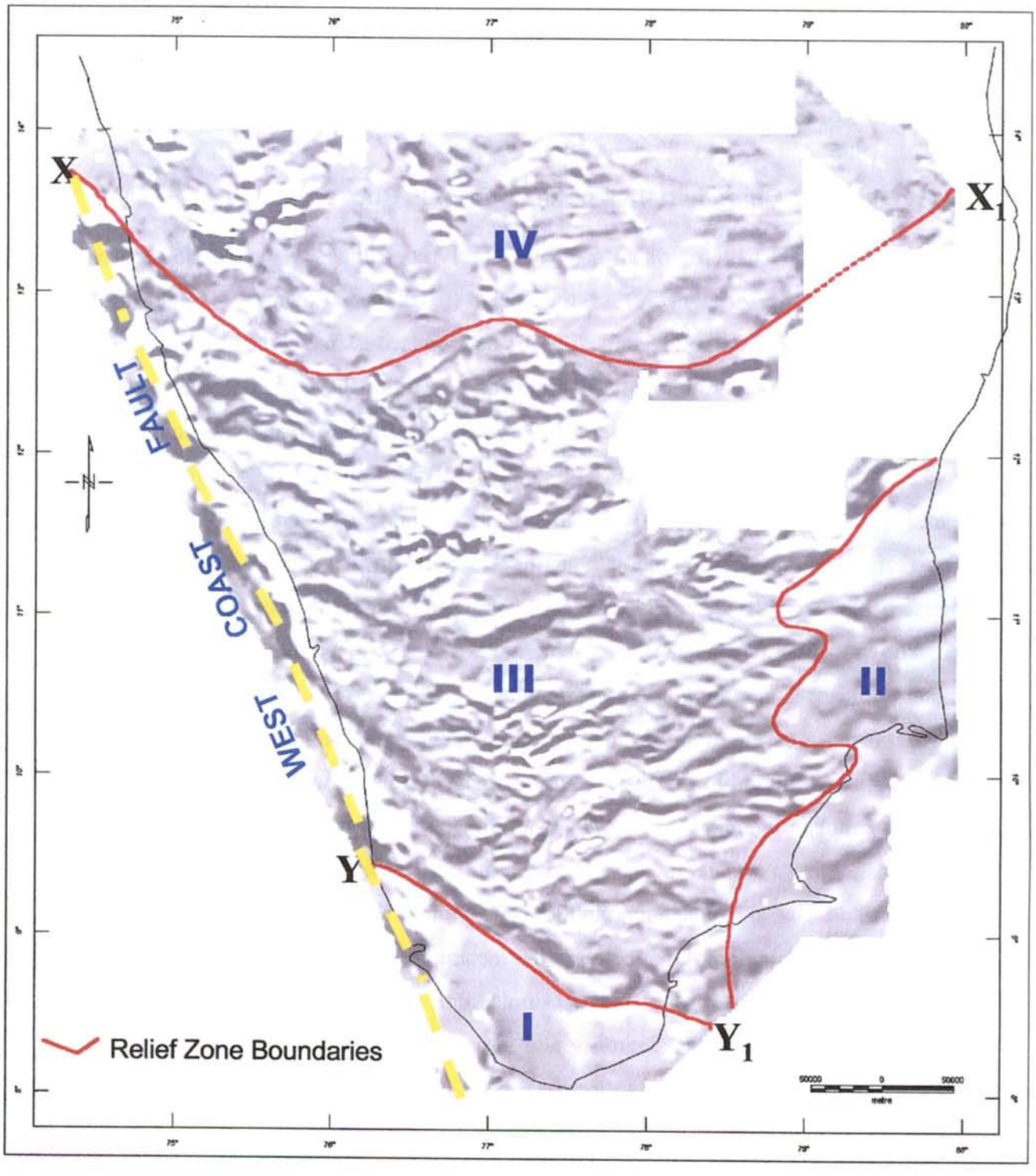

***Figure 5.14**: Grey scale aeromagnetic image showing the magnetic relief zones. Zone I: low (corresponding to the Southern Khondalite Terrain); Zone II: moderate (coastal tracts of Mesozoic and Cenozoic sediment cover); Zone III: moderate to high (granite-greenstone terrains of the Dharwar craton); Zone IV: high (Madurai Block). The West Coast Fault is the most prominent feature in the Aeromagnetic image of southern India.*

wide line spacing), 4 distinct magnetic relief zones are discernible both in the vertical derivative map as well as the analytic signal map (Figure 5.14 and Map 5.4). These 4 zones can be broadly correlated with the regional geology of the corresponding areas.

Relief Zone I: The area south of the Achankovil Shear Zone is marked by a quiet relief zone. High-grade gneisses of the Southern Khondalite Belt dominate this area. As the tectonic trend of the khondalites is NW-SE and outcrop density is considerable, it might be expected that the area should have produced high amplitude analytic signals and high magnetic relief patterns. Lack of such signals implies the existence of low and uniform susceptibility rocks in the area. Thus the khondalites act as magnetically transparent rocks and the magnetic anomalies are mostly from the rocks of the presumably underlying migmatite complex.

Relief Zone II: This zone, also a low relief one, more or less coincides with the coastal cover sediments in the eastern part of the study area. This is expected in this zone because of the presence of a thick and magnetically transparent Mesozoic and Cenozoic sediment cover. The smoother magnetic anomalies are due to the crystalline basement rocks deeply buried under these sediments.

Relief Zone III: The central part of the study area is dominated by high magnetic relief and high amplitude analytic signals. The western part of the area predominantly comprises granulites and related high-grade charnockite massifs, whereas the eastern part is underlain by high-grade migmatites. A decrease in the magnitude of magnetic relief in the eastern part signifies that the susceptibility of charnockite massifs is higher than that of the migmatites.

Relief Zone IV: This is a moderate to high magnetic relief zone in the northern part of the area. This zone corresponds to the Archean granite-greenstone belts of the Dharwar craton. As these rocks have suffered only greenschist to amphibolite facies metamorphism, production of magnetite during metamorphism must have been less than that in the high-grade granulite blocks to the south. It may be noted that two isolated anomalies with high analytic signals occur in the northwestern corner of the analytic signal map (A1 and A2 in Map 5.4 and Figure 5.21) within this relief zone. One such isolated high-amplitude analytic signal anomaly also occurs in the eastern part of Madagascar (A3 in Figure 5.21). The sources of these anomalies might be similar. The east-west fabric in the total field and derivative maps appears to show

some eminence or due to deeply buried east-west lineaments or even might indicate change in metamorphic grades.

Based on the variation in the magnetic relief and patterns of analytic signals, distinct contrast in the magnetic susceptibility between the low-grade granite-greenstone belt in the north and the high-grade granulite block in the south across line X-X_1 can be clearly observed (Figure 5.14). Though the change in magnetic relief patterns and analytical signals across X-X_1 is primarily due to change in grade of metamorphism, no major tectonic lineament is observed in the aeromagnetic maps. Incidentally, the X-X_1 line broadly coincides with the 'Fermor Line' (Figure 5.13). Similarly the boundary between the Southern Khondalite Belt and the predominantly charnockite belt to the north is interpreted along Y-Y_1 (Figure 5.14) that marks a strong contrast in the magnetic susceptibility between these two terrains.

5.12.2. Structural Interpretation

Study of satellite imageries (Drury *et al.*, 1980 & 1984), systematic geological mapping (GSI, 1994), interpretation of geophysical data (Reddi *et al.*, 1988; GSI, 1994) and analysis of regional structural trends coupled with limited field mapping and isotopic data (Ghosh, 1999) have revealed a number of regional lineaments (shear zones, thrusts and regional faults) in the Precambrian terrains of southern India. These lineaments have been advocated as boundaries between different Precambrian blocks by earlier workers (*e.g.*, ASZ, Srikantappa *et al.*, 1985, de Wit *et al.*, 1998; MSZ, Srikantappa, 1993; PCSZ, Harris *et al.*, 1994; KKPT, Ghosh, 1998). These trans-continental lineaments have subsequently been used as markers for correlation with those of Madagascar and East Antarctica - *e.g.*, ASZ with the Ranotsara Shear Zone (RSZ) of Madagascar (Kriegsman, 1993; Pinna *et al.*, 1993); PCSZ – RSZ- Boundary between Napier and Rayner complexes of Enderby Land, East Antarctica (Sahu and Reeves, 1998), KKPT- RSZ (Ghosh, 1999) – for close reconstruction of central Gondwana. The present study aims at verifying the existence, position and extent of these lineaments through interpretation of regional aeromagnetic data of southern India and evaluating the validity of the hypotheses on terrain boundaries and their Gondwana connection.

Use of aeromagnetic data, especially in the form of enhanced images like shaded relief and vertical derivatives, has proved to be effective in delineation of structural

features that are partially or fully obscured by cover rocks. Thus interpretation of these images provides an opportunity – 1. to refine the inferred features, derived mostly from widely separated exposures, in terms of their spatial disposition and 2. to interpret deeply buried features that have no surficial expression, making it difficult to detect them by conventional methods like field mapping, interpretation of aerial photos and satellite images.

A great degree of agreement between the known lineaments and the magnetic anomaly patterns is obvious in Figure 5.15. However, there is enough scope for refining the spatial disposition of these lineaments.

a. Achankovil and Tenmallai Shear Zones: These NW-trending shear zones are closely spaced and parallel to each other. The Achankovil Shear Zone (ASZ) limits the southern boundary of the charnockite massifs in the north. The Southern Khondalite Province in the south is bounded by the Tenmallai Shear Zone. Both these shear zones are marked by high magnetic gradients (Figure 5.15). The narrow intervening area between this pair of shear zones is marked by a zone of relatively low magnetic susceptibility.

b. The Palghat-Cauvery Shear Zone (PCSZ): This is an east-west trending curvilinear lineament, thought to be a major tectonic break in southern India that separates the granite greenstone belts in the north from the high grade granulite terrain in the south (Drury *et al.*, 1984, GSI, 1994). Though this shear zone is marked by a prominent broad magnetic anomaly zone in the western part, no significant magnetic anomaly is noticed along its eastern extremity. Thus, this shear zone may not be of as much tectonic significance as was thought earlier. It is mostly the Palghat gap, a low topographic zone comprising predominantly of the Peninsular Gneissic Complex (Figure 5.15 and Map 5.2) and bounded on either side by high-rising charnockite massifs, that produces the pronounced negative anomaly. The alignment of this shear zone is redefined based on magnetic anomaly patterns (Figure 5.16).

c. Karur-Kambam-Painavu-Trichur Lineament (KKPT): Ghosh (1999) has described this new shear zone (Figure 5.15) on the basis of striking contrasts in structural style, lithological assemblage and isotopic ages across it. Marked difference in style of folding has been reported from either side of this shear zone, especially in the eastern part. The area south of KKPT is dominated by khondalite, paragneisses

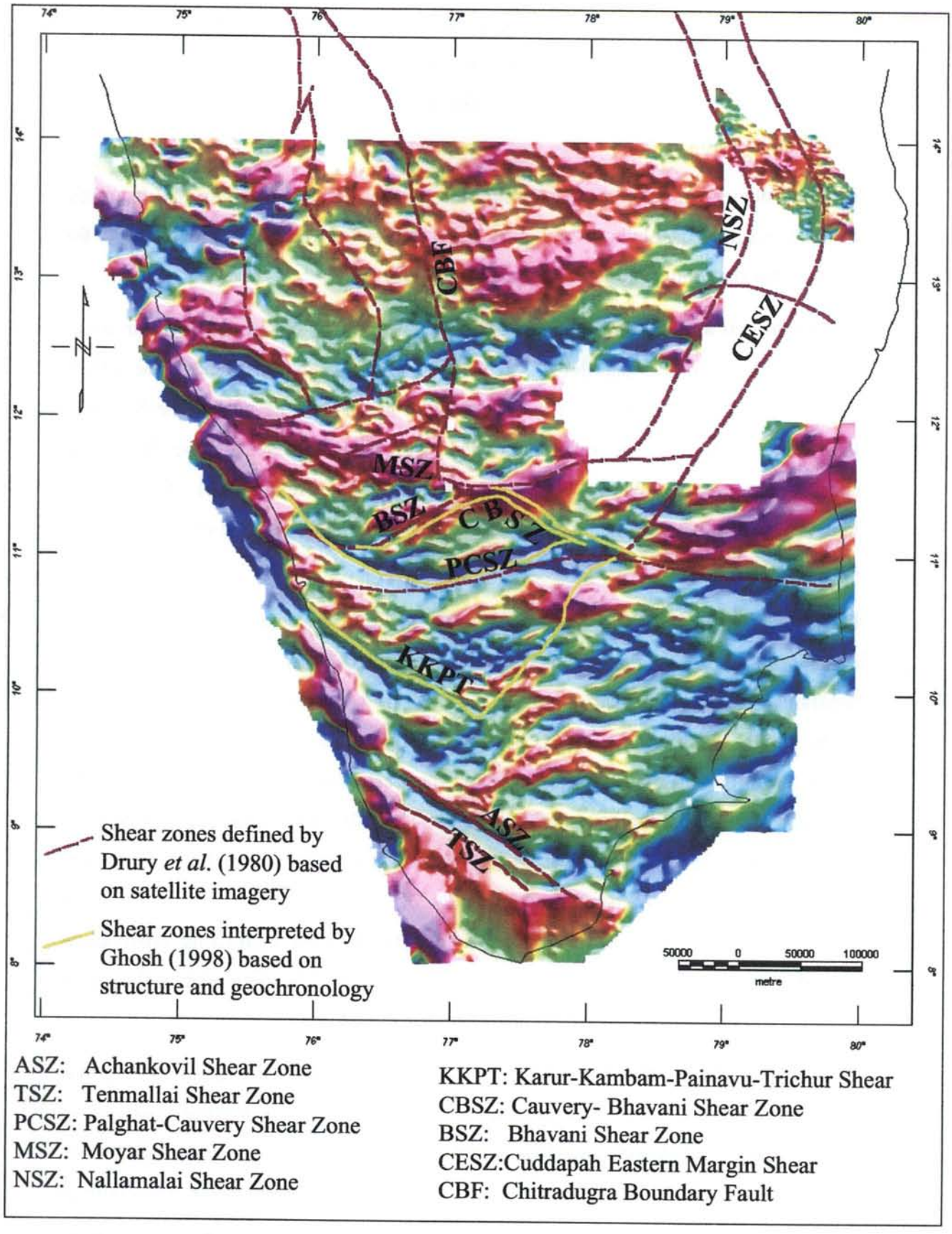

***Figure 5.15**: Total field aeromagnetic image of southern India with previously interpreted shear zones (Drury et al.,1980; GSI, 1994; Ghosh, 1999).*

with intercalated quartzite and calc-silicate bands, whereas to the north of KKPT, the area is dominated by granitic and tonalitic gneisses with mafic granulites, BIF and associated metasediments. Contrast in isotopic ages for the rocks of either sides (~2.9 Ga for metasediments to the north and ~2.5 to 2.0 Ga for khondalites to the south) of the shear zone has been described by Ghosh. He interprets the KKPT as a possible tectonic terrain boundary separating high-grade equivalents of Archean Dharwarian rocks in the north from the Paleoproteriozoic khondalites and associated metasediments in the south.

The aeromagnetic images do not depict significant change in magnetic anomaly patterns across the KKPT. Though there exists a strong curvi-linear low magnetic zone, partially coinciding with the KKPT in the western part, there is no magnetic signature that corresponds to the eastern part. The KKPT is well within the magnetic relief zone III (Figure 5.14) and thus does not seem to be a major tectonic boundary in southern India.

d. Moyar – Bhavani Shear Zone: This is an approximately east-west trending shear system that splits into two – the Moyar Shear Zone (MSZ) and the Bhavani Shear Zone (BSZ) – in the western part. This shear zone, especially the WNW-ESE trending Moyar Shear zone coincides with a high amplitude magnetic zone that seems to be most magnetically prominent shear zone in southern India. Unfortunately, the eastward continuation of this shear zone could not be verified due to lack of data coverage.

e. West-Coast Fault (WCF): The analytic signal map (Map 5.4) shows a strong NW-SE trending linear anomaly zone parallel to the southwest coast of India. It is evident from the total field and first derivative maps that almost all the major ~east-west trending shear zones in southern India bend toward NW in the western parts and finally merge with the West-coast fault. Thus, the West-coast fault is rather a *fault zone* comprising the westernmost parts of the major shears and faults. The northwesterly bend of these faults and shear zones indicates that there must have been significant amount of dextral strike-slip movement along this fault.

f. North-South trending Shear systems: A number of north-south trending shear zones/thrusts (the Cuddapah Eastern marginal fault, the Nallamalai shear zone, the Chitradurga boundary thrust etc., Figures 5.13 and 5.15) have been described by

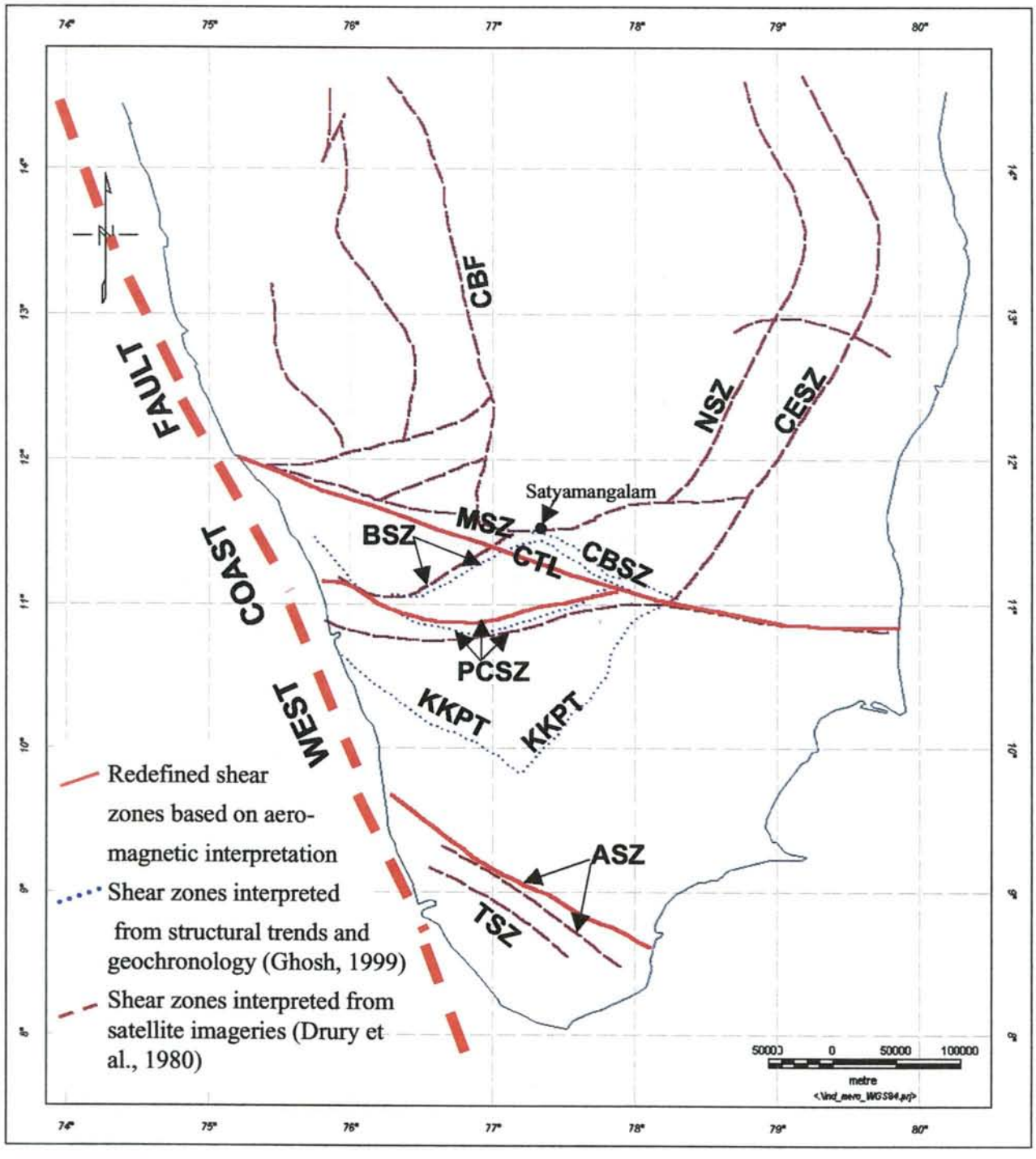

***Figure 5.16**: Proterozoic shear systems of southern India as interpreted by earlier workers and redefined in this study. TSZ: Tenmallai Shear Zone, ASZ: Achankovil Shear Zone, PCSZ: Palghat-Cauvery Shear Zone, BSZ: Bhavani Shear Zone, MSZ: Moyar Shear Zone, CESZ: Cuddapah Eastern Boundary Fault, CBF: Chitradurga Boundary Fault, BCSZ: Cauvery-Bhavani Shear Zone, KKPT: Karur-Kambam-Painavu-Trichur Shear, CTL: Cannanore-Thanzavur Lineament. The West Coast Fault was developed/reactivated during translation between Madagascar and India in Mid Jurassic.*

earlier authors (Drury *et al.*, 1984, GSI, 1994 etc.) to the north of Moyar Shear Zone. However, unlike the east-west shear zones, none of these shear zones have significant magnetic signatures. Absence of magnetic features is probably due to the theoretical considerations and survey parameters – 1. Suppression of amplitude of magnetic anomalies caused due to north-south trending sources in low magnetic latitudes, 2. flying directions at low angles to subparallel to the trends of these shear systems, 3. wide flight line spacing and 4. incomplete data in the eastern part.

g. Other Lineaments: A number of small-scale lineaments have been interpreted from the aeromagnetic images (Figure 5.18) besides the major ones described above. These lineaments can be divided into two groups – 1. ~ east-west trending lineaments mostly confined to the eastern part and 2. NW-SE trending lineaments in the western part. These lineaments might be small-scale faults and shear zones sympathetic to the major east-west shear systems and the West-coast fault respectively.

5.12.3. Integration of Geology and Aeromagnetic Data

Integration of different layers of geoinformation like geology, aeromagnetics, gravity, topography etc. enhances the visibility of geological features, many of which may not be clear on any one of the layers alone. Integration of geology and aeromagnetics of southern India provides a fine example, where major structural and tectonic features stand out clearly. The obvious and most conspicuous feature in the integrated image that catches the eyes is the ENE-WSW trending trans-subcontinental linear magnetic anomaly zone (Z-Z1 in Figure 5.17). This anomaly zone will be referred as the Cannanore-Thanjavur Lineament (CTL) henceforth.

a. Cannanore-Thanjavur Lineament (CTL)

The CTL is a prominent magnetic anomaly that is interpreted as shear zone. (Figure 5.17 and 5.18) The CTL includes of a number of intricate shears and extends from Cannanore in the west coast to near Thanzavur in the east thus transecting the entire South Indian Precambrian crust. The western part of the shear zone roughly coincides with the Moyar Shear Zone, whereas no southeastward extension of it is shown in the earlier maps (Drury *et al.*, 1984; GSI, 1994). The Moyar Shear Zone takes a northeasterly trend from Satyamangalam (Figure 5.16) in the eastern part. Though part of this eastern sector of the Moyar Shear zone coincides with a high and

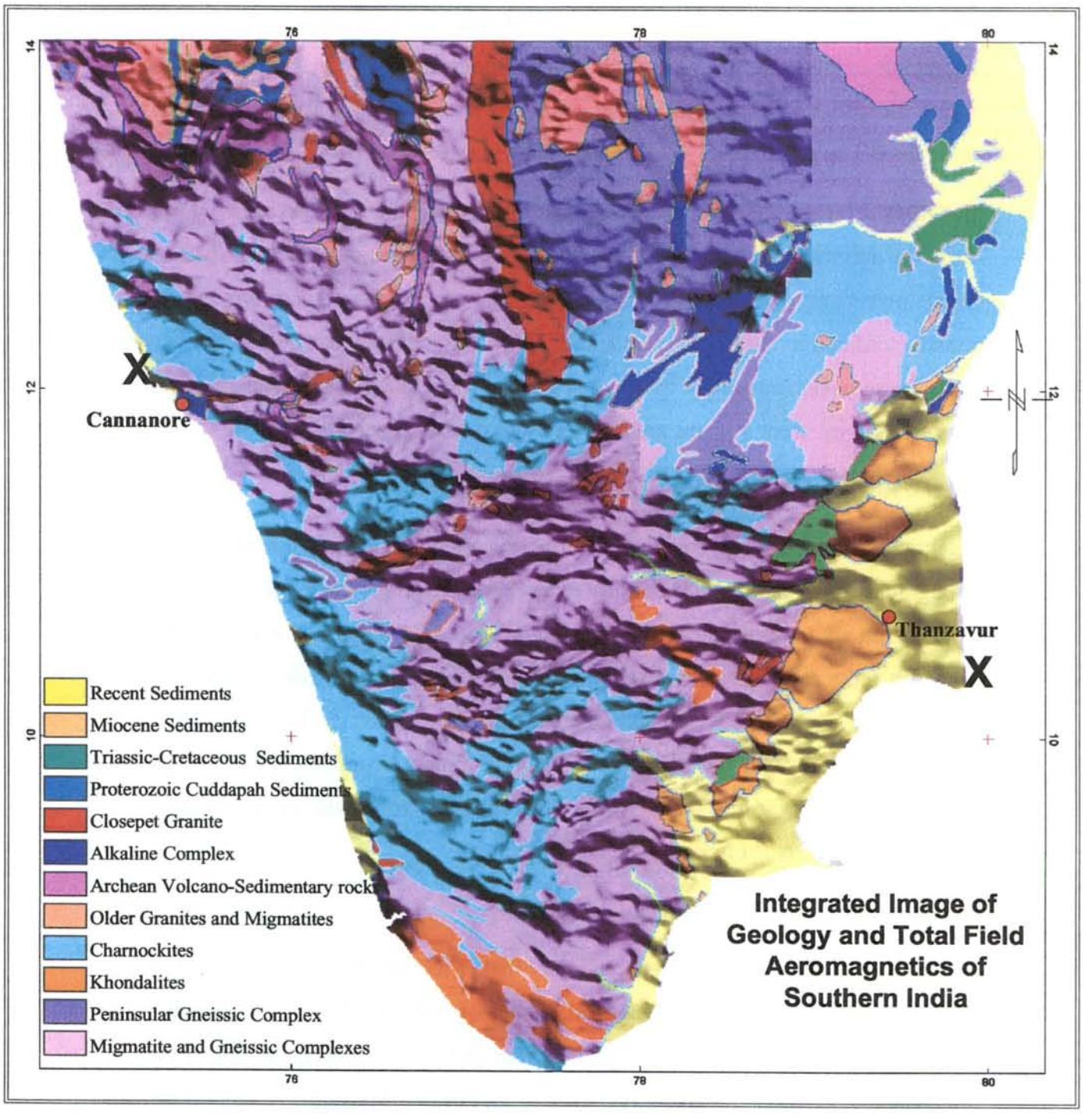

***Figure 5.17**:Composite map of Geology (Geological Survey of India, 1993) and Aeromagnetics (this study) of Southern India. Grey scale shaded relief image of total field aeromagnetic data is draped over geology. Note the prominence of the major shear zones: X-X is the newly defined Cnnanore-Thanzavur Lineament (CTL). In the northwestern part digital aeromagnetic data is not available*

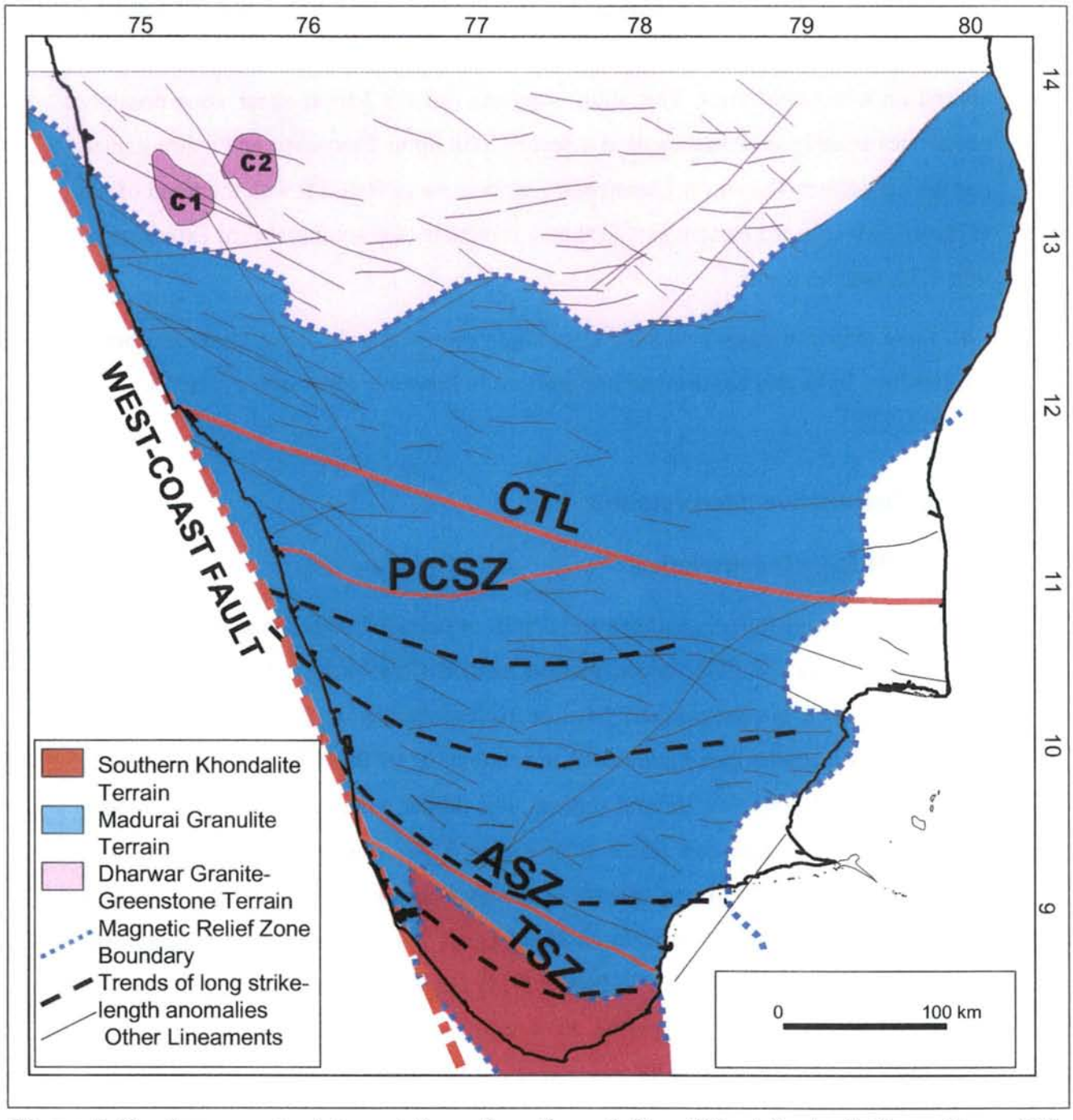

***Figure 5.18**: Aeromagnetic interpretation of southern India. ASZ: Achankovil Shear Zone, CTL: Cannanore-Thanzavur Lineament, PCSZ: Palghat-Cauvery Shear Zone, TSZ: Tenmallai Shear Zone. CTL is the newly defined Lineament. TSZ, ASZ and PCSZ have been redefined. Note the trends of long strike-length magnetic anomalies change to NW in the western part and finally merge with the West-Coast Fault. C1 and C2 are the two high amplitude analytic signals zones within the Dharwar Craton.*

elongated magnetic anomaly, it seems that the eastern and western parts do not meet each other. On the contrary, the western part of the shear zone shows lateral continuity towards southeast in the form of a number of en echelon shears in the integrated map. Furthermore, Ghosh (1999) has shown a NW-SE trending shear zone (Figure 5.15 and 5.16) in continuation with the western part of the Moyar shear zone based on structural trends. This study suggests that the Moyar shear zone possibly continues linearly southeastwards at a deeper level up to Thanzavur and hence named as the Cannanore-Thanzavur Lineament. Coincidence of the CTL with the trend of the Cauvery River in the eastern part further substantiates the southeastward extension of the CTL beyond Karur.

All this evidence suggest that the CTL might represent a fundamental crustal break in southern India that has tectonic implications in Precambrian crustal evolution.

5.13. Quantitative Interpretation

5.13.1. 3D Euler Deconvolution

Quantitative estimation of positions and depths of burial of magnetic sources has been carried out using the Euler deconvolution method (Reid *et al.*, 1990). The various parameters used for the purpose have been described in section 5.5.4. The Euler deconvolution results (see Figure 5.11 in section 'A' of this Chapter) depict source depths up to 23 km below ground surface. The deeper sources (>7.5 km) are mostly confined to the eastern part (Zone II in Figure 5.14), whereas those of shallow depths (<500m) are spread mostly over the Dharwar craton and the Southern Granulite Terrain north of Achankovil Shear Zone. The depth of sources south of the Achankovil Shear Zone (zone I in Figure 5.14) ranges between 1 km and 7 km. The Palghat Gap also shows deeper (1 to 4 km) and fewer solutions signifying the existence of a thick magnetically transparent crustal zone.

Linear alignment of depth solutions (Figure 5.11) was used to delineate lineaments precisely (Figure 5.18). This provides a quantitative support to the lineaments, which are visible in magnetic anomaly (total field and derivative) maps.

5.14. Aeromagnetic Comparison between Southern India and its Gondwana Neighbours

5.14.1. Southwest Sri Lanka

The southwestern part of Sri Lanka was covered by high-resolution aeromagnetic survey in 1957. Digital compilation of this data was completed by Perera in 1997 (see Chapters 1 and 3 for details). Perera (1997) distinguished three distinct magnetic relief zones broadly corresponding to the three Precambrian lithotectonic units- the Wanni Complex, the Highland Complex and the Vijayan Complex (Figure 5.19a) of Cooray *et al.* (1994). The aeromagnetic image (Figure 5.19b) depicts a number of strong NW-SE trending anomalies in the central part which take sharp westward turn and become almost east-west in the extreme west. The long-strike-length magnetic anomalies in the Southern Granulite Terrain of southern India (Map 5.2 and Figure 5.20) also show east-west trend in the eastern part. In the analytic signal map (Figure 5.21), it is evident that the strong analytic signals in the northern part of SW Sri Lanka (WC) corresponds to the high amplitude analytic signals of the central part of southern India. Similarly the weak analytic signals in the southern tip of India (SKT in Figure 5.21) compare well with those of the HC in southwestern tip of Sri Lanka. Thus, the magnetic data corroborates the fit (Figures 5.20 and 5.21). This observation also substantiates the geological similarities between the two terrains described in Chapter 4 of this thesis.

5.14.2. Southern Madagascar

Unfortunately, aeromagnetic coverage in Madagascar is very poor and no data exists in the southern and eastern parts, hindering direct aeromagnetic comparison with southern India. Aeromagnetic data over a small area in the south-central part of Madagascar partly shows trends of the Ranotsara Shear zone and two NE-SW trending shear zones south of RSZ. It is difficult to correlate these shear zones with those of southern India due to incomplete data. However, the analytic signals of the total magnetic field in south-central Madagascar looks similar in patterns with those in the central part of southern India giving some idea on the existence of rocks of comparable susceptibilities in both the terrains. Two circular analytic signal anomalies

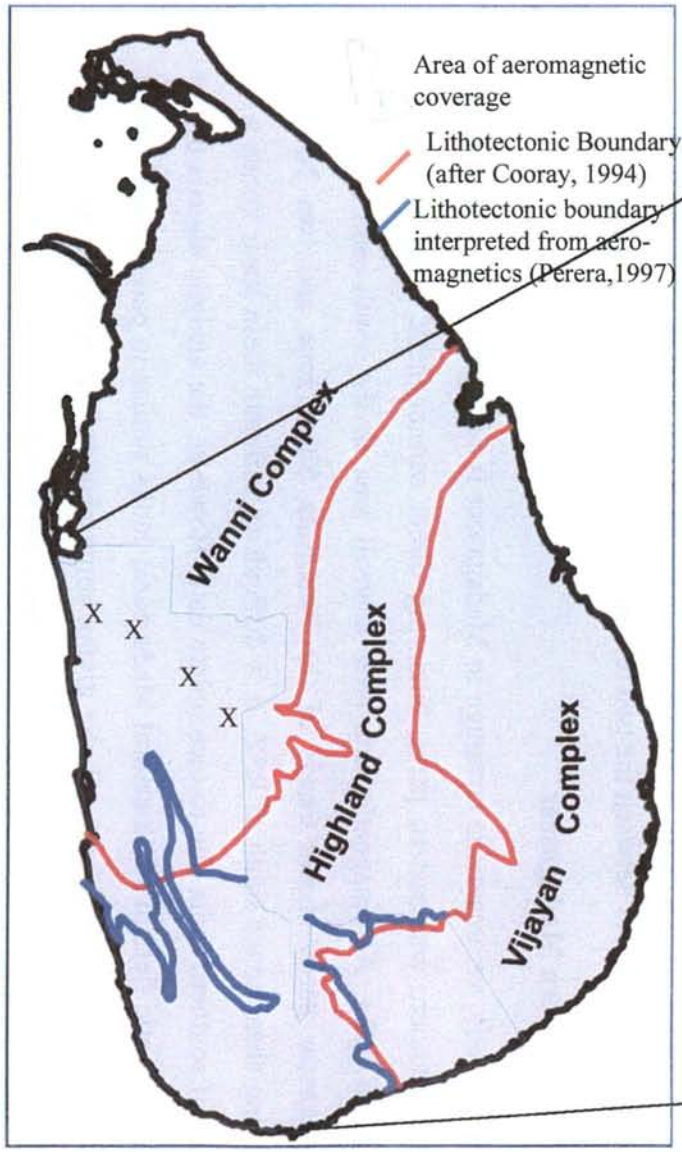

***Figure 5.19a**: Lithotectonic subdivisions of Sri Lanka*

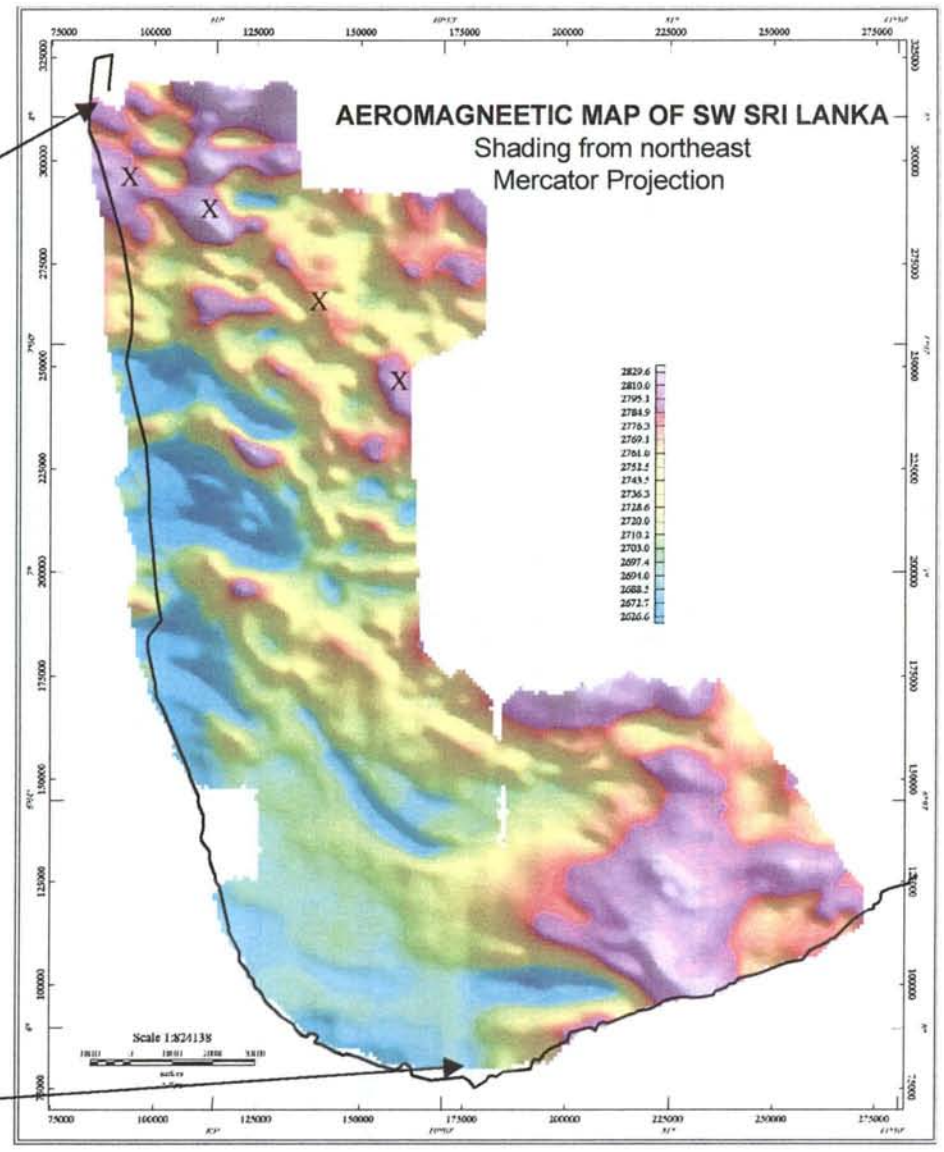

***Figure 5.19b**: Aeromagnetic map of SW Sri Lanka. Note the boundary between the Vijayan and Highland Complexes is clear in the magnetic image, whereas, no clear boundary is discernable between the Highland and the Wanni Complexes. The strike of the anomaly marked by X X X X turns into ~E-W in the western part of the map.Data upward continued to 2100m.*

(A1 and A2 in Figure 5.21) in the northwestern part of southern India are similar to that (A3) in central Madagascar.

5.14.3. Northern Mozambique

Similarity in aeromagnetic anomaly patterns exists between the Madurai Block of southern India and the area north of the Lurio Shear Belt in northern Mozambique (see Map 8.1). The long strike-length magnetic anomalies of both the terrains show change in strike directions suggesting open folds in the magnetic sources. These folds might have been caused due to drag (drag folds) related to the strike-slip movement along a lineament to the west of these folds. Reeves and de Wit (2000) have interpreted a magnetic lineament in northern Mozambique (Xixano-Chivaro Shear Zone, Map 8.1) and have linked this lineament to the rift between India-Madagascar in their Gondwana reassembly. Thus, the Xixano-Chivaro Shear zone might represent the southwestern extension of the West Coast Fault in East Africa.

5.15. Summary and Conclusion

1. Southern India consists of 3 distinct magnetic relief zones corresponding to three Precambrian tectonic provinces – the Archean granite-greenstone belt of the Dharwar craton in the north, the Madurai Block comprising predominantly charnockite massifs and migmatites in the middle and the Southern khondalite belt in the south. The boundary between the Dharwar craton and the Madurai Block lies along the line $X\text{-}X_1$ (Figure 5.14), whereas the Achankovil Shear zone ($Y\text{-}Y_1$ in Figure 5.14) represents the tectonic boundary between the Madurai block and the Southern Khondalite Terrain. The line $X\text{-}X_1$ might represent a change in the metamorphic grade between the two terrains.

2. Though most of the previously described shear zones are depicted in the aeromagnetic images, their positions and extent have been redefined. However, care must be taken, as it is not clear to what extent the magnetic anomalies represent shear zones or change in metamorphic grade or both. These observations must be substantiated with field checks.

3. The Palghat-Cauvery shear zone does not seem to be a tectonic boundary as thought earlier (Harris *et al.*, 1994). Field observations depicting continuity of

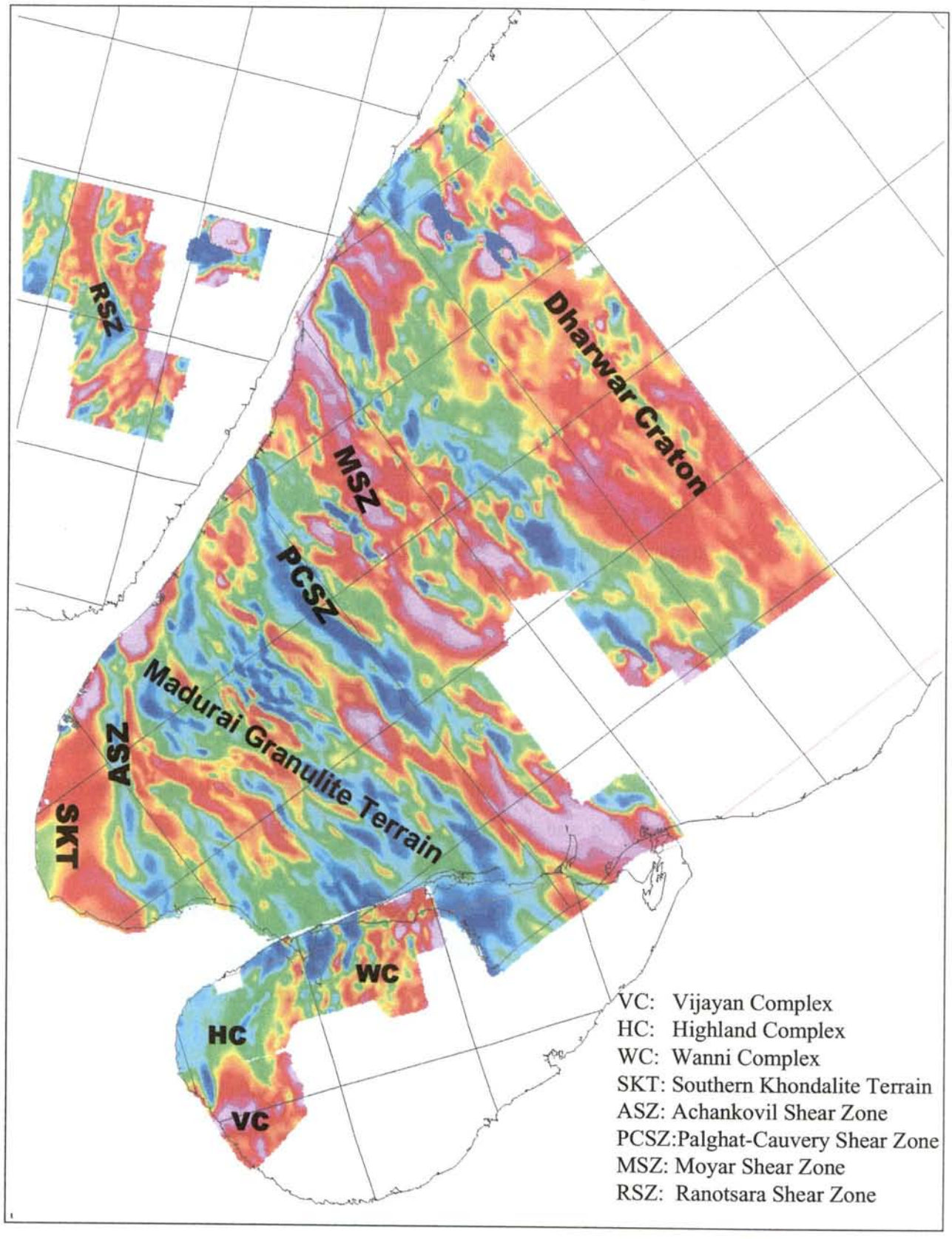

***Figure 5.20**: Aeromagnetic images of parts of southern India, Sri Lanka and Madagascar in a pre-breakup configuration. Model of reconstruction - reev506x at 200 Ma. Aeromagnetic Data Sources: Southern India - this study; Sri Lanka - Perera (1997); Madagascar - African Magnetic Mapping Project (Barritt, 1993).*

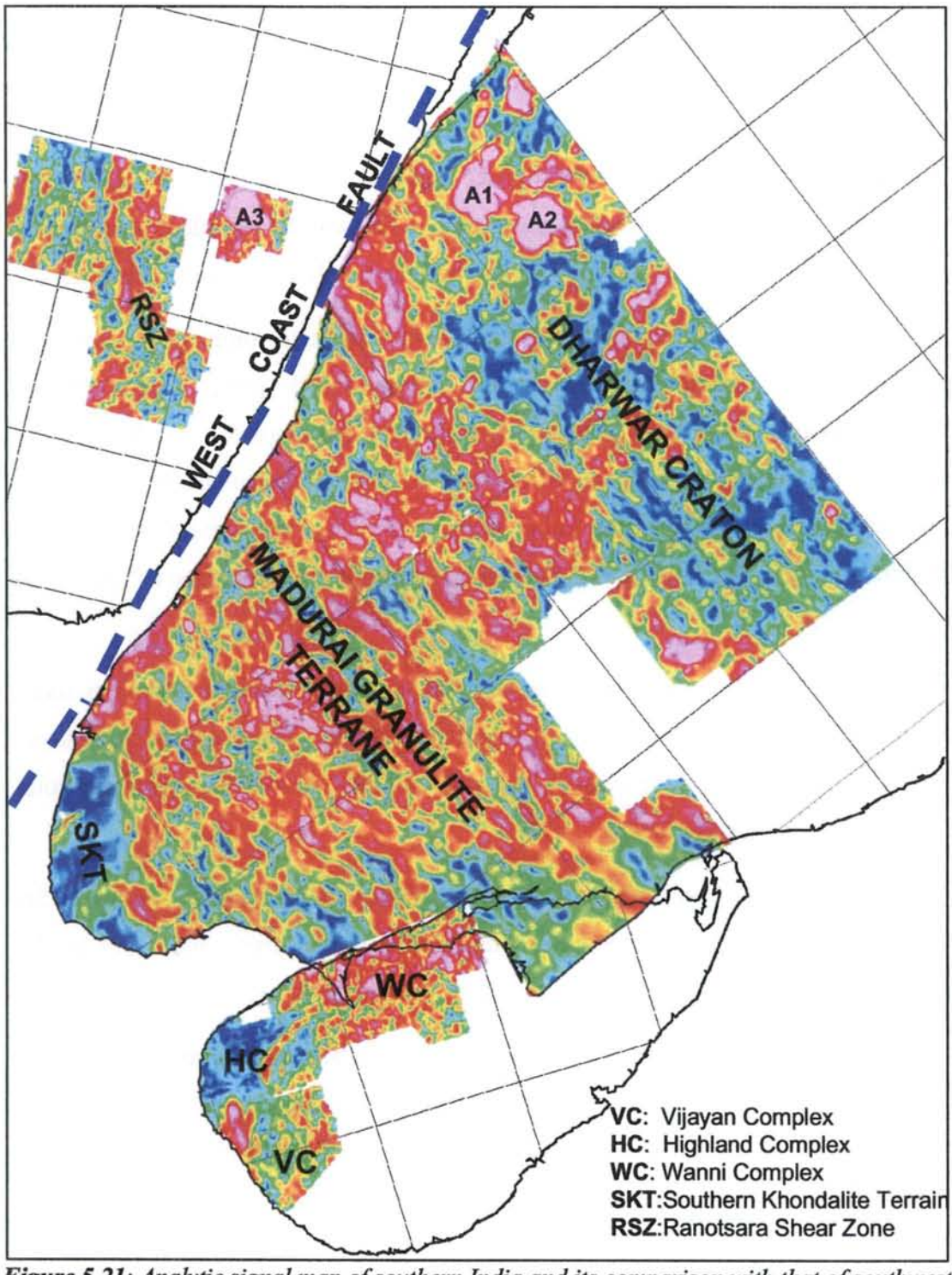

***Figure 5.21**: Analytic signal map of southern India and its comparison with that of southwest Sri Lanka and south-centralMadagascar in a pre-breakup configuration (Model:reeve506x). Note:1. the similarity in analytic signals over Wanni Complex of Sri Lanka, Madurai Granulite Terrane of southern India and south-central Madagascar and 2. near circular analytic signal anomalies (A1 and A2 in India) and (A3) in Madagascar. Note the coincidence of the West Coast Fault with the east coast of Madagascar.*

structural trends across PCSZ and absence of intense shearing in the western part of it (GSI, 1995; Naha and Srinivasan, 1996) do not corroborate the hypothesis of PCSZ being a major tectonic boundary. The present aeromagnetic study reveals that in the western part, the anomaly along the Palghat Gap represents a deep structure, but there is no substantial eastward continuation of it. Thus this study confirms that the PCSZ does not represent a transcontinental shear zone, which can be regarded as a tectonic terrain boundary between the Dharwar craton and the Southern Granulite Terrain.

4. Most of the ~east-west trending long strike-length magnetic anomalies in southern India bend towards northwest in the western part and finally merge with a NW-SE trending lineament, the West Coast Fault (Figure 5.14 and Maps 5.1, 5.2 & 5.3). The bend in the magnetic trends signifies dextral strike-slip movement along the lineament, possibly related to the initial shearing between Madagascar and India in Mid Jurassic. Thus the West Coast Fault might represent the shoulder of the India-Madagascar rift. It is also pertinent to note that a strong lineament in northern Mozambique, north of the Lurio shear zone trending NNE (Maps 6.2-6.4 and 8.1) lies on the direct continuation southward of the WCF (Map 8.1).

5. Integration of geology and aeromagnetic data clearly reveals an unbroken shear system (CTL, Figure 5.17), broadly corresponding to the western part of the Moyar Shear zone (GSI, 1994) in the western part and with the Cauvery-Bhavani shear zone (Ghosh, 1998) in the eastern part.

6. Strong correlation of aeromagnetic anomaly patterns exists between southwest Sri Lanka and southern India. Continuity of long strike-length magnetic anomalies in SW Sri Lanka to southern India can be used to argue for a close fit between them.

6. Digital compilation of the existing aeromagnetic data and its interpretation need to be completed urgently to understand the regional tectonics of India. Attempts also should be made to complete aeromagnetic surveys for the still uncovered parts of India, Sri Lanka and Madagascar to facilitate comparison among these Gondwana neighbours.

6. AEROMAGNETICS OF SOUTHERN AND EASTERN AFRICA

6.1. Introduction

Africa is relatively better covered by aeromagnetic surveys (Figure 6.1) among the central Gondwana fragments. Most of the available aeromagnetic data for Africa (Figure 6.2) was compiled under the African Magnetic Mapping Project (AMMP, Barritt, 1993). A near-total aeromagnetic coverage of southern and eastern Africa exists in the AMMP data. A gap in the AMMP coverage in the western part of Namibia has been filled in this study by merging the data from Namibia (Geological Survey of Namibia) with rest of the AMMP dataset. The compiled dataset - covering South Africa, Namibia, Botswana, Zimbabwe, Malawi, Mozambique, Zambia, Tanzania and Kenya - was processed and interpreted for continental scale tectonic features and used to correlate them with those interpreted from Dronning Maud Land, East Antarctica, Madagascar, India and Sri Lanka in a reassembled central Gondwana (Map 8.3).

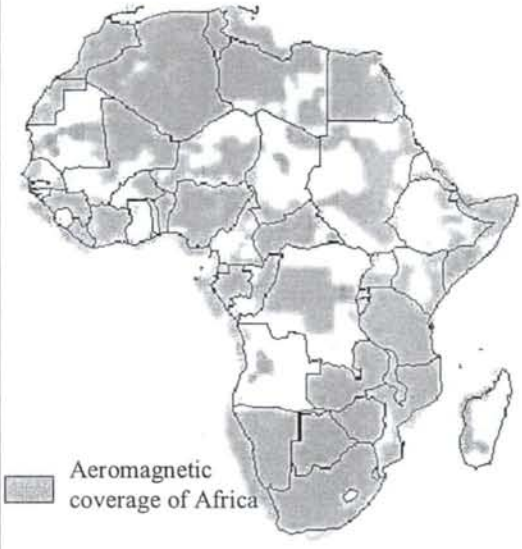

***Figure 6.1**: Known aeromagnetic coverage of Africa (from Reeves et al., 1998). No data exists for the blank areas mostly in central Africa.*

6.2. Processing

6.2.1. Compilation of Namibian Data with AMMP Data

Gridded data (Geosoft GXF format) for Namibia (Figure 6.3) was obtained from the Geological Survey of Namibia (ref. Rainer Wackerle - Senior Geophysicist, 1998) through Reeves. The original data was available at a grid size 500x 500 m in Albers

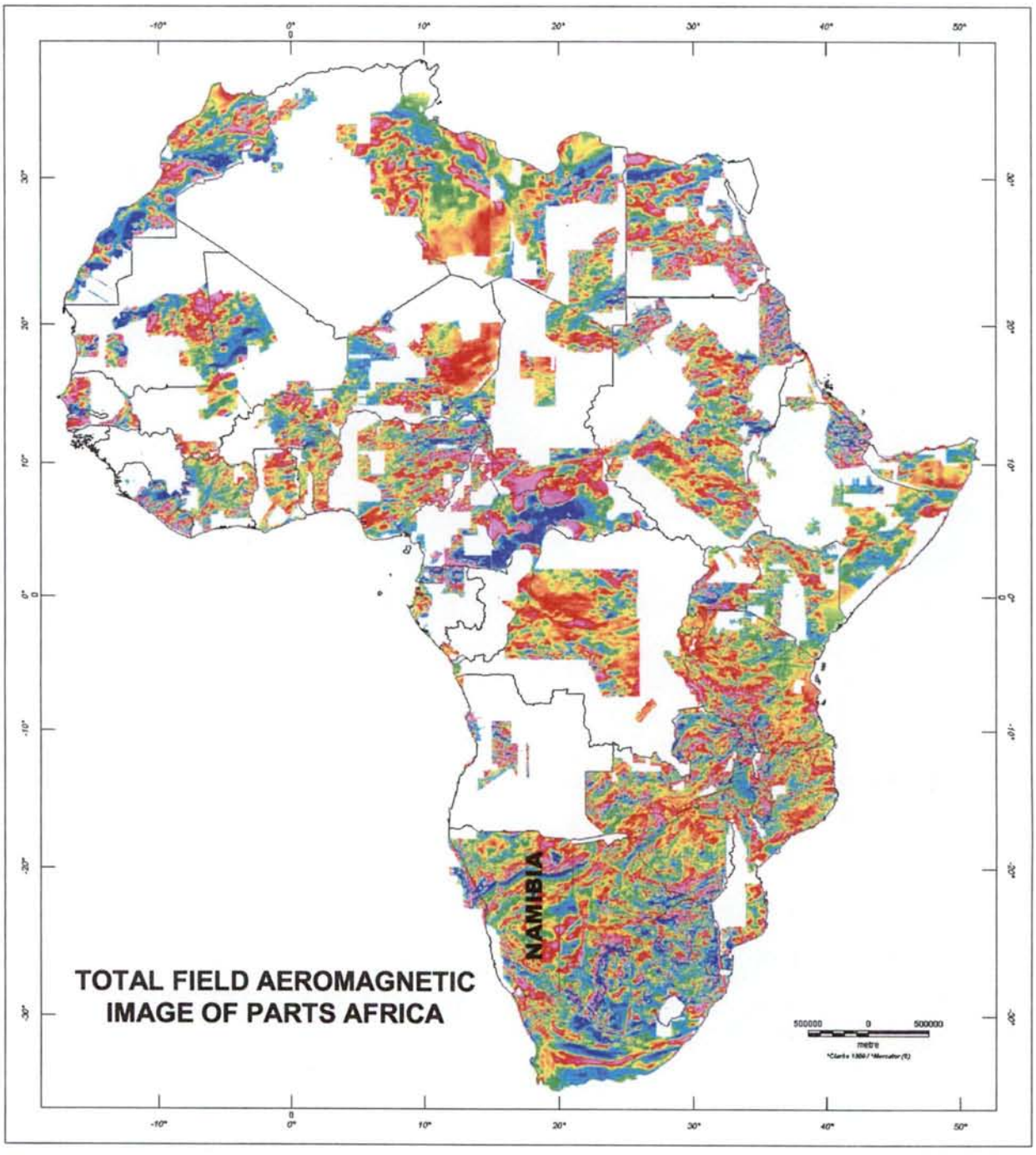

***Figure 6.2**: Total field aeromagnetic image of the available digital data for Africa. Data sources: Geological Survey of Namibia for Namibia and African Magnetic mapping Project (AMMP, Barritt, 1993) for other countries. Note the huge gaps in the aeromagnetic coverage.*

Equal Area projection. The data was regrided at 1000 x 1000 m and reprojected to Mercator projection same as that of AMMP. The data, then, was merged with the AMMP data for southern and eastern Africa (Figure 6.3) using the Boolean functions between two grids. The grids were merged by averaging the total intensity values of both the grids at each point of the overlapping area.

The AMMP data and Namibian grids were available as IGRF-corrected data. The merged data was subjected to Fourier transformation for converting the data into wave-number domain. A number of filtering operations were carried out to calculate the analytic signal amplitudes and vertical derivatives of total intensity and analytic signals and apparent susceptibility mapping to produce enhanced images for interpretation of regional structural and tectonic features like the hidden boundaries of cratons and mobile belts, major lineaments –faults and shear zones and trend of dyke swarms.

6.3. Interpretation

Aeromagnetic interpretation for parts of southern and eastern Africa has been done by many earlier workers (*e.g.* Reeves, 1978; Batterham, 1983; Reeves *et al.*, 1986/87; Corner, 1994). These interpretations were carried out for specific areas mostly from the contour and profile maps. The advantages of the modern processing and visualisation techniques over the traditional data presentation methods (contours and profiles) have been demonstrated elsewhere (*e.g.* Reeves *et al.*, 1998; Milligan and Gunn, 1997). Here, the data is processed using various filtering techniques mostly in the wavenumber domain. The enhanced aeromagnetic images for southern and eastern Africa were used primarily to interpret regional magnetic anomalies for their geological sources and correlate these features with adjacent Gondwana fragments.

6.3.1. Aeromagnetic Domain Map of southern and eastern Africa

An aeromagnetic domain map of southern and eastern Africa (Map 6.7) was prepared based mostly on the magnetic relief patterns, analytic signals and clustering of Euler depth solutions in various tectonic terrains. The Archean cratonic terrains are characterized by relatively lower magnetic relief than the surrounding high-grade granulite and gneissic terrains of Proterozoic ages. The intracratonic Phanerozoic rift

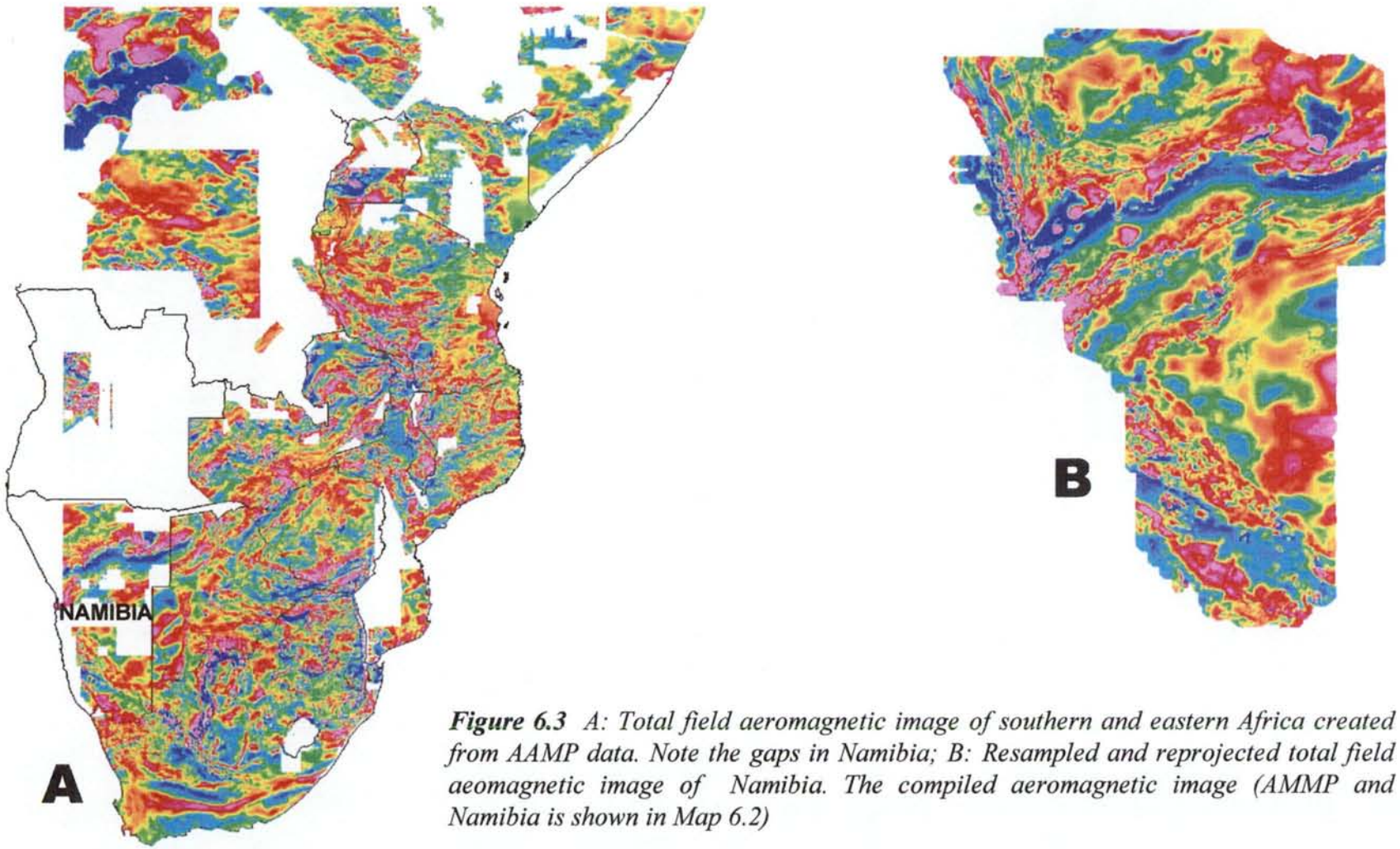

Figure 6.3 *A: Total field aeromagnetic image of southern and eastern Africa created from AAMP data. Note the gaps in Namibia; B: Resampled and reprojected total field aeomagnetic image of Namibia. The compiled aeromagnetic image (AMMP and Namibia is shown in Map 6.2)*

basins filled with magnetically transparent sediments are characterized by quiet magnetic relief.

6.3.2 Aeromagnetic Images

A number of aeromagnetic images were produced at 1: 5 000 000 scale for data presentation and interpretation. A Mercator projection with the spheroid Clarke1880 was used to produce these maps which are enclosed in the back pocket.

a. Total Field Shaded Relief Map

The aeromagnetic data was displayed as a combined colour raster and grey-scale shaded relief image (Map 6.1) to enhance features in preferred directions. An HSV (hue, saturation, value) colour scheme was used to display the image. The image was displayed with varying inclination and declination of light source interactively. It was found that an inclination of 30° and a declination of 45° for the light source produced the desired result.

b. Vertical Derivative Map

First Vertical derivative (Map 6.2) of the total field magnetic anomalies was calculated in the wavenumber domain to enhance the shallow geologic features and better resolve the closely spaced geological sources. This map was particularly useful in tracing the magnetic trends (Map 6.7), which are much better resolved that any other presentation of the data. The magnetic trends in combination with lithological and geochronological information were used to decipher the boundaries of different tectonic blocks.

c. Analytic Signal Map

The theoretical aspects of the analytic signal calculation are described in the Chapters 3 and 5. The analytical signal of the total magnetic field produces simple anomalies whose maxima mark the edges of the magnetised body irrespective of its magnetisation vectors (MacLeod *et al.*, 1993). Thus, areas of analytic signal highs are located over high magnetic sources. This is clearly demonstrated in the Analytic signal map (Map 6.3), where the exposed and near surface Precambrian rocks and basic magmatic rocks are represented by strong analytic signals (shades of magenta) and the basins filled with thick sequence of magnetically transparent sediments are

represented by weak analytic signals (blue). This property has been used in delineation of boundaries of cratons and basins.

d. Vertical Derivative of Analytic Signals

Processing the derivatives of the analytical signal amplitudes, instead of the original analytic signal amplitudes, produces more effective separation of the anomalies caused by close sources (Debeglia and Corpel, 1997). First vertical derivative of the analytic signal amplitudes was calculated in frequency domain. The vertical derivative image (Map 6.4) was of immense help in mapping the rift-related structures and craton boundaries in southern and eastern Africa.

e. Susceptibility Mapping

Susceptibility mapping is an inverse modelling method for converting the continuously varying magnetic anomaly field into a function closely representing the discontinuous geology of the source rocks (Grant, 1973). The susceptibility filter calculates the apparent magnetic susceptibility of the magnetic sources using the following assumptions:

- The magnetic field has had the IGRF or a similar trend surface removed.
- The magnetisation is purely due to induction and absolutely free of any remanent magnetization.
- All magnetic response is caused by a collection of vertical, square-ended prisms, one per cell of the original data grid, extending to infinite depth extent (Bhattacharyya, 1966). The magnetic susceptibility of each of these prisms is calculated such that the combined magnetic effect of all the prisms is the observed magnetic field data. Thus, the validity of the results is naturally subject to how well the actual observed field conforms to these assumptions.

Calculation of apparent susceptibility from the total field aeromagnetic data is done in the wavenumber domain. A susceptibility filter is, in fact, a compound filter that performs – (i) Reduction-to-pole, (ii) downward continuation to the source depth, and (iii) correction for the geometric effect of a vertical square ended prism and division by the total magnetic field to yield susceptibility. The filtering was carried out

basins filled with magnetically transparent sediments are characterized by quiet magnetic relief.

6.3.2 Aeromagnetic Images

A number of aeromagnetic images were produced at 1: 5 000 000 scale for data presentation and interpretation. A Mercator projection with the spheroid Clarke1880 was used to produce these maps which are enclosed in the back pocket.

a. Total Field Shaded Relief Map

The aeromagnetic data was displayed as a combined colour raster and grey-scale shaded relief image (Map 6.1) to enhance features in preferred directions. An HSV (hue, saturation, value) colour scheme was used to display the image. The image was displayed with varying inclination and declination of light source interactively. It was found that an inclination of 30° and a declination of 45° for the light source produced the desired result.

b. Vertical Derivative Map

First Vertical derivative (Map 6.2) of the total field magnetic anomalies was calculated in the wavenumber domain to enhance the shallow geologic features and better resolve the closely spaced geological sources. This map was particularly useful in tracing the magnetic trends (Map 6.7), which are much better resolved that any other presentation of the data. The magnetic trends in combination with lithological and geochronological information were used to decipher the boundaries of different tectonic blocks.

c. Analytic Signal Map

The theoretical aspects of the analytic signal calculation are described in the Chapters 3 and 5. The analytical signal of the total magnetic field produces simple anomalies whose maxima mark the edges of the magnetised body irrespective of its magnetisation vectors (MacLeod *et al.*, 1993). Thus, areas of analytic signal highs are located over high magnetic sources. This is clearly demonstrated in the Analytic signal map (Map 6.3), where the exposed and near surface Precambrian rocks and basic magmatic rocks are represented by strong analytic signals (shades of magenta) and the basins filled with thick sequence of magnetically transparent sediments are

represented by weak analytic signals (blue). This property has been used in delineation of boundaries of cratons and basins.

d. Vertical Derivative of Analytic Signals

Processing the derivatives of the analytical signal amplitudes, instead of the original analytic signal amplitudes, produces more effective separation of the anomalies caused by close sources (Debeglia and Corpel, 1997). First vertical derivative of the analytic signal amplitudes was calculated in frequency domain. The vertical derivative image (Map 6.4) was of immense help in mapping the rift-related structures and craton boundaries in southern and eastern Africa.

e. Susceptibility Mapping

Susceptibility mapping is an inverse modelling method for converting the continuously varying magnetic anomaly field into a function closely representing the discontinuous geology of the source rocks (Grant, 1973). The susceptibility filter calculates the apparent magnetic susceptibility of the magnetic sources using the following assumptions:

- The magnetic field has had the IGRF or a similar trend surface removed.
- The magnetisation is purely due to induction and absolutely free of any remanent magnetization.
- All magnetic response is caused by a collection of vertical, square-ended prisms, one per cell of the original data grid, extending to infinite depth extent (Bhattacharyya, 1966). The magnetic susceptibility of each of these prisms is calculated such that the combined magnetic effect of all the prisms is the observed magnetic field data. Thus, the validity of the results is naturally subject to how well the actual observed field conforms to these assumptions.

Calculation of apparent susceptibility from the total field aeromagnetic data is done in the wavenumber domain. A susceptibility filter is, in fact, a compound filter that performs – (i) Reduction-to-pole, (ii) downward continuation to the source depth, and (iii) correction for the geometric effect of a vertical square ended prism and division by the total magnetic field to yield susceptibility. The filtering was carried out

separately for southern Africa (Map 6.5a)[1] and Eastern Africa (Map 6.5b)[1] as the magnetic vectors differ spatially. Though it is not fully correct to calculate susceptibility values for large areas using a set of magnetic parameters, a judicious selection of a set of parameters that are closely representative for the whole area can produce useful results for interpretation in regional scale. The parameters used for susceptibility filtering in the two regions are given in Table 6.1.

Parameters	Southern Africa	East Africa
Total Intensity	28500	33000
Inclination	-65	-40
Declination	-20	-2
Amplitude Correction	65	40

***Table 6.1**: Parameters used for calculation of apparent magnetic susceptibility*

As 'reduction-to-pole' is involved as the first step in the calculation of apparent susceptibility, the data from the equatorial regions (Kenya and Tanzania), where the magnetic inclination is very low do not produce satisfactory result. However, the southern African data below 20° S, where the magnetic inclination is greater than 50°, the susceptibility map (Map 6.5a) produced better results. The data was downward continued by 1000 m (terrain clearance for AMMP data) to calculate the susceptibility values at the ground level. A comparison between the total field map (Map 6.1) and the apparent susceptibility maps (Maps 6.5a and 5b) shows that the latter, like the vertical derivative maps (Map 6.2 and 6.4), better resolves the closely-spaced geological sources. This can be better appreciated by comparing the resolution of the dyke swarms in southern Africa.

6.3.3 Aeromagnetic Characteristics of Tectonic Terrains

The geology and tectonic framework of southern and eastern Africa are dealt with in detail in Chapter 4. An account of the aeromagnetic characteristics of these tectonic terrains is described in this section. Refer to Figure 6.4 and Map 6.7 for location of different tectonic terrains described below.

---

[1] *The susceptibility maps are produced on 1: 10 000 000 scale in this thesis for limitations of production of the thesis. But these maps can be reproduced on 1: 5 000 000 scale from the digital files (Map 5.5a & Map 6.5b) in the CD-ROM provided with this thesis.*

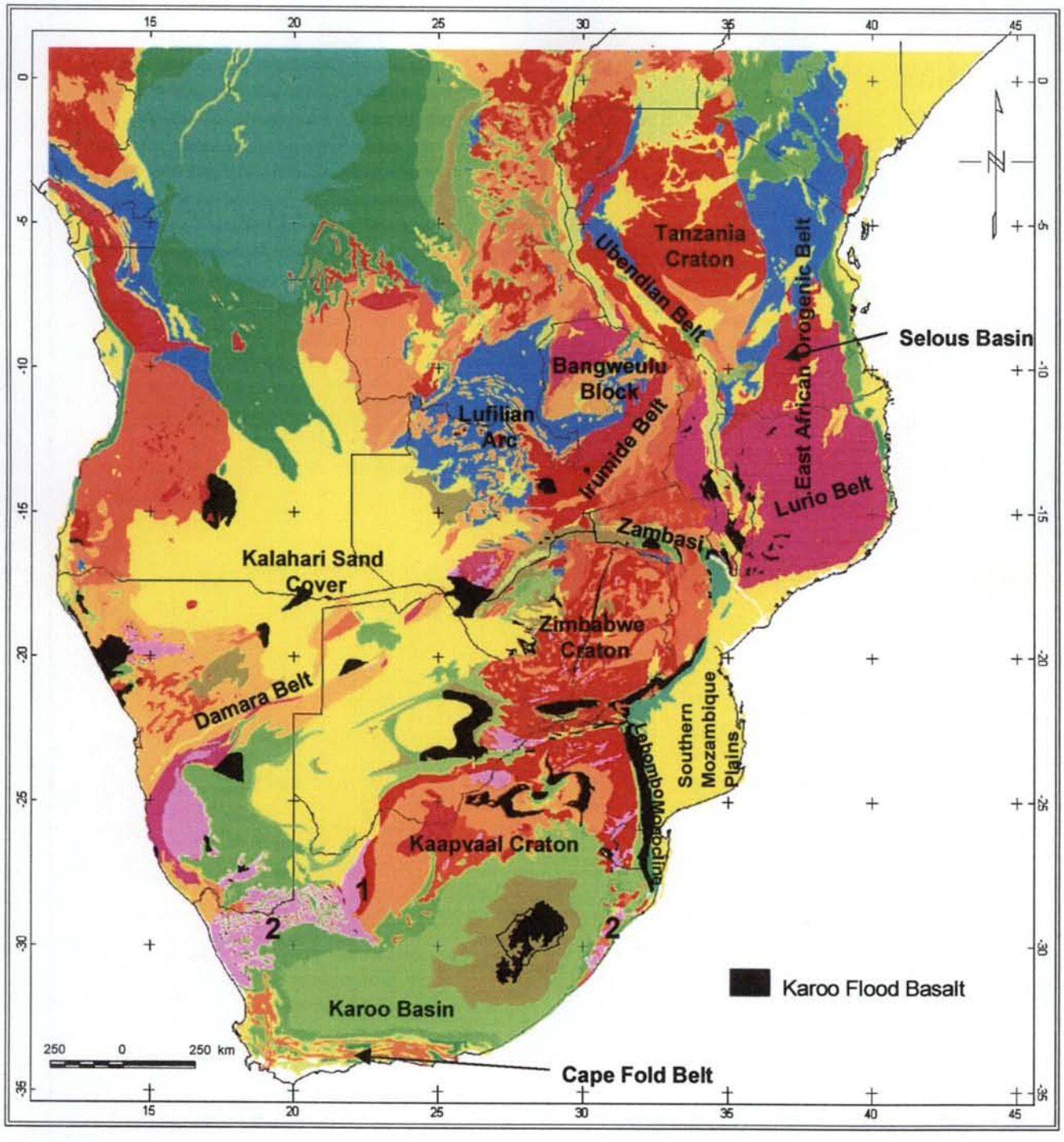

***Figure 6.4**: Geological Map of southern Africa created from digital data (Gondwana GIS) University of Cape Town). This figure is used only to show locations of different tectonic terrains referred in text. Detailed legend for all the units is beyond the scope of this figure.*

a. The Kaapvaal Craton

The margins of the Kaapvaal craton are buried under thick Karoo sediments in the south and the Kalahari sands in the west. To the east, the craton is bounded by the Lebombo monocline, represented by a north-south trending high-amplitude magnetic anomaly. To the north, the craton is bounded by the ENE-WSW trending Zoetfontein Fault (ZF). In the northwestern part the craton is apparently cut by the Zoetfontein Fault (Map 6.1). The block north of this fault (Okwa block in Map 6.1) has a distinctly lower magnetic relief than most parts of the craton south of the ZF. This suggests that the sediment cover is thicker in this part, which is reflected in the Euler depth map (Map 6.6).

b. The Zimbabwe Craton

The Zimbabwe craton is bounded by the Proterozoic mobile belts – the Irumide belt in the west, the Zambesi belt in the north, the Mozambique belt in the east. To the south, the craton is bounded by the Limpopo mobile belt of Archean age. The Zimbabwe craton is represented by moderate magnetic relief with high amplitude magnetic anomalies at the periphery. The elliptical shape of the craton is clearly discernable by tracing these anomalies. The greenstone belts distinctly stand out as relatively longer wavelength with moderate amplitude anomalies within the overall low relief of the granitoid-gneissic terrain.

c. The Rehoboth Triangle

The Rhehoboth triangle (Map 6.1) to the west of the Kaapvaal craton is the most enigmatic feature in aeromagnetic maps of southern Africa. It is represented by a mild magnetic relief with long wavelength anomalies. This suggests that the magnetic basement is deeply buried under the Kalahari cover and is at a much lower level than the surrounding Precambrian metamorphic terrains of the Kaapvaal craton to the east, the Namaqua metamorphic belt to the west and the Damara belt to the north.

d. The Kheis Belt

The Kheis belt is a narrow north-south trending zone at the western margin of the Kappvaal craton. This belt is represented by curvilinear north-south strike length anomalies that suggests presence of alternate bands of magnetic and nonmagnetic

rocks. This is also supported by the linear alignment of shallow (500 to 1000 m) Euler solutions (Map 6.6)

e. The Namaqua-Natal Belt

The Namaqua-Natal belt (Map 6.7) to the south of the Kaapvaal craton is mostly covered by the Karoo sediments and volcanic rocks in the central part. Parts of this belt are exposed in the west (Namaqua province) and in the east (Natal metamorphic province). The link between these two provinces is well demonstrated in all the aeromagnetic images. The southern margin of this belt coincides with a long strike length high amplitude magnetic anomaly (Beattie anomaly, Map 6.1). This anomaly has been modelled by Maher and Pitts (1989) who suggested a low-angle thrust that dips away from the Kaapvaal craton. The belt is bounded by a NW-SE trending narrow zone of high amplitude anomalies in the northeast. In the southwestern part the belt is represented by predominantly east-west magnetic trends.

f. The Damara Belt, Lufilian Arc and the Zambesi belt

The aeromagnetic images clearly show that the Pan-African Damara belt (Hartnady *et al.*, 1985) in Namibia is in physical continuity with the Lufilian arc of Zambia and Zaire and the Zambezi belt (Hanson and Wilson, 1988; Wilson *et al.*, 1993; Porada and Berhorst, 1999) below the Kalahari sediments. The Damara belt is represented by NE-SW magnetic trends and has alternate bands of high and low susceptibility rocks. At least 3 bands of high magnetic zones separated by two intermittent low magnetic zones are clearly decipherable in the analytic signal map (Map 6.3). The Damara belt merges with the Lufilian arc in South Zambia. The Lufilian arc is represented by overall low magnetic relief with predominantly east-west curvilinear magnetic trends and is bounded by the NE-SW trending high-relief Irumide belt in the east.

The east-west trending Zambezi belt cuts across the NE-SW Irumide belt without displacing the structural trends on either side. The Zambezi belt consists of marginal zones of remobilised basement which is overlain by a thick sequence of metasedimentary rocks with minor metavolcanics metamorphosed to amphibolite facies (Hanson and Wilson, 1988). The east-west trend of the Zambezi belt gradually turns to NW-SE around the northeastern part of the Zimbabwe craton. Though the east-west Zambezi trend is predominant within the Irumide belt in southern Zambia, weak NE-SW trend of the Irumide belt is still reflected in the magnetic images. This

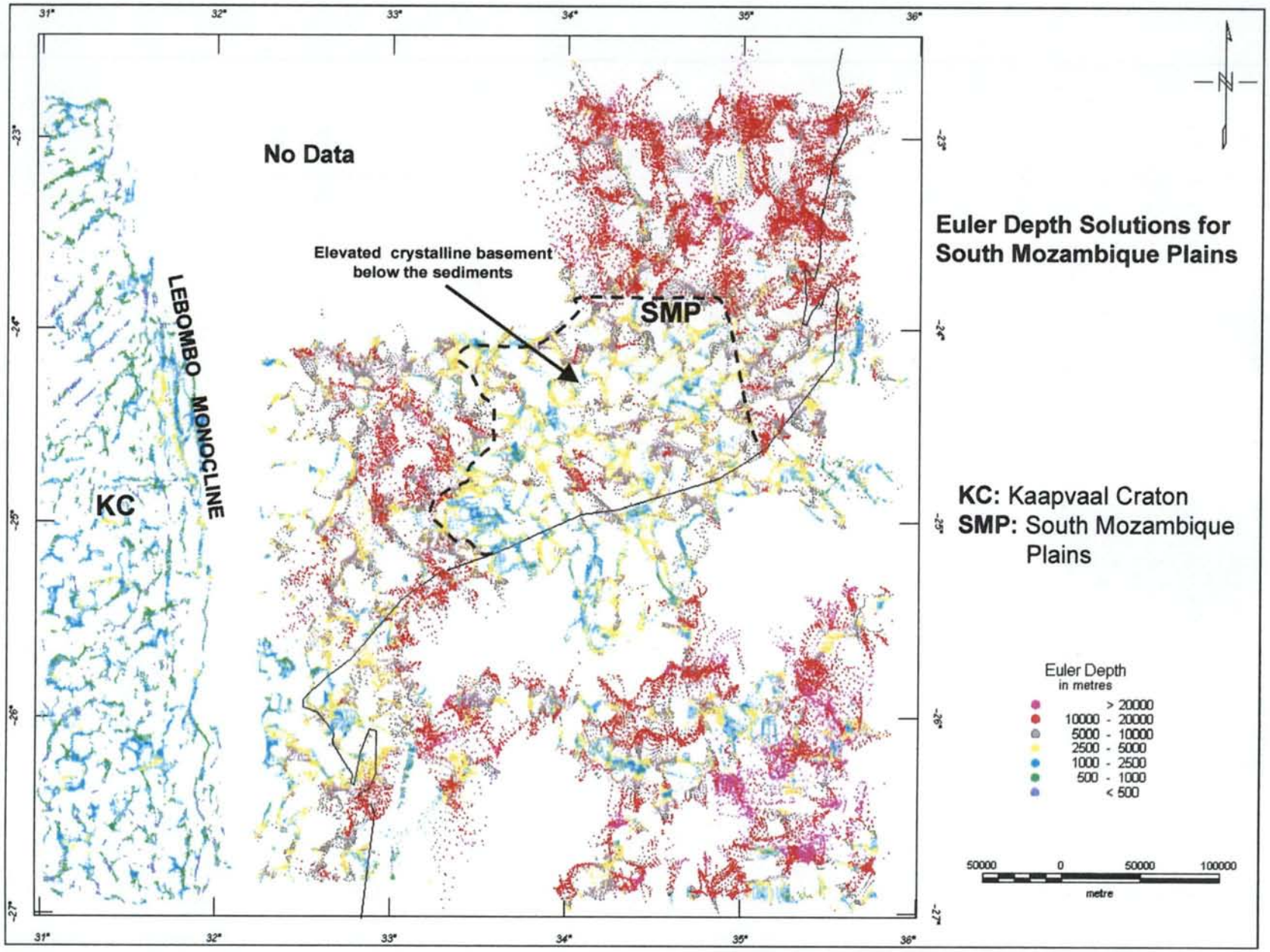

Figure 6.5: *Spatial distribution of the 3D Euler depth solutions for South Mozambique Plains and adjoining areas. Note the drastic difference in the depth of magnetic sources between the Kaapvaal craton (shallow sources) and South Mozambique (up to 25 km).*

craton. The southern margin is marked by a very strong analytic signal zone. The northern and western extent is not very clear in the magnetic images. The western margin (Map 6.7) was tentatively drawn west of the Lake Victoria based on analytic signals. Absence of data farther west is also a constraint in drawing the western margin. The northern margin seems to extend beyond the study area. Two distinct dyke swarms – 1. the north-south trending swarm in the southern part and 2. the semi-circular swarm in the western part - are the prominent features in the magnetic images.

j. The Bangweulu Block

The Bangweulu Block (Drysdall, *et al.*, 1972) is a Mesoproterozoic cratonic block in northern Zambia. This block is surrounded by the Irumide belt to the southeast, the Ubendian belt to the northeast, the Kibaran belt to the northwest and the Lufilian arc to the southwest. Mesoproterozoic granitoid rocks (~1850 Ma, *e.g.*. Schandelmeier, 1980) form majority of the basement complex with few schist belts and metavolcanic rocks (Andersen and Unrug, 1984). The basement complex is overlain by metamorphosed and deformed Mesoproterozoic to Neoproterozoic sedimentary cover. The Bangweulu block is characterized by east-west long strike-length magnetic anomalies and shows relatively lower magnetic relief than the surrounding belts. The distribution pattern of the Euler depth solutions suggests varied depth for the magnetic sources. In the southeastern part the NE-SW long strike-length anomaly yields depth to the basement up to 20 km. Similarly, in the northwestern part deeper, depth solutions corresponding to the low magnetic relief zone representing the supracrustal cover suggest that these sediments are magnetically transparent.

k. The East African Orogen

The north-south trending East African Orogen (Stern, 1994; Meert and Van der Voo, 1997) extends over 3000 km along eastern part of Africa from Egypt to Mozambique. While this belt includes the low-grade Nubian-Arabian shield in the north and the Mozambique belt in the south, the aeromagnetic studies carried out here cover mostly the high-grade terrains of the Mozambique belt. The Mozambique belt is characteristically represented by a higher magnetic relief (both in total field anomaly and analytic signal maps) than the granite-greenstone belts of the Archean cratons. The belt is bounded by the East Africa Coastal Fault (Map 6.7) in the east, where the

high-relief zone is abruptly terminated against a magnetically quiet zone. Similarly the western margins were also delineated from the difference in the magnetic relief. The Mozambique belt shows magnetic trends in varied directions suggesting a complex metamorphic and deformation history. The belt is cut across by the NE-SW trending Lurio Thrust Belt (LTB), which is defined by a narrow low magnetic anomaly zone in the total field shaded relief image (Map 6.1). The thrust belt is also well defined in the Euler deconvolution map (Map 6.6) by linear clustering of shallow depth solutions along the belt. The magnetic trends on either side of the LTB show different characteristics. The trends south of the LTB are predominantly east-west and show broad warps, whereas those to the north are mostly NE-SW and show variation in strike.

The Mozambique belt is cut across by the NE-SW trending Permo-Triassic rift basins (Selous and Ruvu basins) in southeastern Tanzania. The terrains to the north of these rift basins show similar magnetic anomaly patterns with predominantly NW-SE magnetic trends in parts of Kenya .

l. The Ubendian Belt

The Ubendian belt (Cahen and Snelling, 1984) is a NW-SE trending early Mesoproterozoic (~1800 – 2000 Ma) orogenic belt in east-central Africa bordering the Tanzania craton in the southwest. This belt extends from Lake Tanganyika in the northwest to Lake Malawi in the southeast (Shackelton, 1973; Tack, 1995). However, the southeastward continuation of the NW-SE Ubendian trend is clearly depicted in the aeromagnetic images, especially in the vertical derivative map (Map 6.2) in northern Mozambique. The belt is terminated against a NE-SW trending fault (Map 6.7). Thus the Ubendian belt extends much farther northeastward below the Permo-Triassic Selous basin than earlier thought.

6.3.4. Major Dyke Swarms

Major dyke swarms of southern Africa and east-central Africa (Tanzania-Uganda) are better resolved in the vertical derivative map (Map 6.2) and the susceptibility map (Map 6.5a and 6.5b). The sharpness of anomaly amplitudes of the individual dykes is much more enhanced in these images. Mapping of individual dykes is beyond the scope of this work and has already been done (Mubu, 1995; Reeves, 2000; Chavez-Gomez, 2000). The dykes can be mapped later from the images produced in this thesis

and added to the already existing dyke database for southern and eastern Africa (Reeves, 2000).

6.3.5. Regional Faults/Shear Zones

a. Trans-Southern African Shear Zone

A linear belt from the coast in central Namibia continues northeastward through northwestern Botswana, southern Zambia and finally to the east coast of Africa in Tanzania. This belt is a prominent trans-continental lineament that runs across southern Africa and is represented by a series of long strike-length magnetic anomalies. This belt is also clearly depicted in the regional Bouguer gravity anomaly map (Figure 7.4).

b. Zoetfontein Fault

This is an ENE-WSW trending major fault in the northern margin of the Kaapvaal craton. It is clearly depicted in the total filed shaded relief map (Map 6.1) and the Euler deconvolution map (Map 6.6). It is also interesting to note that a number of Karoo rift basins occur along the eastern half of the fault suggesting its reactivation during late Paleozoic and Mesozoic times.

c. East African Coastal Fault

The Precambrian rocks of East Africa from northern Mozambique to Somalia are bounded by a ~north-south trending fault (East African Coastal Fault in Maps 6.4 and 6.7). In the southern part in northern Mozambique and southern Tanzania, this fault trends in a NNW-SSE direction separating the high grade rocks of the Mozambique belt (represented by high magnetic relief) in the west from the Jurassic rift basins (represented by mild magnetic relief) in the east. In the northern part in Kenya, this fault trends in a north-south direction. While the fault can be easily delineated in almost all the aeromagnetic images, it is best represented in the vertical derivative of the analytic signal (Map 6.4), where the Phanerozoic sedimentary basins to the east are represented by orange colour. This fault is also well defined by contrast in the Euler solution results (Map 6.6). Deeper Euler solutions (>5 km) are clustered in the eastern part and are separated by sudden change in the Euler depths (<2.5 km) to the west. Another important observation from the Euler solutions is the rough estimation of throw of this fault. In the southern part the throw of the fault seems to be much less

(1.5 km) as compared to that in the northern part, where the throw is estimated to be more than 5 km.

c. The Lurio Thrust Belt

The ENE-WSW trending Lurio Thrust Belt (Map 6.6 and 6.7) in north-central Mozambique has been considered as an important crustal structure and has been used for correlation with the thrust boundary between the Highland and Vijayan complexes (refer to Figure 4.8) in Gondwana reassembly (*e.g.*. Pinna *et al.*, 1993; de Wit *et al.*, 2000). Recent geochronological studies (Kröner *et al.*, 1997; Jamal, *pers. comm.*, 2000) have also established that the Lurio belt represents a major Pan-African tectonic zone, either side of which the tectonic evolution is different. Thus, precise delineation of this belt and its correlation with similar zones in eastern Gondwana fragments is of prime importance in continental reassembly. The Lurio belt is well represented in all the images. But alignment of depth solutions along this belt (Map 6.6) is, by far, one of the best examples of the utility of Euler deconvolution in delineation of linear crustal structures.

d. Other Lineaments

A number of lineaments (Map 6.7) mostly buried under thick cover rocks were interpreted from the aeromagnetic images. Shaded relief of total magnetic field, vertical derivatives and susceptibility images were mostly used to interpret magnetic lineaments. The lineaments can be broadly grouped into two categories based on orientation – 1. the E-W to ENE-WSW lineaments and 2. ~N-S lineaments. The first category of lineaments are sympathetic to the major shear zones and faults like the Lurio Shear and the Zoetfontein Fault and the second category are mostly related to the extensional episode related to Jurassic rifting of Gondwana fragments.

6.3.6. Rift Valleys

Vertical derivative maps, especially that of the analytic signal amplitudes, have proved to be useful in interpretation of the margins of rift valleys. The Euler depth maps also helped in giving a rough idea on the thickness of sediments in these rift basins.

a. East African Rifts

East Africa is well known for its high density of Phanerozoic rift structures (see Lambiase, 1989 for review). Here an attempt has been made to delineate the limits and depth persistence of the Permo-Triassic and Jurassic rift basins as accurately as possible with the help of aeromagnetic data. The Mozambique belt is cut by a series of NE-SW trending and ~100 km wide Permo-Triassic basins (Selous, Ruvu, Rufiji) in southern Tanzania. The basins are represented by mild magnetic relief and very weak analytic signals suggesting thick nonmagnetic sediment accumulation. The boundary of these basins could be mapped easily in the analytic signal map (Map 6.3) and its vertical derivative (Map 6.4). Plotting of Euler depth solutions (Map 6.6) shows marked difference in depth ranges between the basin and the adjacent Precambrian terrains. The depth to the magnetic basement ranges from 2.5 km to 10 km. Approximate depth to the basement interpreted from earlier geophysical interpretations with limited drilling data (TPDC, 1995) also broadly agree with this result. It is interesting to note that deeper solutions (5 to 10 km) align along two north-south trending parallel zones probably indicating block faulting along these lineaments.

The Permo-Triassic basins are limited by NNE-SSE to N-S trending Jurassic rift basins from northern Mozambique to northern Kenya and beyond. These basins also show very mild magnetic relief and weak analytic signals. Clustering of Euler depth solutions suggest depth ~ 10 km for the basement in these basins.

6.4. Quantitative Interpretation

6.4.1. 3D Euler Deconvolution

Euler 3D deconvolution (Thompson, 1982; Reid *et al.*, 1990) for the total field aeromagnetic data was carried out for a rough quantitative estimation of depth and position of various magnetic sources. A window size of 10 x 10 was found suitable to obtain good results for a grid size of 1000 x 1000 m and a structural index of 1 (dipping dyke model). Major lineaments and tectonic features like shear zones, faults, craton boundaries could be mapped precisely from the clustering of focussed Euler solutions (Map 6.6). Most of the cratonic areas are represented by shallow depth

(<500 m), except for areas covered by thick sedimentary cover. In southernmost Africa, solutions deeper than 10 km cluster along the Beattie and other east-west long strike-length anomalies. The result also shows that the thickness of the sediments in the Karoo basin increases southward from < 500 m in the north to ~10 km in the south. Very deep solutions (~10- 15 km) were obtained from the thickly covered Rehoboth triangle in Namibia and western Botswana. In southern Mozambique, depth solutions up to 25 km suggests the large thickness of magnetically transparent sediment cover east of the boundary fault (Map 6.6). Clustering of depth solutions over the buried dykes also quantitatively define their spatial extent and depth of burial.

In eastern Africa, the distribution of depth solutions quantitatively define the depth and spatial extent of the rift basins. Most of the Phanerozoic rift basins have sediment thickness ranging from about 1 km up to ~10 km.

6.4.2. Inverse Modelling

Quantitative modelling of selected anomalies was carried out for determination of depths, dimensions and magnetisation parameters of the magnetic sources using the MAGMOD tool in GEOSOFT®. Best possible over-all match between an observed anomaly and its theoretical anomaly caused due to an inductively magnetised body of simple geometry was calculated for each of the anomalies modelled. This was done to find a correlation with the depth parameters calculated by Euler deconvolution.

(a). Beattie Anomaly: Five sections across the Beattie anomaly were extracted from the AMMP grid and the anomaly peaks were modelled. The results are shown in the Table 6.2 and Figure 6.6. The modelling result suggests that the anomaly is caused by a southerly dipping magnetic body. The amount of dip varies from 30° to 60°. The modelling results also indicate lateral variation of depth to the top of the causative

Table 6.2: Results of inverse modeling of Beattie anomaly, southern Africa

Lines/ Parameters	Depth to top (km)	Half Width (km)	Dip
A	13.3	22.5	45°S
B	12.1	12.2	68°S
C	4.4	14.6	35°SE
D	6.6	15.7	65°SE
E	15.5	9.5	32°S

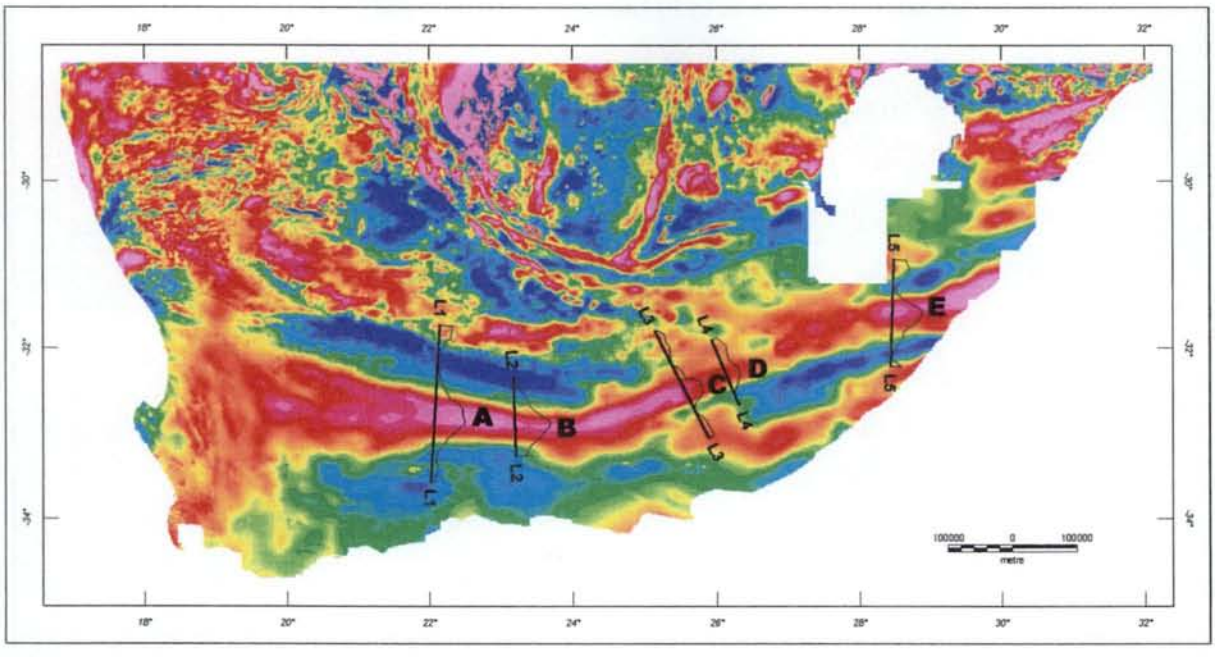

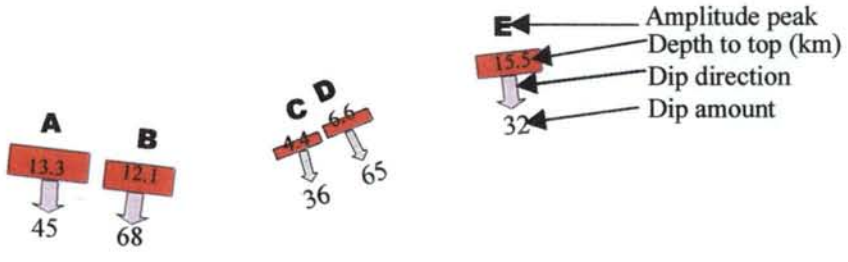

***Figure 6.6**: Aeromagnetic map of southernmost Africa with magnetic profiles across the Beattie Anomaly (top). Plan view of the modeling results of the anomalies (bottom). Note the drastic difference in the depth to the top of the magnetic source in different sections. The middle part of the anomaly (C & D) gives much less depth (~5 km), whereas the western and eastern parts give depth ~20 km.*

(~15 km) in the eastern part. This result corresponds to the results obtained from Euler deconvolution, where the solutions in the middle part of the Beattie anomaly is < 10 km flanked by deeper solutions (10 to 20 km) to the east and west. This implies that there might be vertical movement of blocks across this anomaly with respect to each other. This result shows that the depth to the top of the causative body lies at a little deeper level in the western part than earlier interpreted from seismic data (9-11 km, Harvey, 1999). An offset in the trend between the eastern part and the central part of the anomaly can be observed in the Euler deconvolution map. The offset is caused by a north-south fault (Z-Z1 in Map 6.6), defined by alignment of depth solutions along it.

***Table 6.2**: Results of inverse modeling of Beattie anomaly, southern Africa*

Lines/ Parameters	**Depth to top** (km)	**Half Width** (km)	Dip
A	13.3	22.5	45°S
B	12.1	12.2	68°S
C	4.4	14.6	35°SE
D	6.6	15.7	65°SE
E	15.5	9.5	32°S

6.5. Summary of Interpretation

1. The southeastward extension of the Ubendian trends across the generally north-south trending East African Orogenic Belt (EAO) has implications in the overall tectonic evolution of East Africa. Recent geochronological studies (Kröner *et al.*, 1997; Jamal, *pers. comm.*, 2000) suggest that there is little evidence of existence of pre-Pan-African crustal materials north of the Lurio belt and the belt is formed (~600 Ma) during the collision between East and West Gondwana. Unfortunately, no date is available from the area interpreted as the southeastward extension of the Ubendians in the EAO. Thus, it is suggested that the rocks of this area must be dated to ascertain the southeastern extent of the Ubendian belt. If the rocks of this area yield Ubendian ages (~1800 Ma), it would imply that at least a part the EAO to the north of the Lurio belt was in existence much prior to the overall Pan-African evolution of the belt.

2. A good correlation between the depth results obtained by two different methods – Euler deconvolution and inverse modelling - was demonstrated in limited areas of

episodes. A clear example is the development of Karoo rift basins along the periphery of the Zimbabwe craton (Map 6.7).

4. The Trans-Southern African Shear Zone seems to be a major tectonic structure which separates the two shield areas – the Kalahari and the Congo shields – in southern Africa (Map 6.7). But no significant strike-slip movement along this mega-lineament has been observed from the magnetic data. Only anomalies due to the youngest magmatic episode (*e.g.*. Jurassic dykes) cut across the lineament. This indicates that no significant lateral movement has taken place along this lineament after the Karoo magmatism (≅ Gondwana breakup).

5. The overall NE-SW orientation of the Permo-Triassic Karoo basins of south and eastern Africa suggests that the region was subjected to an extensional regime with a NW-SE extensional stress axis from upper Paleozoic triggering the development of these basins. Sedimentation continued until Triassic followed by eruption and intrusion of huge quantities of basic rocks in southern Africa during early Jurassic (~183, Duncan *et al.*, 1997), when East Antarctica drifted away from southeast coast of Africa initiating development of Indian Ocean.

6. The new aeromagnetic maps produced in this thesis show many new features that can be (re)interpreted. A detailed interpretation of all the features is beyond the scope of this thesis. Hopefully, the new maps will help others to analyse the tectonic history of southern and eastern Africa in greater details.

7. GEOPHYSICAL CORRELATION

7.1. Introduction

With the near completion of surface geological mapping at 1: 1000 000 scale, most of the surface and near-surface features including lithological outcrops, structural trends and exposed mineral occurrences are now adequately known. Priority must be now given to explore the subsurface geology and relate it to the known geology. Airborne and satellite geophysical methods have assumed significance due to their ability in mapping subsurface geological features rapidly and cost-effectively, especially in the areas of little or no outcrop (Reeves, 1998). Release of the high-resolution satellite altimetry data (Smith and Sandwell, 1997) for the whole of world's oceans has added a new dimension in understanding the processes of ocean development and continental drift.

Continental scale tectonic features (*e.g.* major faults, rift valleys, shear zones, lithotectonic boundaries *etc.*) play a significant role in continental breakup processes. Matching of such features with similar geological history (*e.g.* age, lithological assemblages, metamorphic episodes, structural style *etc.*) across the drifted continents provides valuable constraints for reassembly into their predisruption configuration. Airborne and satellite geophysical methods have been proved to be useful for precise delineation of these features (*e.g.*. Lurio Belt in Mozambique, this thesis; North Botswana dyke swarms, Reeves, 1978).

A fragment to fragment correlation of geophysical features is attempted in this chapter to verify their spatial continuity in reassembled Gondwana. A compiled aeromagnetic interpretation map of central Gondwana is produced to substantiate a close fit.

7.2. Compilation of Geophysical Interpretation

Interpretation of geophysical anomalies of various areas of the southern continents exists in different formats. Each of these interpretations either describes the geology

magnetic breaks *etc.* These local-scale geophysical interpretations would better help understanding regional problems when they are compiled together and interpreted in a broader perspective (continental scale). For details of the methodology of compilation of such geophysical interpretations, refer to Chapter 3 of this thesis.

7.3. Correlation of Interpreted Features between Adjacent Fragments

Correlation of compiled geophysical features is done between conjugate fragments that were once in physical continuity within a Gondwana framework. The conjugate fragments are – 1. Southern Africa – Dronning Maud Land, 2. Eastern Dronning Maud Land/Enderby Land – Sri Lanka/India, India – Madagascar, and Madagascar – East Africa.

7.3.1. Southern Africa – Dronning Maud Land (East Antarctica)

(a) Dronning Maud Land

Geophysical mapping of Antarctica assumes special significance due to the thick ice cover in most of its continental landmass. In most Gondwana reconstructions (*e.g.* Grantham *et al.*, 1988; Stern, 1994; Unrug, 1996), Dronning Maud Land is juxtaposed against southern Africa on the basis of geological similarities. Correlation of aeromagnetic anomaly patterns also supports their juxtaposition (Corner, 1994). Though western Dronning Maud Land is extensively covered by aeromagnetic surveys (30°W to 2°E) by the Russians, the data has been compiled, processed and interpreted by Corner (1994) (Figure 7.1). Corner identified two groups of long strike-length regional magnetic anomalies caused by – 1. highly magnetised crust with variable degree of uplift along strike (east-west anomalies) and 2. Jurassic volcanics related to the extensional regime prior to and at the time of Gondwana break-up (NE-SW anomalies). A number of regional structures including shear zones, thrusts, faults and plutons have also been identified. It is evident that the NE-SW trending faults and shear zones are parallel to the Explora Wedge, perhaps suggesting their genetic relationship with the eruption of basalts during the breakup of Antarctica from southern Africa in mid-Jurassic as a result of extensional stress. A tentative southern boundary of the Grunehogna cratonic province (Figure 7.1) has also been delineated

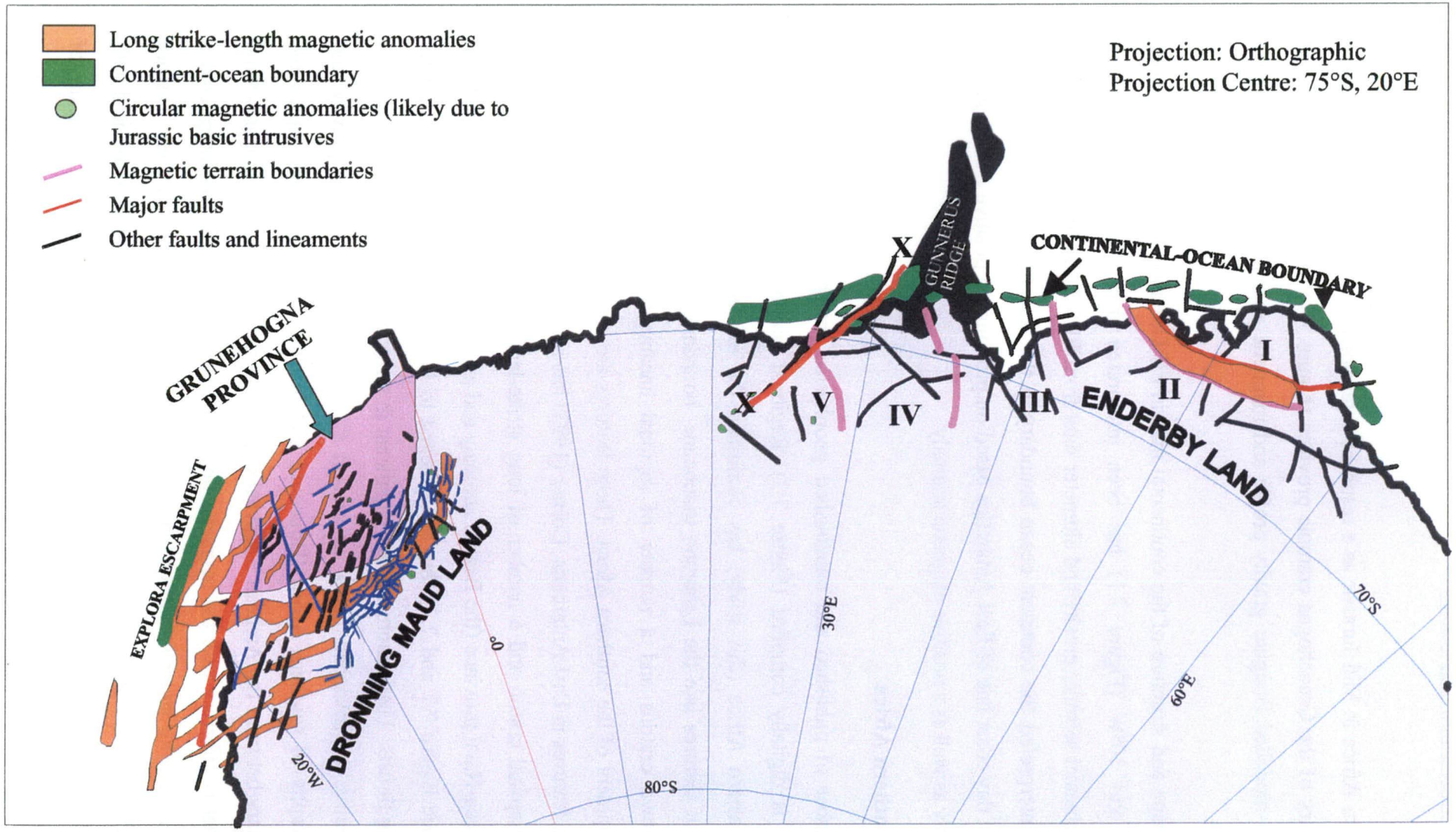

***Figure 7.1**: Geophysical interpretation map of East Antarctica (compiled and modified from: Corner, 1994; Jokat et al., 1996; Golynsky et al., 1996). **I**: Napier Complex, **II**: Rayner Complex, **III**: Lützow-Holm Terrane, **IV**: Yamato-Belgica Terrane, **V**: Sør-Rondane Terrane; X-X: Faulted margin of the Sør-Rondane Mountains*

from a modelled Bouguer gravity profile and magnetic anomaly patterns by Corner (1994).

The shape and structure of the continental margin off Dronning Maud Land between 10°W and 30°W (Figure 7.1) has been interpreted from the geophysical data (multichannel seismic, gravity and altimeter data from ERS-1) by Jokat *et al.*, (1996). They interpreted the continent-ocean boundary in the area that runs parallel to the present day coastline of East Antarctica based on pronounced positive free air gravity anomaly as well as a positive magnetic anomaly.

(b) Southern Africa

A number of published and unpublished geophysical interpretations from southern Africa are digitally compiled (Figure 7.2). Regional aeromagnetic interpretation of southeastern Africa (this study) has confirmed the existence and extent of broad tectonic features like the Lebombo monocline, boundaries of the Kaapvaal and the Zimbabwe cratons and a number of regional lineaments related to the tectonic development of the southern Africa. These features are important for correlation with similar features in East Antarctica. Corner (1993) has also interpreted the boundary of the Kaapvaal craton and a number of long strike-length magnetic anomalies in the Namaqua-Natal province (the Beattie anomaly and anomalies parallel to it in the Natal province Figure 7.2 and 7.3) that are believed to be related to low angle southerly dipping thrusts. These anomalies are significant in terms of correlation in a Gondwana perspective as described below in section C (ii). Study of Bouguer gravity and topography of southern Africa (Doucouré and de Wit, 1996) has also shown the boundary between the Archean Kaapvaal craton and the Proterozoic Namaqua-Natal belt that is coherent with the magnetic observations. Mubu (1995) has interpreted a number of dyke swarms namely Lebombo, Limpopo, North Botswana *etc.* (Figure 7.12) from the aeromagnetic data. The alignment of these dyke swarms associated with limited geochronological data provides valuable constraints on the break-up of Gondwana (see Reeves, 2000 for review).

The broad tectonic fabric of southern and eastern Africa (Map 6.7) has been brought out in this study based on aeromagnetic interpretation.

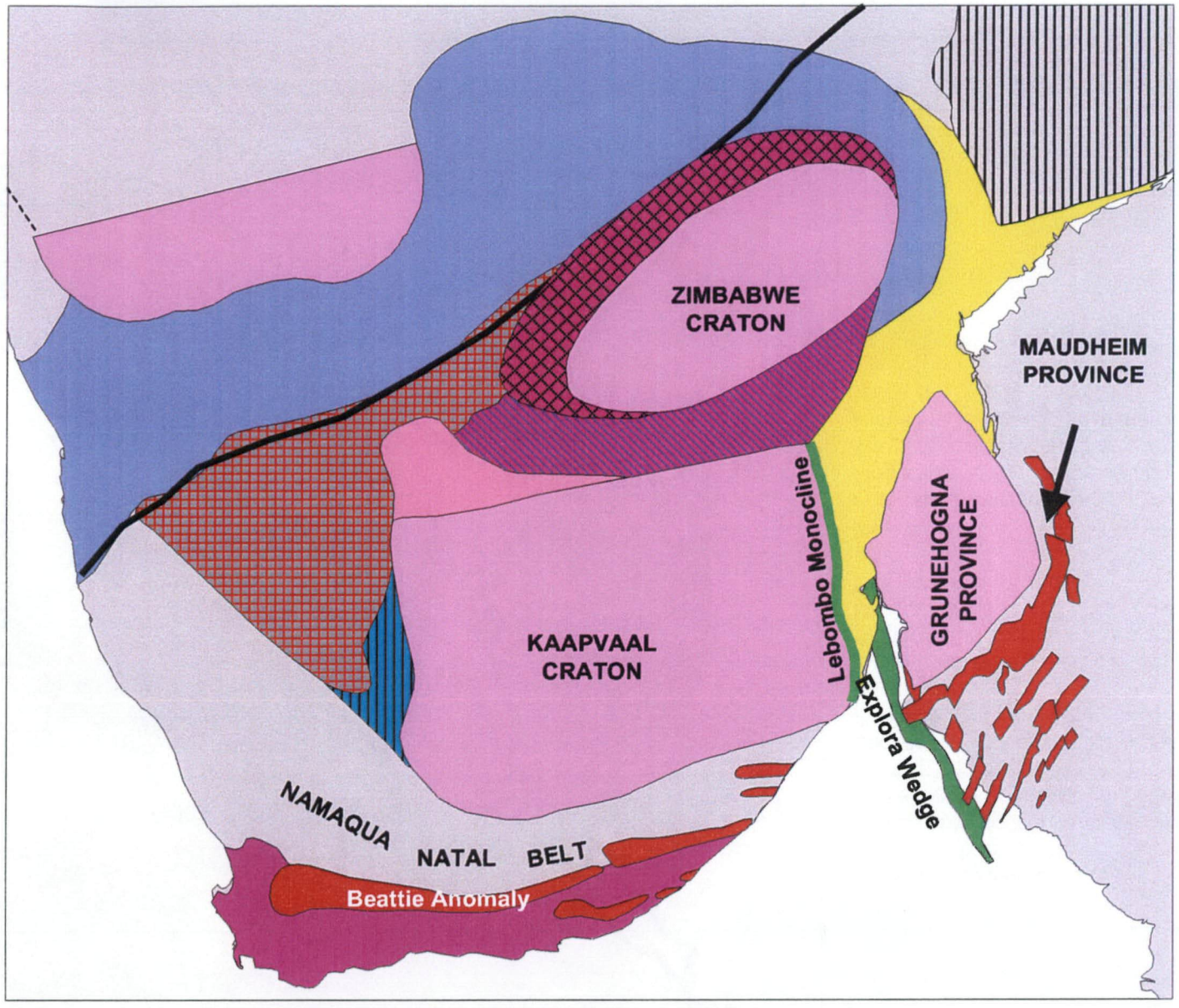

***Figure 7.2**: Correlation of long strike-length magnetic anomalies in southern Africa and western Dronning Maud Land, East Antarctica. Note the presence of long strike-length anomalies (red filled) in the Maudheim Province similar to the Beattie anomaly in southern Africa.*

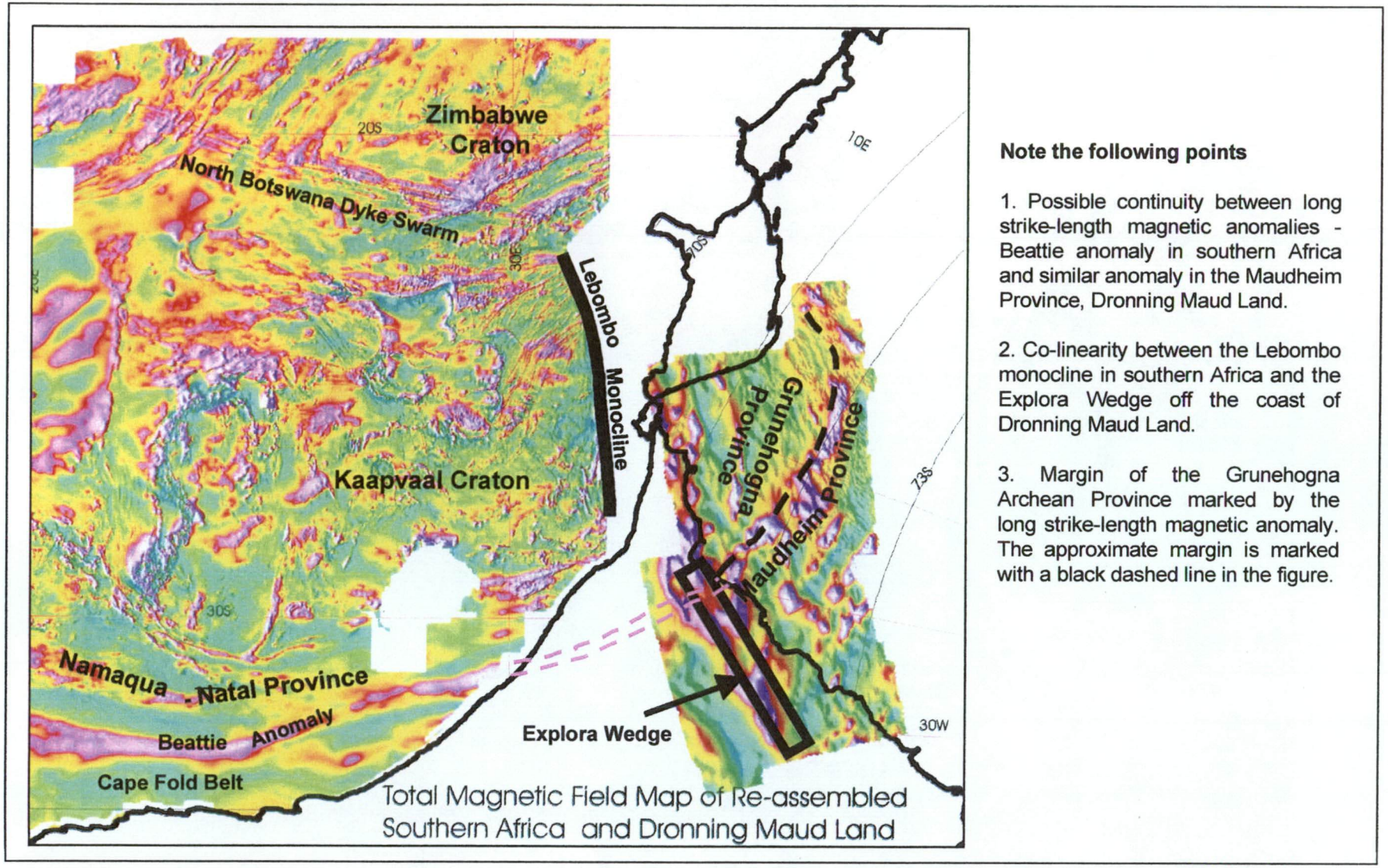

Note the following points

1. Possible continuity between long strike-length magnetic anomalies - Beattie anomaly in southern Africa and similar anomaly in the Maudheim Province, Dronning Maud Land.

2. Co-linearity between the Lebombo monocline in southern Africa and the Explora Wedge off the coast of Dronning Maud Land.

3. Margin of the Grunehogna Archean Province marked by the long strike-length magnetic anomaly. The approximate margin is marked with a black dashed line in the figure.

***Figure 7.3**: Aeromagnetic anomaly images of southeastern Africa and western Dronning Maud Land, East Antarctica plotted on a reassembly by Reeves (model 464, pers. comm.)*

(i) Gravity Interpretation of sub-Saharan Africa

Coarse Bouguer gravity data of sub-Saharan Africa (see Chapter 3 for source and quality of data) was imaged (Figure 7.4) for limited interpretation of obvious regional features to substantiate the aeromagnetic interpretation. The data is too course for a detailed interpretation. The most obvious feature in the image is the NE-SW trending Trans-Southern African Shear Zone (TSASZ in Figure 7.4), supporting aeromagnetic and geological interpretation (Map 6.7). The Archean cratons (Kaapvaal, Zimbabwe and Tanzania) are represented by relatively low gravity values than the surrounding mobile belts. The extent of dykes and volcanic rocks along Mateke-Sabi belt (see Figure 7.4 for location) is not clear due to lack of aeromagnetic coverage in southern Mozambique and eastern Zimbabwe (Map 6.1). But the Bouguer gravity image clearly shows the nature of Middle Jurassic magmatic belts in southeastern Africa. The southeastward extension of the Ubendian belt beyond the Trans-South African Shear Zone is also clear in the gravity data (Figure 7.4).

(c) Comparison of Geophysical Features

(i) Explora Wedge and Lebombo Monocline

The Explora Wedge (Figure 7.2 and 7.3) off the coast of Dronning Maud Land is represented by a 1500 km long and 140 km wide curvilinear positive magnetic anomaly that runs parallel to the coast of western Dronning Maud Land (Johnson *et al.*, 1992). This anomaly with amplitudes reaching 400 nT at places is believed to be associated with a volcanic wedge of seaward dipping sub-basement reflectors (Kristoffersen and Hinz, 1991) and considered to have resulted from sub-aerial sea-floor spreading during the early stages of continental break-up. The Explora Wedge has been well identified between 17°W and 10°W with gravity values +5 to +20 mgal (Jokat *et al.*, 1996). These observations suggest that the Explora Wedge might have been formed by oblique spreading rather than pure strike-slip, as suggested by Miller *et al.*, (1990). But it seems logical to consider the steep sea-ward dipping Explora Wedge/Escarpment as one half of the basalt eruption (the other half being the Lebombo monocline in southern Africa) along an already existing weak zone during the onset of the continental breakup process in mid-Jurassic.

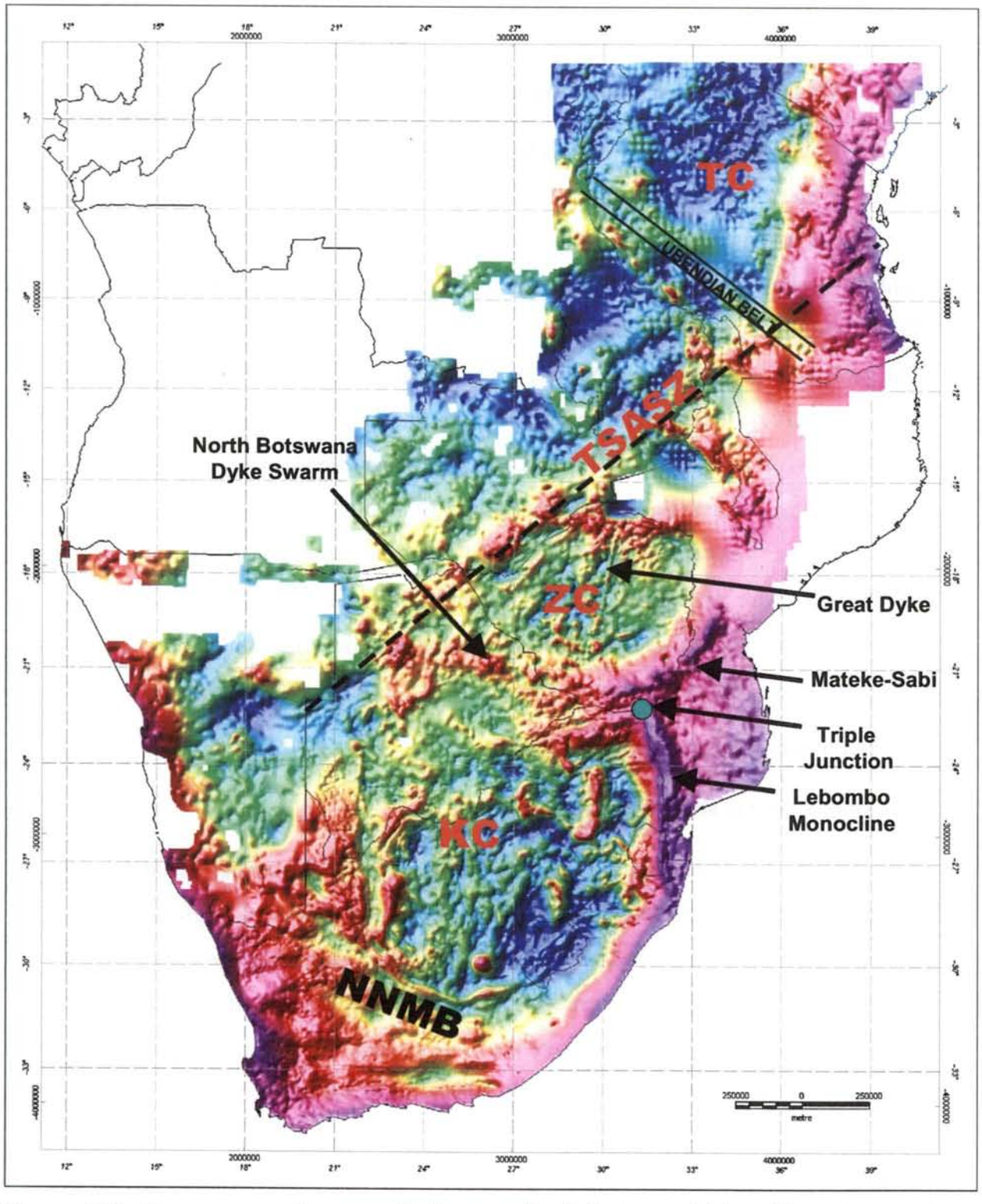

Figure 7.4: *Bouguer gravity anomaly image of sub-Saharan Africa. Note the prominent tectonic blocks and lineaments are clearly depicted in the gravity image. NNMB: Namaqua-Natal Metamorphic Belt, KC: Kaapvaal Craton, ZC: Zimbabwe Craton, TC: Tanzania Craton, TSASZ: Trans-Southern African Shear Zone.* The southeastern extension of the Ubendian Belt beyond TSASZ is clearly depicted in the image.

The aeromagnetic image (Figure 7.3) of southern Africa (AMMP; Barritt, 1993) shows a north-south trending magnetic high at the eastern margin of the Kaapvaal craton. This anomaly corresponds to the Karoo lavas and associated dykes along the Lebombo monocline. These basalts have been correlated with those of the Explora Wedge in a predisruption configuration by Cox (1992) (refer to Figures 4.5a and 4.5b, Chapter 4). It can be argued that the basalts along the Lebombo monocline and the Explora Wedge are parts of a single volcanic episode and are syntectonic with the initial rifting between East and West Gondwana ~183 Ma (Duncan *et al.*, 1997).

(ii) Beattie Anomaly and its eastward extension in the Falkland Plateau and East Antarctica

One of the most striking features in the southern African aeromagnetic map is the east-west running Beattie anomaly (Figure 7.3) with a strike length of over 900 km. De Beer and Meyer (1984) have observed that this anomaly does not have any gravity expression and occurs within a major deep-crustal conductivity anomaly. But recent gravity interpretation by Doucouré (*pers. comm.*, 1999) has revealed a strong positive anomaly corresponding the Beattie anomaly. Comparable linear anomalies have been identified in the Maudheim Province of western Dronning Maud Land (Kirwan anomalies) and in the Falkland plateau (Maccelari, 1991; Corner, 1994; Figure 7.3). Forward modelling of the magnetic profiles across the Beattie anomaly by Maher and Pitts (1989) and Pitts *et al.*, 1992, the magnetic anomaly in the Maudheim province of DML by Hodgkinson (1990) and the extension of the Beattie anomaly in the Falkland plateau by Maccelari (1991) reveals low angle thrusts dipping away from the Kaapvaal Craton (Corner *et al.*, 1991). This is substantiated by field observations and paleomagnetic sampling of highly magnetic thrusts causing the Kirwan anomalies which are the proposed extensions of the Beattie anomaly in Dronning Maud Land (Corner, 1994)

7.3.2. Eastern Dronning Maud Land/Enderby Land) – Sri Lanka/India

(a) Eastern Dronning Maud Land/Enderby Land

Aeromagnetic data for the eastern part of Dronning Maud Land and Enderby Land, East Antarctica has been compiled and interpreted by Golynsky *et al.*, (1996). The

magnetic anomaly patterns of this area, in general, are complex and perhaps related to an extended history of terrain development and structural evolution with polyphase deformation and metamorphism during Kibaran and Pan-African times (see Section 4.3 in Chapter 4 for geological details). Golynsky *et al.* (1996) delineated boundaries between various Precambrian blocks based on change in magnetic anomaly patterns (Figure 7.1).

The boundary between the Napier and Rayner complexes is represented by an elongated band of high intensity magnetic anomalies. The boundary between the Lützow-Holm terrain and the Yamato-Belgica terrain is marked by an abrupt change in the magnetic fabric. A prominent positive magnetic anomaly belt along the continental slope and shelf areas extending from Enderby Land to Dronning Maud Land and further westward to the Weddell Sea is attributed to the discontinuity in the continental crust formed during Gondwana breakup by Golynsky *et al.*, (1996). A number of faults and lineaments have also been identified in the region. The most prominent among them is the north-south fault (X-X in Figure 7.1) along the western margin of the Sør Rondane Mountains. This fault extends farther northwards along the western margin of the Gunnerus Ridge.

The faults and lineaments in the area can be broadly grouped into two sets based on their orientation. The north-south trending faults are parallel/subparallel to the interpreted terrain boundaries and might be related to the vertical movement of the tectonic blocks relative to each other. The other set of lineaments having approximately an east-west strike are parallel to the boundary between continental and oceanic crusts and probably developed due to north-south stretching of the crusts during breakup of India from Antarctica.

(b) Geophysical Interpretations of Peninsular India

(i) Bouguer Gravity Image of India

Images (Figures 7.5a and 7.5b) of Bouguer gravity data (Sreedhar Murthy, *pers. comm.*, 1999) were produced in this study to delineate major gravity features and facilitate comparison between the aeromagnetic features (Figure 5.18) and gravity

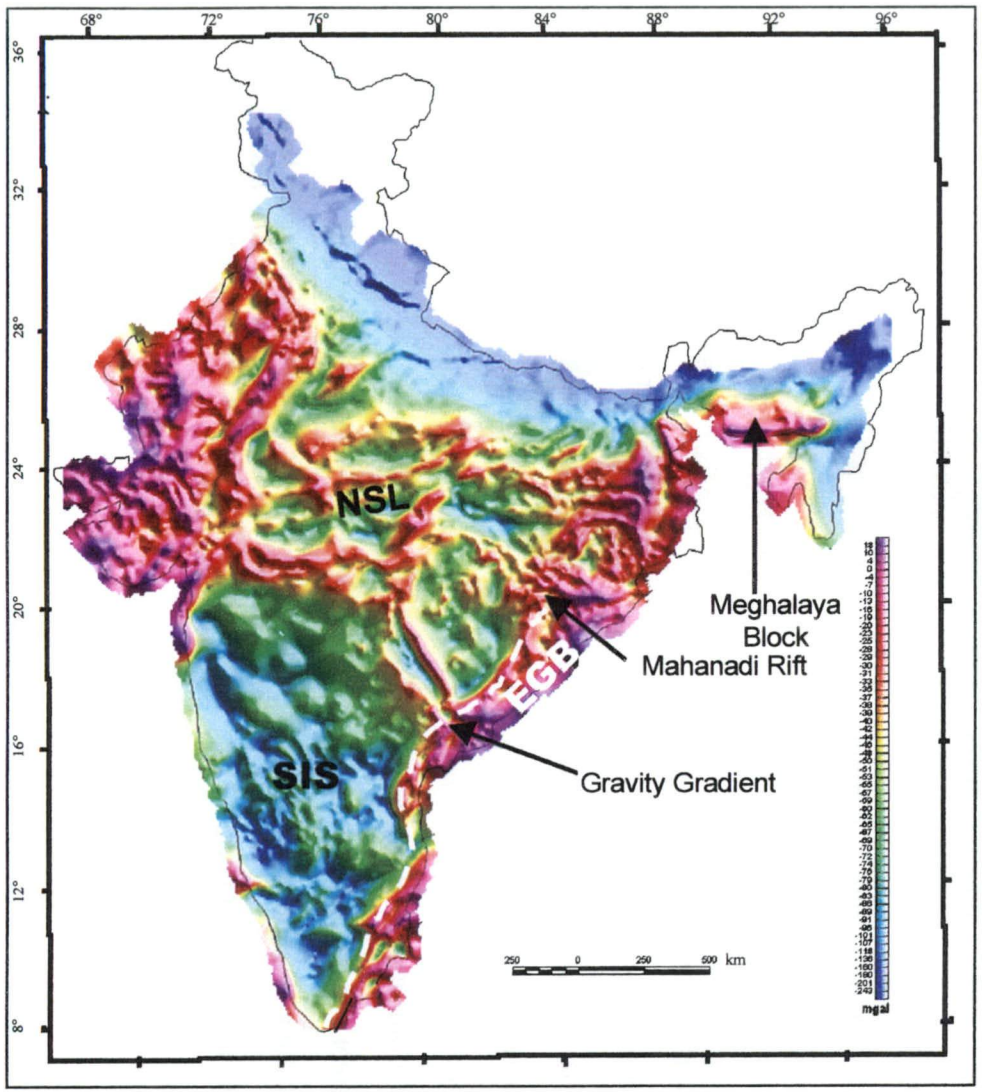

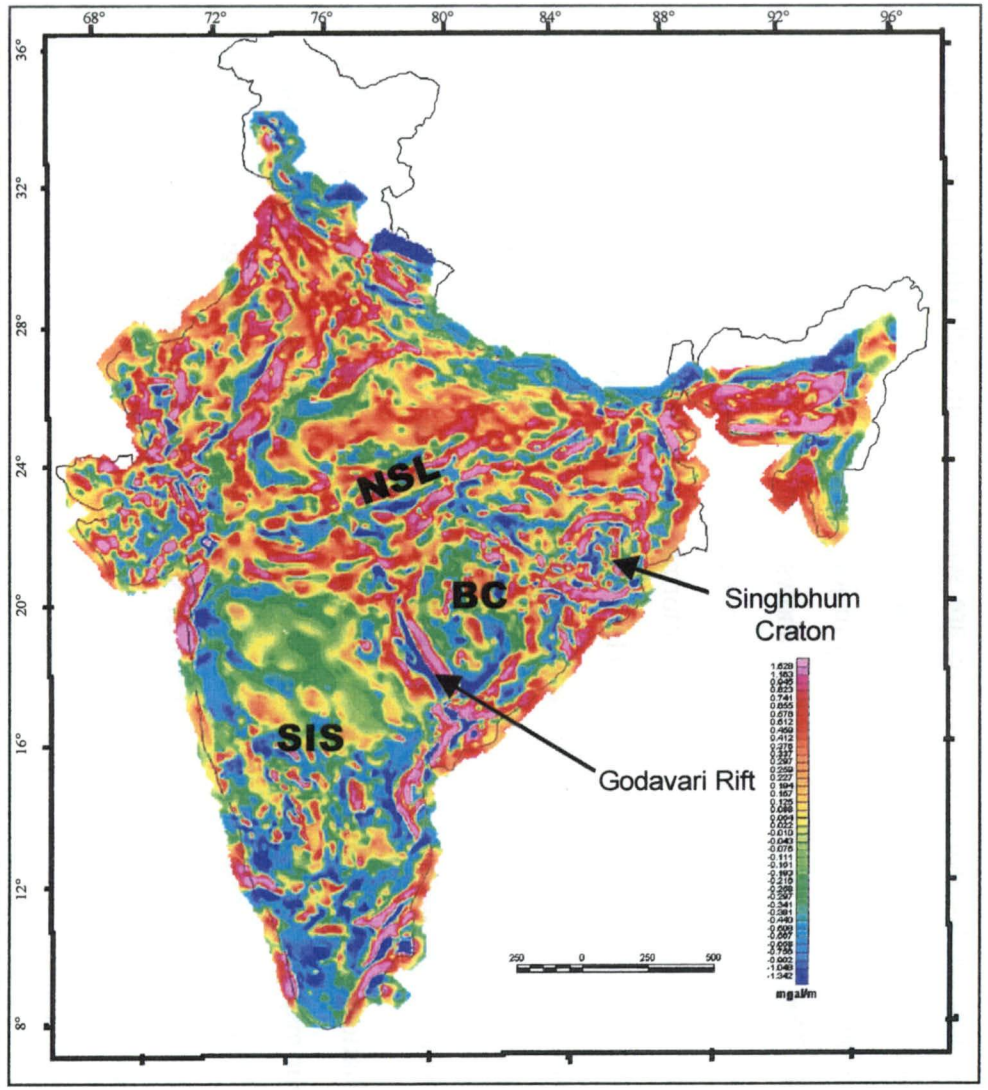

***Figure 7.5a**: Colour Shaded relief Bouguer Gravity map of India.* ***Figure 7.5b**: First Vertical Derivative map of Bouguer Gravity data of India*

Note the strong gravity gradient in the eastern part and the strong gravity highs flanking a narrow gravity low zone along the Narmada-Son Lineament in both the maps.
BC: Bastar Craton, SIS: South Indian Shield, EGB: Eastern Ghats Belt, NSL: Narmada-Son Lineament.

features. The Archean cratonic areas (Dharwar, Bastar and Singhbhum cratons) are characterised by relatively low gravity relief and lower gravity values than the surrounding mobile belts. The cratons are separated from each other by rift valleys represented by narrow gravity lows flanked by highs. Though the gravity images do not show prominent east-west fabric in the South Indian Shield as the magnetic images, a WNW trending lineament corresponding to the CTL (Figure 5.17) is observed. The Bouguer gravity image shows a strong gravity gradient parallel to the southeastern coast that continues farther northward marking the western boundary of the Eastern Ghats Belt. This is in conformity with the observations made by Subrahmanyam (1978 a & b) and Hari Narain and Subrahmanyam (1986). The Narmada-Son Lineament is prominently represented by a low gravity zone flanked by magnetic highs.

(ii) Gravity Interpretations of Southern Indian Shield

The National Geophysical Research Institute (NGRI) published a series of gravity contour maps on 1:5 000 000 covering almost whole of India between 1975 and 1978. Since then a number of workers have interpreted this gravity data. The earlier interpretations for the area south of the Narmada–Son Lineament are discussed here.

Based on gravity anomalies, Hari Narain and Subrahmanyam (1986) divided the South Indian Shield into four distinct geophysical domains -1. Deccan trap and adjoining areas, 2. Dharwar Geotectonic blocks and the Chitradurga Belt, 3. Eastern margins of Cuddapah basin and the Eastern Ghats and 4. Gravity high around the Cuddapah basin. These domains, in general, are consistent with the major lithotectonic subdivisions of Peninsular

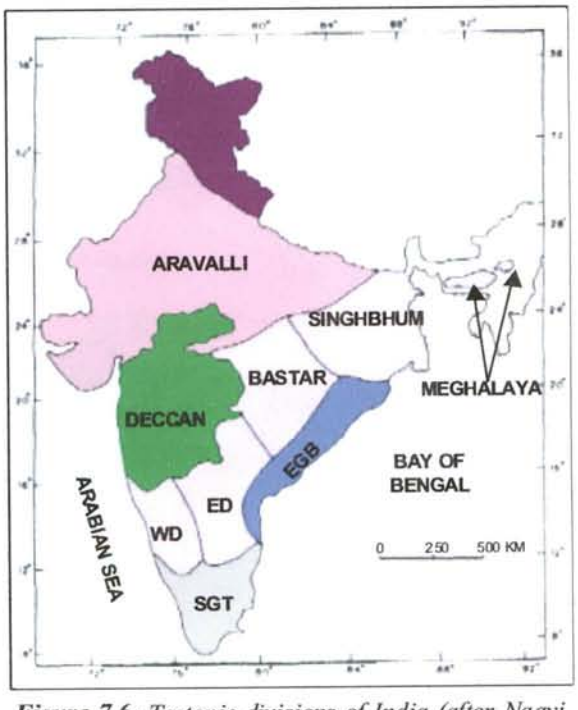

***Figure 7.6**: Tectonic divisions of India (after Naqvi and Rogers. WD: Western Dharwar, ED: Eastern Dharwar, SGT: Southern Granulite Terrain, EGB: Eastern Ghats Belt.*

India (Figure 7.6). Though the interpretation of LANDSAT imageries (Drury *et al.*, 1984) has revealed a number of major east-west shear zones (Figure 7.7), only a few such are evident in the gravity images (Figure 7.5). Rather the gravity contours exhibit continuity from the Dharwar granite-greenstone terrains to the Southern Granulite Terrain only with a change in the trend from N-S over the granite-greenstone belts to a NE-SW trend over the granulite terrain. Hari Narain and Subrahmanyam (1986) argue that the gravity provides no evidence of any deep faults/shear zones in the region since no strong gradient in the gravity anomalies is evident. However, Mishra (1990) interpreted a gradient in the Bouguer gravity anomaly along Palghat-Tiruchi line (Figure 7.5a) and related it to a deep-seated fault. Reeves (*pers. comm.*, 1999) also identified a gravity feature (Figure 6.7) similar to that of Mishra.

The gravity gradient from Cape Comorin to Mahanadi rift (Figure 7.5) separates the high gravity regions of the Eastern Ghats Belt in the East from the low gravity areas of the Dharwar craton in the west. Subrahmanyam (1978a, 1978b) earlier interpreted this boundary as a cryptic suture zone between the stable craton of 'normal' density (Dharwar craton) and a younger reactivated crustal block of relatively higher density (Eastern Ghats).

(iii) Narmada-Son Lineament

One of the most striking features in the gravity map of India (NGRI, 1978) is the ENE-WSW trending Narmada-Son Lineament (NSL) running across peninsular India (Figures 7.5). The NSL has long been considered as a fundamental crustal discontinuity that limits the northern extension of the Southern Indian Shield (*e.g.* Mishra, 1977; Sen, 1991; Verma and Banerjee, 1992). The lineament is a well-studied zone in the Indian subcontinent. It is represented by an elongated narrow gravity low (Valadiya, 1984) flanked by Bouguer anomaly highs corresponding to the shoulders of a rift basin (Sivaji and Agarwal, 1995) and has been considered to have characteristics of a rift valley on the basis of geophysical evidence (Nayak, 1990). Results of five deep seismic sounding (DSS) sections across the NSL (Kalia *et al.*, 1981, 1986 and 1987) coupled with the gravity interpretation (Verma and Banerjee, 1992) support the idea of rift valley. Presence of prominent aeromagnetic anomalies all along its length (Gupta, 1983), high heat flow (*e.g.* Ravi Shankar, 1988), occurrence of hot springs and

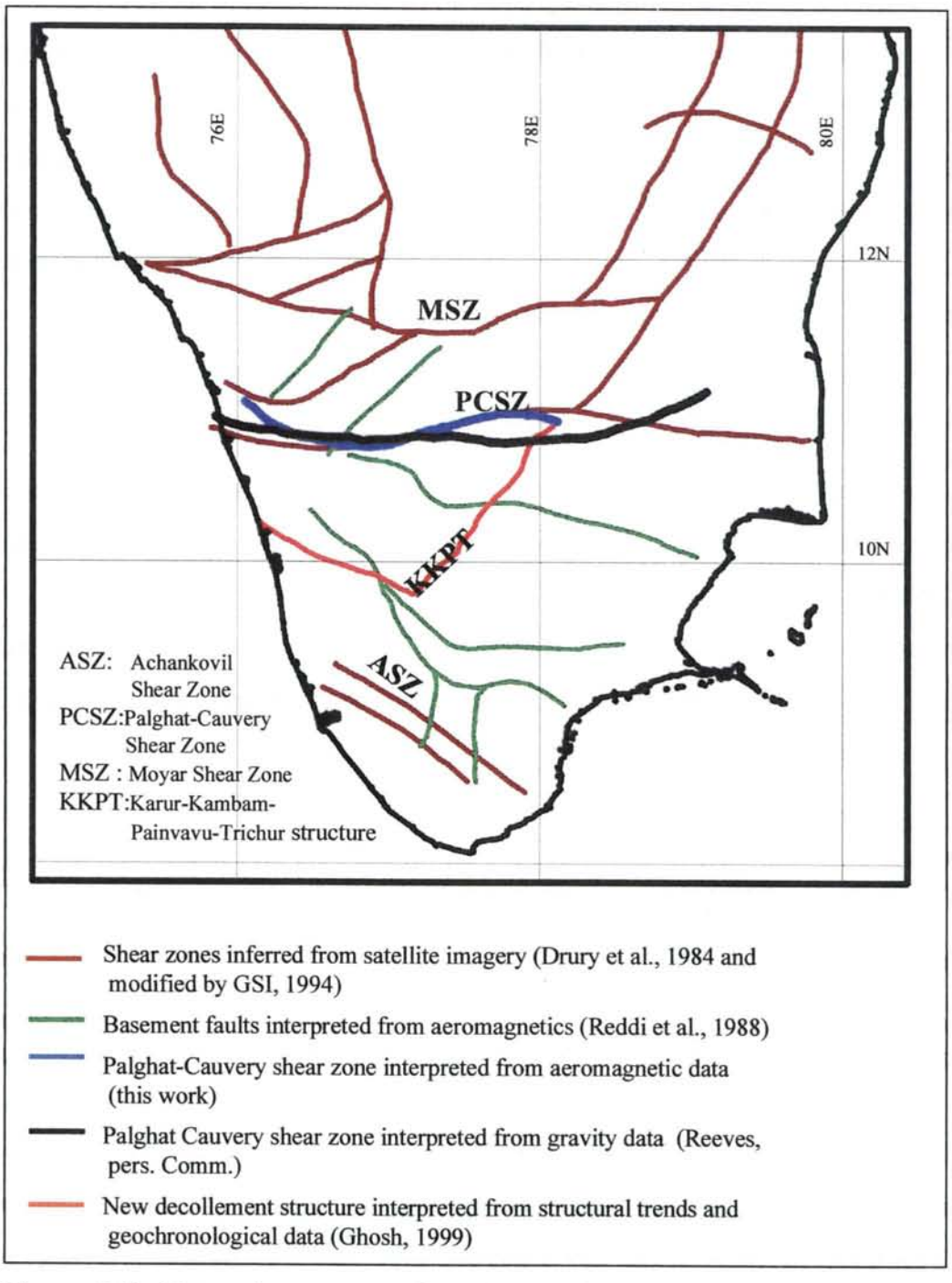

***Figure 7.7**: Major shear zones of southern India compiled from the various sources mentioned above.*

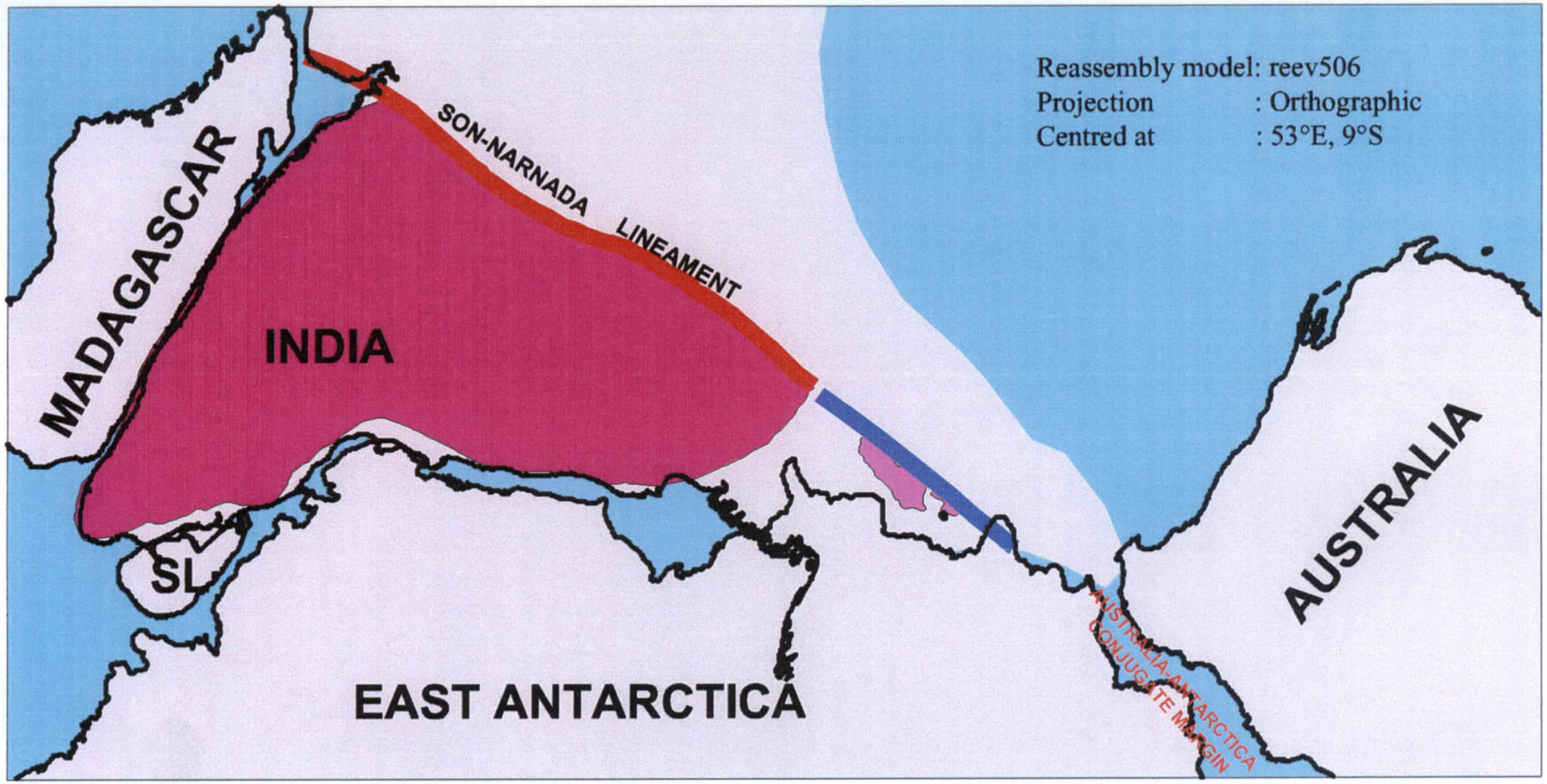

***Figure 7.8**: India-Australia-Antarctica fit at 200 Ma. Note the linearity between the eastward extension of the Son-Narmada Lineament and the rifted conjugate margins of Australia and Antarctica.The magenta colour in India represents the Precambrian basement rocks interpreted from gravity anomaly image.*

noticeable seismicity along the NSL suggests that it is an active tectonic feature even today (Verma and Banerjee, 1992). Mishra (1977) has suggested eastward extension of the NSL in the eastern syntaxial bend of the Himalayas. The NSL and its eastward extension seem to be in the same trend as of the rifted margins of Antarctica and Australia in a predisruption configuration (Figure 7.8) suggesting a possible reactivation of the NSL might have triggered the Antarctica-Australia rift in Mid-Jurassic.

(iv) Aeromagnetic features of Southern India

Regional airborne magnetic contour maps of South India up to 12°N flown at altitudes of 5000' - 9000' at 4 km line spacing have earlier been interpreted by Suryanarayana and Bhan (1985), Ramachandran *et al.* (1986), Reddi *et al.* (1988) and Geological Survey of India (1994). The results of their interpretation depict east-west magnetic trends in the south that changes to a NE-SW trend towards the east coast. They have interpreted the turn in magnetic trend (implying structural trend) from E-W to NE-SW as the impact of severe stress from southern and southeastern sides on the entire region during the break-up of India from East Antarctica.

Reddi et al (1988) recognised several crustal blocks separated by deep faults in the basement of the Southern Granulite Terrain (Figure 7.7). These crustal boundaries mostly show NW-SE and NE-SW trends which are at an angle to the east-west trending Palghat-Cauvery shear zone (PCSZ) interpreted from satellite imagery (Drury and Holt, 1980). The PCSZ is not reflected in the basement structure inferred by Reddi *et al.* (1988). This implies that the Palghat–Cauvery shear zone might represent a near-surface feature without having much depth persistence. Aeromagnetic interpretation by Geological Survey India (1994) marks the magnetic highs and lows related to regional structures.

Digital compilation and interpretation of aeromagnetic images for southern India (Figure 5.18) brought out 4 distinct aeromagnetic relief zones representing tectono-metamorphic terrains. The aeromagnetic images depict various regional lineaments broadly coinciding with those earlier interpreted from satellite imageries (Drury and Holt, 1980). However, the spatial extents of these lineaments have been redefined. A

new trans-subcontinental lineament (Cannanore-Thanzavur Lineament, Figure 5.17) has been interpreted from integration of geology and aeromagnetic data.

(c) Sri Lanka

(i) Aeromagnetics

Aeromagnetic coverage of Sri Lanka is restricted to the southwestern part of the country only. Perera (1997) has interpreted three areas of different magnetic relief-high, intermediate and low - corresponding to the three major lithotectonic units of Sri Lanka namely the Wanni Complex, the Vijayan Complex and the Highland Complex respectively (Figure 5.19a). The aeromagnetic map of Sri Lanka (Figure 5.19b) shows NW-SE trending anomalies. The trend of these anomalies becomes almost E-W towards the western coast and matches with those in the southern granulite terrain of India. Lack of aeromagnetic coverage in the central and eastern parts of Sri Lanka is a hindrance in comparison of aeromagnetic features between East Antarctica and Sri Lanka. However, based on the geological similarities (Chapter 4) and the geometry of the continental boundary of East Antarctica (inferred from geophysical interpretations), Sri Lanka can be satisfactorily placed in the gap between the Lützow-Holm area of East Antarctica and the southern granulite terrain of India. The possibility of the granulite terrains of Sri Lanka as an extension of the Mozambique Belt of east Africa (Pinna *et al.*, 1993) is ruled out based on the comparison of magnetic anomalies of both the terrains by Perera (1997) and ocean floor evidence by Reeves and de Wit *et al.* (2000, in press).

(i) Bouguer Gravity Image

Bouguer gravity image of Sri Lanka (Figure 7.9) is based on digitised contour map (Hatherton *et al.*, 1975). The Bouguer gravity image does not reveal much of the lithotectonic and structural fabric of Sri Lanka. This is mostly due to sparse and uneven distribution of gravity stations. A strong north-south negative anomaly in the southwestern part is evident in the Bouguer gravity image, the axis of which coincides partly with the lithotectonic boundary (Cooray, 1994) between the Highland Complex and the Vijayan Complex (Figure 7.9). Similarly, The boundary between the Wanni Complex and the Highland Complex broadly coincides with a narrow zone of

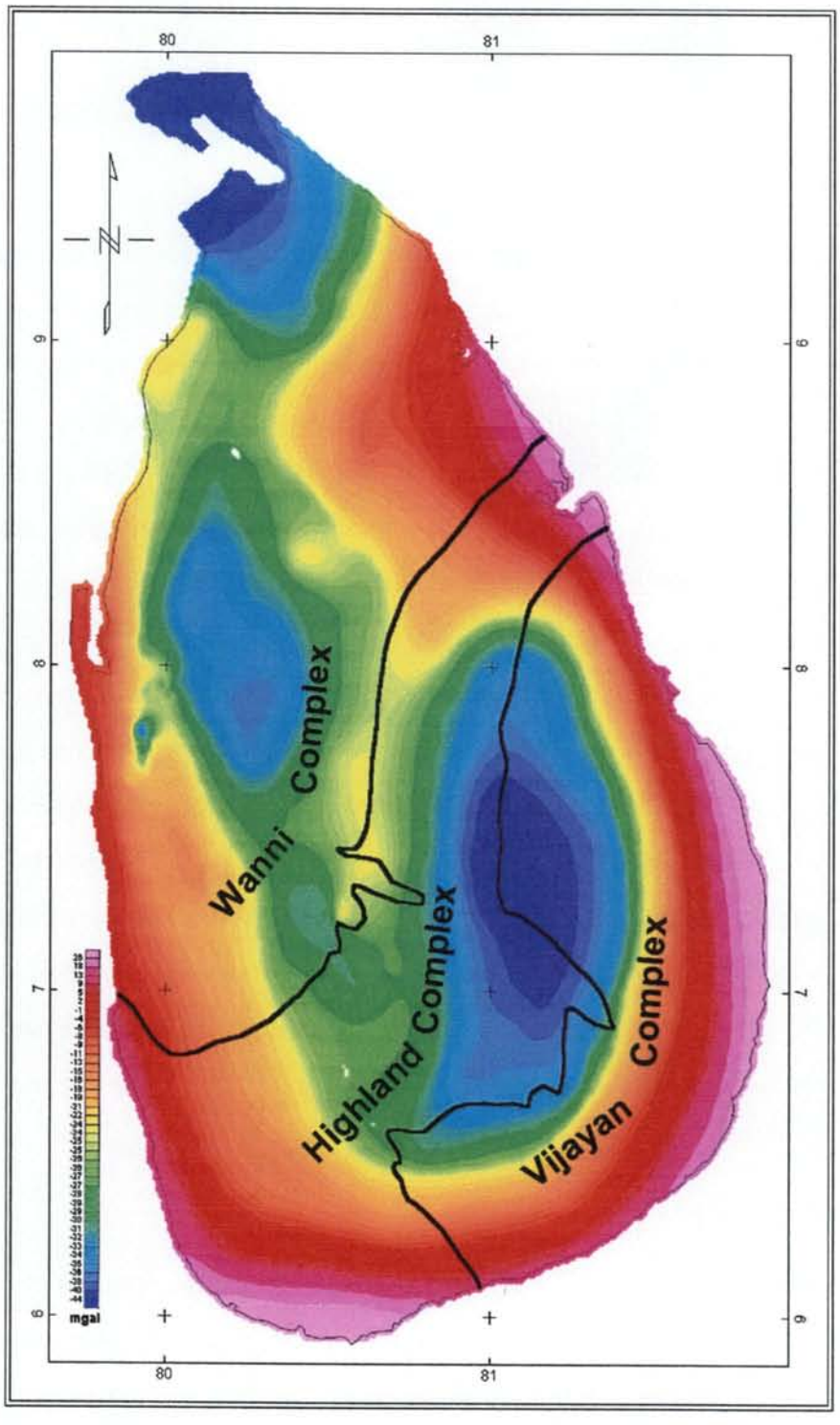

***Figure 7.9**: Bouguer gravity anomaly image of Sri Lanka. Data digitised from contour map (Hatherton et al., 1975). Note the coincidence of HC-VC boundary with the axis of the gravity low in the southeastern part and the WC-HC boundary with the the gravity high axis in the central part.*

Bouguer gravity high that separates the gravity lows to the NW and SE. The near coastal areas are represented by higher Bouguer gravity values.

(d) Gunnerus Ridge and its Gondwana connection

The Gunnerus Ridge is about 100 km wide, a submerged ridge off the coast of eastern Dronning Maud Land, East Antarctica. The high-resolution satellite altimetry (gravity) data precisely defines the outline of the Ridge and the Kainanmaru Seamount off its northern extremity. These are characterized by high gravity anomalies (Figure 7.10a). Saki *et al.* (1987) observed basement velocities of 5.4 and 5.8 km^{-1} below the Gunnerus Ridge, which resemble the 6.0 km^{-1} of the adjacent Antarctic continental basement. This observation suggests that the ridge is of continental nature. Dredging in the valley between the Gunnerus Ridge and the Kainanmaru Seamount has yielded gneisses, amphibolites, pegmatites and granites of continental provenance. Seismic profiles along and across the Gunnerus Ridge (Roeser *et al.*, 1996) have revealed rift structures with tilted fault blocks on the flanks of the ridge that resemble passive continental margins.

A gravimetric map constructed from the line data (Roeser *et al.*, 1996) shows gravity highs over the Gunnerus Ridge and the Kainanmaru Seamount and gravity lows on both flanks. The present gravity contour map (produced from the satellite altimetry data (GEOSAT)) for the Gunnerus Ridge and surrounding area (Figure 7.10b) reveals gravity values comparable to those shown by Roeser et al (1996). The magnetic data show anomalies of up to 200 nT over the Gunnerus Ridge and weak anomalies over the Kainanmaru Seamount. All these observations lead to the conclusion that the Gunnerus Ridge is continental in nature. Roeser *et al.* consider this ridge as a remnant of continental crust left behind when Madagascar and India separated from Antarctica. But continental reconstruction based on retracing the transforms (interpreted from satellite altimetry data) of the Indian Ocean (Reeves and de Wit, 1998 &, 2000) shows the western margin of the ridge against northern Mozambique and eastern margin against the southern coasts of Sri Lanka and India.

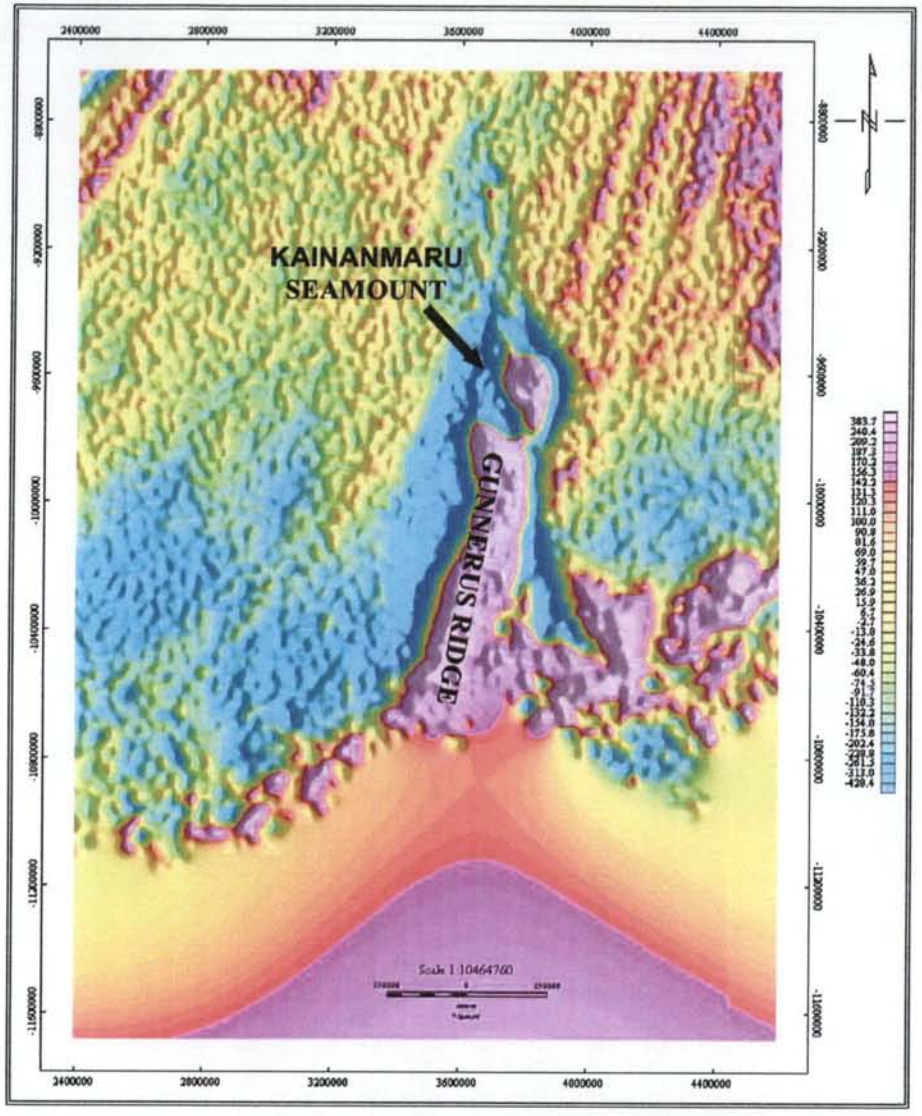

***Figure 7.10a**: Satellite altimetry derived gravity image of the Gunnerus Ridge (Data source: GEOSAT data from World Data Centre, USA)*

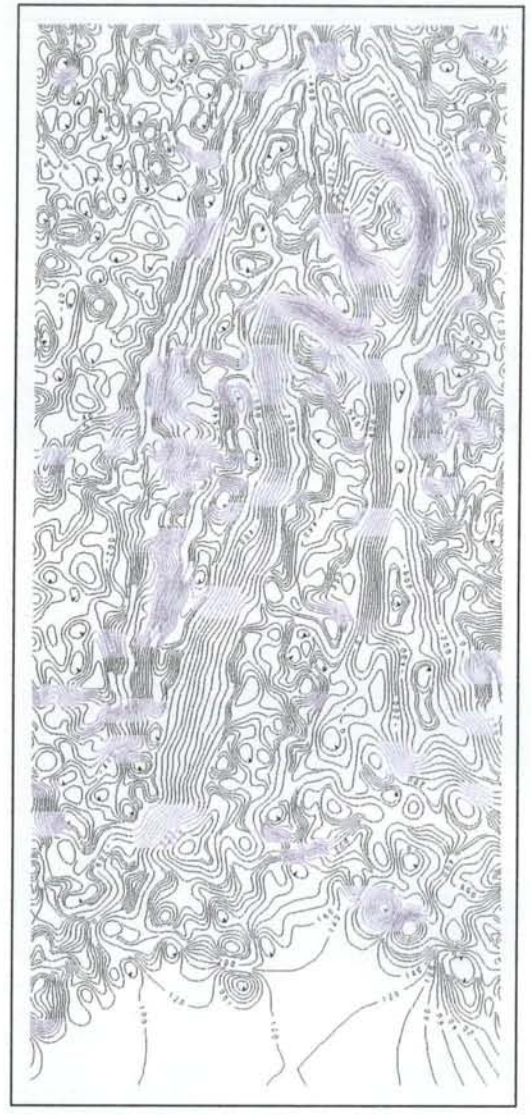

***Figure 7.10b**: Gravity contour map of the Gunnerus Ridge. Note high contour gradients on either flanks of the Ridge.This contour map is produced from the GEOSAT data by the author.*

7.3.3. India – Madagascar

(a) Comparison of aeromagnetic and gravity features with the major structures of South India

Aeromagnetic data of South India has been interpreted by several workers (*e.g.* Ramachandran *et al.*, 1986; Reddi *et al.*, 1988) and the results are discussed in section 6.3.2. (iii). More recent interpretation of the data by Geological Survey of India (1994) depicts the trends of magnetic highs and lows and major magnetic discontinuities corresponding mostly with the general strikes of the litho-units. No major structures corresponding to those interpreted from satellite imagery (Drury *et al*, 1984) or from structural trend lines (Ghosh, 1999) are evident from this magnetic interpretation. However, the magnetic images in this thesis (see figures and maps in Chapter 5) clearly depict some of the major lineaments at least in parts (Palghat-Cauvery, Achankovil and Moyar-Bhavani shear zones).

The gravity gradients interpreted by the GSI (1994) in southern India mostly trend NE-SW and E-W. But none of these gradients coincides with the major shear zones. More recently Reeves (*pers. comm.* 1999) has interpreted the gravity data of southern India that shows the Palghat-Cauvery Shear Zone more or less consistent with that of Drury *et al.* (1984). However, in Reeves' interpretation the trend of the shear zone becomes NE-SW in the eastern part (Figure 7.7). Thus the existence of major lineaments (Drury *et al.*, 1984; GSI, 1994) can not be ruled out. The recent interpretations of gravity (Reeves, *pers. comm.*, 1999 and this thesis) and magnetic data (this thesis) confirms the persistence of these lineaments, which are redefined.

Paucity of aeromagnetic coverage of eastern Madagascar makes it difficult to geophysically substantiate its fit with western India, as described in the geological correlation. However, satellite magnetic anomalies (MAGSAT) for Madagascar and India show excellent correlation between these two fragments (Agrawal *et al.*, 1992; Figure 2.8 in Chapter 2). Such correlation of satellite magnetic anomaly patterns is of limited use due to lack of desired level of resolution for precise delineation of geological features that can be used for correlation purposes. Interpretation of the aeromagnetic data in parts of the Ranotsara Shear Zone (Yardimcilar, 1998) precisely defines the orientation of the Shear Zone and associated faults that are significant in

correlation of similar features of the juxtaposed fragments (India and East Africa) in a Gondwana framework. As described in Chapter 4, the Ranotsara Shear Zone (RSZ) represents a major break in the continuity of structural trends on either sides of it. Though geophysically, no drastic change in anomaly patterns is observed across the Palghat-Cauvery Shear Zone (PCSZ), broad geological differences on either side are similar to that in Madagascar across the RSZ. Thus, the PCSZ might represent the eastward extension of the RSZ in India. The West Coast Fault (Figure 5.14), interpreted from the aeromagnetic images, however, provides the strongest evidence in favour of a strike-slip motion between India and Madagascar before they finally departed from each other.

7.3.4. Madagascar – East Africa

(a) Geophysical Interpretations of East Africa

Geology of East Africa is dominated by the north-south trending Meso/Neoproterozoic East African Orogen (EAO) and a number of Permo-Jurassic sedimentary basins. Interoperation of aeromagnetic data in parts of Kenya and Tanzania was earlier done by Reeves *et al.* (1986/87) and Batterham *et al.* (1983) respectively. Reeves *et al.* interpreted the presence of a triple junction of Jurassic age in eastern Kenya, two arms of which developed into a part of the Indian Ocean that lead to the separation of Madagascar from East Africa. They also identified a number of isolated magnetic anomalies along the Mombassa coast of Kenya and interpreted these as buried plutons genetically related to the separation between Madagascar and East Africa. Yardimcilar and Reeves (1998) interpreted the Precambrian margin in Tanzania and Kenya from aeromagnetic data and suggested a Madagascar-East Africa fit based on correlation of these Precambrian margins with those in Madagascar (Figure 7.11).

Interpretation of aeromagnetic images of Eastern Africa is done in this thesis (see Chapter 6 for details). The eastern margin of Precambrian rocks is delineated from the derivative maps (Maps 6.2 and 6.4) and the Euler deconvolution map (Map 6.6).

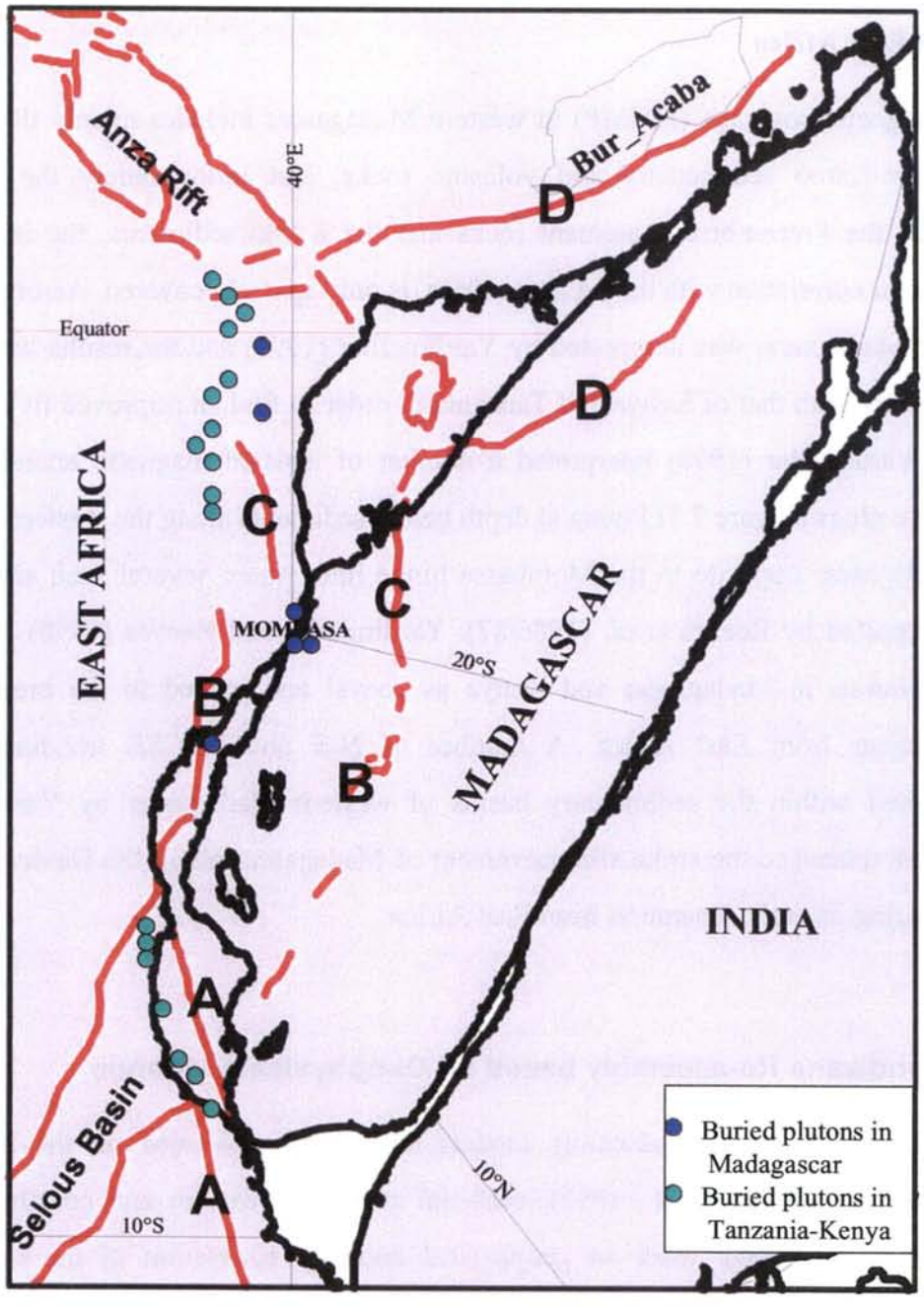

***Figure 7.11**: A close fit between Madagascar and East Africa based on matching of Precambrian margins and alignment of buried plutons interpreted from aeromagnetic data (modified from Yardimcilar and Reeves, 1998; Model: Reeve464d). A-A: geophysically interpreted faulted margin of Precambrian rocks in SW Tanzania, B-B: western Precambrian margin in SW Madagascar- Precambrian margin of NE Tanzania, C-C: western margin of Precambrian between 20° and 18°S in Madagascar- hinge line north of Mombassa (Reeves et al., 1986/87), D-D: Precambrian margin in NW Madagascar- parallel margin south of Buur-Acaba massif in southern Somalia.*

(b) Geophysical Interpretation of western Madagascar and its comparison with that of East Africa

Aeromagnetic coverage (AMMP) in western Madagascar includes mainly the Karoo and Post-Karoo sedimentary and volcanic rocks. But unfortunately the contact between the Precambrian basement rocks and the Karoo sediments, the important feature for correlation with that in East Africa, is only sparsely covered. Aeromagnetic data of Madagascar was interpreted by Yardimcillar (1998) and the results were used to correlate with that of Kenya and Tanzania in order to find an improved fit between them. Yardimcilar (1998) interpreted a number of isolated magnetic anomalies as intrusive plugs (Figure 7.11) lying at depth below sediments along the western margin of Madagascar opposite to the Mombassa hinge line, where several such anomalies were reported by Reeves *et al.* (1986/87). Yardimicilar and Reeves (1998) consider these plutons in Madagascar and Kenya as coeval and related to the breakup of Madagascar from East Africa. A number of N-S and NW-SE trending faults interpreted within the sedimentary basins of western Madagascar by Yardimcilar might be related to the strike slip movement of Madagascar along the Davie fracture zone during its early separation from East Africa.

7.4 Gondwana Re-assembly based on Geophysical Evidence

Though a number of re-assembly models have been advocated on the basis of lithology (*e.g.* Pinna *et al.*, 1993), surficial structural features and coastline (*e.g.* Bullard *et al.*, 1965), work on geophysical anomaly correlation of the separated continents has been sparse. In the present study, reassembly of the continental fragments (Figure 7.12) of central Gondwana has been attempted by matching the geophysical anomaly patterns and geological features interpreted from these anomaly patterns and from the ocean floor evidence derived from the satellite altimetry (gravity) interpretation (Reeves and de Wit, 1998)

7.4.1. Precambrian Geology

The faulted boundary of the Precambrian rocks (A-A in Figure 7.12) and associated faults in western Dronning Maud Land interpreted from the aeromagnetic data

(Corner, 1994) are parallel to the eastern boundary of the Kaapvaal craton, suggesting a close fit between the two terrains prior to the extrusion of basalts along the Lebombo monocline/Explora Wedge and subsequent separation of East Antarctica from Africa in Early Jurassic. The similar nature of the long strike length anomalies in both the terrains assumed to be low-angle thrusts dipping away from the cratons, further substantiates the fit (Figures 7.2 and 7.3).

Interpretation of the magnetic anomalies of the coastal region of Enderby Land, East Antarctica (Golynsky *et al.*, 1996) defines the boundary between the Archean Napier Complex and the Proterozoic Rayner complex. I consider this boundary as the westward extension of the Palghat-Cauvery Shear Zone in south India based on the fact that they separate the Archean cratonic rocks and the Proterozoic granulite belts. A normal fault, inferred in the Sør Rondane Mountains (Golynsky *et al.*, 1996) that extends farther northwards along the western margin of the Gunnerus Ridge, matches well with the Achankovil Shear Zone in South India. The marked parallelism and closeness of the Precambrian boundary of India and the continental margin (interpreted from the aeromagnetics, Golynsky *et al.*, 1996) in Enderby Land in East Antarctica further support a tight fit between these two fragments. Sri Lanka fits well in the gap between the Southern Granulite Terrain of India and the Lützow-Holm Bay of East Antarctica in this fit. The continental nature of the Gunnerus Ridge and the shape of its eastern margin comfortably place Sri Lanka in the gap between Antarctica and India in this close fit. The left laterally truncated NW-SE trending magnetic anomalies in the granulite belts in SW Sri Lanka seem to be in continuity with the E-W trending magnetic anomalies over the southern granulite belt of India (Figure 7.12). Aeromagnetic interpretation of SW Sri Lanka (Perera, 1997) and its comparison with that of northern Mozambique does not support the idea of continuance of the Lurio belt of Mozambique.

Though the aeromagnetic coverage of Madagascar is poor, it includes an important sector covering a part of the Ranotsara Shear Zone. Geophysical data is too limited in both India and Madagascar to achieve a fit based on geophysical anomaly patterns. However, the Ranotsara Shear Zone in Madagascar and the Palghat-Cauvery Shear Zone in South India interpreted from aeromagnetic data line up well to form parts of a

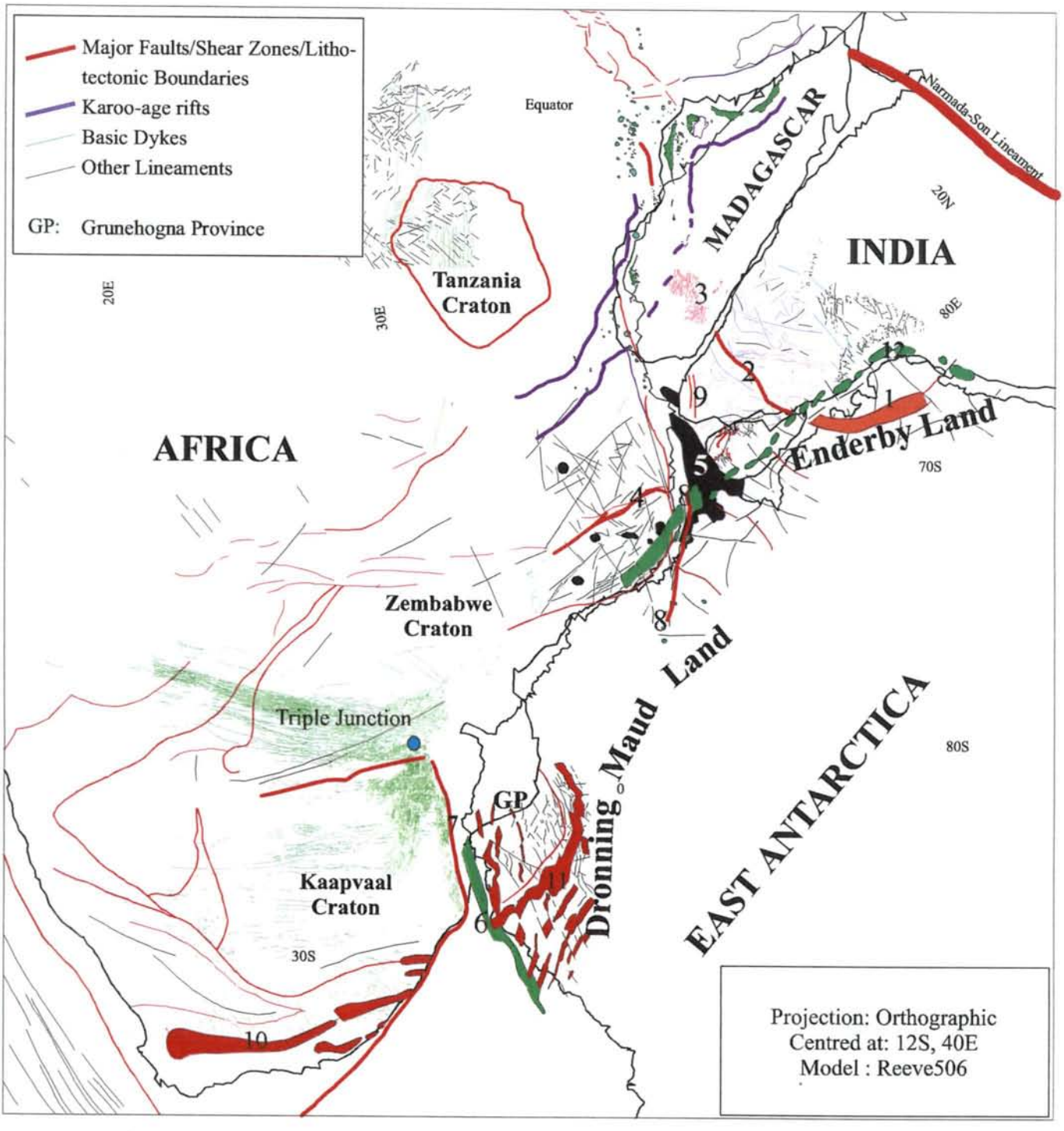

Figure 7.12: Reconstructed map of central Gondwana based on geophysical features.1: Boundary between Rayner and Napier complexes, 2.Palghat-Cauvery Shear Zone, 3.Ranotsara Shear Zone, 4. Lurio Shear Zone, 5. Gunnerus Ridge, 6. Explora Wedge, 7. Lebombo Monocline, 8. Western faulted boundary of Sor Rondane terrane, 9. Achankovil Shear Zone, 10. Beattie Anomaly, 11.Long strike-length anomaly in Maudheim Province, 12. Magnetic anomalies along continent-ocean Boundary off Enderby Land..

shear zone running from Enderby Land in Antarctica to Madagascar. The straightness of the Precambrian margins of the west coast of India and east coast of Madagascar also support a tight fit of the rifted margins of Precambrian rocks.

The Madagascar–East Africa fit is well constrained with the conjugate pairs of Precambrian margins in both the fragments (Yardimcilar and Reeves, 1998). Madagascar is placed between 9°S and 3°N latitudes primarily based on the parallelism of the conjugate margins- (1). the faulted margin in SW Madagascar and the geophysically interpreted Precambrian margin in SE Tanzania and NE Mozambique, (2). the western Precambrian margin of southern Madagascar and the Precambrian margin in NE Tanzania as shown by Batterham *et al.*, (1983), (3). the western Precambrian margin of Madagascar between 20°S and 18°S latitudes with the hinge line interpreted north of Mombassa by Reeves *et al.* (1986/87) and (4). the Precambrian margin in northwest Madagascar and that of south of Buur Acaba massif in southern Somalia.

7.4.2. Syn-rift features

The parallelism between the dyke swarm and basalt forming the Lebombo monocline in southeastern Africa (Mubu, 1995; present work) and the Explora wedge off the coast of western Dronning Maud Land (Jokat *et al.*, 1996) is suggestive of a simultaneous phase of magmatism in the region, probably during the earliest phase of rifting between East and West Gondwana in the Early Jurassic. Eruption of basaltic material along N-S trending zones suggests the prevalence of a east-west tensional regime leading to the onset of rifting between East and West Gondwana in the southern part at ~183 Ma (Duncan *et al.*, 1997), *i.e* at least 20 Ma prior to the actual drifting of fragments. The array of dyke swarms in southern Africa (Figure 7.12) compiled from geophysical and geological sources (Reeves, 1978; Mubu, 1995; Reeves, 2000) in combination with the geochronological data (*e.g.* Duncan *et al.*, 1990 and 1997) suggests the presence of a triple junction (Figure 7.12), the two successful arms of which occurred along the Lebombo and the Sabi monoclines and the Botswana dyke swarm being the failed third arm. It supports the proposed location of the triple junction at the intersection of the Kaapvaal craton, the Limpopo Belt and the Mozambique Belt (Cox, 1992; Goldberg, 1998). The dyke swarms along the Lebombo and Sabi monoclines and their northward

extension in the southern part of northern Mozambique (dykes interpreted from the aeromagnetic anomalies, this thesis; 'B' in Figure 7.12) limits the continental margin of southeastern Africa that lies parallel to the continental margin interpreted from magnetic anomalies (Golynsky *et al.*, 1996; Jokat *et al.*, 1996) off the coast of Dronning Maud Land, East Antarctica. The arcuate shape of the Precambrian boundary in northern Mozambique fits well with the corresponding margin formed by the Gunnerus Ridge and the continental margin magnetic anomaly off the coast of the Sør Rondane terrain (Figure 7.12).

A number of isolated circular magnetic anomalies in Tanzania and Kenya interpreted as basic intrusive bodies (Reeves, 1986/87; Yardimicilar and Reeves, 1998) are aligned along a linear zone (Figure 7.12). These intrusions, along with the Lebombo and Sabi dyke swarms, form a continuous zigzag north-south belt all along the eastern coast of Africa indicating the prevalence of an E-W tensional regime in the area preceding the separation between East and West Gondwana during the mid-Jurassic (Reeves and de Wit, 2000). Based on the quantitative interpretation (depth to the top of the source) of these magnetic anomalies and the stratigraphic constraints from seismic mapping (TPDC, 1995), Yardimcilar and Reeves (1998) have inferred that these intrusive bodies pre-date the Upper Jurassic sedimentation in eastern Tanzania. This result implies that the emplacement of these plutons occurred during Lower Jurassic and probably synchronously with the initial rupture between East Africa and Madagascar.

8. DATA INTEGRATION AND CENTRAL GONDWANA REASSEMBLY

This Chapter reports the methodology and usefulness of integration of various layers of geoscience data (e.g. lithology, aeromagnetics, gravity). The integrated images are interpreted and the results are used in finding constraints for a tight fit of the Precambrian blocks of central Gondwana.

8.1 Data Integration

Integration of various layers of geoscience datasets provides additional information, which might not be well depicted in any one of the layers when displayed in isolation. In this study, an attempt at integration of two data layers – regional geology and aeromagnetics – was carried out for the areas (*e.g.* South India, Southern and Eastern Africa, Southwest Sri Lanka), where both the datasets were available.

8.1.1. Methodology

Spatial integration of different data layers (raster and vector) was carried out using principles of GIS (Geographical Information System). The digital data was prepared by digitising hard copy maps. As the original maps were in different projections and scales, all the digitised data for a particular area were resampled and reprojected to a common grid cell size and projection respectively. The grid cell size was determined depending upon the quality of original data – *e.g.* a grid cell size of 250 m was used for the high resolution aeromagnetic data for Sri Lanka, whereas a grid cell size of 1000 m was used for high-altitude aeromagnetic data for southern India. Similarly grid cell size of 1000 m was used for African geology and aeromagnetic data, following that of the original AMMP data. A simple latitude-longitude projection with WGS84 Ellipsoid was used for all the datasets for simplicity and easy handling of data.

The different layers of geological data used in the integration and interpretation are – 1. lithology and 2. structural data. Though the lithology layer could have been used as a vector layer (in the form of polygons) in the integrated image, a raster format was preferred as manipulation of data is easier in raster format with most of the commercially available software. The steps followed in digital integration of various datasets are given in the flow chart (Figure 8.1).

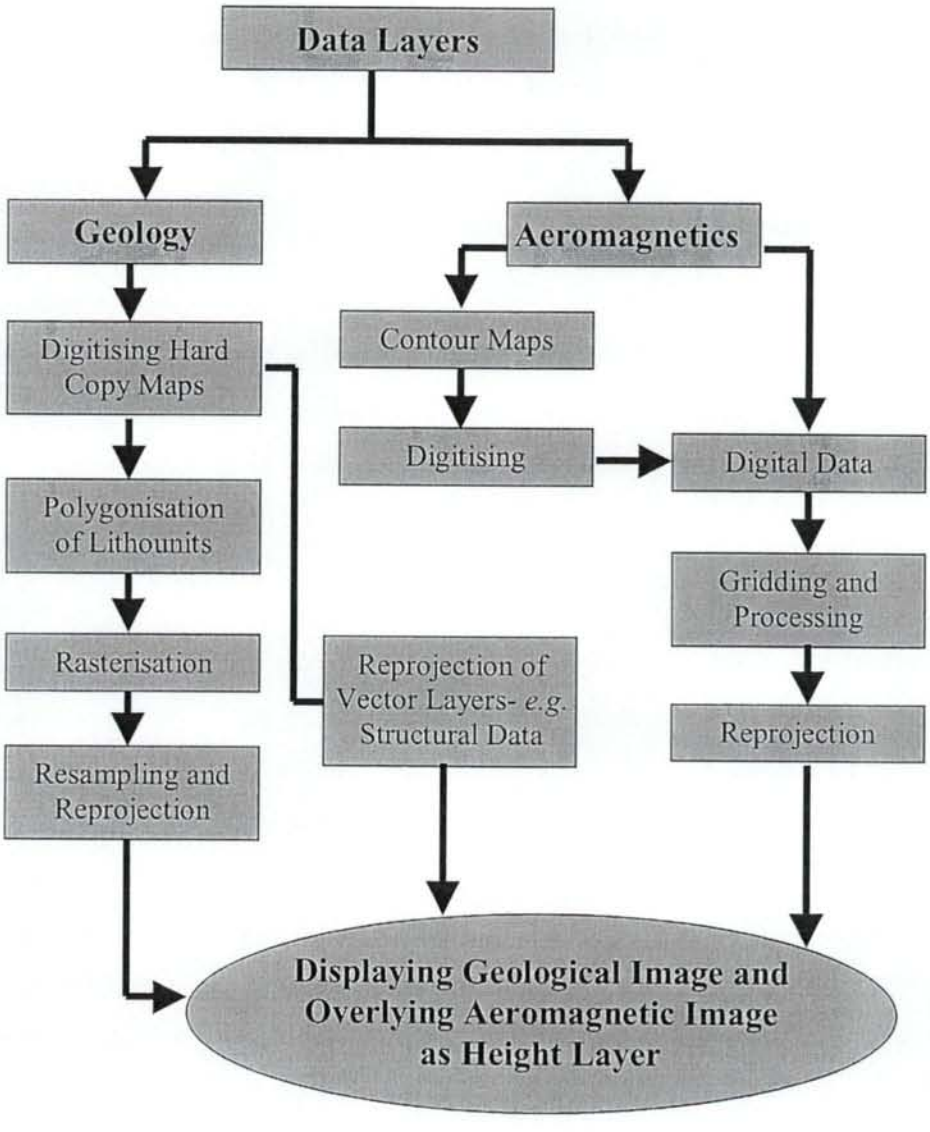

***Figure 8.1**: Flow chart for steps involved in digital integration of various data layers.*

8.1.2. Integrated Images

Overlying of aeromagnetic data on the geological maps integrates surface geological features with the subsurface features. Thus, the integrated images bring out the subsurface extension of the sparsely exposed geological features. Integration of aeromagnetic and geological data is done for three areas – 1. southern and eastern Africa, 2. South India and 3. Southwest Sri Lanka. See Chapters one and three for sources and quality of various data used for this study.

a. Southern and Eastern Africa

The data integration for southern Africa and Eastern Africa is done separately as the datasets are very large in size. In southern African image (Figure 8.2), aeromagnetic data for Namibia has not been used. The following features are more prominently displayed in the integrated image than in the aeromagnetic images (Aeromagnetic maps enclosed in the back pocket) alone.

1. The Kheis Belt: The north-south magnetic anomaly trends in the Kheis Belt (KB in Figure 8.2) are clear in the image and extends much beyond the boundary shown in the geological map.

2. The Zoetfontein Fault marking the northern limit of the Kaapvaal craton in the northeastern part is better-resolved in integrated image.

3. The individual dykes seem to be better resolved.

A direct correlation between the aeromagnetic data and the lithology in the Eastern African image (Figure 8.3) is not very clear because of the lack of geological details. However, the integrated image convincingly substantiates the following facts.

1. The east-west magnetic trend in the Lufilian Arc and the Zambezi Belt to the north of the Zimbabwe craton cuts across the overall northeast-soutwest trend of the Irumide Belt.

2. The Tanzania craton extends much farther eastward at depth than it is shown in the surface geological map.

3. The NW-SE trending Ubendian Belt continues farther southeastward beyond the Irumide belt. The magnetic trends similar to that of the Ubendian Belt is clear even to the southeast of the Selous rift basin in southern Tanzania. However, field check of

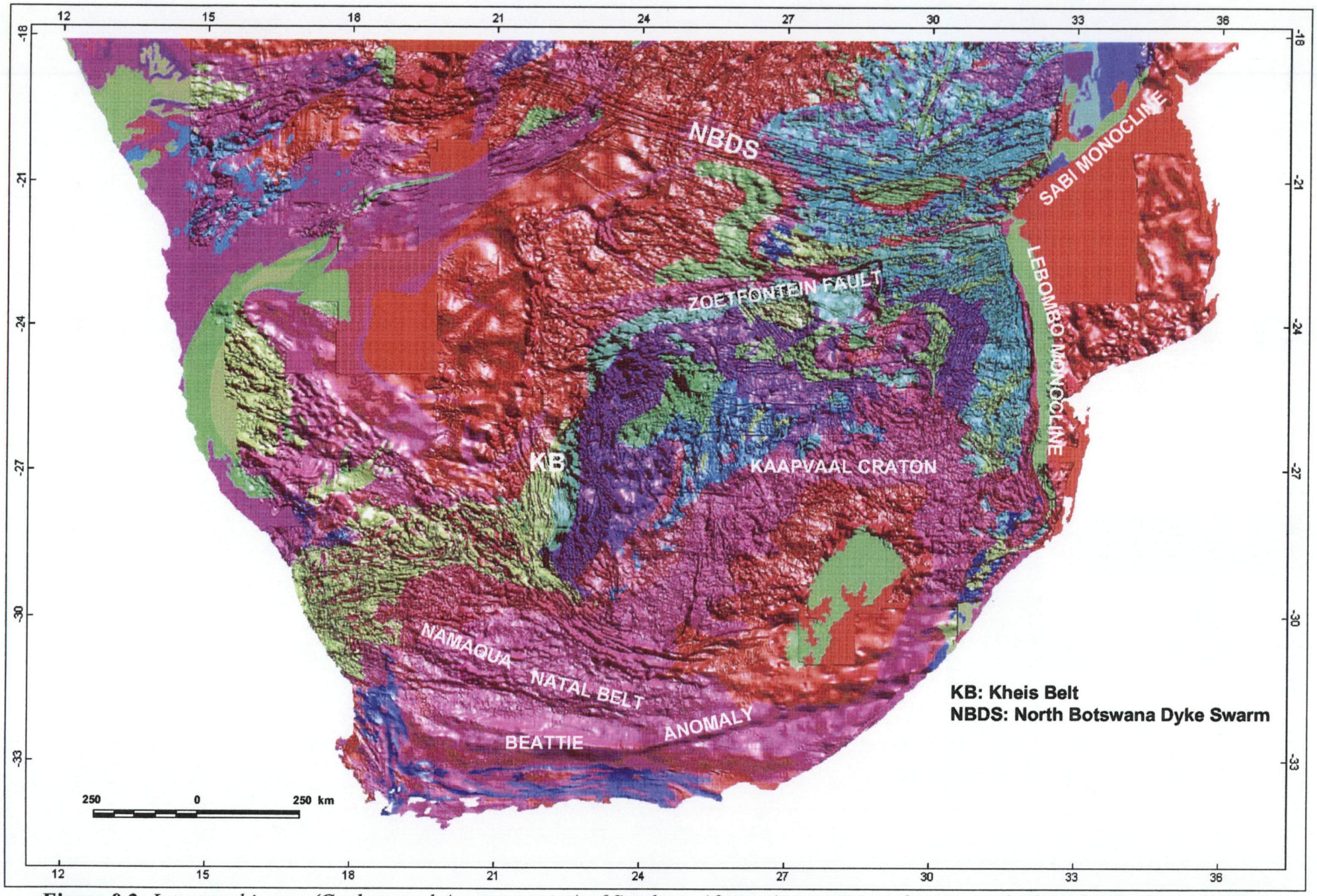

***Figure 8.2**: Integrated image (Geology and Aeromagnetics) of Southern Africa Aeromagnetic data is overlaid on the Geological Map. Data: Aeromagnetics - AAMP and Geology - CIGCES, University of Cape Town*

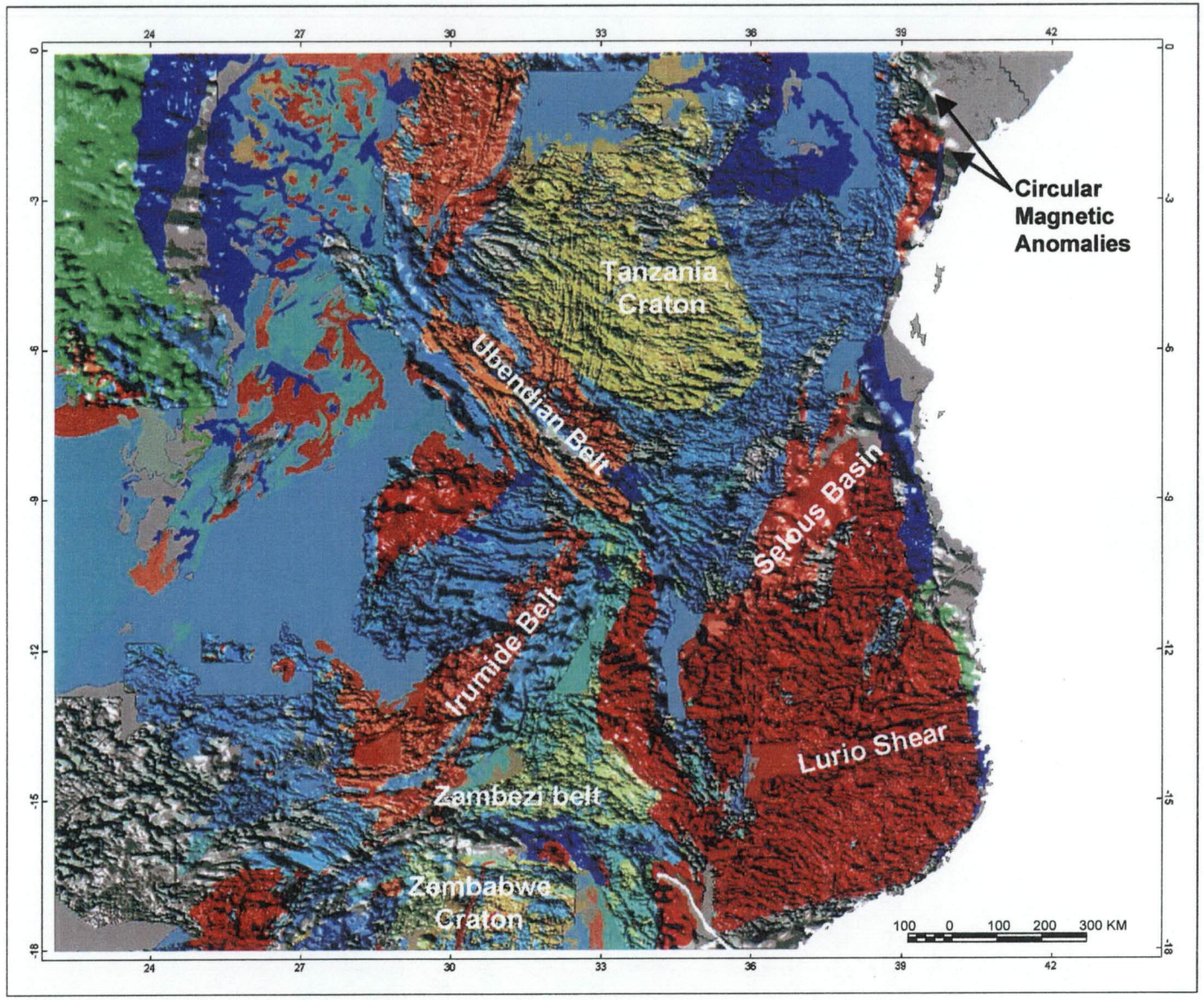

***Figure 8.3**: Aeromagnetic data overlaid on regional geological map. Data Sources: Aeromagnetics - African Magnetic Mapping Project and Geology - Gondwana GIS database, CIGCES, University of Cape Town.*

the lithology and structural trend of the area is necessary to ascertain the presence of Ubendian rocks within the East African orogenic Belt in southern Tanzania and northern Mozambique.

b. Southern India

The results of aeromagnetic and geological data integration (Figure 5.17) are described in Subsection 5.12.3 in Chapter 5. The most obvious outcome of the integration is the identification of the Cannanore-Thanjavur Lineament (CTL), which is probably the most important one among several such features identified from satellite imageries (Drury *et al.*, 1980) and structural trend analysis (Ghosh, 1999). Other linear features like the Achankovil Shear Zone, the Palghat-Cauvery Shear Zone etc. is very well depicted in the integrated image. Figure 8.4 shows the earlier defined shear zones over the integrated image. This clearly demonstrates the need to redefine the spatial disposition of the shear zones in the region (see Figure 5.18 for redefined shear zones based on interpretation of aeromagnetic data and integrated data).

c. Southwest Sri Lanka

A good degree of conformity between the mapped geology and their aeromagnetic signature is observed in the integrated image (Figure 8.5) of Southwest Sri Lanka. A gradual change in strike direction of geological units from NNW-SSE in the southern part to WNW-ESE in the western coastal areas of the study area is evident in the map. The magnetic trends continue farther northwesterly, although the geological units cease to crop out beyond ~7.3° in the west-central coastal areas of Sri Lanka. The coincidence of geological units and the magnetic anomaly trends in the southwestern part gives confidence to map the subsurface extension of those units in the northwest direction up to the coast. This interpretation has implications in fixing the paleoposition of Sri Lanka with respect to India in Gondwana. This is described in the next Section of this Chapter. The datasets used for this study vary a great deal in terms of resolution. The geology is too course (1: 506 880) for a fair comparison with the relatively higher resolution (~ 500 m line spacing and 150 m terrain clearance) aeromagnetic data. Better results could be expected if larger scale geological maps (1: 50 000) with better information on geological units are used.

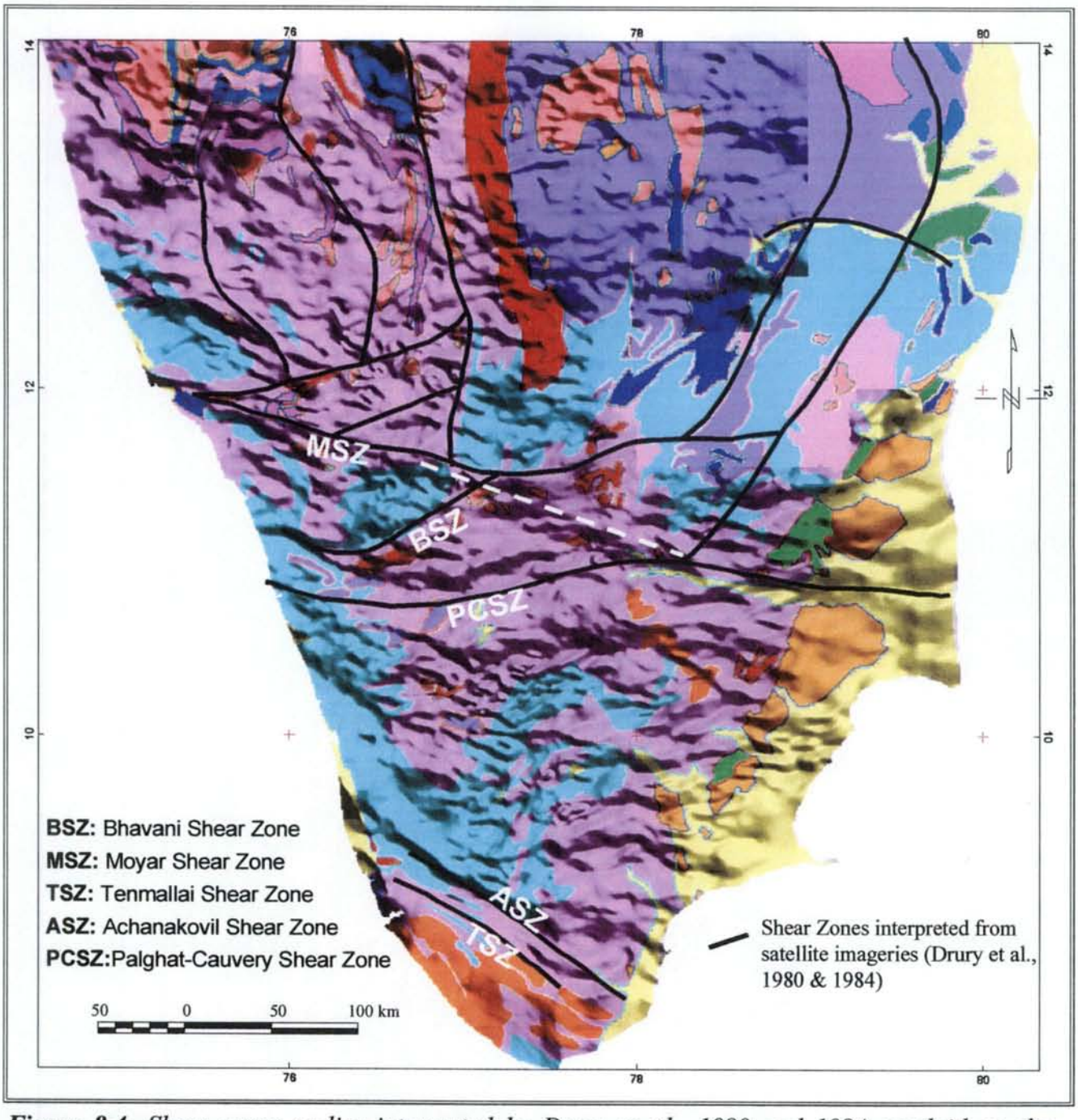

***Figure 8.4**: Shear zones earlier interpreted by Drury et al., 1980 and 1984 overlaid on the integrated image (geology and aeromagnetic) of southern India. Note the correlation between the shear zones and the integrated image. The MSZ, BSZ and ASZ are well depicted in the image, whereas the PCSZ needs to be redefined as in Figure 5.16. The white dashed line in the image represents the missing link between the Moyar Shear Zone in the west and the eastern part of the PCSZ in the east to define a continuous lineament - the Cannanore-Thanzavur Lineament (see Figure 5.17 for geological legend).*

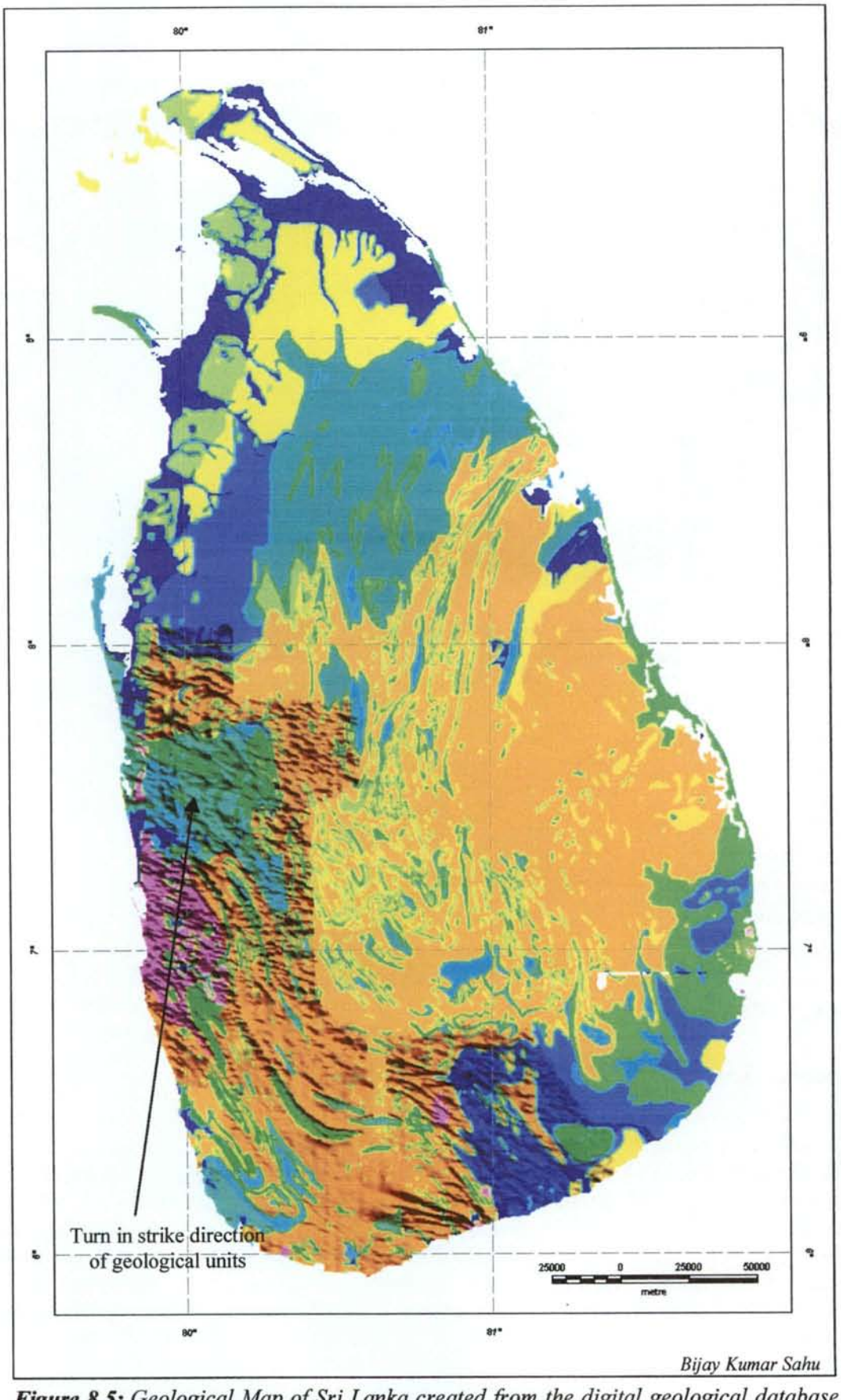

Figure 8.5: *Geological Map of Sri Lanka created from the digital geological database created in this study with aeromagnetic data overlain in the Southwestern part. Note the change in geological trend from NW-SE to WNW-ESE from south to north.*

Though the integration of different layers of data is done here in a regional/subcontinental scale, similar method could be applied to small areas with high-resolution datasets to refine geological maps. Coincidence of geophysical anomalies with the known geology boosts the confidence for interpretation of similar anomaly patterns in areas of limited or no exposure.

8.1.3. Discussion

Digital integration of aeromagnetic and geological data of few of the central Gondwana fragments demonstrates the following:

1. A direct correlation between the geology and the aeromagnetic anomaly patterns can be made by displaying both the datsets as in one image.

2. Better results could be obtained by using geological maps incorporating lithological and structural details.

3. Similarly, other geoscience datasets (*e.g.* gravity, topography) can be used to integrate with geology for producing more complex (2-layer, 3-layer) maps, which might provide much more information on subsurface geological features.

8.2. Central Gondwana Reassembly

A tight re-assembly of the central Gondwana continents flanking the Indian Ocean (Map 8.3 and 8.4) was attempted using the results of the geological and geophysical evidence gathered in this study. Constraints for reassembly of central Gondwana fragments was derived from the combination of geological information (lithology, geochronology and structure) and geophysical interpretation compiled in this study. All these informations were stored in an ATLAS database and different models were tested interactively to find a tight (±100 km) reconstruction for the Precambrian central Gondwana. The recent reconstruction model (Reeves and de Wit, 2000) based primarily on retracing of ocean floor transforms was taken as the base and the model was tested using the geological and geophysical evidence from the continents.

8.2.1. Comparison of Aeromagnetic Anomalies

The shape and amplitude of aeromagnetic anomalies are largely dependant on a number of geological and geophysical factors – *e.g.* strength of the inducing field, magnetic inclination and declination, remanent magnetisation, and magnetic susceptibility and attitude of the source rock. The quality and resolution of aeromagnetic data are greatly affected by survey parameters like flight height and direction and spacing of survey lines. Processing factors like grid cell size also affect the quality and resolution of data. So direct comparison of magnetic anomalies produced by widely varied parameters mentioned above is not correct and could be misleading. It is therefore a prerequisite to minimise the effects of these factors on the anomaly patterns as far as practicable before comparing them. This was achieved by systematically reducing the aeromagnetic data for all the fragments as if they all were acquired with a similar set of parameters. Mostly the parameters used for compilation of AMMP data were used, as the AMMP data constitutes about 70% of the total data used in this study.

a. Methodology for Data Reduction

1. All the datasets except that of the AMMP were reduced to 1 km height and resampled at 1 km grid to largely remove the influence of survey parameters. As the terrain clearance for the Antarctica data was not available, the data was used unchanged.

2. In most metamorphic terrains the influence of remanent magnetisation is negligible compared to that of the induced magnetisation (Henkel, 1991). Thus, ignoring the remanence, it can be assumed that the anomalies are produced predominantly due to induced magnetisation that is directly proportional to the inducing field (Earth's magnetic field at the time of survey or IGRF). For comparison of magnetic anomalies due to crustal sources, removal of IGRF for the corresponding years/epochs of each survey must be done. But removal of IGRF alone does not fully eradicate the effects of the field strength on anomalies over widely separated areas. Thus, to balance the anomalies, the rocks must be subjected to same inducing fields. This could be achieved by amplifying the anomalies of one of the areas by multiplying a factor equal to the ratio of inducing field of the area and that of the area to be compared. For

example, a comparison between southern India and northern Mozambique can be carried out as follows.

Southern India:	IGRF in 1980	= ~40150 nT
	Magnetic Inclination	= 3°
Northern Mozambique:	IGRF in 1975	= ~33300
	Magnetic Inclination	= -50°
Ratio of IGRF (Mozambique to India)		= 0.829

The amplitudes of magnetic anomalies for southern India were amplified by a factor of 0.829 to neutralise the effect of difference in the inducing fields of the two terrains at the time of surveys.

3. To minimise the contribution of magnetic inclination and declination on the anomalies, it is required to reduce the data to the pole (RTP). But no useful RTP could be applied due to the obvious problems associated with RTP for low magnetic latitude data (McLeod *et al.*, 1993). Instead, the analytical signal amplitudes, which are virtually independent of the effects of the magnetic vectors, for each of the dataset (Map 8.2) were calculated for a fair first order comparison of data.

After minimising the effects the parameters that affect the amplitudes of magnetic anomalies, the reduced data were used to produce two aeromagnetic anomaly maps – 1. Total Field Map (Map 8.1) and 2. Analytic Signal Map (Map 8.2) - of central Gondwana for direct comparison of anomalies.

b. Comparison of Anomaly patterns among Central Gondwana Fragments

The projection parameters of the available digital data were also different for different fragments. It was necessary to convert all the datasets into a global projection for comparison. The datasets were reprojected to the Mercator projection (origin at 0°, 0°) on a WGS84 spheroid. The data were posted on the central Gondwana map (Reeves and de Wit, 2000) to ascertain the continuity of anomaly patterns across the rifted margins. Results of comparison of anomaly patterns between hitherto conjugate fragments have been discussed in preceding chapters (*e.g.* correlation between India and Sri Lanka in Chapter 5). A summary of the comparison is given below.

***Table 8.1**: Specification of digital data used for preparing aeromagnetic map of central Gondwana*

Fragments	Data Source	Terrain Clearance (metres)	Grid Size (m x m)	Projection Parameters	
				Projection	Spheroid
Africa	AMMP	1000	1000 x 1000	Mercator	Clarke1880
East Antarctica	Corner	not available	2000 x 2000	Lamberts Conic Conformal	WGS84
Sri Lanka	Perera	152	250 x 250	Transverse Mercator	Everest1930
India	This study	2100	1000 x 1000	Polyconic	Everest1930
Madagascar	AMMP	1000	1000 x 1000	Mercator	Clarke1880

(i) Although the quality of data for the two terrains are greatly different, a broad comparison of the anomaly patterns between the two terrains show similar long strike-length anomalies in the Maudheim Province of Dronning Maud land as the Beattie anomaly in southern Africa. The other prominent feature is the colinearity between the anomalies over Lebombo monocline in southeastern Africa and the Explora Wedge off the coast of Dronning Maud Land.

(ii) A direct comparison of anomalies could not be done between India and Enderby Land due to non-availability of data for Enderby Land. However, a comparison of the aeromagnetic interpretations of the two terrains is described in Chapter 7.

(iii) Juxtaposition of Sri Lanka against southeastern tip of India is constrained by comparison of anomalies of the two terrains (Map 8.1 and 8.2). A direct comparison between India and Madagascar could not be done due to lack of data in Madagascar.

(iv) Magnetic anomalies over the near coastal tracts of Madagascar and East Africa show similar anomaly patterns with very low magnetic relief. A number of circular anomalies in both the terrains have been interpreted as subsurface plutons temporally related to the breakup between the two.

8.2.2 Aeromagnetic Interpretation Map

A digital database in ATLAS format including all the available (published and unpublished) aeromagnetic interpretations of parts of central Gondwana fragments was prepared in this study. Aeromagnetic interpretation for regional structures was done by the author for southern India and southern and eastern Africa. These interpretations were appended to the aeromagnetic interpretation database and an aeromagnetic interpretation map (Map 8.3) of central Gondwana was prepared. The map shows all the important aeromagnetic features of the continents and their relationship in Gondwana.

8.2.3 Tectonic map of central Gondwana

A database of the geophysical and geological features for each of the continental fragments of central Gondwana was prepared. Geology of each fragment was subdivided into five lithotectonic domains (Map 8.4) based on aeromagnetic anomaly patterns, litho-assembages and geochronology. The boundaries of these tectonic domains were mostly interpreted from the geophysical anomaly patterns.

a. Pre-Kibaran/Grenvillian-age (~1100 Ma) Shields

All the terrains that were cratonised prior to the widely recognised orogeny at ~1100 Ma have been considered as single units for the purpose of this study. These terrains, in general, have not been affected by the later tectonothermal episodes (*e.g.* Pan-African) except intracontinental rifting in the Phanerozoic (Karoo rifting and Jurassic-Cretaceous rifting related to Gondwana breakup). In Africa the Kalahari craton (Map 8.4), the Congo Craton and the Dodoma-Bangweulu shield, in East Antarctica the Grunehogna Province and the Napier Complex, in Peninsular India the southern Indian Shield, in Madagascar, the Anglonkil Block are the Pre-Kibaran shields.

b. Meso-Neoproterozoic (~Kibaran\Grenville-age) Mobile Belts

These belts represent the sites of collision between Pre-Kibaran continental blocks during the formation of Rodinia (Chapter 2). Thus identification of these terrains helps in understanding the history of Rodinia that split into a number of fragments at around 725 Ma. These fragments later amalgamated to form Gondwana in Neoproterozoic.

c. Proterozoic Terrains affected by Neoproterozoic tectonothermal events (~Pan-African)

Many Paleoproterozoic to Neoproterozoic terrains (*e.g.* southern and central Madagascar, Sri Lanka, Southern Granulite Terrain of India) show effects of a Late Neoproterozoic to Early Cambrian (~ 500-600 Ma) thermo-tectonism indicating these terrains lie within or near the collisional belts among continental fragments which amalgamated to form Gondwana. Thus identification and correlation of these belts constrain the suturing locii among these continental masses.

d. Phanerozoic Rift Basins

Intracontinental rift basins developed during Late Paleozoic to Early Jurassic in response to the lithospheric extension. These basins are known as the Karoo basins in Africa and Madagascar and Gondwana basins in India. As these basins developed during the lifetime of Gondwana, correlation of these basins provides valuable clues for assembling rifted Gondwana fragments.

e. Syn-breakup Magmatic Provinces

Huge volumes of magmatic rocks related to the breakup of Gondwana have erupted/intruded in many parts of Africa, Antarctica and India. In South Africa the Karoo magmatic provinces are the best example of this event. Eruption of flood basalt along the Lebombo monocline and Mateke-Sabi in southern Africa and the Explora Escarpment off the coast of Western Dronning Maud Land in East Antarctica is the result of rifting between the two fragments.

8.3 Comparison with the Recently Published Gondwana Models

8.3.1. Lawver and Scotese (1987)

Lawver and Scotese (1987) suggested a tight reconstruction of the central Gondwana fragments (see Chapter 2 for details). Although, their reconstruction closely matches with the fit presented in this thesis, there is scope for further refinement of the reconstruction based on the results of this study. The fits between East Africa-Madagascar and India and Enderby Land are in conformity with the present model. A tighter fit between Madagascar and India is suggested based on the findings of

aeromagnetic interpretation of southern India. Position of Sri Lanka with respect to India and east Antarctica is almost analogous in both the models. However, the wide gap between northern Mozambique and eastern Dronning Maud Land in Lawver and Scotese reassembly could be reduced in the present model to constrain a tight fit between the two.

8.3.2. Pinna *et al.* (1993)

Pinna *et al.* (1993) studied geology of northern Mozambique and suggested its fit (Figure 8.6) with adjacent Gondwana fragments. His original figure shows a number of subplates within Africa separated by failed rifts of various ages. By contrast, the non-African fragments have been drifted away from Africa as a result of rifting that successfully turned into dispersal and ocean creation. Thus a post-Karoo and predrift reassembly of these figments should resemble the post-Karoo appearance of Africa (Reeves, Sahu and de Wit, *in prep.*). Figure 8.6b shows a tighter reconstruction, where the similar tectonic terrains (*e.g.* Zimbabwe, Kaapvaal and Grunehogna cratons; Zambezi Belt, Mozambique belt and Queen Maud Land) are juxtaposed.at closer proximity. The eastern margin of the Zimbabwe craton and the southern margin of the Grunehogna Province are aligned almost along a straight line.

8.3.3. Windley *et al.* (1994)

In contrast to the tight fit model of Lawver and Scotese (1987), Windley *et al.* (1994) suggested a 'loose' fit of the southern continents (Figure 8.7) based on comparison of Precambrian geology of Madagascar with that of the adjacent fragments and continuity of certain regional features mapped in Madagascar across India and East Africa. Such a 'loose' reassembly does not account for the wide gaps shown between conjugate fragments in Gondwana. Geophysical studies and recent geochronological works in Madagascar, India and East Africa (*e.g.* Kröner *et al.*, 1997; Collins *et al.*, 2000, de Wit *et al.*, 2000, Ghosh, 1999) favour a more northerly position of Madagascar with respect to India and East Africa. An alternative tighter reconstruction (Figure 8.7b) based on the results of the present study does not pose any difficulty and reunites the Gondwana-age geology satisfactorily (see Chapter 4 for detail geological correlation).

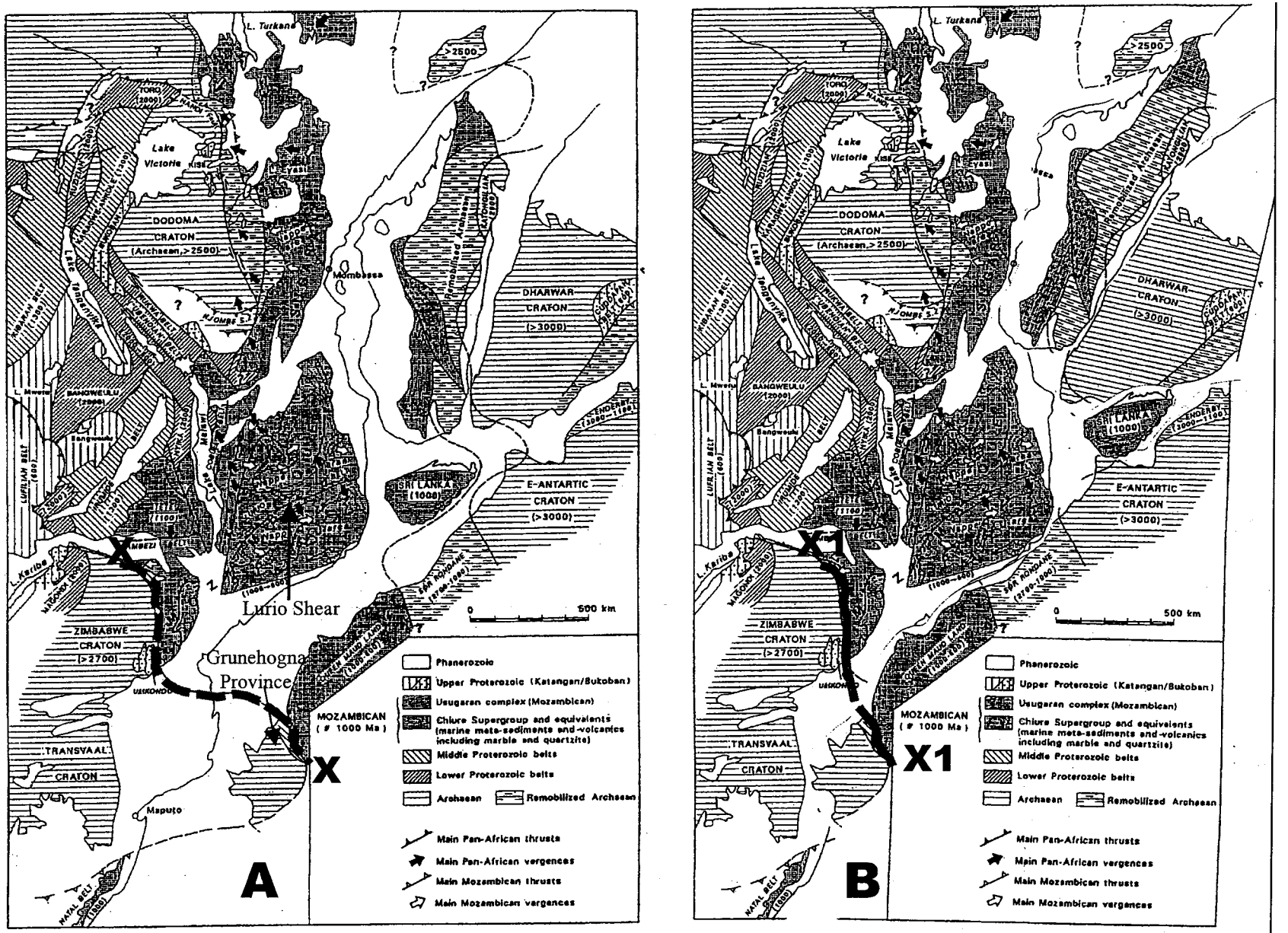

***Figure 8.6**: A.Central Gondwana reassembly by Pinna et al.,(1995) based on geological comparison. Wide gaps exist between the fragments. B. A tight fit of the fragments with the same geology better defines the sutures between East and West Gondwana. For example, the eastern boundary of the Zimbabwe craton and the southern margin of the Grunehogna Province (X-X and X1-X1) align in a straight line Figure B (from Reeves, Sahu and de Wit, in prep.).*

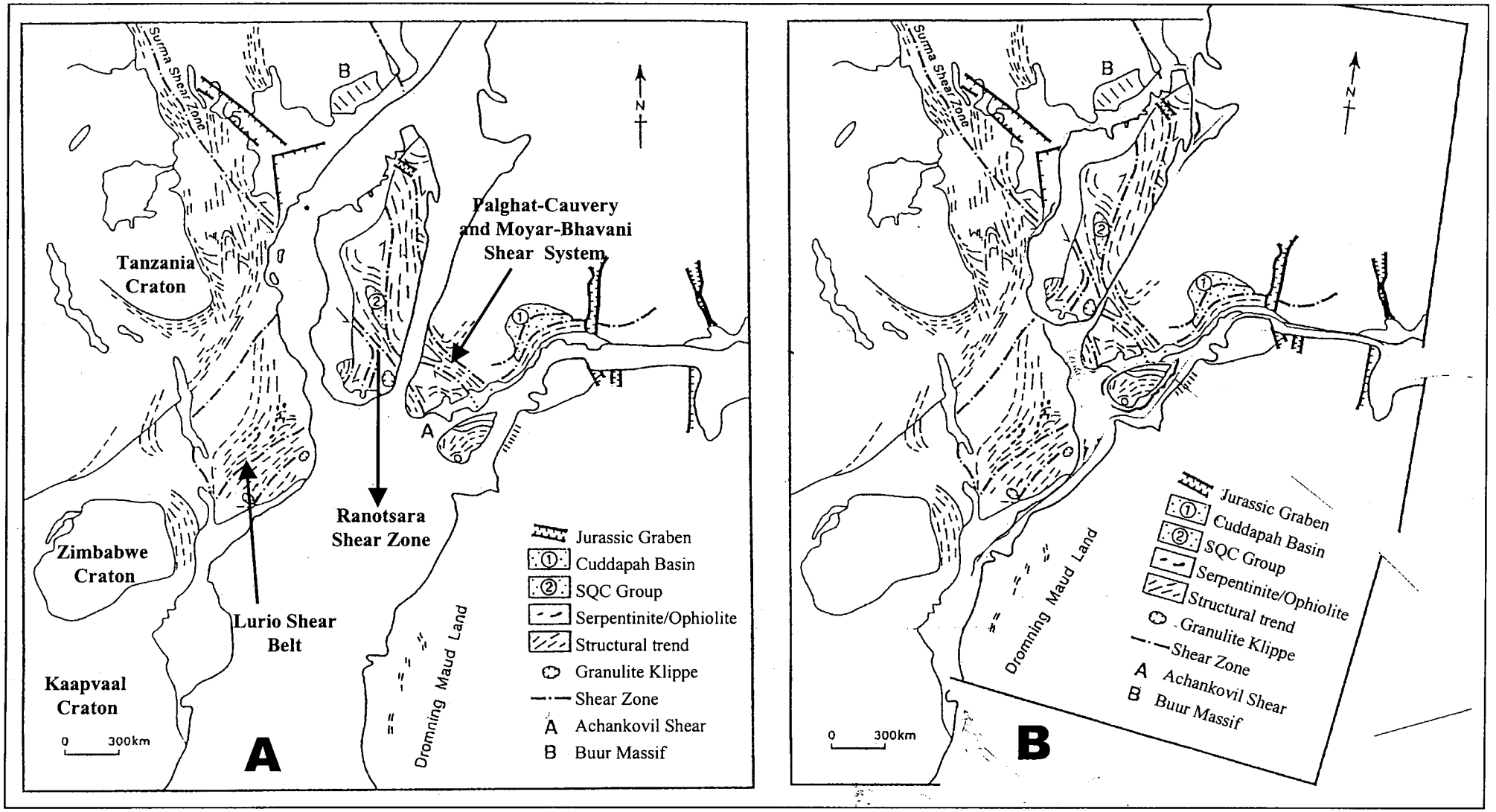

***Figure 8.7**: A. Central Gondwana reassembly by Windley et al., 1994 based on geology of Madagascar and its comparison with India and East Africa. Note wide gaps between the conjugate fragments. The Achankovil Shear Zone of India is correlated with the Ranotsara Shear Zone. B. Tight reconstruction of the fragments based on geological and geophysical evidence. Note the farther northerly position of Madagascar with respect to East Africa. The Palghat-Cauvery and Moyar-Bhavani Shear system is compared with the Ranotsara Shear Zone in the tight reassembly (from Reeves, Sahu and de Wit, in prep).*

8.3.4. Ghosh (1999)

Ghosh (1999) proposed a fit of India with Madagascar, Sri Lanka and Enderby Land (Figure 2.14) based on new geochronological data from southern India. Though there is not much difference in the paleopositions of fragments adjacent to India, this study certainly favours a tighter reassembly. Geophysical data from SW Sri Lanka and southern India suggests a closer fit (Map 8.3).

8.4. Summary and Conclusions

1. Large areas of all the fragments of central Gondwana have records of Neoproterozoic tectonothermal events in the form of high-grade granulite facies metamorphism and magmatism. These areas, someway or other, have suffered impact of the collision among the continental blocks during their amalgamation to form Gondwana. Recent dating of the Pan-African events (*e.g.* Pinna *et al.*, 1993; Ghosh *et al.*, 1999; Kröner *et al.*, 1997; Collins *et al.*, 2000; de Wit *et al.*, 2000) in these terrains indicate the amalgamation of continents to form Gondwana was complete by ~500 Ma.

2. The NNW-SSE trending major fault (West-coast Fault) in the West Coast of India seems to have been active during the initial separation of Madagascar from India. The aeromagnetic images show a sudden turn in the strike of generally east-west magnetic trends towards northwest in the western parts and finally merge with the West-coast Fault. This implies that India and Madagascar had substantial dextral strike-slip movement along the WCF prior to drifting, where India moved southward with respect to Madagascar. Unfortunately, eastern part of Madagascar is not aeromagnetically covered to substantiate this observation. However, limited aeromagnetic coverage in south central Madagascar reveals an over all 'S' shape of the Ranotsara Shear Zone, where the eastern end bends southward. The trends of magnetic lineament interpreted (Yardimcilar, 1998) in south central Madagascar (Figure) show a gradual change from NNW-SSE to NW-SE, which also might have resulted from the initial northward movement of Madagascar along the WCF. The Archean terrains in the northeastern and east-central parts of Madagascar (Antongil Block in Figure 4.10) possibly were parts of the Dharwar craton whereas, the rest of

the Precambrian terrains of Madagascar with Pan-African metamorphism, deformation and magmatism were parts of a broader Pan-African mobile belt in continuity with the East African Orogen.

3. Juxtaposition of Madagascar against East Africa (Yardimcilar and Reeves, 1998) is well constrained by geophysical evidence (see Chapter 7 for details). This study is in full agreement with their fit. Recent geochronological and structural studies in southern and central Madagascar (*e.g.* de Wit *et al.*, 2000; Collins *et al.*, 2000; Kröner *et al.*, 2000,) suggest most parts of Madagascar, except the Archean Antongil block in the northeastern and east-central parts (refer to Figure 4.10 in Chapter 4), were constituent parts of the East African Orogeny that was formed by collision between East and West Gondwana.

4. The position of Sri Lanka in reassembled Gondwana is poorly constrained by geophysics as only less than a third of the whole country is aeromagnetically covered. This coverage is restricted to the southwestern part. However, continuity of the long strike-length aeromagnetic anomalies in SW Sri Lanka into the Southern Granulite Terrain of India provides strong argument for their predrift juxtapositioning. Geological similarities – high-grade granulite facies metamorphism during Pan-African times – in the Southern Granulite Terrain of India, Sri Lanka and Meso-Neoproterozoic metamorphic belts (the Lützow-Holm Complex and the Rayner Complex of Enderby Land, East Antarctica – suggest that they were part of a single mobile belt during Pan-African times.

5. Lack of aeromagnetic data from eastern India and Enderby Land, East Antarctica is a hindrance in their direct geophysical correlation. The complex aeromagnetic anomaly zone at the boundary between the Archean Napier Complex and the Proterozoic Rayner Complex (Golynsky *et al.*, 1996), must have its counterpart in Sri Lanka/Southeast India if the tight reassembly models are true. The Napier Complex is sandwiched between the Proterozoic belts - Eastern Ghats Belt of India to the west and the Rayner Complex in to the east. So it is certain that the Archean Napier Complex had a separate character prior to the amalgamation of Gondwana and possibly it was never a part of the Dharwar Craton.

6. The nature of the crust below the thick sequence of Cenozoic sediments in southern Mozambique is still uncertain. Limited aeromagnetic coverage in the eastern and

southern parts suggests a very deep basement (up to 25 km). Moreover, the geophysical and geological similarities between the Lebombo monocline in southeastern Africa and the Explora Wedge off the coast of Dronning Maud Land in East Antarctica indicates that they were parts of a single volcanic province erupted syntectonically during rifting between southern Africa and Dronning Maud Land. Thus, it can be reasonably speculated that the crust below the sediments in southern Mozambique is oceanic or contains extended continental crust produced by east-west stretching for about 30 million years (~190 ma to ~160 Ma) before it failed to produce the rift between southern Africa and Dronning Maud land. That means that this part of Mozambique (except, perhaps, part of the Mozambique Rise) did not exist prior to the Gondwana breakup in Jurassic times. Thus, an overlap of about the width of the southern Mozambique plains (~250 km) can be allowed to constrain a tight reassembly between the Precambrian rocks of southern Africa and Dronning Maud Land.

7. Clearly, geophysics plays an important role in delineation of deep crustal structures, particularly in the areas of little or no outcrop. However, the geophysical surveys have not yet been utilised to their full potential. The utility of these methods is gradually gaining appreciation by majority of the geoscientific community. Combination of geophysical interpretations with the existing geological knowledge of a particular area can drastically improve the understanding of subsurface geology in a 3D perspective. Geophysics (especially airborne and satellite) plays an even greater role in continental reconstructions because continental scale structures and lithotectonic units can be delineated more continuously and accurately in a relatively short timespan. The best example of the utility of geophysical data is the satellite-derived gravity data for whole of the world's ocean, where the ocean floor topography is virtually 'laid bare'. Still huge gaps in the aeromagnetic coverage in many parts of the continents need to be filled. Thus, geophysical (aeromagnetic and gravity) coverage for the whole of the world's continental mass is urgently needed to do away with the great degree of ambiguity that prevails on the lateral and depth persistence of the continental features – 'lifelines' for any continental reassembly. Huge gaps in the aeromagnetic coverage of India, Sri Lanka, Madagascar and Antarctica (Maps 8.1 and 8.2) are evident due to non-availability (not flown) or non-accessibility of the data sources. Existence of such gaps in today's world is a scientific shame and need to be filled with utmost urgency

to help resolve problems that no other traditional geological methods are capable of. It is true, however, that geophysical surveys are expensive and beyond the economic capability of most countries. It necessitates co-operative exploration. It is hoped that this will be pursued in future in an effective and equitable way.

REFERENCES

Abdelaziz, A.M.S, 1996. A GIS data base of faulting and fracturing in eastern and southern Africa based on published geological maps and new aeromagnetic interpretation. MSc Thesis, Dept. of Earth Resource Survey, ITC, Delft, The Netherlands.

Agrawal, P.K., Pandey, O.P. and Negi, J.G., 1992. Madagascar: a continental fragment of the paleo-super Dharwar craton of India. Geology 20, 543-546.

Allsopp, H. L., Krammers, J. D., Jones, D. L. and Erlank, A. J., 1989. The age of the Umkondo Group, Eastern Zimbabwe and implications for paleomagnetic correlations. South African Journal of Geology 92, 11-19.

Andersen, L.S. and Unrug, R., 1984. Geodynamic evolution of the Bangweulu Block, Northern Zambia. precambrian research 25,187-212.

Armstrong, R.A., Compston, W., Retief, E.A., Williams, I.S. and Welke, H.J., 1990. Zircon ion microprobe studies bearing on the age and evolution of the Witwatersrand triad. Precambrian Research 53, 243-266.

Asfaha, W. and Erren, H., 1990, Cal91tb software to digitise the flight line and counter line intersections of aeromagnetic contour maps (developed in-house), ITC, Delft, The Netherlands.

A.S.G.A./UNESCO, 1968. International Tectonic map of Africa. (1: 5 000 000)

Atlaswin Pro, Cambridge Paleomap Services Ltd., Cambridge, UK.

Barritt, S.D., 1993. The African Magnetic Mapping project. Special Issue ITC Journal 1993-2, 119-199.

Bartlett, J. M., Harris, N. B. W., Hawkesworth, C. J. & Santosh, M., 1995. New isotope constraints on the crustal evolution of South India and Pan-African metamorphism. In Yoshida, M. and Santosh, M. (eds) India and Antarctica during the Precambrian, Mem. 34 Geol. Soc. Ind., 391-397.

Bartlett, J. M., Dougherty-Page, J. S., Harris, N. B. W., Hawkesworth, C. J. and Santosh, M. 1998. The application of single zircon evaporation and model Nd ages to the interpretation of polymetamorphic terrains: an example from the Proterozoic mobile belt of south India. Crontrib. Minreal Petrol. 131, 181-195.

Barton, J. M., Klemd, R., Allsop, H. L., Auret, S. H. and Copperthwaite, Y. E., 1987. The geology and geochronology of the Annandagstoppane granite, western Dronning Maud Land, Antarctica. Contributions to Mineralogy and Petrology 97, 488-496.

Barton, J.M., 1990. Geochronological and isotopic constraints. In Van Reenen, D.D. and Roering, C. (eds) The Limpopo Belt: a field workshop on granulites and deep crustal tectonics, 28-30.

Barton, J.M. and Van Reenen, D.D., 1992. When was the Limopo orogeny? Precambrian Research 55, 7-16.

Batterham, P.M., Bullock, S.J. and Hopgood, D. 1983. Tanzania: integrated interpretation of aeromagnetic and radiometric maps for mineral exploration. Trans. Instn Min. Metall. (Sect B: Appl Earth Sci) 92, 83-92.

Bauer, W., Jacobs, J., Raab, M., Siegesmund, S., Spaeth, G., Thomas, R.J. and Weber, K., 1998. New geological map of the Heimefrontfjella (Antarctica). Journal of African Earth Sciences, Vol 27 (1A): Special Abstracts Issue: Gondwana10: Event stratigraphy of Gondwana, 23-24.

Berhe, S. M., 1990. Ophiolites in Northeast and East Africa: implications for Proterozoic crustal growth. J. Geol Soc. London 147, 41-57.

Berhe, S. M., 1997. The Arabian-Nubian Shield. In de Wit, M.J. and Ashwal, L.D. (eds) Greenstone Belts. Oxford Monographs on Geology and Geophysics 35. Clarendon Press, Oxford.

Besairie, H., 1967. The Precambrian Madagascar. In Rankama, K. (ed) The Precambrian. Wiley, London.

References

Besse, J. and Courtillot, 1988. V. Paleogeographic maps of the continents bordering the Indian Ocean since the Early Jurassic. Journal of Geophysical Research 93(B10): 11791-11808.

Besse, J. and Ricou, L.E., 1998. Pangea of type B at the end of Permian: new paleomagnetic clues. Journal of African Earth Sciences, Vol 27 (1A): Special Abstracts Issue: Gondwana10: Event stratigraphy of Gondwana, p. 26.

Bhaskar Rao, Y. J., Sivaraman, T. V., G. V. C. Pantulu, Gopalan, K. and Naqvi, S. M. 1992. Rb-Sr ages of Late Archean metavolcanics and granites, Dharwar craton, South India and evidence for Early Proterozoic thermotectonic event(s). Precambrian Research, **62**, 145-170.

Bhattacharyya, B.K., 1966. Continuous spectrum of the total magnetic field anomaly due to a rectangular prismatic body. Geophysics 31, 97-121.

Black, L. P., Harley, S. L., Sun, S. S. & McCulloch, M. T., 1987. The Rayner Complex of East Antarctica: complex isotopic systematics within a Proterozoic mobile belt. Journal of Metamorphic Geology 5, 1-26.

Black, L.P. and McCulloch, M.T., 1987. Evidence for isotopic equilibration of Sm-Nd whole-rock systems in early Archean crust of Enderby Land, Antarctica. Earth and Planetary Science Letters 82, 15-24.

Blenkinsop, T., Martin, A., Jelsma, H.A. and Vinyu, M.L., 1997. The Zimbabwe craton. In de Wit, M.J and Ashwal, L.D. (eds) Greenstone Belts. Oxford Monographs on Geology and Geophysics 35. Clarendon Press, Oxford. 567-580.

Board, W.S. and Frimmel, H.E., 2000. Tectonothermal evolution of the Eastern H.U. Sverdrupfjella, Western Dronning Maud Land, Antarctica (abstr.), Geocongress 2000, Stellenbosch, Geological society of South Africa, p 4.

Bond, C.G., Nickeson, P.A., and Kominz, M.A., 1984. Breakup of a supercontinent between 625 Ma and 555 Ma: new evidence and implications for continental histories. Earth and planetary Sciences Letters 70:325-345.

Bonavia, F.F. and Chorowicz, J., 1992. Northward expulsion of the Pan-African of northeast Africa guided by a reentrant zone of the Tanzania craton. Geology 20, 1023-1026.

Borg, S.G.and DePaolo, D.J., 1994. Laurentia, Australia and Antarctica as a Late Proterozoic supercontinent: constraints from isotopic mapping. Geology 22, 307-310.

Borg, G. and Shackleton, R.M., 1997. The Tanzania and NE-Zaire Cratons. In de Wit, M.J and Ashwal, L.D. (eds) Greenstone Belts. Oxford Monographs on Geology and Geophysics 35. Clarendon Press, Oxford. 567-580.

Brandl, G. and de Wit, M.J., 1997. The Kaapvaal Craton. Chapter 5.8 in de Wit, M.J and Ashwal, L.D. (eds) Greenstone Belts. Oxford Monographs on Geology and Geophysics 35. Clarendon Press, Oxford. 581-607.

Brandon, A. D. & Meen, J. K., 1995. Nd isotopic evidence for the position of southernmost Indian terrains with East Gondwana. Precamb. Res. 70, 269-280.

Büchel, G., 1994. Gravity, magnetic and structural patterns at the deep crustal plate boundary zone between West and East Gondwana. Precamb. Res. 66, 77-94.

Bullard, E., Everette, J.E., and Smith, A.G., 1965. The fit of the continents around Atlantic. Philosophical Transactions Royal Society London 258(A): 41-51.

Burton, K. W. and O'Nions, R. K. 1990. The timescale and mechanism of granulite formation at Kurunegala, Sri Lanka. Contr. Minl. Petrol. 106, 66-89.

Cahen, L., Snelling, N. J., Dehal, J. and Vail, J. R., 1984. The geochronology and Evolution of Africa. Clarendon Press, Oxford, 512 pp.

Carlson, R.W., Grove, T.L., Bowring, S.A., Schmitz, M.D., Bell, R.D., Gurney, J.J., Richardson, S.H., and Pearson, D.G., 2000. Continental growth, preservation, and modification in Southern Africa. GSA Today 10(2), 1-5.

CGMW/UNESCO, 1985-90. International Geological map of Africa (1: 5 000 000)

Chandrasekhar, P., 1997. Digital aeromagnetic compilation over parts of southern India. Short Course on Geophysical Mapping (EXG5) Project Report, Exploration Geophysics Division, ITC, Delft.

Chavez-Gomez, S., 2000. A database of dykes in eastern and southern Africa supported by aeromagnetic survey interpretation. MSc thesis. International Institute for Aerospace Survey and Earth Sciences (ITC), The Netherlands.

Chetty, T.R.K., 1996. Proterozoic shear zones in Southern Granulite Terrain, India In M. Santosh and M.Yoshida (Eds) The Archean and Proterozoic terrains in southern India within East Gondwana. Gondwana Research Group Memoir 3, 77-89.

Chorowicz, J., Fournier, J.L. and Vidal, G., 1987. A model for rift development in Eastern Africa. Geological Journal 22, 495-513.

Choudhary, A. K, Harris, N. B. W., Van Calsteren, P. and Hakesworth, C. J., 1992. Pan-African charnockite formation in Kerala, South India. Geol. Mag., 129. 257-264.

Clark, D.A. and Emerson, D. W., 1991. Notes on rock magnetisation characteristics in applied geophysical studies. Exploration Geophysics, 22, 547-555.

Clifford, A.C., 1986. African oil - past, present and future. In M.T.Halbouty (ed.) Future Petroleum provinces of the world. AAPG. Mem. 40. 339-373.

Collins, A.S., Windley, B.F., Kroner, A., Razakamanana, T., Hegner, E., and Nemchin, A.A., 2000. The tectonic architecture of central and northern Madagascar: a structural and geochronological framework. Precambrian Res. (in press).

Compston, W. and Kröner, A., 1988. Multiple zircon growth within early Archean tonalitic gneisses from the Ancient Gneissic Complex, Swaziland. Earth and Planetary Sciences Letters 87, 13-28.

Cooray, P. G., 1994. Precambrian of Sri Lanka: a historical review. Precamb. Res. 66, 3-20

Cornell, D.H., Kröner A., Humphreys, H. and Griffin, G., 1990. Age of origin of the polymetamorphosed Copperton Formation, Namaqua-Natal Province, determined by single grain zircon Pb-Pb dating. South African Journal of Geology 93, 709-716.

Corner, B., Maccelari, J.C. and Niccol, S., 1991. Major magnetic anomalies in western Dronning Maud Land: their possible origin and correlates in southern Africa. In Absrtacts: Sixth International Symposium on Antarctic Earth Sciences, Tokyo. National Institute of Polar Research 113.

Corner, B., 1993. The nature of the deep crust of the Kaapvaal craton. Congr. S. Afr. Geophys. Ass., 34-37.

Corner, B., 1994. Geological evolution of western Dronning Maud Land within a Gondwana frame work: Geophysical subprogramme. Final project report to SACA, Pretoria.

Corner, B., 1995. The Namaqua-Natal-Maudheim Belt: geophysical signatures within Gondwana. Geological Society South Africa Centennial Congress (Extended Abstracts 1, 210-213.

Cox, K. G., 1992. Karoo igneous activity and the early stages of the break-up of Gondwanaland. In Storey, B. C., Alabaster, T. & Pankhurst, R. J. (eds) Magmatism and the causes of continental break-up. Geological Society Special Publication No. 8, 137-148.

Crawford, A.R. and Compston, 1969. Reconnaissance Rb-Sr dating of the Precambrian rocks of southern peninsular India. J geol. Soc India 10, 117- 166.

Daly, M.C., Chakraborty, S.K., Kasolo, P., Musiwa, m., Mumba, P., Naidu, B., Namateba, C., Ngambi, O. and Coward, M.P., 1984. The Lufilian arc and Irumide belt of Zambia: results of a geotraverse across their intersection. Journal of African Earth Sciences 2 (4), 311-318.

Dalziel, I.W.D., 1991. Pacific margins of Laurantia and East Antarctica-Australia as a conjugate rift pair: Evidence and implications for an Eocambrian Supercontinent. Geology 19, 598-601.

Dalziel, I.W.D., 1992. On the organisation of American plates in the Neoproterozoic and the breakout of Laurentia. GSA Today .2(11), 237-141.

Dalziel, I.W.D., 1997. Neoproterozoic-Paleozoic geography and tectonics: review, hypothesis, envirionmental speculation. Geol. Sci. Am. Bull. 109, 16-42.

De Beer, J.H. and Meyer, R., 1984. Geophysical characteristics of the Namaqua-Natal belt and its boundaries, South Africa. Jour Geodyn. 1, 473-494.

Debegla, N. and Corpel, J., 1997. Automatic 3-D interpretation of potential field data using analytic signal derivatives. Geophysics 62(1): 87-96.

References

Deters-Umlauf, P., Srikantappa, C. and Köhler, H., 1997. Pan-African ages in the Moyar-Bhavani shear zone (South India): First geochronological results. In R.Cox and L.D.Ashwal (eds), Proc.of the UNESCO-IUGS-IGCP-348/368 Int. Field Workshop on Proterozoic geology of Madagascar, Antananarivo, Madagascar, 18-19.

De Waele, B., Tembo, F., and Key, R., 1999. A review of geochronological data on the Irumide Orogeny, Zambia. in Abstract Volume IGCP - 418/419 Conference 1999, Kitwe, Zambia, Geological Society of Zambia. 9-10.

De Wit, M., Jeffery, M. Bergh, H. and Nicolaysen, L., 1988. Geological map of sectors of Gondwana. Am. Ass. Petr. Geol. Tulsa, Oklahoma and University of Witwatersrand.

De Wit, M.J., Roering, C., Hart, R.J., Armstrong, R.A., de Ronde, C.E.J., Green, R.W.E., Tredoux, M., Peberdy, E. and Hart, R.A., 1992. Formation of an Archean continent. Nature 357, 553-562.

De Wit, M.J. and Hart, R.A., 1993.Earth's earliest continental lithosphere, hydrothermal flux and crustal recycling. Lithos 30, 309-335.

De Wit, M.J., Vitali, E. and Ashwal, L., 1995. Gondwana reconstruction of the East Africa-Madagascar-India-Sri Lanka-Antarctica fragments revisited. Geokongres (abstract).

De Wit, M.J., Ghosh, J.G., Bowrin, S. and Ashwal, L., 1998. Late Neoproterozoic shear zones in Madagascar and India: "Gondwana lifelines". Journal of African Earth Sciences 27(1A), p. 58.

De Wit, M.J., Bowring, S.A., Ashwal, L.D., Morel, V.P.I., Randrianasolo, L.G. and Rambeloson, R.A., 2000. Age and tectonic evolution of Neoproterozoic ductile shear zones in southwestern Madagascar, with implications for Gondwana studies. Tectonics (in press).

Divakar Rao, V., Rama Rao, P., Subba Rao, M.V., Govil, P.K., Rao, R.U.M., Walsh, J.N., Thompson, M. and Reddy, G.R., 1990. Trace and rare earth element geochemistry and origin of the Closepet Granite, Dharwar Craton, India. In S.M. Naqvi (ed), Precambrian Continental Crust and its Economic Resources. Developments in Precambrian Geology 8. Elsevier, Amsterdam, 203-222.

Doucouré, M.C. and de Wit, M.J., 1996. Effective elastic thickness of the continental lithosphere in South Africa. Jour Geophy. Res. 101(B5), 11291-11303.

Doucouré, C.M., de Wit, M.J. and Reeves, C.V., 1998. Towards a gravity map of Gondwana. Journal of African Earth Sciences 27(1A), p. 62.

Doucouré, C.M., de Wit, M.J. and Reeves, C.V., 2000 (in press). Towards a gravity map of Gondwana.

Drysdall, A.R., Johnson, R.L., Moore, T.A. and Thieme, J.G., 1972. Ouline of the geology of Zambia. Geologie Mijnbouw 51, 265-276.

Drury, S.A. and Holt, R.W., 1980. The tectonic framework of south Indian craton: a reconnaissance involving Landsat imagery. Tectonophysics 65. T1-T15.

Drury, S. A., Harris, N.B.W., Holt, R.W., Reeves-Smith, G.J. and Wightman, R.T., 1984. Precambrian tectonics and crustal evolution in south India. Jour Geol. 9, 277-287.

Duncan, A. R., Armstrong, R. A., Erlank, A. J., Marsh, J. S. and Watkins, R. T., 1990. MORB related dolerites associated with the final phase of Karoo flood basalt in southern Africa. In Parker, Rickwood and Tucker (eds). Mafic dykes and emplacement mechanism. Balkema, Rotterdam.

Duncan, R.A., Hooper, P.R., Rehacek, KJ., Marsh, J.S. and Duncan, A.R., 1997. The timing and duration of Karoo igneous event, southern Gondwana. Journal of Geophysical Research 102. 18, 127-138.

Dutta, K.K., Choudhary, S.V., Rajurkar, S.T. and Deshmukh, S.S. (eds), 1990. Scientific papers presented at the Workshop on Precambrian of Central India. Geological Survey of India Special Publication 28.

Du Toit, A. L., 1937.Our wandering continents: Oliver and Boyd, Edinburg, 366 pp.

Eldridge, J., Walsh, D. and Scotese, C.R. Commercial software 'Plate Tracker' ISBN # 0-9700020-1-7. (http://www.scotese.com/software.htm).

References

Elliot, D.H. and Fleming, T.H., 2000.Weddell triple junction: The principal focus of Ferrar and Karoo magmatism during initial breakup of Gondwana. Geology 28,6, 539-542.

Encarnación, J., Fleming, T.H., Elliot, D.H., and Eales, H.V., 1996. Synchronous em-placement of Ferrar and Karoo dolerites and the early breakup of Gondwana: Geology, v. 24, p. 535–538.

Erren, H., 1997, AAIME: Aeromagnetics of Arabia, India and the Middle East, Abstract submitted to the IAGA Session, August 1997.

Fairhead, J.D., Bennett, K.J., Gordon, R.H. and Huang, D., 1994. Euler: beyond the 'Black Box'.

Fermor, L.L., 1936. An attempt at correlation of the ancient schistose rocks of Peninsular India. Geol. Surv. India Mem. 70. 1-324.

Ferreira, E. D., 1986. The sedimentology and stratigraphy of the Ahlmannryggen Group, Antarctica. Geol. Soc. S. Afr. Geocongress '86. Abstracts Vol., 719-722.

Fuller, A.O., 1999. Alex Logan du Toit. Journal of African Earth Sciences 28 (1), 3-9.

Geological Survey Department, Sri Lanka, 1982&1983. Geological and Structural maps of Sri Lanka (1: 506 880).

Geosoft GridKnit™, Grid Stitching tool for Oasis montaj™: Tutorial and User's Manual, (http:\\www.geosoft.com).

Geological map of Mozambique, 1987. Scale 1: 1 000 000. National Geological Institute

Ghosh, J.G., Zartman, R.E. and de Wit, M.J., 1998. Re-evaluation of tectonic framework of southernmost India: new U-Pb geochronological and structural data and their implication for Gondwana reconstruction. Journal of African Earth Sciences 27 (1A), p. 86.

Ghosh, J.G., 1999. U/Pb geochronology and structural geology across major shear zones of southern granulite terrain of India and $^{13}C_{org}$ stratigraphy of the Gondwana coal basins of India: their implications for Gondwana studies. PhD thesis, Dept. of Geological Sciences, University of Cape Town, South Africa.

Ghosh, J. G., de Wit, M.J., Zartman, R.E., Bowring, S. and Kinny, P., (in press). Where is the southern boundary of the Dharwar craton of India.

Goldberg, A.S., 1998. The Botswana dyke swarm and its relationship to the break-up of Gondwana. Journal of African Earth Sciences. Vol 27-1A, p.89.

Golynsky, A.V., Masolov, V.N., Nogi, Y., Shibuya, K., Tarlowski, C. and Wellman, P. 1996. Magnetic anomalies of Precambrian terranes of the East Antarctica shield coastal region (20°E-50°E). Proc. of the NIPR Symposium on Antarctic Geosciences 9, 24-39.

Grant, F.S., 1973. The magnetic susceptibility mapping method for interpreting aeromagnetic surveys. Presented at the 43rd Annual International meeting of the Society of Exploration Geophysicists, Mexico City, November 1973.

Grantham, G. H., Groenewald, P. B. and Hunter, D. R., 1988. Geology of the northern H.U.Sverdrupfjella, western Dronning Maud Land and implications for Gondwana reconstruction. S. Afr. J. Antarc. Res. 18, 2-10.

Grantham, G. H., 1995. The tectonothermal evolution of Kirwanveggen- H.U. Sverdrufjella areas, Dronning Maud Land, Antarctica. Precamb. Res. 75, 209-229.

Grobler, D.F. and Walraven, F., 1992. Geochronology of the Gaborone Granite Complex extensions in the area north of Mafeking, South Africa. Extended Abstracts, Geocongress '92. Geological Society of South Africa, Bloemfontein

Groenewald, P. B. & Hunter, D. R., 1991. Granulites of northern Sverdrupfjella, western Dronning Maud Land: metamorphic history from garnet pyroxene assemblages, coronas and rehydration reactions. In Thomson, M. R. A. Crame, J. A. & Thomson, J. W. (eds.) Geological evolution of Antarctica: 61-66. Cambridge: Cambridge University Press.

Groenewald, P.B., 1993. Correlation of cratonic orogenic provinces in southern Africa and Dronning Maud Land, Antarctica. In Findley, Unrug, Banks & Veevers (eds). Gondwana Eight. Balkema, Rotterdam, 111-122.

Groenewald, P.B., Moyes, A.B., Grantham, G.H. and Krynauw, J.R., 1995. East Antarctica crustal evolution: Geological constraints and modelling in western Dronning Maud Land. Precamb. Res. 75, 231-250.

References

Grunow, A., Hanson,R. and Wilson, T., 1996. Were aspects of Pan-African deformation linked to Iapetus opening? Geology 24, 1063-1066.

Grunow, A., 1999. Gondwana events and paleogeography: a paleomagnetic review. Journal of African Earthsciences 28 (1). 53-59.

GSI (Geological Survey of India), 1993. Geological Map of India (1: 5 000 000). Geological Survey of India, Calcutta, India.

GSI (Geological Survey of India), 1994. Project Vasundhara: geoscientific analysis, database creation and development of GIS for parts of South Indian peninsular shield. Special Publication, National Workshop.

GSI (Geological Survey of India). 1995a. Geological and Mineral map of Tamilnadu and Pondichery (scale 1:0.5 million).

GSI (Geological Survey of India). 1995b. Geological and Mineral map of Kerala (scale 1:500 000).

GSI (Geological Survey of India), 1995. Catalogue of Aero geophysical maps of India

GSI (Geological Survey of India), 1998. Geological Map of India (1:2 000 000). 7th Edition

Guerrot, C., Cocherie, A. & Ohnenstetter, M., 1993. Origin and evolution of the West Andriamena Pan-African mafic-ultramafic complexes in Madagascar as shown by U-Pb, Nd isotopes and trace element constraints. Terra Nova (Abstr.) 5, 387.

Gupta, A., 1983. A preliminary qualitative interpretation of the total intensity aeromagnetic data for blocks I, II and III, Narmada-Son Lineament. Unpub. Report. Geological Survey of India.

Hanson, R.E., Wilson, T.J. and Wardlaw, M.S., 1988. Deformed batholiths in the Pan-African Zambezi belt, Zambia: age and implications for regional Proterozoic tectonics. Geology 16, 1134-1137.

Hansen, E. C., Hickman, N. H., Grant, N. K. and Newton, R. C., 1985. Pan-African age of "Peninsular Gneiss" near Madurai South India (abstract). EOS (Trans. American Geophys. Union). 66, 419-420.

Hari Narain, and Subrahmanyam, C., 1986. Precambrian tectonics of the south Indian shield inferred from the geophysical data. Journal of Geology. Vol.94, 187-198.

Harley, S. L. and Black, L. P., 1997. A revised Archean chronology for the Napier Complex, Enderby Land, from SHRIMP ion-microprobe studies. Antarctica Science. 9. (1), 74-91.

Harris, N. B. W., Bartlett, J. M. and Santosh, M., 1996. Neodymium isotopic constraints on the tectonic evolution of East Gondwana. Journal of Southeast Asian earth Sciences, Vol.14, 119-125.

Harris, N.B.W., Santosh, M. and Talor, P.N., 1994. Crustal evolution in South India: constraints from Nd isotopes. Jour. Geology 102, 139-150.

Harris, C., Watters, B.R. and Groenewald, P.B., 1991. Geochemistry of the Mesozoic regional basic dykes of western Dronning Maud Land of Antarctica. Contrib. Mineral. Petrol. 107, 100-111.

Hartnady, C., Joubert, P., and Stowe, C., 1985. Proterozoic crustal evolution in Southwestern Africa. Episodes 8(4), 236-244.

Harvey, J., 1999. The use of seismic receiver functions in determining the thickness, structure and azimuthal variations of the crust in the southwestern Cape. BSc (Honours) dissertation, Deptt of Geological Sciences, University of Cape Town, South Africa.

Hatherton, T., Pattiaratchi, D.B. and Ranasinghe, V.V.C., 1975. Gravity map of Sri Lanka (1: 1000000). Professional Paper No.3. Geological Survey Department, Sri Lanka.

Henkel, H., 1991, Petrophysical properties (density and magnetization) of rocks from the northern part of the Baltic Shield: Tectonophysics 192, 1-19.

Henkel, O., 1994. Early Permian to Middle Jurassic rifting and sedimentation in East Africa and Madagascar. Geologische Rundschau 83, 703-710.

Hiroi, Y., Shirashi, K. and Motoyoshi, Y., 1991. Late Proterozoic paired metamorphic complexes in East Antarctica, with special reference to the tectonic significance of ultramafic rocks. In Thomson, M.R.A., Crame, J.A. and Thomson, J.W. (eds). Geological Evolution of Antarctica: Cambridge University Press, 83-87.

References

Hodgkinson,G.K., 1990. Paleomagnetic studies in the western Dronning Maud Land, Antarctica. MSc dissertation, Department of Geophysics, University of Witwatersrand, South Africa.

Hoffman, P.F., 1991. Did the breakout of Laurentia turn Gondwanaland inside out? Science 252, 1409-1412.

Hoffman, P.F., 1998. The Rodinia hypothesis and the birth of Gondwana. Journal of African Earth Sciences 27 (1A), 111-112.

Hoffman Paul F., 1999. The break-up of Rodinia, birth of Gondwana, true polar wander and the snowball Earth, Journal of African Earth Sciences (28) 1, 17-33.

Hölzl, S., Köhler, H., Kröner, A., Jaeckel, P. & Liew, T. C., 1991. Geochronology of Sri Lankan basement. In A. Kröner (ed.) The crystalline crust of Sri Lanka, part I. Summary of Research of the German-Sri Lankan Consortium. Geological Survey Department of Sri Lanka. Professional Paper 5, 237-257.

Hölzl, S., Hoffmann, A.W., Todt, W. and Köhler, H., 1994. U-Pb geochronology of the Sri Lankan basement. Precambrian Research 66, 123-149.

Hunter, D.R., 1991.Crusta processes during Archean evolution of the southeastern Kaapvaal Province. Journal of African Earth Sciences 13, 13-26.

Hurley, P.M., de Almeida, F.F.M., Melcher, G.C., Cordani, U.G., Rand, J.R., Kawashita, K., Vandoros, P., Pinson, Jr., W.H., Fairbairn, H.W., 1967. Test of continental drift by comparison of radiometric ages. Science 157 (3788), 495-500.

Jacobs, J., Fanning, C. M., Henjes-Kunst, F., Olesch, M. and Paech, H., 1998. Continuation of Mozambique belt into East Antarctica: Grenville- age metamorphism and polyphase Pan-African high-grade events in Central Dronning Maud Land. Journal of geology 106, 385-406.

Jamal, D.L., Zartman, R.E. and de Wit M.J., 1999. U-Pb single zircon dates from the Lurio belt, northern Mozambique: Kibaran and Pan-African orogenic events highlighted. Journal of African Earth Sciences, 28 (4A), p. 32.

Jayanand, M. and Peucat, J.J., 1995. Archean crust formation in southern India: geochronologic and isotopic constraints. In M.Yoshida, M.Santosh and A.T.Rao (eds) India as a fragment of East Gondwana. Gondwana Research Group Mem. 2, Field Science Pub., Osaka, Japan, 15-21.

Jayanand, M., Janardan, A. S., Sivasubramanian, P. and Peucat, J. J., 1995. Geochronologic and isotopic constrains on granulite formation in the Kodaikkanal area, southern India. In India and Antarctica during the Precambrian, Mem.34 (edited by Yoshida, M. & Santosh, M.), 373-390. Geological Society of India, Bangalore.

Johnson, A.C., Aleshkova, N.D, Barker, P.F., Golynsky, A.V., Masolov, V.N and Smith, A.M., 1992. A preliminary aeromagnetic anomaly compilation map for the Weddell Sea Province of Antarctica. In Y.Yoshida et al. (eds): Recent Progress in Antarctic Earth Science. Terra Scientific Publishing Company (TERRAPUB), Tokyo, 545-553.

Jokat,W., Hubscher,C., Meyer, U., Oszko,L., Schone, T., Versteeg, W. and Miller, H., 1996. The continental margin off East Antarctica between 10°W and 30°W. In Weddel Sea tectonics and Gondwana break-up, Storey, B.C., King, E.C, & Livermore, R.A. (eds) Geological Society special publication No.108, 129-141.

Joubert, P., 1986. Namaqualand – a model of Proterozoic accretion. Trans. Geol. Soc. South Africa 89, 79-96.

Kagami, H., Owada, M., Osanai, Y. & Hiroi, Y., 1990. Preliminary geochronological study of Sri Lankan rocks. In Y. Hiroi and Y. Motoyoshi (eds.) Interim Report of Japan-Sri Lanka Joint Research, 55-70.

Kalia, K.L., Roy Choudhury, K., Reddy, P.R., Krishna, V.G., Hari Narain, Subbotin, S.I, Sollogub, V.B., Chekunov, A.V., Kharetchko, G.E., Lazarenko, M.A., 1979. Crustal structure along Kavali-Udipi profile in the Indian peninsular shield from deep seismic sounding. Geological Soc. India Jour. Vol.20, 307-333.

References

Kalia, K.L. and Bhatia, S.C., 1981. Gravity study along the Kavali-Udipi Deep Seismic Sounding Profile in the Indian Peninsular Shield: some inferences about the origin of anorthosites and the Eastern Ghat Orogeny, Tectonophysics 79, 129-143.

Kalia, K.L., Tewari, H.C., 1985. Structural trends in the Cuddapah basin from Deep Seismic Soundings (DSS) and their tectonic implications. Tectonophysics 115, 69-86.

Kalia, K.L., 1986. Tectonic framework of Narmada-Son Lineament – a continental rift system in central India from deep seismic soundings. In Reflection Seismology – a Global Perspective. American Geophysical Union, Geodynamics Series 13, 133-150.

Kalia, K.L., Murthy, P.R.K., Mall, D.M. and Dixit, M.M., 1987. Deep seismic soundings along Hirapur-Mandala profile., Central India. Geophysics J. R. Astron. Soc., 89. 399-404.

Kamenev, E.N., 1993. Structure and evolution of the Antarctica shield in Precambrian. In Findlay et al. (Eds) Gondwana Eight: Assembly, Evolution and Dispersal. Balkema, Rotterdam. 141-151.

Kelley, S. P.; Bartlett, J. M. and Harris, B. W. 1997. Pre-metamorphic Ar-Ar ages from biotite inclusions in garnet. Geochemia et Coscochemica Accta 61 (18), 3873-3878.

Kenedy, W.Q., 1964. The structural differentiation of Africa in the Pan-African (500 m.y.). Tectonic Episode. Eighth Ann. Rep. Inst. African Geology, Session 1962-1963, 8, 48-48. Leeds University.

Krabbendam, M. and Barr, T. D., 2000 (in press). Proterozoic orogens and the breakup of Gondwana: why did some orogens not rift?

Kriegsman, L.M., 1993. Geodynamic evolution of the Pan-African lower crust in Sri Lanka: structural and petrological investigation into a high-grade gneiss terrane. PhD thesis. Utrecht University, the Netherlands.

Kriegsman, L.M., 1995, The Pan-African event in East Antarctica:A view from Sri Lanka and the Mozambique belt: Precamb. Res., 75, 263-277.

Kristoffersen, Y. and Hinz, K., 1991. Evolution of the Gondwana plate boundary in the Weddell Sea area. In M.R.A. Thomson, J.A.Crame and J.W. Thomson (eds) Geological Evolution of Antarctica. Cambridge University Press, 225-230.

Krogstad, E.J., Balakrishnan, S., Mukhopadhyay, D.K., Rajamani, V. and Hanson, G.N., 1989. Plate tectonics 2.5 billion years ago: evidence at Kolar, South India. Science 243, 1337-1340.

Kröner, A., Williams, J S., Compton, W., Baur, N., Vitanage, P. W. & Perera, L. R. K., 1987. Zircon ion microprobe dating of high grade rocks in Sri Lanka. Journal of Geology 95, 775-791.

Kröner, A., Cooray, P.G. and Vitanage, P.W., 1991. Lithotectonic subdivision of the Precambrian basement in Sri Lanka. In Kröner, A. (ed) The crystalline crust of Sri Lanka, Part I: Summary of research of German-Sri Lanka consortium. Geological Survey Department of Sri Lanka, 5-21.

Kröner, A., Kehelpannala, K.V.W. and Kriegsman, L.M., 1994, Origin of compositional layering and mechanism of crustal thickening in the high-grade gneiss terrain of Sri Lanka: Precam. Res. 66, 21-34.

Kröner A., Sacchi, R., Jaeckel, P. and Costa, M., 1997. Kibaran magmatism and Pan-African granulite metamorphism in northern Mozambique: single zircon ages and regional implications. Journal of African earth Sciences 25, 467-484.

Kröner, A., Jaeckel, P., Brandl G., Nemchin A.A., Pidgeon R.T., 1999. Single zircon ages for granitoid gneisses in the Central Zone of the Limpopo Belt, Southern Africa and geodynamic significance, Precambrian Research (93) 4, 299-337.

Kröner, A., Jackle, P., Windley, B.F., Brewer, T. and Razakamanna, T., 1999. New zircon ages and regional significance for the evolution of the Pan-African orogen in Madagascar. Journal of the Geological Society of London 156, 1125-1135.

Kröner, A., Hegner, E., Collins, A.S., Windley, B.F., Brewer, T., Razakamanana, T., and Pidgeon, R.T. Age and mgmatic history of the Antananarivo block, central Madagascar, as devised from zircon geochronology and Nd isotopic systematics. in press , 2000.

References

Kreuser, T., Wopfner, h., Kaaya, C.Z., Markwort, S., Semkiwa, P.M. and Aslanidis, P., 1990. Depositional evolution of Permo-Triassic basins in Tanzania with reference to their economic potential. Journal of African Earth Sciences 10, ½, 151-167.

Lambiase, J.J., 1989. The framework of African rifting during the Phanerozoic. Journal of African Earth Sciences 8(2/3/4): 183-190.

Lawver,L. A. and Scotese, C.R., 1987. A revised reconstruction of Gondwana. In McKenzie, G.D. (ed.) Gondwana Six: Structure, Tectonics and Geophysics. Geophysical Monograph 40, 17-23.

Li, Z.X. and Powell, C.M., 1993. Late Proterozoic to early Paleozoic paleomagnetism and the formation of Gondwanaland. In R.H. Findley et al. (eds) Gondwana Eight: Evolution and Dispersal. Balkema, Rotterdam, 9-21.

Maboko M.A.H., 2000. Nd and Sr isotopic investigation of the Archean--Proterozoic boundary in northeastern Tanzania: constraints on the nature of Neoproterozoic tectonism in the Mozambique Belt, Precambrian Research (102)1-2, 87-98.

Maccelari, J.C.D., 1991. A reconstruction of Gondwana through the use of magnetic data. BSc Honours dissertation, Department of Geophysics, University of Witwatersrand, South Africa.

Maher, M.J. and Pitts, B.E. (1989). Interpretation of potential field profile over the Cape Fold Belt. South African Geophysical Association, First Technical Meeting. Extended Abstracts, 135-140.

MapInfo Professional, MapInfo Corporation, New York, USA. WWW: http://www.MapInfo.com.

McElhinny, M.W., 1970. Formation of the Indian Ocean. Nature 228(December 5): 977-979.

McKenzie, D. and Sclator, J.G., 1971. Evolution of Indian Ocean since Late Cretaceous. Geophys. J. R. Astro. Soc 25:437-528.

McLeod, I.N., Jones, K., and Dai, T.F., 1993. 3-D Analytic Signal in the interpretation of total magnetic field data at low magnetic latitudes. Exploration Geophysics 24(3/4), 679-687.

Meen, J.K., Rogers, J.J.W. and Fullagar, P.D., 1992. Pb isotopic compositions of the Western Dharwar craton, southern India: evidence for distinct middle Archean terranes in a Late Archean craton. Geochemica et Cosmochimica Acta 56, 2445-2470.

Meert, J.G. and van der Voo, R., 1997. The assembly of Gondwana 800-550 Ma. Journal of Geodynamics, 23. 223-235.

Mezger, K. and Cosca, M.A., 1999. The thermal history of the Eastern Ghats Belt (India) as revealed by U-Pb and 40Ar/39Ar dating of metamorphic and magmatic minerals: implications for the SWEAT correlation. Precambrian Research, 94, 251-271.

Miller, H., De Batist, M., Jokat, W., Kaul, N., Steinmetz, S., Uenzelmann-Nwben, G. and Versteeg, W., 1990. Revised interpretation of tectonic features in the Southern Weddell Sea, Antarctica from new seismic dada. Polarforschung, 60, 33-38.

Milligan, P.R., Morse, M.P., and Rajagopalan, S., 1992. Pixel map preparation using the HSV colour model. Exploration Geophysics, 23, 219-224.

Milligan, P.R. and Gunn, P.J., 1997. Enhancement and presentation of airborne geophysical data. AGSO Journal of Australian Geology and Geophysics 17(2): 63-75.

Milsenda, C. C., Liew, T. C., Hoffman, A. W. and Kröner, A., 1988. Isotopic mapping of age provinces in Precambrian high-grade terrains: Sri Lanka. J. Geol. 96, 608-615.

Milsenda, C. C., Liew, T. C., Hofmann, A. W. and Köhler, H., 1994. Nd isotopic mapping of the Sri Lanka basement: update and additional constraints from Sr isotopes. Precamb. Res. 66, 95-110.

Minor, D., and Mukasa, S., 1997, Zircon U-Pb and hornblende 40 Ar-39 Ar ages for the Dufek layered mafic intrusion, Antarctica: Implications for the age of the Ferrar large igneous province: Geochimica et Cosmochimica Acta, v. 61, p. 2497–2504.

Minty, B.R.S., 1991. Simple microlevelling for Aeromagnetic data. Exploration Geophysics, 22, 591-592.

References

Mishra, D.C., 1977. Possible extensions of the Narmada-Son lineament towards Murrray Ridge (Arabian Sea) and the eastern syntaxial bend of the Himalayas. Earth and Planetary Science Letters 36, 301-308.

Mishra, D.C., 1984. Magnetic anomalies- India and Antarctica. Earth and Planetary Sciences Letters 71, 173-180.

Mishra, D.C., 1990. Precambrian rifts and associated tectonics of peninsular India. In S.M. Naqvi (ed) Precambrian continental crust and economic resources- Developments in Precambrian Geology.

Möller, A., 1994. Crustal evolution of the Mozambique belt in Tanzania: evidence from Sm-Nd whole rock systematics and Pb isotopes of leached feldspars. Proceedings of the International Geological Field Conference, Mozambique Belt, p.19. Nairobi.

Moorbath, S. and Taylor, P.N., 1988. Early Precambrian crustal growth in eastern India: the ages of the Singhbhum Granite and included remnants of older gneisses. Geol. Soc. India 31, 82-84.

Moore, J.M., 1989. A comparative study of metamorphosed supracrustal rocks from the western Namaqualand Metamorphic Complex. Bull. Precambrian Research Unit 37., University of Cape Town, 370 pp.

Moores, E.M., 1991. Southwest-US- East Antarctica (SWEAT) connection: a hypothesis. Geology 19, 425-428.

Morgan, W.J., 1981. Hotspot traces and the opening of the Atlantic and the Indian Oceans in Emiliani, C. (ed.) The Sea Vol. 7, 443-487, Wiley Interscience, New York.

Moyes, A. B. & Barton, J. M.Jr., 1990. A review of isotopic data from western Dronning Maud Land, Antarctica. Zeitblatt Geologie und Palaontologie 1, 19-31.

Moyes, A. B and Haris, P.D., 1996. Geological evolution of western Dronning Maud land within a Gondwana framework – radiogenic Isotope Geology Project. Final Project Report submitted to SACAR, 38 p.

Mubu, S.M. 1995. Aeromagnetic mapping and interpretation of mafic dyke swarms in southern Africa. M.Sc. thesis 63p. International Institute for Aerospace Survey and Earth Sciences (ITC), Delft, The Netherlands.

Mukhopadhyay, D., 1986. Structural pattern in the Dharwar craton. Journal of Geology 94, 167-186.

Nagaraja Rao, B.K., Rajurkar, S.T., Ramalingaswamy, G. and Ravindra Babu, B., 1987. Stratigraphy, structure and evolution of the Cuddapah basin. In Purana Basins of Peninsular India. Geological Society of India Memoir 6, 33-86.

Naha, K. and Srinivasan, R., 1996. Nature of the Moyar and Bhavani Shear Zones, with a note on its implication on the tectonics of the southern Indian Precambrian shield. Earth and Planetary Sciences 105:173-189.

Nance, D.R., Worsley, T. and Moody, J.B., 1988. The Supercontinent cycle. Scientific American. July 1988. 44-51.

Naqvi, S.M. and Rogers, J.J.W., 1987. Precambrian Geology of India, Oxford Monographs on Geology and Geophysics 6. Clarendon, New York.

Nayak, P.N, 1990. Deep crustal configuration of central India. Geological survey of India. Spl.Pub. 28, 67-98.

Neethling, D.C., 1972. Comparative geochemistry of Proterozoic and Paleo-Mesozoic tholeiites of Western Dronning Maud Land. In Aide, R.J. (ed), Antarctic Geology and Geophysics: Universitetsforlaget, Oslo, Norway. 603-616.

Nyakaana, J., 1994. Ground geophysical studies near the Kilembe mine, Uganda and their relation to the interpretation of regional aeromagnetic data in central Africa. MSc thesis, ITC, Delft, the Netherlands.

NGRI, 1975-1978. Gravity map series of India. Published by National Geophysical research Institute, Hyderabad, India.

References

NGRI, 1978-81. Total intensity aeromagnetic map of parts of the Cuddapah basin and adjoining crystallines. Unpublished contour maps (1:2 50 000) by National Geophysical Research Institute, Hyderabad, India.

Norton, I.O. and Sclator, J.G., 1979. A model for the evolution of the Indian Ocean and the breakup of Gondwanaland. Journal of Geophysical Research 84, 6803-6830.

Nutman, A. P., Chadwick, B., Ramakrishnan, K. & Viswanatha, M. N., 1992. SHRIMP U-Pb ages of detrital Zircon in Sargur supracrustal rocks in western Karnataka, southern India, J. Geol. Soc. Ind. 39, 367-374.

Oasis montaj™, Geosoft Inc., Canada. WWW: http://www.geosoft.com

Olesen, O., Henkel, H., Kada, K. and Tveten, E., 1991. Petrophysical properties of a prograde amphibolite-granulite facies transition zone at Sigerfjord, Vesteral, northern Norway. Tectonophysics, 192, 33-39.

Paquette, J. L., Nedelec, A., Moine, B. & Rokotondrazafy, M., 1994. U-Pb single zircon evaporation And Sm-Nd isotopic study of a granulite domain in SE Madagascar. J. Geol. 102, 523-538.

Paquette, J.L. and Nédélec, A., 1998. A new insight into Pan-African tectonics in the East-West Gondwana collision zone by U-Pb zircon dating of granites from central Madagascar. Earth and Planetary Science Letters 155:45-56.

Paquette, J.L., Nédélec, A., Moine, B., and Rokotondrazafy, M., 2000. U-Pb single zircon evaporation and Sm-Nd isotopic study of granulite domain. Journal of Geology 102:523-538.

Park, J. K., 1994. Paleomagnetic constraints on the position of Laurentia from middle Neoproterozoic to Early Cambrian times. Precambrian Research 95, 95-112.

Paul, D.K., Ray Barman,Y., McNaughton, N.J., Fletcher, I.R., 1990. Archean-Proterozoic evolution of Indian charnockites: isotopic and geochemical evidence from the granulites of the Eastern Ghat Belt. Journal of Geology 98, 253-263.

Peraraju, P.; Kovach, A.; and Svinger, E. 1979. Rubidium-Strontium ages of some rocks from parts of Eastern Ghats in Orissa and Andhra Pradesh. Jour. Geol. Soc. India. 20, 290-296.

Perera, A. G. S. R., 1997. Aeromagnetic interpretation of SW Sri Lanka and its comparison with northern Mozambique. MSc thesis, ITC, delft, The Netherlands.

Peucat, J.J.; Mahabaleswar R. and Jayananda M., 1993. Age of Younger tonaliteic magmatism and granulitic metamorphism in the South India transition zone (Krishnagiri area); comparison with older Peninsular gneisses from Gorur- Hassan area. Jr. Metamorphic Geology 11, Pp. 879-888

Peucat, J.J., Bouhallier, H., fanning, C. M & Jayananda, M., 1995. Age of the Holenarsipur greenstone belt, relationships with the surrounding gneisses (Karnataka, South India). J. Geol. 103, 701-710.

Pinna, P., Jourde, G., Calvez, J. Y., Mroz, J. P. and Marques, J. M., 1993. The Mozambique belt in northern Mozambique: Neoproterozoic (1100-850 Ma) crustal growth and tectogenesis, and superimposed Pan-African (800-550 Ma) tectonism. Precamb. Res. 62, 1-59.

Pinna, P., 1995. On the dual nature of the Mozambique belt, Mozambique to Kenya. African Journal of Earth Sciences 21, 477-480.

Pinna, P., Cocherie, A., Thieblemont, D., Jezequell, P. and Kayogoma, E., 1999. The Archean evolution of the Tanzanian craton (2.93- 2.53 Ga). Journal of African Earth Sciences 28 (4A). 62-63.

Pitts, B.E., Maher, M.J., de Beer, J.H. and Gough, D.I., 1992. Interpretation of magnetic, gravity and megnetotelluric data cacross the Cape Fold Belt and Karoo Basin. In de Wit, M.J., Ransome, I.G.D. (eds) Inversion Tectonics of the Cape Fold Belt, Karoo and Cretaceous Basins of Southern Africa. Balkema, Rotterdam, 27-32.

Porada, H and Berhorst, 1999. Towards a new understanding of the Neoproterozoic-Early Paleozoic Lufilian and northern Zambezi belts in Zambia and Congo/Zaire (abstr.). IGCP- 418/419 Conference in Kitwe, Zambia, 40-41.

References

Powell, C. McA., 1993. Assembly of Gondwanaland- Open forum, In Frindley, R.H. et al. (eds). Gondwana Eight: Assembly, Evolution and Dispersal. Rotterdam, Netherlands, Balkema, 218-237.

Powell,C. McA and Li, Z.X., 1994. Reconstruction of the Panthalasaan margin of Gondwanaland. In Veevers, J.J. and Powell, C. McA. (Eds), Permian-Triassic Pangean Basins and foldbelts along the Panthalassan Margin of Gondwanaland. Geological Society of America, Memoir 184, 5-9.

Qin, S., 1994. An analytical signal approach to the interpretation of total field magnetic anomalies. Geophysical Prospecting, 42, 665-676.

Radhakrishna, T. and Mathew, J., 1996. Late Precambrian (850-800 Ma) paleomagnetic pole for the south Indian shield from the Harohalli alkaline dykes: geotectonic implications for Gondwana reconstructions. Precambrian Research 80, 77-87.

Raith, M.M., Srikantappa, C., Bhul, D. and Köhler, H., 1999. The Nilgiri enderbites, South India.: nature and age constraints on protolith formation, high-grade metamorphism and cooling history. Precambrian research 98, 129-150.

Rajesh, H.M., Santosh, m. and Yoshida, M., 1998. Dextral pan-African Shear along the southwestern edge of the Achankovil Shear Belt, South India: constraints on Gondwana reconstructions: a discussion. Journal of Geology, 106, Pp. 105-114.

Ramachandran, T.V., Mishra, A. and Mishra, R.S., 1986. Geological evolution of absolute total intensity magnetic data of Tamilnadu. Journal Ass. Expl. Geophys. 7, 151-162.

Ramakrishnan, M. 1993. Tectonic evolution of the granulite terrains of southern India. Geol. Soc. India. Memoir, **25**, 35-44.

Ramakrishna, M., 1996. Tectonic evolution of the granulite terrains of southern India. Geological Society of India Memoir 25:35-44.

Ramakrishnan, M., Nanda, J.K. and Augustine, P.F., 1998. Geological evolution of the Proterozoic Eastern Ghats mobile belt. Geol. Surv. Ind. Spl. Pub. 44, 1-21.

Rakotosolofo, N.A., Torsvik, T.H., Ashwal, L.D., Eide, E.A., and De Wit, M.J., 1999. The Karoo Supergroup revisited and Madagascar Africa fit. Journal of African Earth Sciences 29(1):135-151.

Ravi Shankar, 1988. Heat flow map of India and discussions on its geological and economic significance. Indian Minerals 42 (2). 89-110.

Reddi, A.G.B., Mathew, M.P., Singh, B. and Naidu, P.S, 1988. Aeromagnetic evidence of crustal structure in the granulite terrane of Tamilnadu-Kerala. Journal Geol Soc India, Vol 32, 368-381.

Reeves, C.V., 1978. A failed Gondwana spreading axis in southern Africa. Nature 273:222-223.

Reeves, C.V, Karanja, F.M. and MacLeod, I.N., 1986/87. Geophysical evidence for a failed Jurassic rift and triple junction in Kenya. Earth and Planetary Sciences Letters, 81, Pp. 299-311.

Reeves, C.V., Zeil, P.W., and Yunxuan, Z., 1990. Interpretation of airborne geophysical surveys: some potential application of image processing techniques and geographic information systems in systematic exploration strategy. ITC Journal 2

Reeves, C.V., 1992. New horizons in airborne mapping. Exploration Geophysics 23: 273-280.

Reeves, C.V. 1998. Aeromagnetic and gravity features of continental Gondwana and their relation to continental break-up: more pieces, less puzzle. Journal of African Earth Sciences (special abstract issue), Vol.27-1A.

Reeves, C.V. and de Wit, M., 1998. Conjugate termini in separated oceans and continents: getting Gondwana back together. Journal of African Earth Sciences (special abstract issue), Vol.27-1A.

Reeves, C.V., 1998. Continental scale and global geophysical anomaly mapping. ITC Journal, 1998-2, 91-98.

Reeves, C.V., 1998. Compiling all the world's magnetic anomalies. EOS, July 14, 1998, 338.

Reeves, C.V., 1999. Aeromagnetic and gravity features of Gondwana and their relation to continental break-up: more pieces, less puzzle, Journal of African Earth Sciences 28 (1), 263-277.

Reeves, C.V., 2000. The geophysical mapping of Mesozoic dyke swarms in southern Africa and their origin in the disruption of Gondwana. Journal of African Earth Sciences 30:499-515.

Reeves, C.V. and de Wit, M. J., 2000. Making ends meet in Gondwana: retracing the transforms of the Indian Ocean and reconnecting continental shear zones. Terra Nova (in press).

Reeves, C.V., Sahu, B.K. and de Wit, M.J., in press. A re-examination of the paleoposition of Africa's eastern neighbours in Gondwana.

Reid, A.B., Allsop, J.M., Granser, H., Millet, A.J. and Somerton, I.W., 1990. Magnetic interpretation in three dimensions using Euler deconvolution: Geophysics, 55, 80-91.

Reference Manager®, Research Information Systems, Carlsbad, USA. WWW: http://www.risinc.com

Robb, L.R., Davis, D.W. and Kamo, S.L., 1991. Chronological framework for the Witwatersrand basin and environs: towards a time-constrained depositional model. South African Journal of geology 94, 86-95.

Roering, C., Barton, J.M. and Winter, H de la R., 1990.The Vedefort structure: a perspective with regard to new tectonic data from adjoining terranes. Tectonophysics 171, 7-22.

Roering, C., Van Reenen, D.D., Smit, C.A., Barton, J.M., de Beer, J.H., de Wit, M.J., Stettler, E.H., van Schalkwyk, J.F., Stevens, G. and Pretorious, S.J., 1992. Tectonic model for the evolution of the Limpopo Belt. Precambrian Research, 55, 539-552.

Roeser, H.A., Fritsch, J. and Hinz, K., 1996. The development of the crust off Dronning Maud Land, East Antarctica. In Storey, B.C, King, E.C. and Livermore, R.A. (eds) Weddell Sea Tectonics and Gondwana Break-up. Geological Society Special Publication No. 108, Pp.243-264.

Roest, W.E., Verhoef, J., Pilkington, M., 1992. Magnetic interpretation using 3D analytic signal. Geophysics, 57, 116-125.

Rosers, J.J.W. and Giral, R.A., 1997. The Indian Sheld. Chapter 5.10 in de Wit and Ashwal, L.D. (eds) Greenstone Belts. 620-674.

SACAR (South African Committee for Antarctica Research), 1994. Geological Evolution of western Dronning Maud Land within a Gondwana framework: Geophysics subprogram. Project Report.

Sacchi, R. Marques, J. Costa, M. & Casati, C., 1984. Kibaran events in the southernmost Mozambique belt. Precamb. Res. 25, 141-159.

Sacks, P.E., Nambiar, C. G., and Walters, L. J. 1997. Dextral Pan-African shear along the southwestern edge of the Achankovil shear belt, south India: constraints on Gondwana reconstructions: Jour. Geol., 105, 275-284.

Saha, A.K., Ray, S.L. and Sarkar, S.N., 1986. Early history of the earth-evidence from the eastern Indian shield (abstr.). Group discussion on Precambrian of the Eastern Indian Shield, Dhanbad, Pp. 1-2.

Sahu, B.K. and Reeves, C.V., 1998. Continental scale geophysical anomaly patterns: implications for Gondwana re-assembly. Journal of African Earth Sciences 27(1A): 165-167,

Saki, T., Tamura, Y., Tokushashi, S. Kodato, T., Mizukoshi, I. and Amano, H., 1987. Preliminary report on the geological and geophysical surveys off Dronning Maud Land, East Antarctica. Proc NIPR Symp. On Antarctic Geoscience 1, Pp 23-40.

Santosh, M., Iyer, S. S., Vasconcellos, M. B. A. and Ensweiler, J. 1989. Late Precambrian alkaline plutons in southwest India: geochronologic and rare earth element constraints on Pan-African magmatism. Lithos, 24, 65-79.

Sarkar, A.N., Bhanumathi, L., and Balasubrahmanyan, M. N., 1981: Petrology, geochemistry and geochronology of the Chilka lake igneous complex, Orissa state, India. Lithos, 14, 93-111.

References

Sarkar, S.C., Paul, D.K., de Laeter, J.R., McNaughton, N.J. and Misra, V.P., 1990. A geochemical and Pb, Sr isotopic study of the evolution of granite-gneisses from the Bastar craton, central India. Journal Geological Society of India 35, 480-496.

Schandelmeier, H., 1980. Regionale Gliederung des Präkambrimus und Aspeckte der krustenentwicklung um Mambwe/ Nordost – Zambia. Giessener Geologische Schriften 23. Lenz-Verlag, Giessen, 111 pp.

Seen, N., 1991. The Narmada-Son-Brahmaputra transform: a Mesozoic fracture zone in Gondwanic India. Tectonophysics, 186. 359-364.

Shackleton, R.M., 1973. Implications of continental drift to the earth sciences. In: Implications of Continental Drift to the earth Sciences, edited by Tarling, D.H. and Runcorn, S.K., London and New York: Academic Press, 1091-1095.

Shackleton, R.M., 1996. The final collision zone between East and West Gondwana: where is it? Journal of African Earth Sciences 23(3): 271-287.

Shaw, R.K., Arima, M and Kagami, H., 1996. Preliminary geochronological results of a suite of granulites from Eastern Ghats. Gondwana News Letter 7. Journal of African Earthsciences.

Shaw, R. K.; Arima, M.; Fanning, C. M.; Shiraishi, K. and Motoyoshi, Y., 1997. Proterozoic Events in the Eastern Ghats Granulite Belt, India: Evidence from Rb-Sr, Sm-Nd Systematics, and SHRIMP Dating: Jour. Geol., 105, P.645-656.

Shibata, K., Yanai, K. and Shirashi, K., 1986. Rb-Sr whole-rock ages of metamorphic rocks from eastern Queen Maud Land, East Antarctica. Memoirs of National Institute of Polar Research Special Issue 43, 133-148.

Shirashi, K, Kanisawa, S. and Ishikawa, 1988. Geochemistry of post-orogenic mafic dyke rocks from the eastern Queen Maud Land, East Antarctica. Proc. Nat. Inst. Polar Res. Sym. Antarctic Geoscience 2, 117-132.

Shirashi, K., Ellis, D.J., Hiroi, Y., Fanning, C.M., Motoyoshi, Y. and Nakai, Y., 1994. Cambrian orogenic belts in East Antarctica and Sri Lanka: implications for Gondwana reassembly. Journal of Geology 102, 47-65.

Sivaji, C.H. and Agarwal, B.N.P., 1995. Application of the relaxation technique in mapping of crustal discontinuities from Bouguer anomalies over central India. Mem. Geological Survey of India 31, Pp. 495-518.

Skilbrei, J.R., Skyseth, T. and Olesen, O., 1991, Petrophysical data and opaque mineralogy of high-grade and retrogressed lithologies: implications for the interpretation of aeromagnetic anomalies in Northern Vestranden, Central Norway: Tectonophysics, 192, 21-31.

Smith, A.G., 1999. Gondwana: its shape, size and position from Cambrian to Triassic times, Journal of African Earth Sciences (28) 1. 71-97

Smith, A.G., Hurley, A.M., and Briden, J.C., 1981. Phanerozoic paleocontinental world maps. Cambridge University Press, New York, 102.

Smith, A.G. and Hallam, 1970. A. The fit of the southern continents. Nature 225(`): 139-144.

Smith, W. H. F. and Sandwell, D., 1997. Measured and estimated seafloor topography (Version 4.2), World data Centre A for Marine Geology and Geophysics research publication RP-1, poster, 34"x 53".

Spaeth, G. and Schüll, P., 1987. A survey of Mesozoic dolerite dykes from western Neuschwabenland and their geotectonic significance. Polarforschung 57, 93-113.

Spector, A. and Grant, F.S., 1970. Statistical models for interpreting aeromagnetic data. Geophysics 35(2), 293-302

Sreedhar Murthy, Y., Govindarajan, K., and Babu Rao, V., 1998. Contours to images, Part I - an innovative methodology. Journal of Geophysics 19:141-148.

Srikantappa, C., Raith, M., and Spiering, B., 1985: Progressive charnockitization of a leptynite-khondalite suite in southern Kerala, India evidence for formation of charnockites through decrease in fluid pressure. J. Geol. Soc. India, **26**, 849-872.

Srikantappa, C., 1993. High-pressure charnockites of the Nilgiri Hills, Southern India. In B.P. Radhakrishna (ed) Continental crust of South India. Memoir Geol Soc. India 25, 95-111.

References

Strangway, D.W. and Vogt, P.R., 1970. Aeromagnetic tests for continental drift in Africa and South America. Earth and planetary Science Letters 7, 429-435.

Stern, R.J., 1993. Tectonic evolution of the Late Proterozoic East African Orogen: constraints from crustal evolution of Arabian-Nubian Shield and the Mozambique belt. In Thorweihe, U. and Schandelmeire, H. (eds) Geoscientific Research in Northeast Africa. Balkema, Rotterdam.

Stern, R.J., 1994. Arc assembly and continental collision in the Neoproterozoic East African Orogen. Annu. Rev. Earth Planet Sci. 22, 319-351.

Storey, B.C., 1995. The role of mantle plumes in continental breakup: case histories from Gondwanaland. Nature 377. 301-308.

Subrahmanyam, C., 1978a. On the relation of gravity anomalies to geotectonics of the Precambrian terrains of the Southern Indian Shield. Journal of Geological Society of India 19. 241-263.

Subrahmanyam, C., 1978b. The relationship of gravity field to the structural provinces in the peninsular shield of South India. PhD thesis. Indian School of Mines, Dhanbad, India. 237 pages.

Subrahmanyam, C., 1983. An overview of gravity anomalies. Precambrian metamorphic terrains and their boundary relationships in the southern Indian shield. In: Precambrian of south India. Mem. Geol. Soc. India, 4, p. 553-564.

Suess, E., 1904. The face of the earth. Vol. 1. Oxford Clarendon Press.

Suryanarayana, M. and Bhan, S.K., 1985. Aeromagnetic survey over parts of Kerala and the adjoining offshore region, India. Geophys. Res. Bull. 23, 105-114.

Tack, L., 1995. The Neoproterozoic Malagarazi Supergroup of SE Burundi and its equivalent Bukoban system in NW Tanzania. Ann. Sc. Geol. 101, 121-129.

Tani, Y., 1997. Collision tectonics of the Wanni and Highland complexes in Sri Lanka. Gondwana News Letter.No.7.

Tankard, A.J., Jackson, M.P.A., Eriksson, K.A., Hobday, D.R., Hunter, D.R. and Minter, W.E.L., 1982. Crustal evolution of southern Africa, 3.8 billion years of earth history. Springer-Verlag, Heidelberg, 523 Pp.

Tarlowski, C., Milligan, P.R. and Mackey, T.E., 1996. The magnetic anomaly map of Australia (second edition), scale 1: 5 000 000, Australian Geological survey Organisation, Canberra.

Taylor, P.N., Chadwick, B., Moorbath, S., Ramakrishnan, M. and Vishwanatha, M.N., 1984. Petrography, chemistry and isotopic ages of Peninsular Gneiss, Dharwar acid volcanic rocks and the Chitradurga Granite with special reference to the Late Archaean evolution of the Karnataka craton, South India. Precambrian research: 23, 249-375.

Thomas, R.J., 1989. A tale of two tectonic terranes. South African Journal of Geology 92, 306-321.

Thomas, R.J. and Ellington, B.M., 1990. A Rb-Sr, Sm-Nd and U-Pb zircon isotopic study of the Mzumbe Suite, the oldest intrusive granitoid in southern Natal, South Africa. South African Journal of Geology 93, 761-765.

Thomas, R.J., Von Veh, M.W.A. and MCourt, S., 1993. The tectonic evolution of southern Africa, an overwiew. Journal of African Earth Sciences 16(Special Issue): 5-24.

Thomson, D.T., 1982. EULDPH: A new technique for making computer-assisted depth estimates from magnetic data. Geophysics, 47, 31-37.

TimeTrek, Cambridge Paleomap Services Ltd., Cambridge, UK.

Tingey, R. J., 1991. Commentary on the Schematic Geological Map of Antarctica (1: 10 000 000). BMR Bulletin 238. 30 pp +Map.

Torsvik, T. H. and Smethurst, M. A., 1999. Plate tectonic modelling: virtual reality with GMAP, Computers And Geosciences (25) 4, 395-402.

TPDC, 1995. Tanzania petroleum exploration potential. Tanzania Petroleum Development Corporation. 40p.

Tucker, R.D., Ashwal, L.D., Handke, M.J and Hamilton, M.A., 1999. U-Pb geochronology and isotope geochemistry of the Archean and Proterozoic rocks of north-central Madagascar. Journal of Geology 107 (2).

References

Unnikrishnan-Warrier, C., Santosh, M, Yoshida, M., 1995. First report of Pan-African Sm-Nd and Rb-Sr mineral isochron ages from regional charnockites of southern India. Geol. Mag. 132, 253-260.

Unrug, R., 1996. The assembly of Gondwanaland- Scientific results of IGCP Project 288: Gondwana structures and mobile belts. Episodes. Vol 19 (1&2), 11-20.

Unrug, R., 1997. The Geodynamic map of the Gondwana Supercontinent Assembly. GSA Today.7 (1), 1-6.

Valadiya, K.S., 1984. Aspects of Tectonics: focus on south-central Asia. Tata Mc-Graw-Hill publ.Co.Ltd., 59-75.

van Heiningen, P. S., 1997. The predisruption tectonics in Gondwana: Evolution of Karoo basins in southern and eastern Africa and Madagascar. MSc thesis, Deptt. Of Earth Sciences, University of Utrecht and International Institute for Aerospace Survey and Earth Sciences, Delft, the Netherlands

Van der Voo, R. and Meert, J.G., 1991. Late Proterozoic paleomagnetism and tectonic models: a critical appraisal. Precambrian research 53:149-163.

Verma, R.K. and Banerjee, P., 1992. Nature of continental crust along the Narmada-Son lineament inferred from gravity and deep seismic sounding data. Tectonophysics. Vol 202, 375-397.

Van der Voo, R. and Meert, J.G., 1991. Late Proterozoic paleomagnetism and tectonic models: a critical appraisal. Precambrian Research 53, 149-153.

Van Reenen, D.D., Roering, C., Brandl, G., Smith, C.A. and Barton, J.M.,

Von Frese, R.R.B., Hinze, W.J., Olivier, R. and Bentley, C.R., 1987. Satellite magnetic anomalies and continental reconstructions. In McKenzie (Ed) Gondwana Six: Structure, Tectonics and Geophysics. Geophysical Monograph 40, American Geophysical Union, Washington, D.C.

Watkeys, M.K., 1983. Brief explanatory notes on the provisional geological map of the Limpopo Belt and environs. Geological Society of South Africa, Special Publication 8, 5-8.

Watkeys, M.K. and Uken, R., 1998. Dyking events in the Kaapvaal Craton from the Archean to Gondwana break-up. Abs. Vol., Journal of African Earth Sciences, 27, 1A, 206-207.

Watts, A.B. and Cox, K.G., 1989. The Deccan Traps: an interpretation of progressive lithospheric flexture in response to a migrating load. Earth and Planetary Science Letters 93, 85-97.

Watters, B. R., Krynauw, J. R. & Hunter, D. R., 1991. Volcanic rocks of the Proterozoic Jutulstraumen Group in western Dronning Maud Land, Antarctica. In Thomson, M. R. A., Crame, J. A. & Thomson, J. W. (eds.). Geological evolution of Antarctica, 41-46.

Weaver, B.L., 1990. Early Precambrian basic rocks of India: In Hall, R.P. and Hughes, D.J. (eds) Early Precambrian basic magmatism. Blackie, Glasgow, 339-351.

Wegener, A., 1915. Die Entstehung der Kontinente und Ozeane. Braunschewig: z.uitg.

Weil, A.B., van der Voo, R., Nicoill, C.M. and Meert, J.G., 1998. The Proterozoic supercontinent Rodinia: paleomagnetically derived reconstrctions for 1100 to 800 Ma. Earth and Planetary Science Letters 154, 13-24.

Whitten, D.A.G. and Brooks, J.R.V., 1982. The Penguin Dictionary of Geology. Penguin Books Ltd.

Wison, T.J., 1963. Continental Drift. In Continents Adrift (Readings froMSc ientific American). W.H Freeman and Company, San Francisco, 41-55.

Wilson, T.J., Hanson, R.E. and Wardlaw, M.S., 1993. Late Proterozoic evolution of the Zambezi belt, Zambia: implications for regional Pan-African tectonics and shear displacements in Gondwana. Gondwana Eight, Unrug, Banks and Veers (eds), 69-82.

Wilson, T.J., Grunow, A.M. and Hanson, R.E., 1997. Gondwana assembly: The view from southern Africa and East Gondwana: Journal of Geodynamics 23, 263-286.

Windley, B. F., Razafiniparany, A., Razakamanana, T. & Ackermand, D., 1994. Tectonic framework of the Precambrian of Madagascar and its Gondwana connections: a review and reappraisal. Geol. Rundsch 83, 642-659.

Wolmarans, L.G. and Kent, K.E., 1982. Geological investigations in western Dronning Maud Land, Antarctica- a synthesis. S. Afr. J. Antarc. Res., Suppl. 2, 93 pp.

References

Yardimcilar, C. and Reeves, C.V. 1998. The evidence for the fit of Madagascar against East Africa from magnetic anomaly mapping. Journal of African Earth Sciences (special abstract issue), Vol.27-1A, 215-216.

Yardimcilar, C., 1998. An examination of the evidence from magnetic anomaly mapping for the fit of Madagascar against East Africa. MSc thesis, Exploration Geophysics Division, ITC, Delft, The Netherlands.

Yoshida, M. & Santosh, M., 1994. A tectonic perspective of incipient charnockites in East Gondwana. Precamb. Res. 66, 379-392.

Yoshida, M., 1995. Assembly of East Gondwanaland during the Mesoproterozoic and its rejuvenation during the Pan-African period. In Yoshida, M. and Santosh, M. (eds): India and Antarctica during the Precambrian. Geological Society of India Memoir 34, 25-45.

Yoshida, M., Bindu, R.S., Kagami, H., Rajesham, T., Santosh, M. and Shirahata,, H., 1996. Geochronologic constraints of granulite terranes of South India and their implications for the Precambrian assembly of Gondwana. Journal of Southeast Asian Earth Sciences, Vol 14, 137-147.

Appendices

Appendix I: Figure Captions

Figure Captions **Page**

Appendix II: List of Maps

Appendix III: List of Tables

Appendix IV: An example of *mif* file

```
Version 300
Charset "WindowsLatin1"
Delimiter ","
CoordSys Earth Projection 1,
0
Columns 1
 ID Integer
Data

Pline 32
78.792695 11.749412
78.619303 11.730325
78.524615 11.714267
78.462514 11.710025
78.406254 11.713661
78.268832 11.713358
78.017661 11.700935
77.952178 11.691238
77.875628 11.666996
77.718838 11.60153
77.70654 11.588192
77.567889 11.521494
77.550058 11.520281
77.544217 11.516037
77.319177 11.508456
77.203275 11.522101
77.064931 11.519978
77.022199 11.526649
76.933351 11.557877
76.921976 11.566972
76.850037 11.588192
76.779021 11.616079
76.695707 11.642751
76.424245 11.663662
76.16754 11.729113
76.130341 11.746685
76.08853 11.756683
75.93297 11.81666
75.745744 11.859363
75.613549 11.906903
75.49857 11.92628
75.39804 11.96382
  Pen (1,2,255)
Pline 9
76.211502 11.720024
76.268685 11.7482
76.547832 11.860271
76.656048 11.899636
76.711386 11.927491
76.755041 11.942023
76.801463 11.964425
76.889388 11.989247
76.933351 12.009223
  Pen (1,2,255)
```

Appendix V: An example of *atl* file

(Atlas file format for the mif file in Appendix IV)

```
READ 300
 33  Shear zones in southern India
 1000.00    0.000
  11.749  78.793  11.730  78.619  11.714  78.525  11.710  78.463
  11.714  78.406  11.713  78.269  11.701  78.018  11.691  77.952
  11.667  77.876  11.602  77.719  11.588  77.707  11.521  77.568
  11.520  77.550  11.516  77.544  11.508  77.319  11.522  77.203
  11.520  77.065  11.527  77.022  11.558  76.933  11.567  76.922
  11.588  76.850  11.616  76.779  11.643  76.696  11.664  76.424
  11.729  76.168  11.747  76.130  11.757  76.089  11.817  75.933
  11.859  75.746  11.907  75.614  11.926  75.499  11.964  75.398
0
READ 300
 10  Shear zones in southern India
 1000.00    0.000
  11.720  76.212  11.748  76.269  11.860  76.548  11.900  76.656
  11.927  76.711  11.942  76.755  11.964  76.801  11.989  76.889
  12.009  76.933
0
```

---

300 Fragment number for India

33 Number of coordinates including Dummy co-ordinates

1000.000 0.000 Dummy co-ordinates to draw lines

Appendix VI: Basic Program to convert *mif* files into *atl* files

(Written by Reeves and modified by the author)

```
10 ' program to reformat *.mif files to ATLAS *.atl files
30 DIM LON(1,2500), LAT(1,2500), NN(2500)
40 INPUT "Name of *.MIF file:  "; A$
50 OPEN A$ FOR INPUT AS #1
51 INPUT "Fragment number:  ", F$
52 INPUT "Name of *.ATL file:  "; G$
53 INPUT "Dummy Latitude: "; Y$
56 INPUT "Minimum age: ";U$
57 INPUT "Maximum age: ";X$
60 INPUT "Label for vectors:  "; Z$
62 OPEN G$ FOR OUTPUT AS #2
63 tell=0
65 FOR N=1 TO 8
70 LINE INPUT #1, B$
80 NEXT N
90 WHILE NOT EOF(1)
95 M = 1
100 LINE INPUT #1, C$: 'PRINT C$
110 IF LEFT$(C$,5)="Pline" THEN 115 ELSE 90
115 tell=tell+1
120 N$ = MID$(C$,7,3)
130 NN(M) = VAL(N$)
140 FOR N = 1 TO NN(M)
150   LINE INPUT #1, D$
155   PPOS = INSTR(D$," ")
160   LON(M,N) = VAL(LEFT$(D$,PPOS-1))
170   LAT(M,N) = VAL(MID$(D$,PPOS+1,10))
175   PRINT LON(M,N), LAT(M,N)
180 NEXT N
190 LINE INPUT #1,E$
191 'write the revised vector out
247   COUNT = 0
250   PRINT#2, "READ ";F$
255   PRINT#2, " ";NN(M)+3;"  ";Z$
270   PRINT#2, " ";"4000.000   0.000";"    ";U$; "  ";X$; "  ";Y$; "    ";  "0.000"
280   FOR N = 1 TO NN(M)
290       PRINT#2, USING"#####.###";LAT(M,N);LON(M,N);
310       COUNT = COUNT + 1
320       IF COUNT = 4 THEN PRINT#2,: COUNT = 0
330   NEXT N
340   IF COUNT = 0 THEN 390 ELSE PRINT#2,
390   PRINT#2, "0    "
402 WEND
406 CLOSE #1
410 CLOSE #2
420 END
```

Appendix- VII: Table of Euler rotation parameters used in quoted Gondwana re-assemblies

Fragment	Reev464d			Reev506x		
	Euler latitude	Euler longitude	Rotation angle*	Euler latitude	Euler longitude	Rotation angle*
Africa	-	-	fixed	-	-	fixed
Arabia	+36.50	+18.00	-4.34	+36.50	+18.00	-6.08
Horn of Africa	-	-	fixed	+3.00	+38.50	+8.00
Seychelles	+4.80	57.11	-66.02	+4.80	+57.11	-66.02
Madagascar	-4.73	-85.08	+20.97	-4.73	+85.08	+20.97
Madagascar Rise	+2.90	-78.38	+25.27	+2.90	-78.38	+25.27
India	+29.89	+40.80	-65.23	+29.59	+41.01	-65.62
Sri Lanka	+21.13	+49.16	-81.03	+20.90	+49.28	-81.47
Antarctica	-10.43	-30.53	+58.95	-10.18	-31.04	+58.73
Australia	-25.48	-61.63	+55.53	-25.14	-62.21	+55.62
South America	+42.87	-30.91	+58.65	+42.82	-28.84	+59.52

The pole quoted is that closest to the zero meridian, positive = north and east, negative = south and west.

* counter-clockwise rotations in reverse time are shown as positive.

AEROMAGNETICS OF SELECTED CONTINENTAL AREAS FLANKING THE INDIAN OCEAN; *WITH IMPLICATIONS FOR GEOLOGICAL CORRELATION AND REASSEMBLY OF CENTRAL GONDWANA*

APPENDIX VII

AEROMAGNETIC MAPS OF SOUTHERN AND EASTERN AFRICA (MAPS 6.1, 6.2, 6.3 & 6.4)

Thesis presented for the degree of Doctor of Philosophy in the Department of Geological Sciences University of Cape Town

September 2000

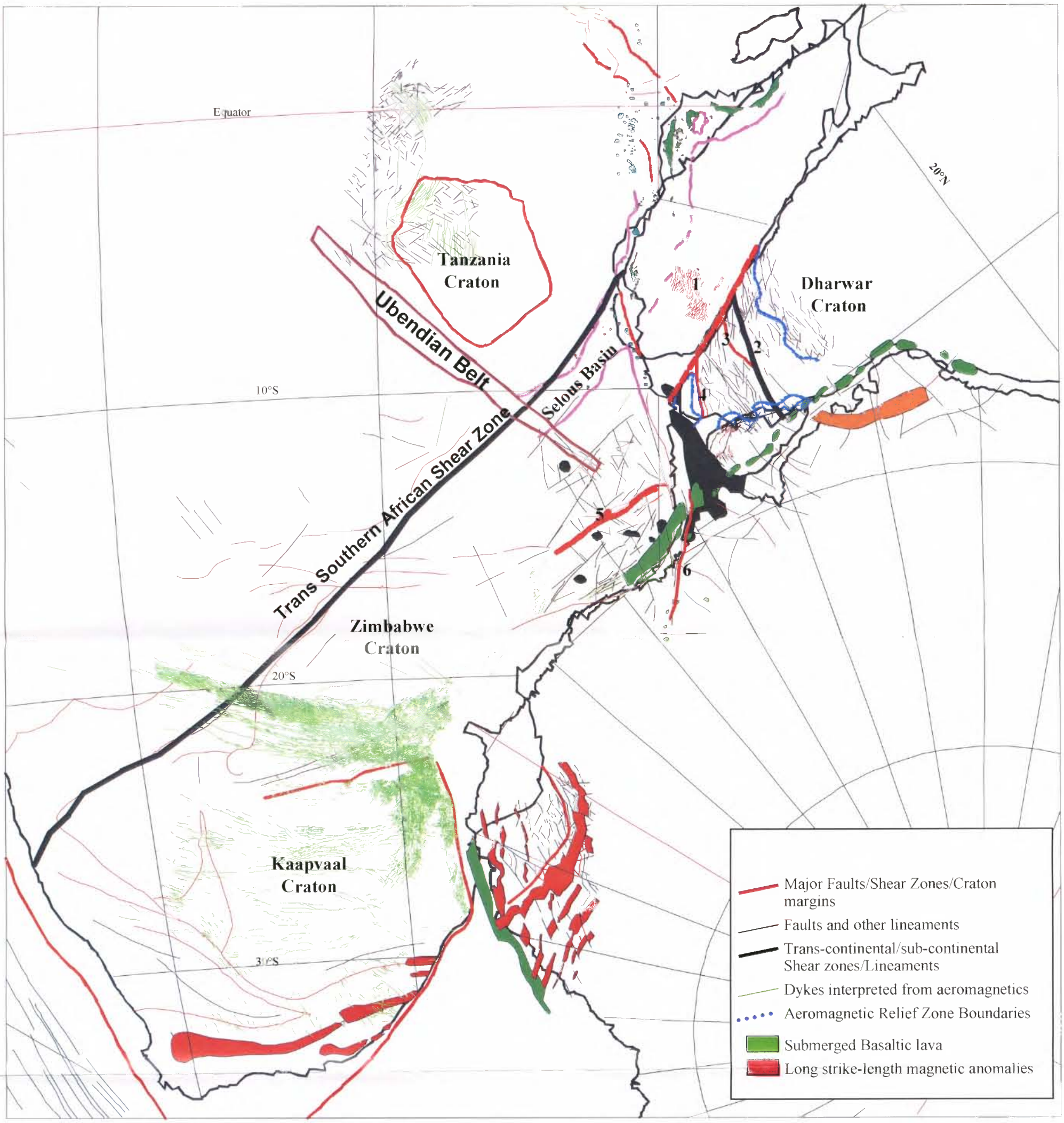

Aeromagnetic Interpretation Map of central Gondwana

1: Ranotsara Shear Zone, 2: Cannonore-Thanzavur Shear Zone, 3: Palghat-Cauvery Shear Zone, 4. Achankovil Shear Zone, 5: Lurio Shear Belt, 6: Western Marginal Fault of Sør Rondane Mountains

Data Sources: Africa - Batterham et al. (1983), Mubu, (1995), Reeves (pers. comm., 1998), this study; Madagascar - Yardimcilar, 1998; India - this study; Antarctica - Golynsky et al. (1996), Corner (1994).

Map 8.3

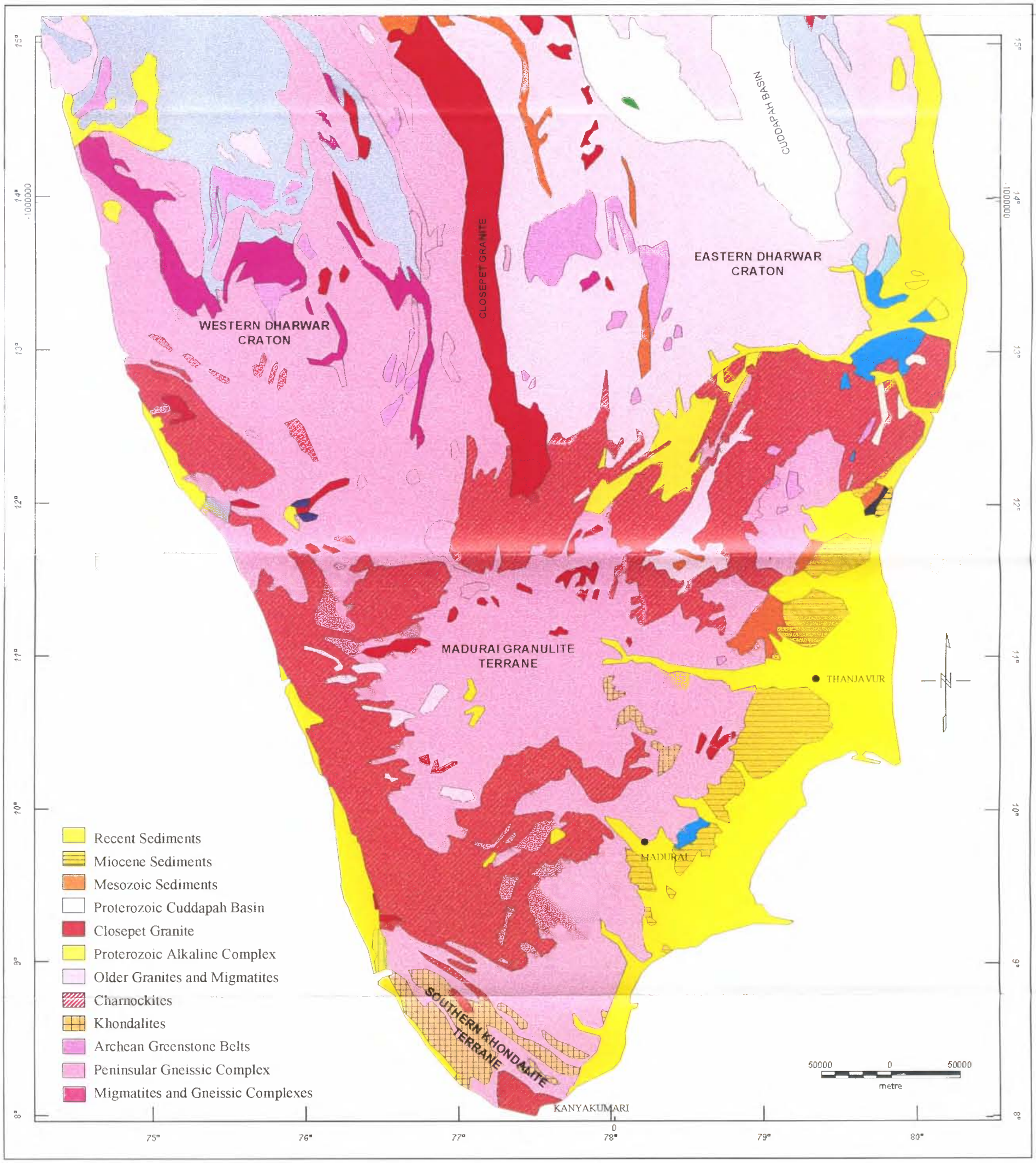

Map 5.1

Generalised Geological Map of India

(digitised and modified from geological maps, GSI, 1994 and 1998)

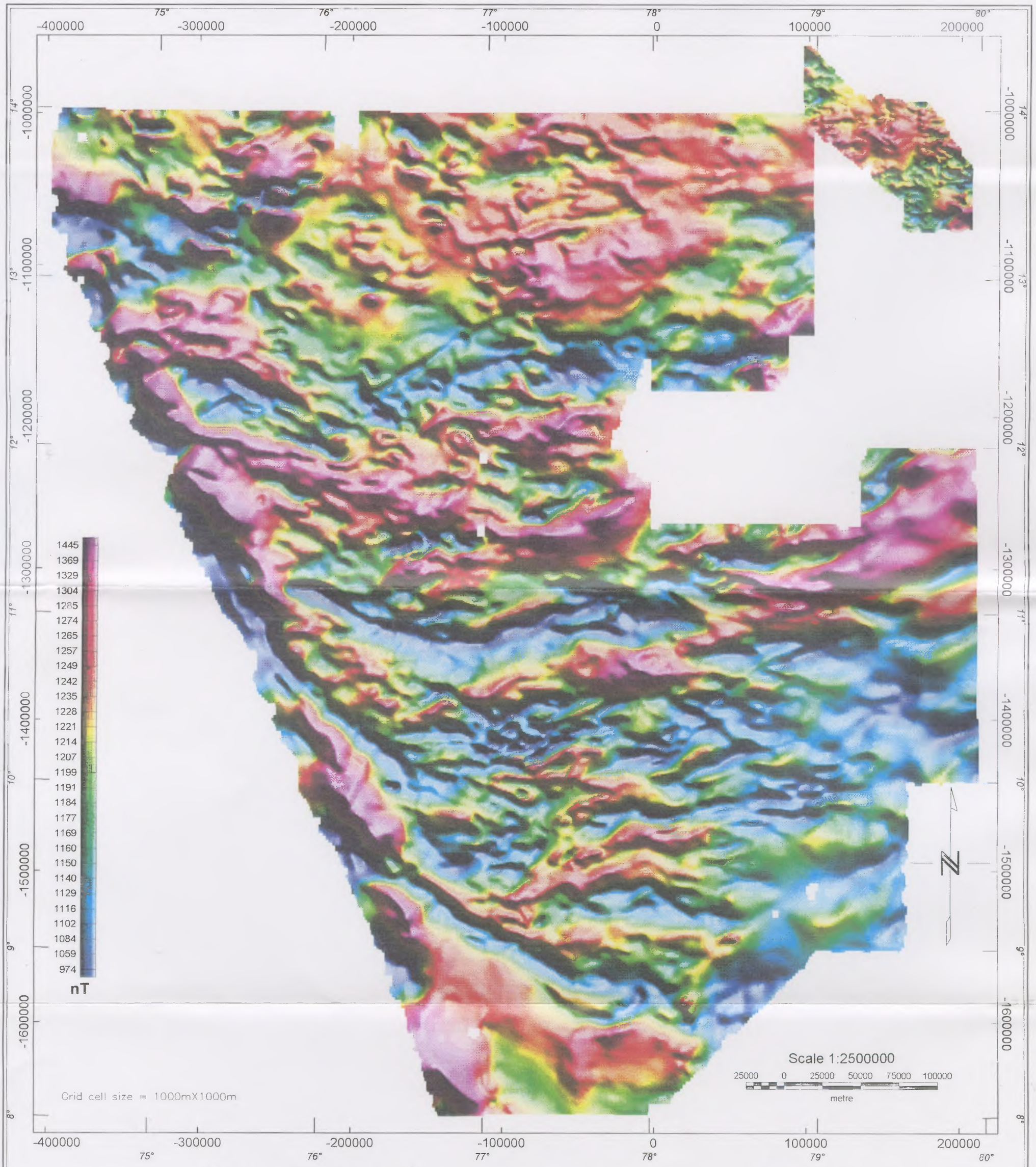

Total Field Aeromagnetic Map of Southern India

Map 5.2

Data reduced to 2100m level (flight height)
Plyconic Projection (Everest 1830 Datum)
Bijay Kumar sahu, ITC, Delft, Netherlands

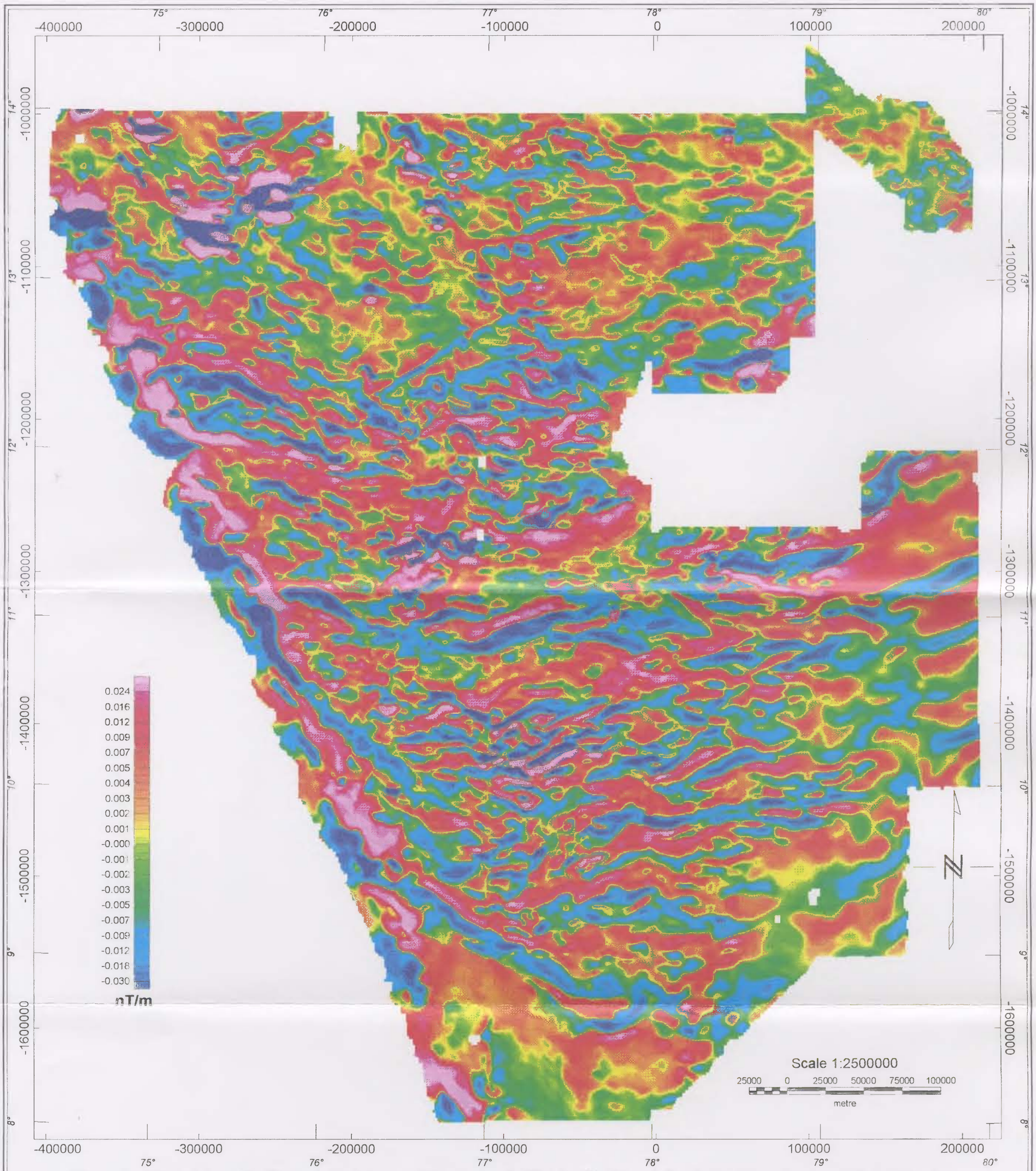

First Vertical Derivative Map of Total Field Aeromagnetic Data Southern India

Map 5.3

Data reduced to 2100m level (flight height)
Plyconic Projection (Everest 1830 Datum)
Bijay Kumar sahu, ITC, Delft, Netherlands

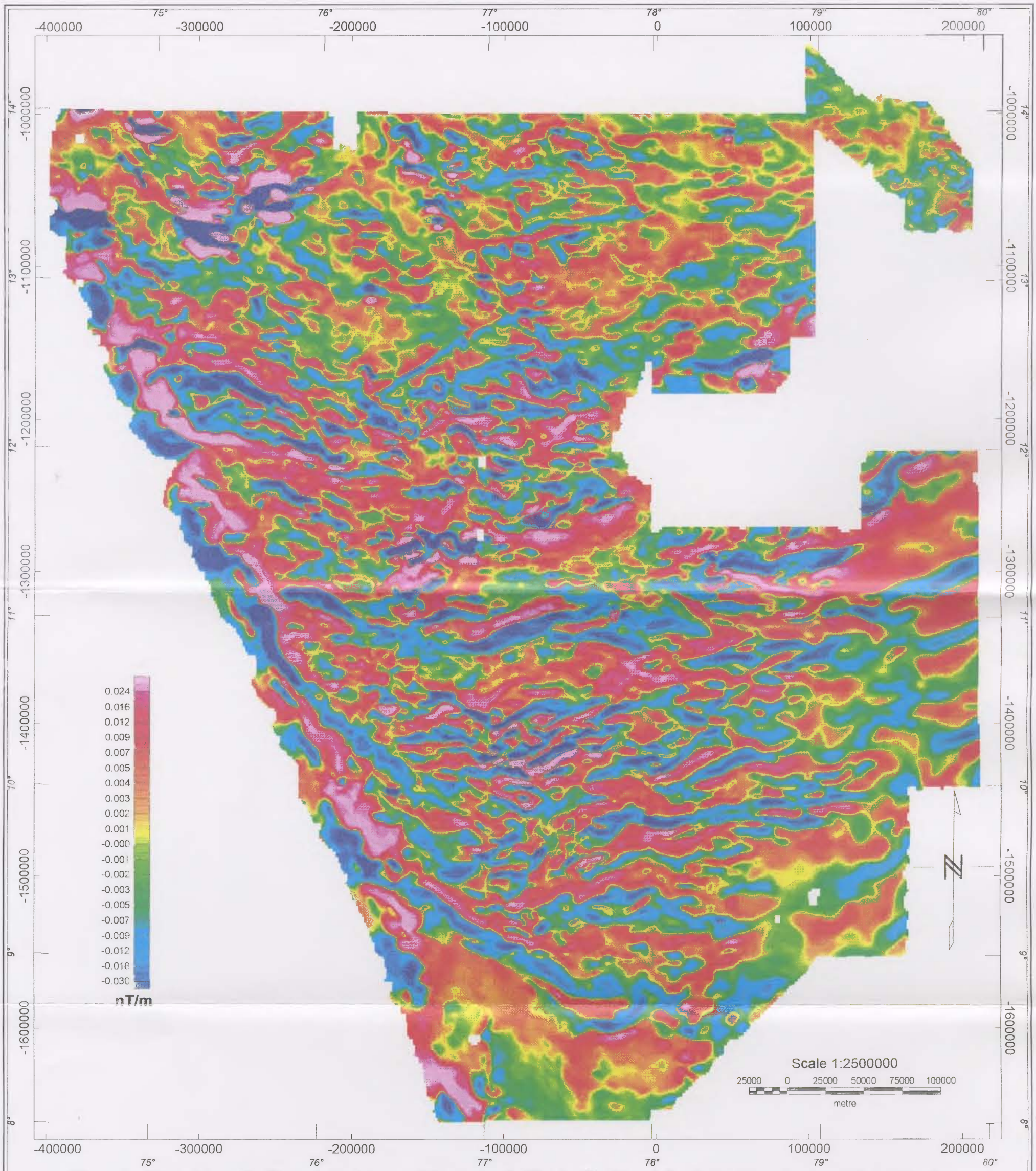

First Vertical Derivative Map of Total Field Aeromagnetic Data Southern India

Map 5.3

Data reduced to 2100m level (flight height)
Plyconic Projection (Everest 1830 Datum)
Bijay Kumar sahu, ITC, Delft, Netherlands

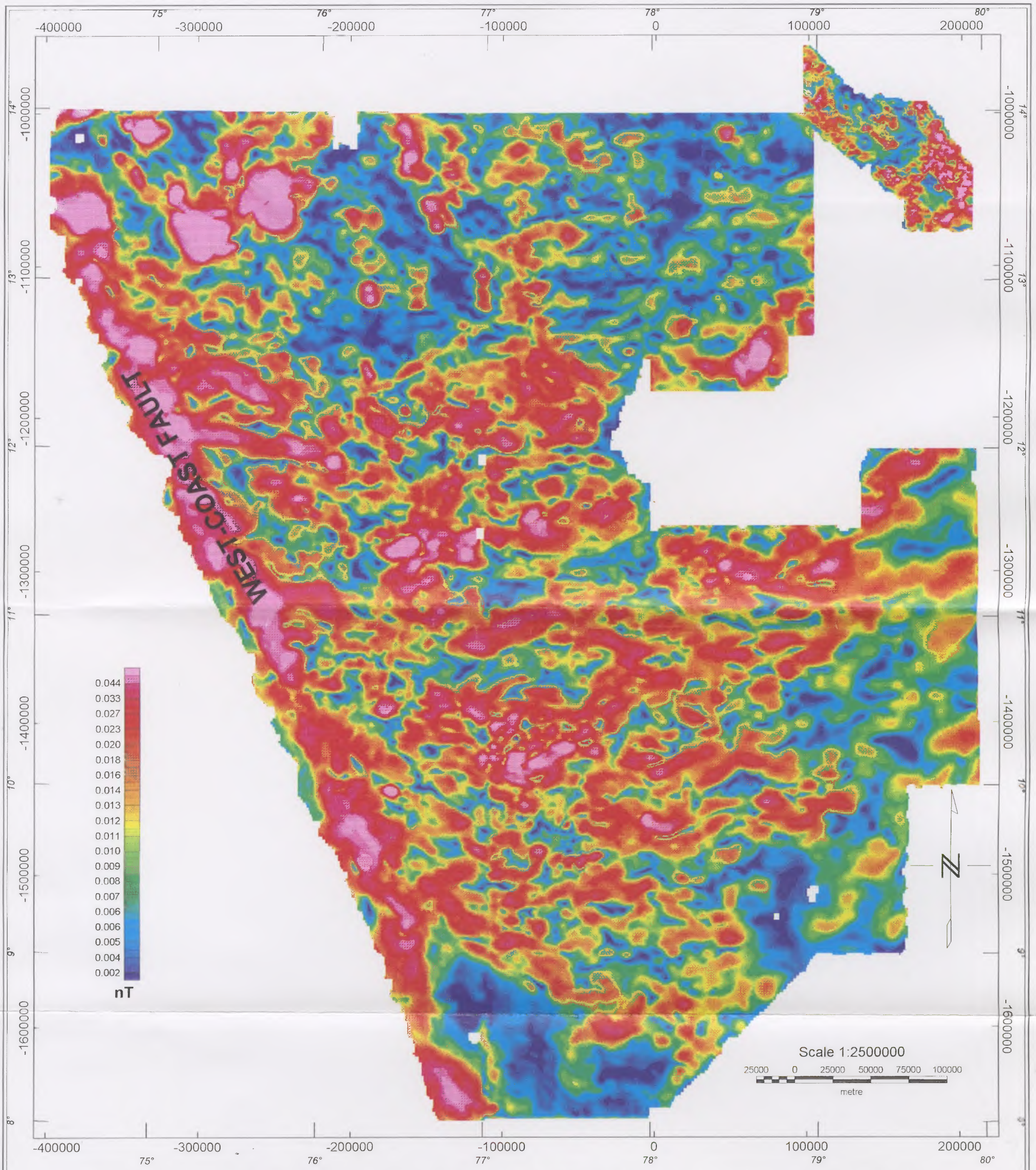

Analytic Signal Map of Total Field Aeromagnetic Data Southern India

Data reduced to 2100m level (flight height)
Plyconic Projection (Everest 1830 Datum)
Bijay Kumar sahu, ITC, Delft, Netherlands

Map 5.4

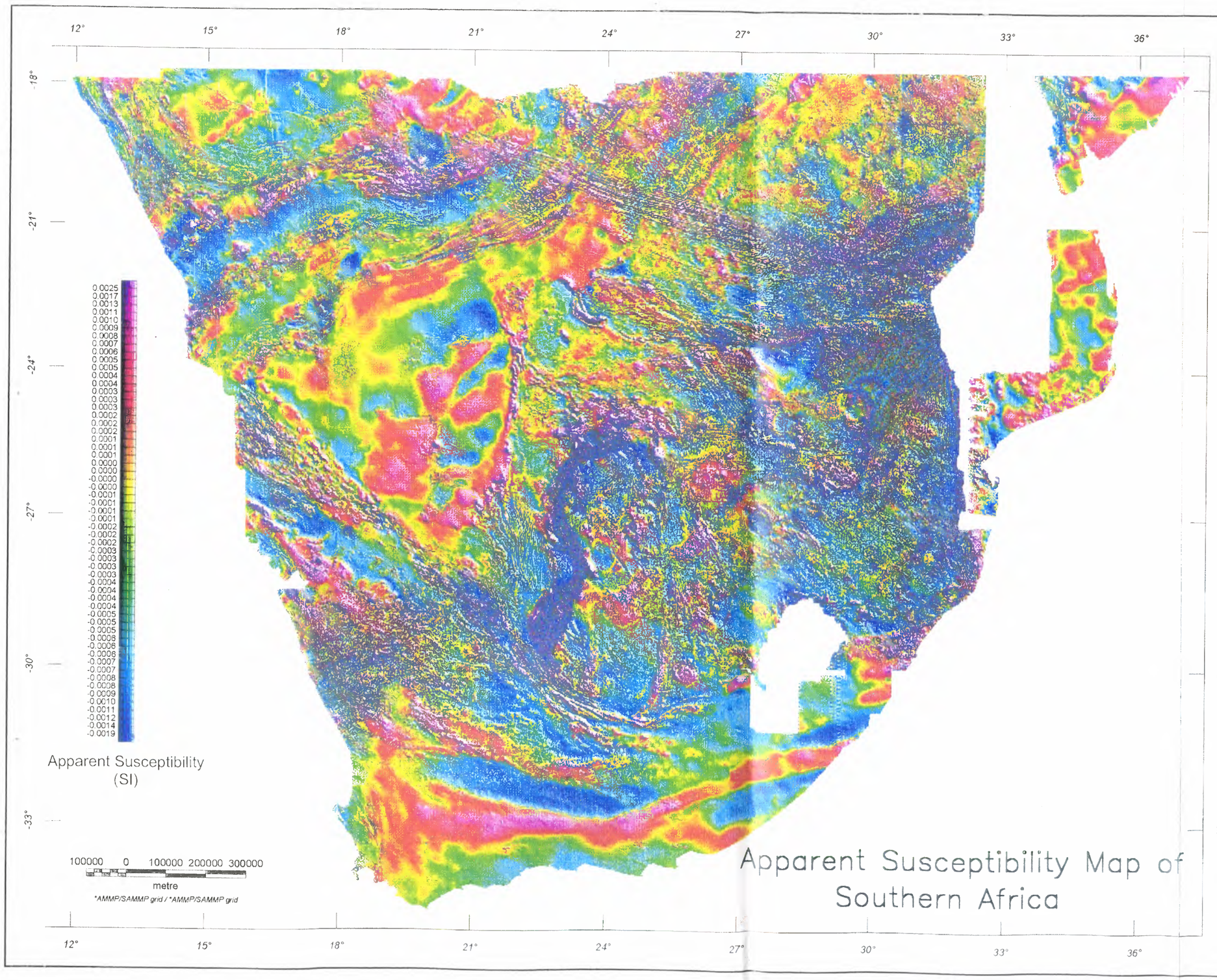

The Apparent susceptibilty was calculated from the total field aeromagnetic data using

Field = 29500 nT

Inclination = – 65

Declination = –20

Apparent Susceptibility Map of Southern Africa

Map 6.5a

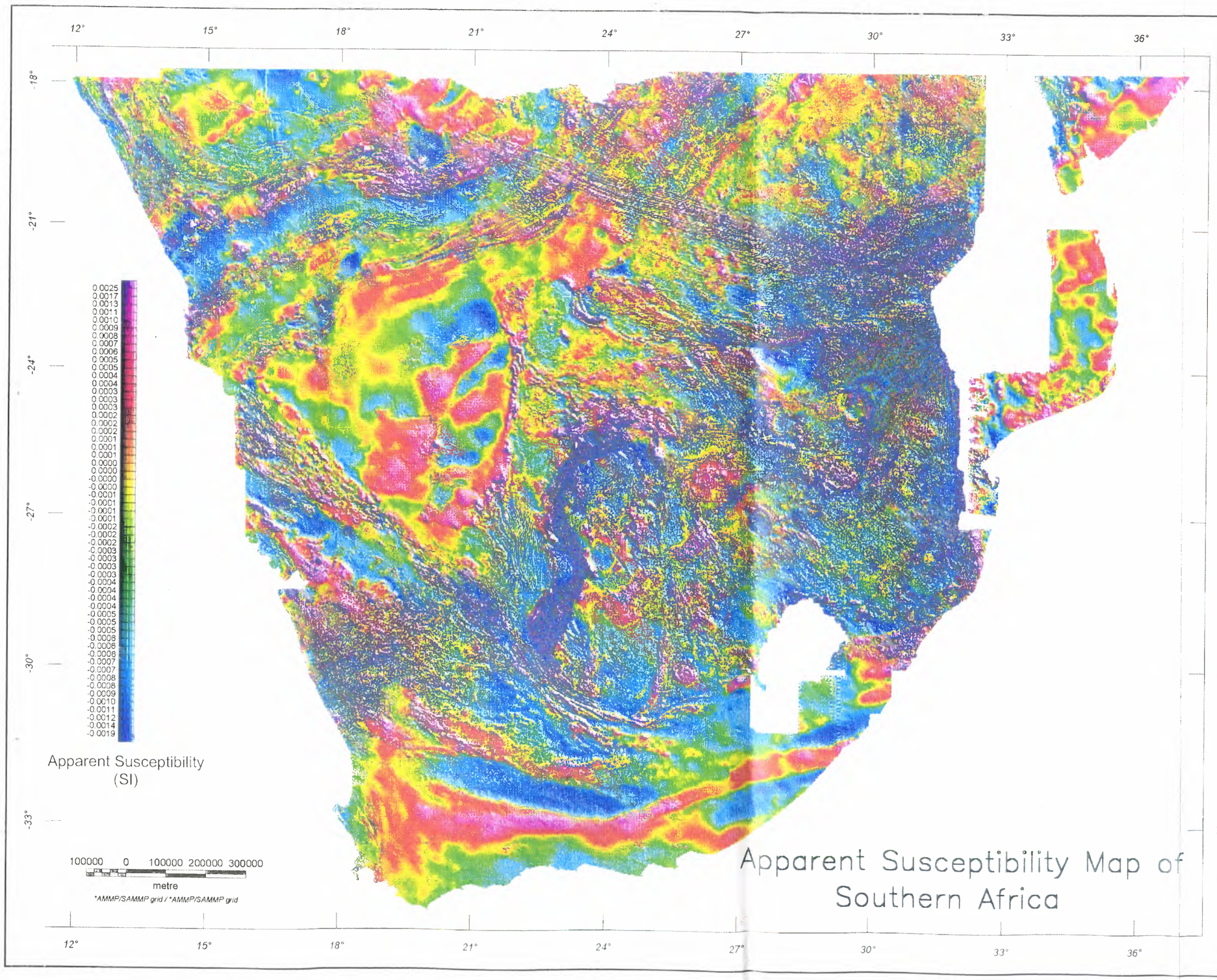

The Apparent susceptibilty was calculated from the total field aeromagnetic data using

Field = 29500 nT

Inclination = – 65

Declination = –20

Apparent Susceptibility Map of Southern Africa

Map 6.5a

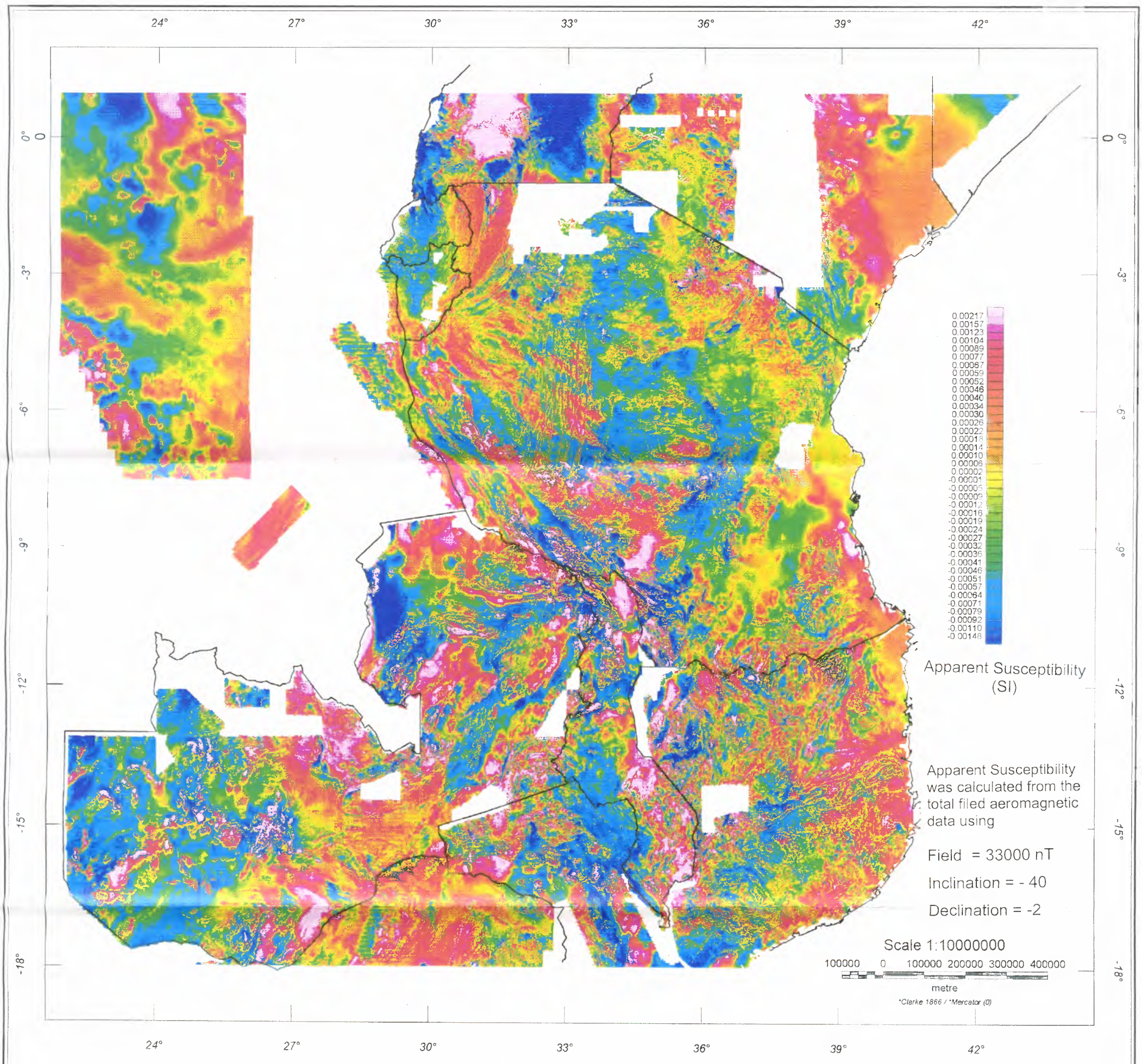

Apparent Susceptibility Map of Eastern Africa

Map 6.5b

Bijay Kumar Sahu, ITC, The Netherlands

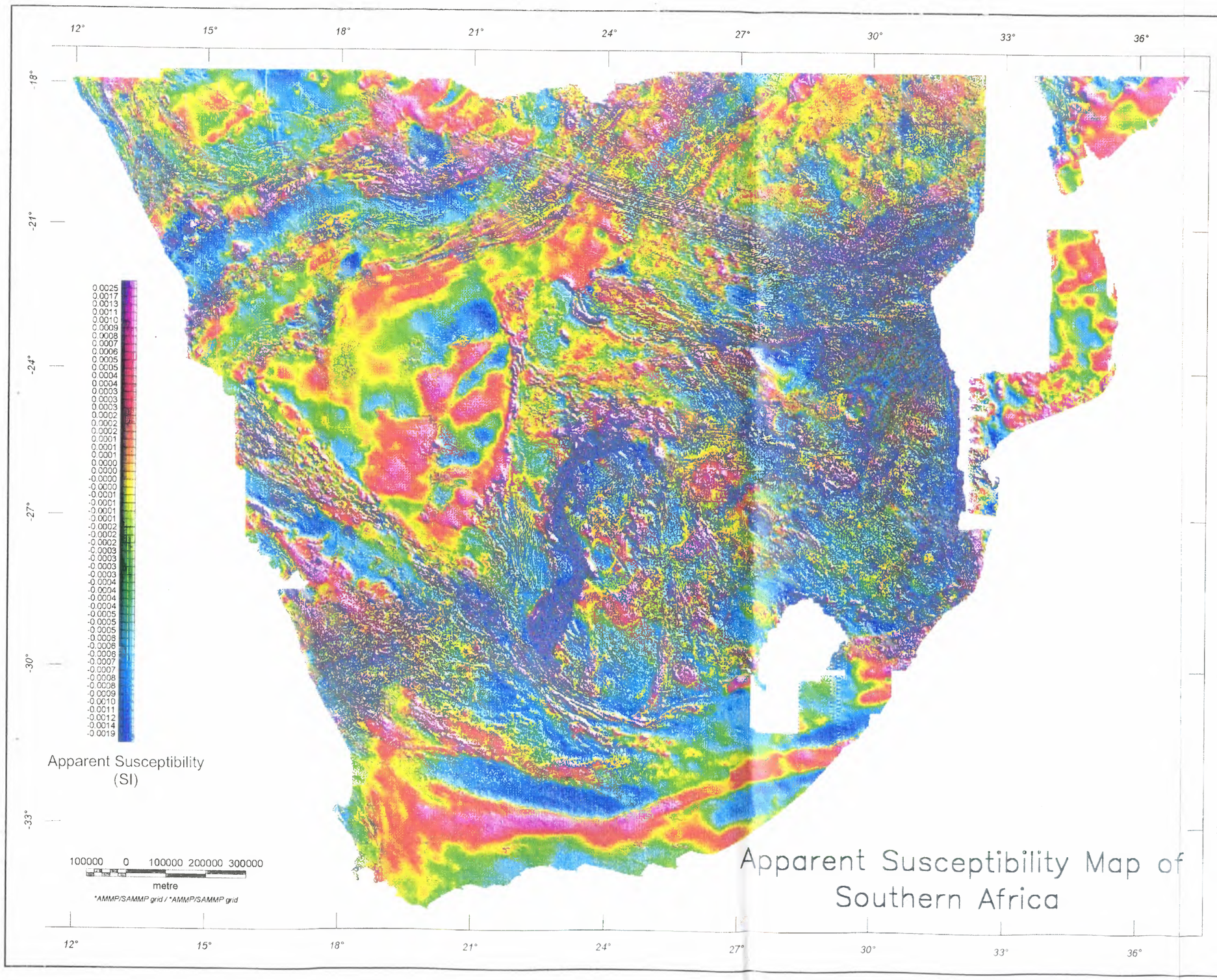

The Apparent susceptibilty was calculated from the total field aeromagnetic data using

Field = 29500 nT

Inclination = – 65

Declination = –20

Apparent Susceptibility Map of Southern Africa

Map 6.5a

24° 27° 30° 33° 36° 39° 42°

0° -3° -6° -9° -12° -15° -18°

0.00217
0.00157
0.00123
0.00104
0.00089
0.00077
0.00067
0.00059
0.00052
0.00046
0.00040
0.00034
0.00030
0.00026
0.00022
0.00018
0.00014
0.00010
0.00006
0.00002
-0.00001
-0.00005
-0.00009
-0.00012
-0.00016
-0.00019
-0.00024
-0.00027
-0.00032
-0.00036
-0.00041
-0.00046
-0.00051
-0.00057
-0.00064
-0.00071
-0.00079
-0.00092
-0.00110
-0.00148

Apparent Susceptibility (SI)

Apparent Susceptibility was calculated from the total filed aeromagnetic data using

Field = 33000 nT

Inclination = - 40

Declination = -2

Scale 1:10000000

100000 0 100000 200000 300000 400000

metre

*Clarke 1866 / *Mercator (0)

Apparent Susceptibility Map of Eastern Africa

Map 6.5b

Bijay Kumar Sahu, ITC, The Netherlands

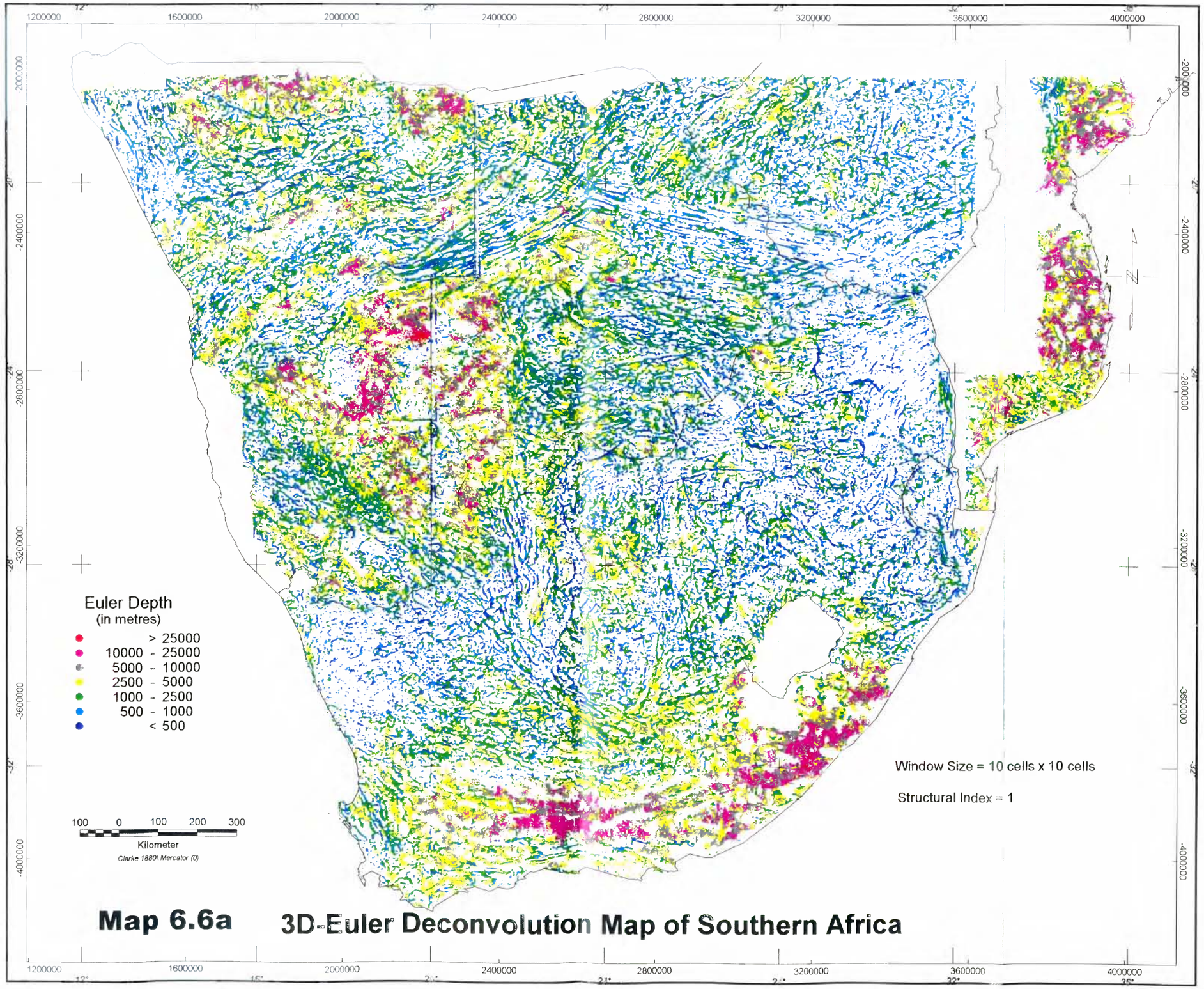

Map 6.6a **3D-Euler Deconvolution Map of Southern Africa**

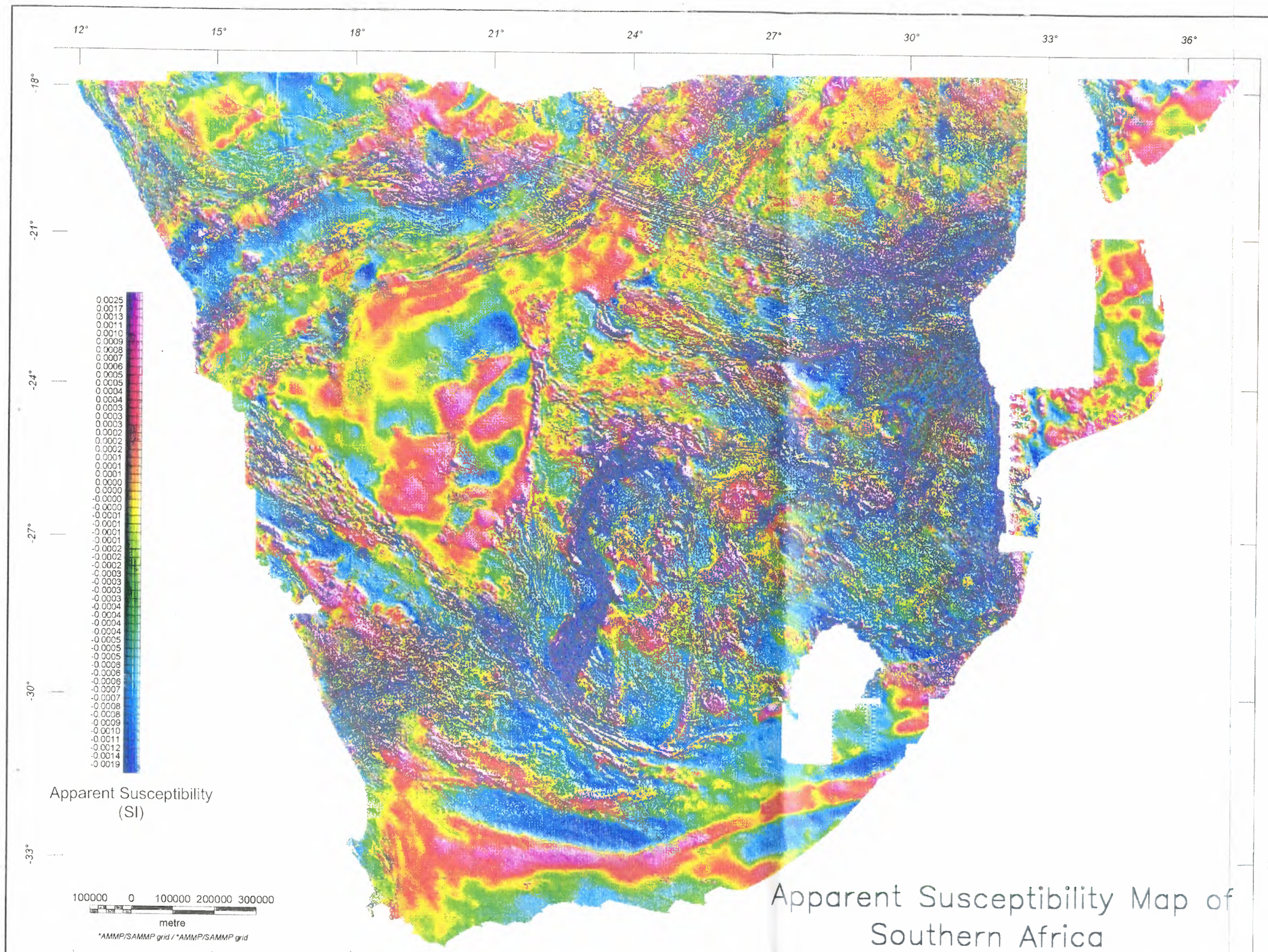

The Apparent susceptibilty was calculated from the total field aeromagnetic data using

Field = 29500 nT

Inclination = – 65

Declination = –20

Apparent Susceptibility Map of Southern Africa

Map 6.5a

24° 27° 30° 33° 36° 39° 42°

0° -3° -6° -9° -12° -15° -18°

0.00217
0.00157
0.00123
0.00104
0.00089
0.00077
0.00067
0.00059
0.00052
0.00046
0.00040
0.00034
0.00030
0.00026
0.00022
0.00018
0.00014
0.00010
0.00006
0.00002
-0.00001
-0.00005
-0.00009
-0.00012
-0.00016
-0.00019
-0.00024
-0.00027
-0.00032
-0.00036
-0.00041
-0.00046
-0.00051
-0.00057
-0.00064
-0.00071
-0.00079
-0.00092
-0.00110
-0.00148

Apparent Susceptibility (SI)

Apparent Susceptibility was calculated from the total filed aeromagnetic data using

Field = 33000 nT

Inclination = - 40

Declination = -2

Scale 1:10000000

100000 0 100000 200000 300000 400000

metre

*Clarke 1866 / *Mercator (0)

Apparent Susceptibility Map of Eastern Africa

Map 6.5b

Bijay Kumar Sahu, ITC, The Netherlands

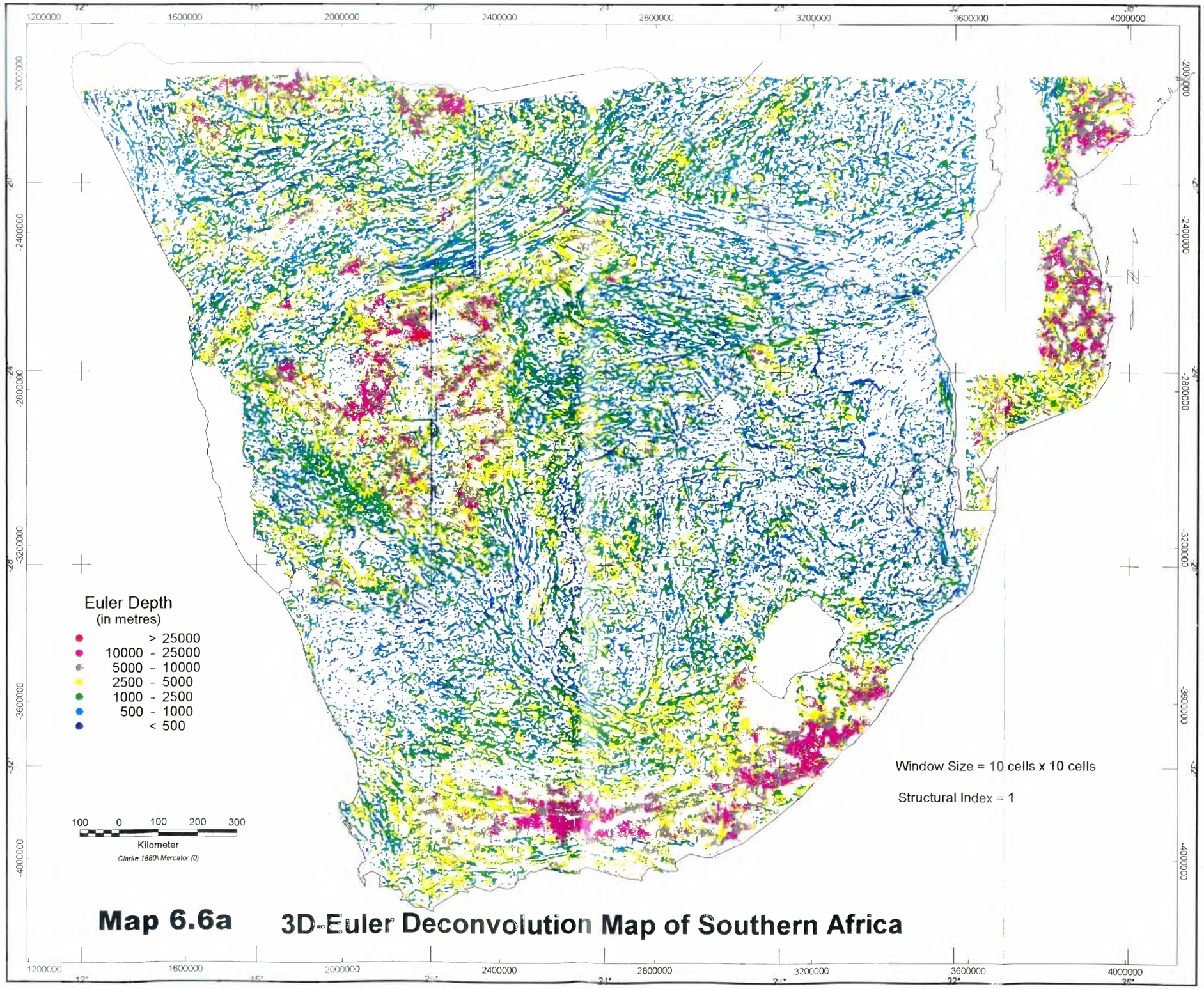

Map 6.6a **3D-Euler Deconvolution Map of Southern Africa**

3D Euler Deconvolution Map
Eastern Africa

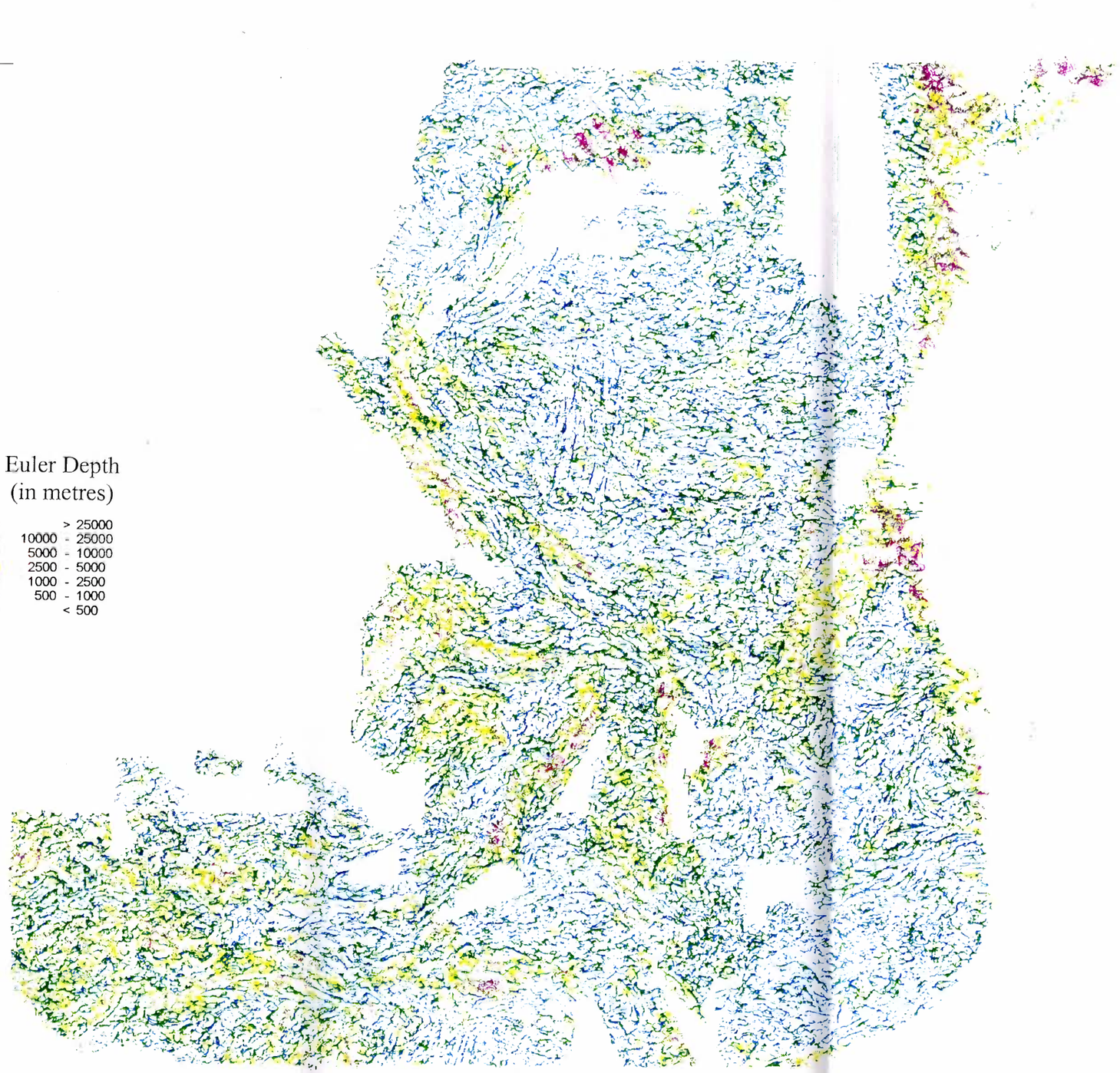

Cell Size = 1000 m

Window Size = 10 cells x 10 cells

Structural Index = 1

Map 6.6b

TECTONIC MAP OF SOUTHERN AND EASTERN AFRICA BASED ON AEROMAGNETIC INTERPRETATION

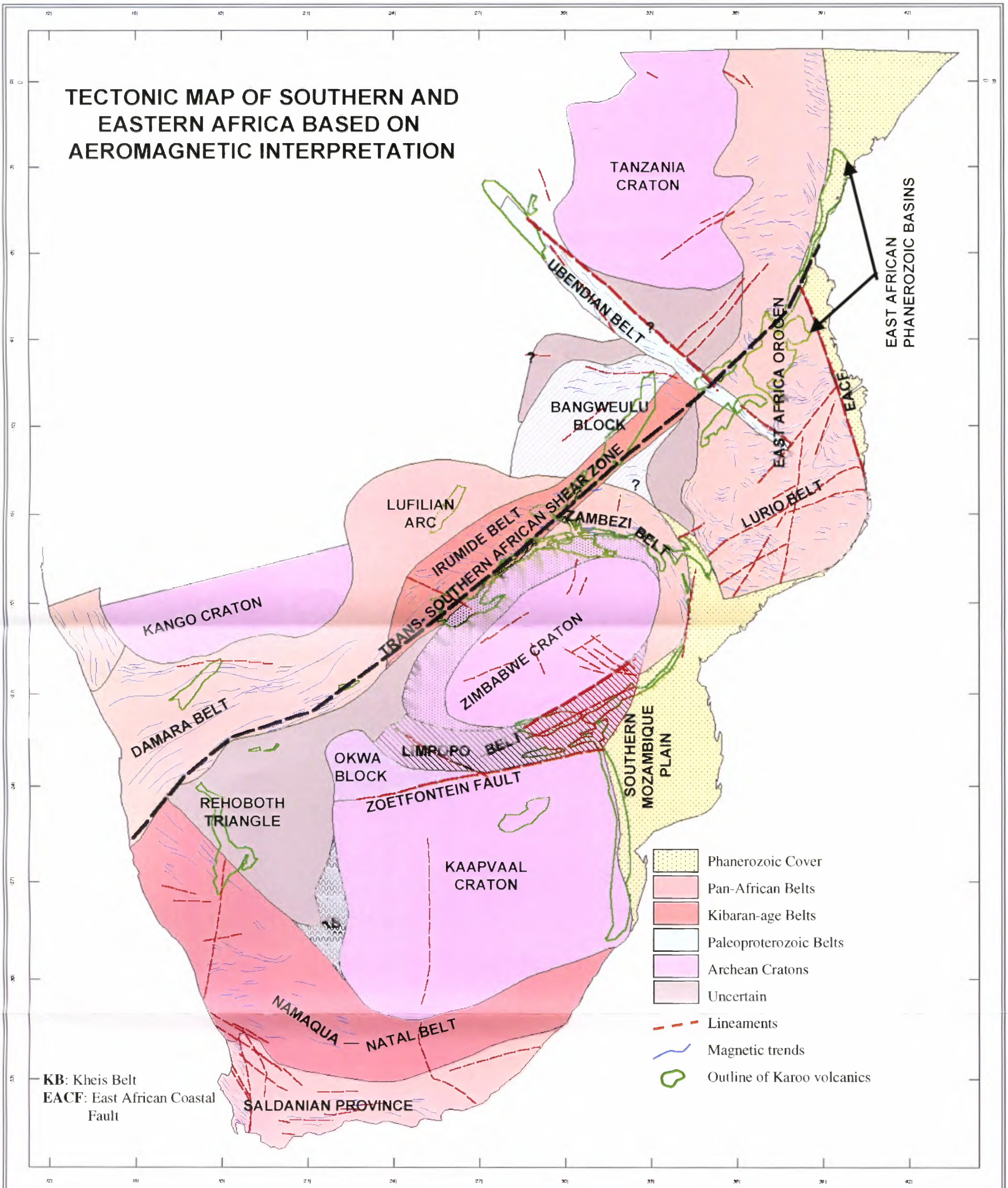

Map 6.7

Bijay Kumar Sahu

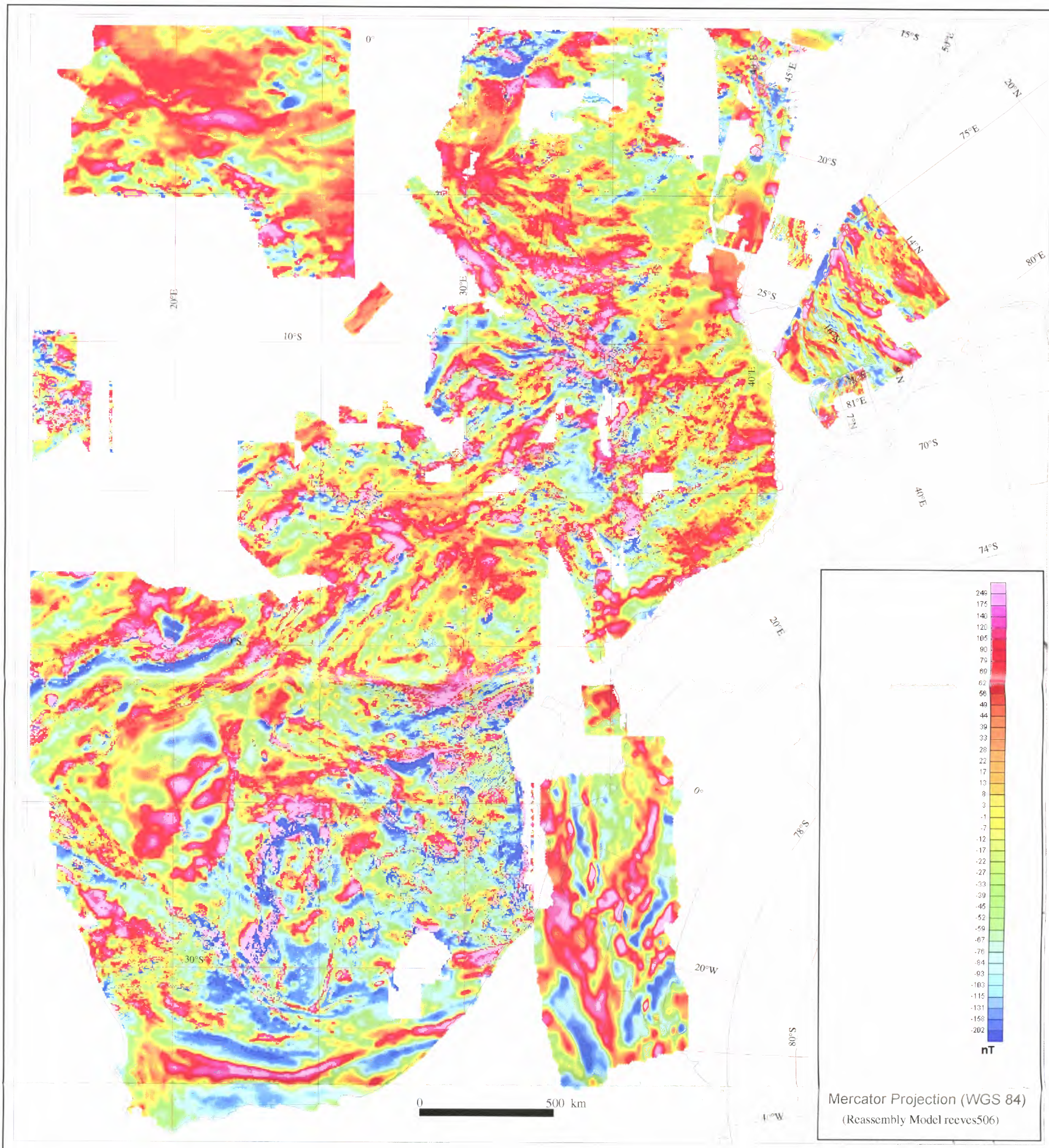

TOTAL FIELD AEROMAGNETIC MAP OF PARTS OF CENTRAL GONDWANA

Data Sources:	Africa and Madagascar	African magnetic Mapping Project
	Namibia	Geological Survey of Namibia
	Southern India	Digital data compiled in this thesis
	Southwest Sri Lanka	Perera (1997)
	Dronning Maud Land	Corner (1994)

Map 8.1

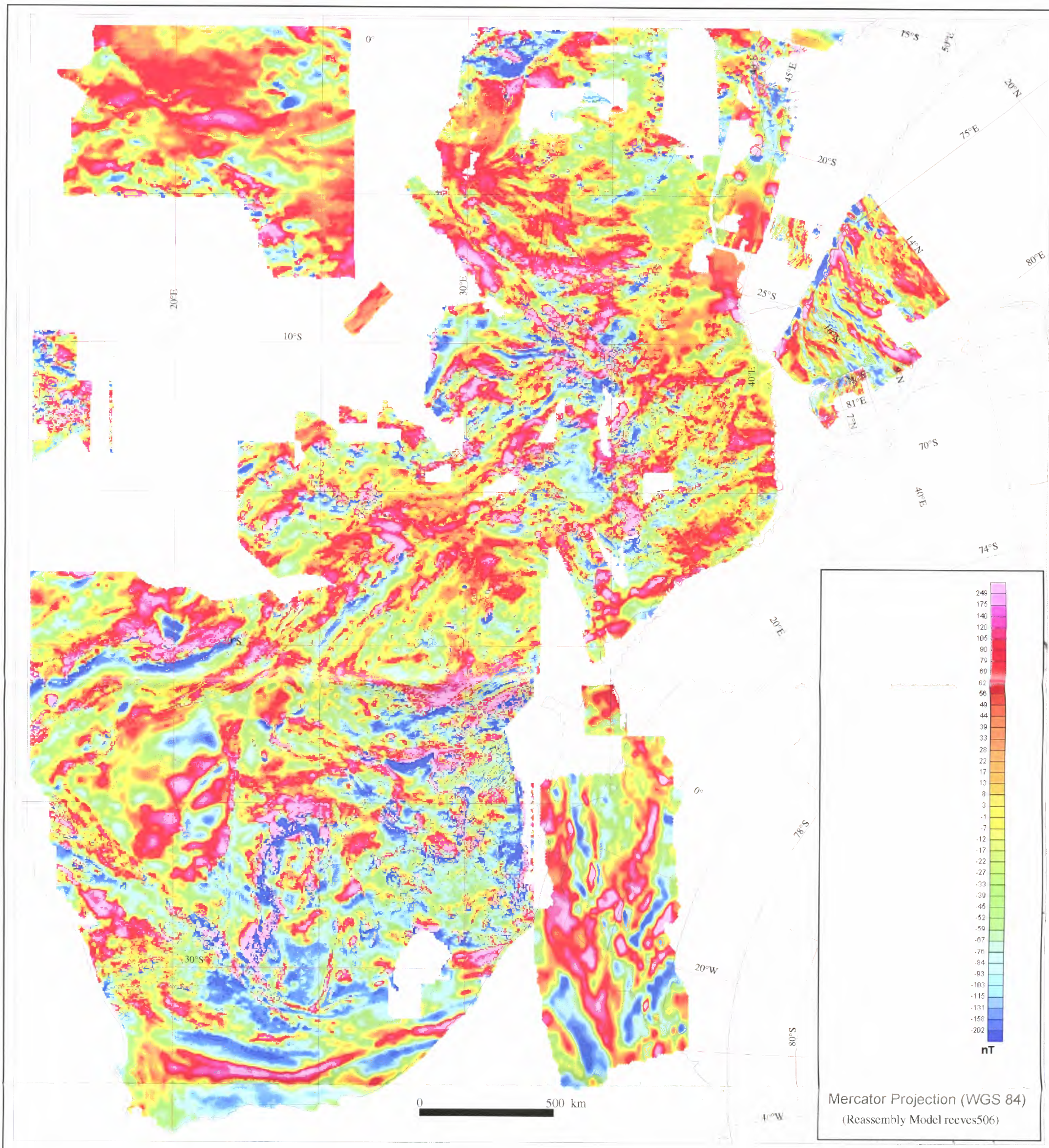

TOTAL FIELD AEROMAGNETIC MAP OF PARTS OF CENTRAL GONDWANA

Data Sources:	Africa and Madagascar	African magnetic Mapping Project
	Namibia	Geological Survey of Namibia
	Southern India	Digital data compiled in this thesis
	Southwest Sri Lanka	Perera (1997)
	Dronning Maud Land	Corner (1994)

Map 8.1

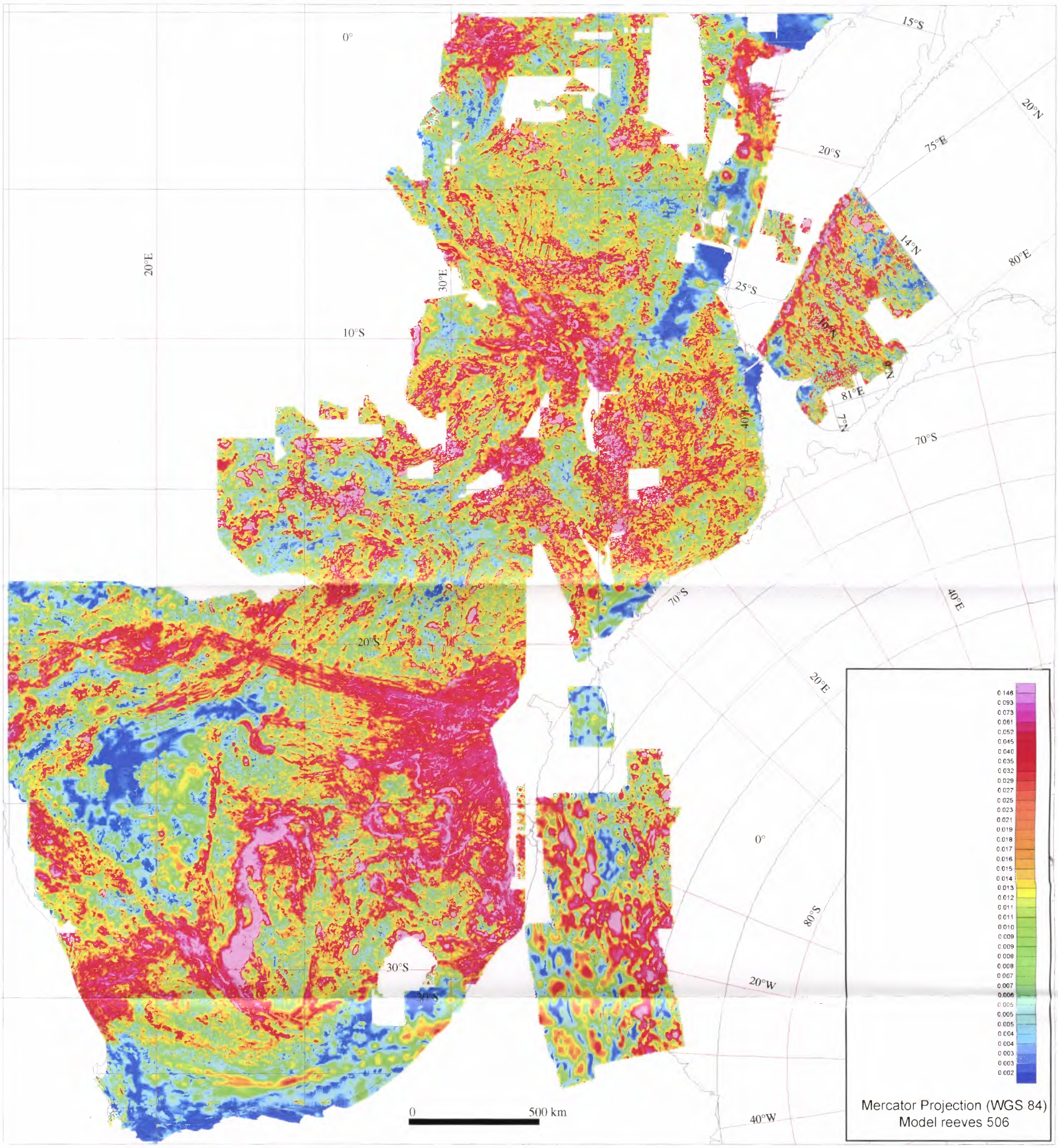

ANALYTIC SIGNAL MAP OF PARTS OF CENTRAL GONDWANA

Data Sources:	Africa and Madagascar	African magnetic Mapping Project
	Namibia	Geological Survey of Namibia
	Southern India	Digital data compiled in this thesis
	Southwest Sri Lanka	Perera (1997)
	Dronning Maud Land	Corner (1994)

Map 8.2

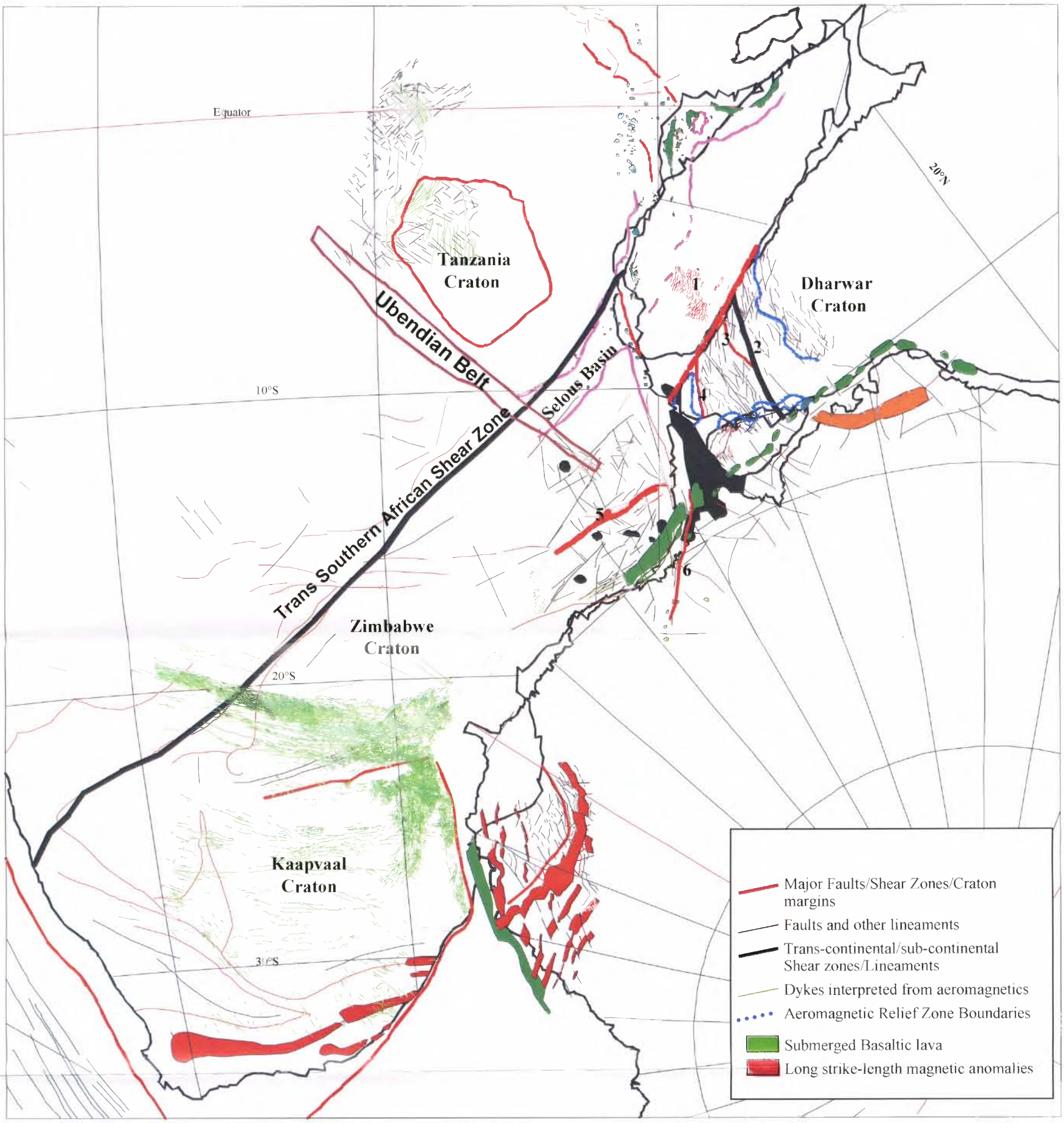

Aeromagnetic Interpretation Map of central Gondwana

1: Ranotsara Shear Zone, 2: Cannonore-Thanzavur Shear Zone, 3: Palghat-Cauvery Shear Zone, 4. Achankovil Shear Zone, 5: Lurio Shear Belt, 6: Western Marginal Fault of Sør Rondane Mountains

Data Sources: Africa - Batterham et al. (1983), Mubu, (1995), Reeves (pers. comm., 1998), this study; Madagascar - Yardimcilar, 1998; India - this study; Antarctica - Golynsky et al. (1996), Corner (1994).

Map 8.3

Tectonic Map of Central Gondwana

Cylindrical Equidistant Projection

0 1000 km

TC
UB
EAO
SM
AB
DT
DC
GR
MR
DR
SGT
NC
RC
S
BB
LA
IB
CC
ZC
DB
LB
KC
LM
GP
MP
EW
NNB
SP

- Syn-breakup magmatism
- Phanerozoic rift basins
- Proterozoic belts affected by Pan-African (~550 Ma) tectonothermal activities
- Kibaran-age(~1100 - 1000 Ma) Mobile Belts
- Pre-Kibaran\Grenvile Cratons
- Uncertain

SP: Saldanian Province
NNB: Namaqua-Natal Belt
KC: Kaapvaal Craton
LB: Limpopo Belt
ZC: Zimbabwe Craton
DB: Damara Belt
CC: Congo Craton
LA: Lufilian Arc
IB: Irumide Belt
BB: Bangweulu Block
EAO: East African Orogen
UB: Ubendian Belt
TC: Tanzania Craton
SM: South Madagascar

AB: Antongil Block
DC: Dharwar Craton
DC: Deccan Trap
GR: Godavari Rift
MR: Mahanadi Rift
DR: Damodar Rift
SGT: Southern Granulite Belt
S: Sri Lanka
NC: Napier Complex
RC: Rayner Complex
MP: Maudheim Province
GP: Grunehogna Province
EW: Explora Wedge
LM: Libombo Monocline

Map 8.4